

LIBRARY
Michigan State
University

This is to certify that the
dissertation entitled

SYNTHESIS AND PROPERTIES OF COMB-LIKE
POLYLACTIDES

presented by

XUWEI JIANG

has been accepted towards fulfillment
of the requirements for the

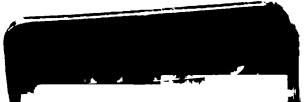
Ph.D. degree in Chemistry

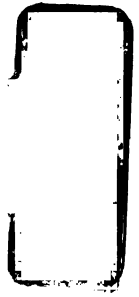


Major Professor's Signature

24 August 2006

Date





SYNTHESIS AND PROPERTIES OF COMB-LIKE POLYLACTIDES

By

Xuwei Jiang

A DISSERTATION

Submitted to
Michigan State University
in partial fulfillment of the requirements
for the degree of

DOCTOR OF PHILOSOPHY

Department of Chemistry

2006

ABSTRACT

SYNTHESIS AND PROPERTIES OF COMB-LIKE POLYLACTIDES

By

Xuwei Jiang

Because of their biodegradability and biocompatibility, lactide based polymers are extensively studied for biomedical applications. To have the broad range of physical properties that make them suitable for these applications, certain modifications of polylactides are necessary. This objective can be partially accomplished by synthesizing substituted polylactides.

A series of substituted glycolides, substituted with *n*-alkyl groups of various lengths (*n* (number of carbons in the alkyl group) = 6, 8, 10, 12, 14, 16), were synthesized and subsequently polymerized to high molecular weight polymers. Depending on the side chain length, low T_g polylactides and side chain crystalline polylactides were obtained. Hydrolytic degradation rates are independent of side chain length within experimental error. Thermal degradation temperatures of these alkyl comb polylactides are around 320 °C. Kinetic studies showed that lactide polymerizations are first order reactions in both melt and solution processes. The apparent polymerization rates initially decrease with the increase of side chain length. When side chain exceeds a critical length, the polymerization rates became independent of side chain length. For side chain crystalline polylactides, X-ray data revealed the formation of hexagonally packed side chain crystallites and lamellar structure in bulk. The melting temperature of the polymer can be easily tuned through copolymerization.

Novel glycolides with oligo(ethylene oxide) containing substituent groups were synthesized and polymerized to yield PEO-grafted polylactides with well-defined architecture. The introduction of PEO pendant groups onto the polylactide backbone improved its hydrophilicity and eventually made the polymer water-soluble. Aqueous solutions of water-soluble PEO grafted polylactides underwent reversible phase transitions when the temperature is above or below a critical point. The phase transition was studied by cloud point measurements, variable temperature ¹HNMR analysis, and variable temperature DLS measurements.

Amphiphilic substituted lactide monomers were synthesized by coupling of PEG containing α -hydroxy acids and 2-bromo-octadecanoyl chloride. DSC analysis of the polylactides derived from these amphiphilic monomers suggested side chain crystallization. Azobenzene encapsulation study by solvent displacement method showed that water solubility of azobenzene can be improved using the amphiphilic polylactide.

An acetylene functionalized glycolide was successfully synthesized. Subsequent homopolymerization and copolymerization led to pendant acetylene group containing polylactides. These functional polylactides were used as substrates for introduction of functional moieties onto polylactide backbone by click chemistry. PEG, alkyl, and PEG/alkyl grafted polylactides have been prepared through this approach. Among those grafted polymers, DiEG and DiEG/alkyl grafted polylactides exhibit lower critical solution temperature (LCST) in aqueous solution at ~80 °C and ~30 °C respectively.

ACKNOWLEDEMENTS

I would like to sincerely thank my advisor Greg Baker for his guidance. It is because of him I decided to come to MSU, it is because of him I had the chance to stay at MSU, and it is also because of him I chose to stay as a Spartan. I value tremendously his training and encouragements in all these years.

Secondly, I would like to thank Prof. Mitch Smith for his invaluable scientific guidance and discussions, and for his free lunches. I would like to thank Professor Maleczka and Blanchard for helpful discussions and suggestions, as well as Professor Mackay and his group members for use of their equipments.

Special thanks go to Jon for his help with my language and research, as well as for his interesting jokes. I would like to thank former and current group members Tianqi, JB, Feng, Qin, Ying, Bao, Erin, Leslie, D.J., and Ping for their friendship and profitable discussions.

Finally and most importantly, I would like to thank Guangyan, my wife, for your love and support, as well as our coming daughter for the anticipation you bring me. I would also like to thank my parents, sister, brother-in-law, and all other family members for their support and encouragements during my graduate career.

TABLE OF CONTENTS

List of Figures	vii
List of Schemes	xvii
List of Tables.....	xviii
List of Abbreviations.....	xix
Chapter 1 Introduction.....	1
Structure and Properties of Comb-like Polymers.....	1
Alkyl Comb Polymers with flexible backbone	1
Poly(acrylate)s, poly(methacrylates), poly(acrylamides).....	1
Poly(vinyl ethers) and poly(vinyl esters).....	3
Poly(α -olefins), polyaldehydes, and poly(oxiranes).....	4
Polystyrenes, poly(1,3-butadienes), and polyitaconates	7
Alkyl comb polymers with rigid backbone.....	9
Polypeptides	9
Poly(3-alkyl thiophene)s.....	12
Stiff-chain polyesters, polyamides, and polyimides.....	13
Other stiff-chain alkyl comb polymers	15
PEG comb polymers	17
Poly(vinyl ethers)	17
Poly(methacrylates)	20
Polystyrenes	21
PEG/Alkyl comb polymers.....	23
Application of Click Chemistry in polymer synthesis and functionalization.....	27
Chapter 2 Alkyl Comb Polylactides	39
Introduction	39
Results and Discussion	41
Monomer Synthesis	41
Bulk Polymerizations.....	44
Solution Polymerizations.....	48
Homopolymer Properties	49
Polymer Degradation	63
Alkyl Comb Copolymers.....	66
Experimental Section	69
Chapter 3 PEO-grafted Comb Polylactides	78
Introduction	78
Results and Discussion	80
Monomer synthesis.....	80

Bulk polymerization.....	84
Polymer properties.....	86
Aqueous solubility and solution properties of PEO-grafted polylactides	87
Conclusions.....	92
Experimental Section	92
Chapter 4 Functionalization of Polylactides by “Click” Chemistry.....	103
Introduction	103
Results and Discussion	105
Monomer synthesis.....	105
Polymerization	107
“Click” functionalization	111
Conclusions.....	121
Experimental Section	122
Chapter 5 PEG/Alkyl-Grafted Comb Polylactides.....	129
Introduction	129
Results and Discussion	131
Conclusions.....	139
Experimental Section	140
Appendicies	148
Appendix A. NMR Spectra	149
Appendix B. FT-IR Spectra	232
References.....	247

List of Figures

Figure 1. Chemical structures of comb-like poly(acrylates), poly(methacrylates), and poly(acrylamides).....	2
Figure 2. Possible side chain packing motifs for poly(acrylates) and poly(methacrylates) as proposed by Jordan et al.....	3
Figure 3. Chemical structures of comb-like poly(vinyl ester)s and poly(vinyl ether)s.....	4
Figure 4. Chemical structures of comb-like poly(α -olefin)s, poly(oxiranes)s, and polyaldehydes.....	5
Figure 5. Packing of comb polymers with parallel main chains and fully extended side chains as proposed by Turner-Jones.....	5
Figure 6. Possible packing arrangements for comb polymers with side chains tilted to main chain axis as proposed by Turner-Jones.....	6
Figure 7. Chemical structures of comb-like polystyrenes, poly(1,3-butadiene)s, and polyitaconates.....	8
Figure 8. Chemical structures of comb-like polypeptides.....	9
Figure 9. Model for the packing of poly(α -glutamates) at low temperatures.....	10
Figure 10. Schematic model illustrating the structural changes as function of temperature for side chain crystalline poly(β -aspartate)s.....	11
Figure 11. Chemical structure and proposed possible molecular packing of poly(3-alkyl thiophene)s.....	12
Figure 12. Chemical structures of comb-like rigid-rod polyesters, polyamides, and polyimides I (R represents linear alkyl groups).....	14
Figure 13. Chemical structures of comb-like rigid-rod polyesters, polyamides, and polyimides II (R represents linear alkyl groups).....	15
Figure 14. Chemical structures of several other alkyl comb-like polymers.....	16
Figure 15. Chemical structures of PEG comb-like poly(vinyl ether)s.....	17
Figure 16. Chemical structures of PEG comb-like poly(vinyl ether)s block copolymers.....	18

Figure 17. Chemical structures of comb-like PEG poly(methacrylate)s	20
Figure 18. Chemical structure of comb-like PEG polystyrenes	21
Figure 19. Chemical structures of PEG/alkyl comb polymers with well-defined structures	23
Figure 20. Chemical structures of PEG/alkyl comb polymers with ill-defined structures	25
Figure 21. A proposed model for a hypothetical bilayer structure formed by the graft copolymers poly(PEOMA- <i>ran</i> -ODMA).	26
Figure 22. Mechanism of click chemistry proposed by Sharpless et al.	27
Figure 23. Structure of a divergent dendrimer synthesized by Hawker and Wooley et al.	28
Figure 24. Structure of an unsymmetrical dendrimer synthesized by Lee et al. ...	29
Figure 25. 500 MHz ¹ H NMR spectra of hexadecyl glycolide and its polymer....	43
Figure 26. Bulk polymerization kinetics of substituted glycolides. Polymerization conditions: 130°C, [Sn(2-ethylhexanoate) ₂]/[<i>tert</i> -butylbenzyl alcohol] = 1, [monomer]/[catalyst] = 50. Each data point is the average of three independent runs and corrected for equilibrium.....	45
Figure 27. Relationship between apparent rate constant and the length of side chains for bulk polymerization of substituted glycolides.....	46
Figure 28. Solution polymerization kinetics of substituted glycolides. Polymerization conditions: 90°C in toluene, [Sn(2-ethylhexanoate) ₂]/[<i>tert</i> -butylbenzyl alcohol] = 1, [monomer]/[catalyst] = 100. Each data set corresponds to a single kinetics run.	47
Figure 29. Relationship between apparent rate constant and the length of side chains for solution polymerization of substituted glycolides.	48
Figure 30. TGA results for substituted polyglycolides. (10 °C/min in air, no aging)	50
Figure 31. DSC scans for substituted polyglycolides. The data are second heating scans, taken after heating to 70 °C and flash cooled. Heating rate: 10 °C /min in N ₂	51
Figure 32. The relationship between ΔH _f and side chain length	52

Figure 33. WAXS profiles of flash-cooled polyC14 and polyC16 (polyC14-1 and polyC14-2, polyC16-1 and polyC16-2 are two different runs from the same polyC14 and polyC16 sample, respectively.)	54
Figure 34. DSC traces of polyC14 samples with different thermal histories. First heating scan. 10 °C/min in N ₂ . (black line: flash cooled in freezer for 8 minutes; pink line: annealed at 27 °C for four hours; blue line: annealed 32 °C for six weeks)	56
Figure 35. WAXS profiles of polyC14 samples with different thermal histories. (black line: flash cooled in freezer for 8 minutes; pink line: annealed at 27 °C for four hours; blue line: annealed 32 °C for six weeks)	56
Figure 36. DSC traces of polyC16 samples with different thermal histories. First heating scan. 10 °C/min in N ₂ . (black line: annealed at room temperature for 12 hours; pink line: annealed at 45 °C for two weeks; blue line: annealed at 45 °C for two months)	57
Figure 37. WAXS profiles of polyC16 samples with different thermal histories. (black line: annealed at room temperature for 12 hours; pink line: annealed at 45 °C for two weeks; blue line: annealed at 45 °C for two months)	57
Figure 38. DSC traces of annealed alkyl comb polyglycolides. 10 °C/min in N ₂ . (black line: polyC10, annealed at room temperature for a year; pink line: polyC12, annealed at room temperature for a year; red line: polyC14, annealed at 32 °C for six weeks; blue line: polyC16, annealed at 45 °C for two weeks)	60
Figure 39. WAXS profiles of annealed alkyl comb polyglycolides. (black line: polyC10, annealed at room temperature for a year; pink line: polyC12, annealed at room temperature for a year; red line: polyC14, annealed at 32 °C for six weeks; blue line: polyC16, annealed at 45 °C for two weeks).....	60
Figure 40. Evolution of d-spacings with side chain length. (■ crystalline polymer samples; ▲ melt polymer samples)	61
Figure 41. Proposed molecular packing of annealed alkyl comb polylactides	62
Figure 42. WAXS profiles of alkyl comb polyglycolides.....	63
Figure 43. Molecular weight change of polyglycolides during hydrolytic degradation in pH = 7.4 phosphate buffer at 55 °C	65
Figure 44. Molecular weight change of polyglycolides during hydrolytic degradation fitted to random chain scission model	65

Figure 45. DSC heating scans of C14 and C16 random copolymers. Second heating scan, 10 °/min in N ₂	67
Figure 46. DSC heating traces of polyC14 and polyC16 blends. Second heating scan, 10 °C/min in N ₂	68
Figure 47. DSC heating scan of polyC16 – <i>block</i> - polyC14). Second heating scan, 10 °C/min in N ₂	69
Figure 48. ¹ H NMR spectra for 4b, 5b, and poly(5b).....	82
Figure 49. GPC traces of PEO-grafted polylactides.....	85
Figure 50. TGA of PEO-grafted polylactides (10 °C/min in air, samples were held at 135 °C for 30 min prior to run. Pink line: poly(5a); red line: poly(5b); black line: poly(5c); blue line: poly(5d)).....	86
Figure 51. DSC traces of PEO-grafted polylactides (second heating scan, 10 °C/min in N ₂).....	87
Figure 52. 500 MHz ¹ H NMR spectra of poly(5c) (M _n = 59,800 g/mol, PDI = 1.16) in D ₂ O (15 mg/mL) at different temperatures.....	88
Figure 53. 500 MHz ¹ H NMR spectra of poly(5d) (M _n = 10,600 g/mol, PDI = 1.12) in D ₂ O (15 mg/mL) at different temperatures.....	89
Figure 54. DLS results of poly(5c) (M _n = 59,800 g/mol, PDI = 1.16) in water (3 mg/mL) at different temperatures.....	91
Figure 55. DLS results of poly(5d) (M _n = 10,600 g/mol, PDI = 1.12) in water (3 mg/mL) at different temperatures.....	91
Figure 56. 300 MHz ¹ H NMR spectra of propargyl glycolide and poly(propargyl glycolide).....	107
Figure 57. Relationship between M _n and the degree of polymerization for propargyl glycolide bulk polymerization.....	108
Figure 58. 75 MHz ¹³ C NMR carbonyl region of propargyl glycolide homopolymer, copolymers, and polylactide.....	110
Figure 59. GPC traces of the PPGL macroinitiator, and PPGL- <i>block</i> -polylactide. (black line: PPGL; pink line: PPGL- <i>block</i> -polylactide).....	111
Figure 60. GPC traces of PPGL and C10-grafted PPGL. (pink line: PPGL; black line: C10-grafted PPGL).....	113

Figure 61. GPC traces from a control reaction where PPGL was exposed to click conditions, but without added azide. (black line: PPGL before the reaction; pink line: PPGL after the reaction).....	114
Figure 62. GPC traces of a polylactide sample exposed to “click” conditions. (black line: polylactide before the click reaction; pink line: polylactide after reaction).....	116
Figure 63. GPC traces for the poly(propargyl glycolide-co-lactide) click PEGylation. The concentration of propargyl glycolide in the copolymer was 7.9 mol %. (black line: copolymer before the click reaction; pink line: copolymer after click reaction).....	116
Figure 64. DLS of DiEG/alkyl-grafted PPGL (5 mg/mL in water).....	119
Figure 65. DLS of PEGylated PPGL- <i>block</i> -polylactide in water	120
Figure 66. 300 MHz ¹ H NMR spectra of PEG containing α-hydroxy acids	133
Figure 67. 500 MHz ¹ H NMR spectra of amphiphilic glycolide monomers	134
Figure 68. 500 MHz ¹ H NMR spectra of amphiphilic polyglycolides.....	135
Figure 69. GPC traces of amphiphilic polyglycolides (pink line: poly(4a); black line: poly(4b)	136
Figure 70. DSC heating traces of amphiphilic polylactides (second heating scan, 10 °C/min in N ₂)	136
Figure 71. DLS of polymeric micelles and azobenzene loaded polymeric micelles (5mg/mL in water, pink line: polymer only; black line: polymer + azobenzene). 137	
Figure 72. UV-vis spectra of polymeric micelles, azobenzene loaded polymeric micelles, and azobenzene in water. (black line: azobenzene; pink line: poly(4a); blue line: poly(4a) + azobenzene).....	138
Appendix A 1. ¹ H NMR spectrum of C6-α-hydroxy acid.....	150
Appendix A 2. ¹³ C NMR spectrum of C6-α-hydroxy acid.....	151
Appendix A 3. ¹ H NMR spectrum of C6 dimer	152
Appendix A 4. ¹³ C NMR spectrum of C6 dimer	153
Appendix A 5. ¹ H NMR spectrum of C8-α-hydroxy acid.....	154

Appendix A 6. ^{13}C NMR spectrum of C8- α -hydroxy acid.....	155
Appendix A 7. ^1H NMR spectrum of C8 dimer	156
Appendix A 8. ^{13}C NMR spectrum of C8 dimer	157
Appendix A 9. ^1H NMR spectrum of C10 α -hydroxy acid	158
Appendix A 10. ^{13}C NMR spectrum of C10 α -hydroxy acid.....	159
Appendix A 11. ^1H NMR spectrum of C10 dimer.....	160
Appendix A 12. ^{13}C NMR spectrum of C10 dimer	161
Appendix A 13. ^1H NMR spectrum of C12 α -hydroxy acid	162
Appendix A 14. ^{13}C NMR spectrum of C12 α -hydroxy acid.....	163
Appendix A 15. ^1H NMR spectrum of C12 dimer	164
Appendix A 16. ^{13}C NMR spectrum of C12 dimer	165
Appendix A 17. ^1H NMR spectrum of C14 α -hydroxy acid	166
Appendix A 18. ^{13}C NMR spectrum of C14 α -hydroxy acid.....	167
Appendix A 19. ^1H NMR spectrum of C14 dimer	168
Appendix A 20. ^{13}C NMR spectrum of C14 dimer	169
Appendix A 21. ^1H NMR spectrum of C16 α -hydroxy acid	170
Appendix A 22. ^{13}C NMR spectrum of C16 α -hydroxy acid.....	171
Appendix A 23. ^1H NMR spectrum of C16 dimer	172
Appendix A 24. ^{13}C NMR spectrum of C16 dimer	173
Appendix A 25. ^1H NMR spectrum of polyC6.....	174
Appendix A 26. ^1H NMR spectrum of polyC8.....	175
Appendix A 27. ^1H NMR spectrum of polyC10	176
Appendix A 28. ^1H NMR spectrum of polyC12.....	177

Appendix A 29. ^1H NMR spectrum of polyC14.....	178
Appendix A 30. ^1H NMR spectrum of polyC16.....	179
Appendix A 31. ^1H NMR spectrum of MonoEG-C6 bromide	180
Appendix A 32. ^{13}C NMR spectrum of MonoEG-C6 bromide.....	181
Appendix A 33. ^1H NMR spectrum of MonoEG-C6- α -hydroxy acid.....	182
Appendix A 34. ^{13}C NMR spectrum of MonoEG-C6- α -hydroxy acid	183
Appendix A 35. ^1H NMR spectrum of MonoEG-C6 dimer	184
Appendix A 36. ^{13}C NMR spectrum of MonoEG-C6 dimer.....	185
Appendix A 37. ^1H NMR spectrum of DiEG-C6 bromide.....	186
Appendix A 38. ^{13}C NMR spectrum of DiEG-C6 bromide	187
Appendix A 39. ^1H NMR spectrum of DiEG-C6- α -hydroxy acid	188
Appendix A 40. ^{13}C NMR spectrum of DiEG-C6- α -hydroxy acid.....	189
Appendix A 41. ^1H NMR spectrum of DiEG-C6 dimer.....	190
Appendix A 42. ^{13}C NMR spectrum of DiEG-C6-dimer	191
Appendix A 43. ^1H NMR spectrum of TriEG-C6 bromide.....	192
Appendix A 44. ^{13}C NMR spectrum of TriEG-C6 bromide.....	193
Appendix A 45. ^1H NMR spectrum of TriEG-C6- α -hydroxy acid	194
Appendix A 46. ^{13}C NMR spectrum of TriEG-C6- α -hydroxy acid	195
Appendix A 47. ^1H NMR spectrum of TriEG-C6 dimer.....	196
Appendix A 48. ^{13}C NMR spectrum of TriEG-C6 dimer.....	197
Appendix A 49. ^1H NMR spectrum of TetraEG-C6 bromide.....	198
Appendix A 50. ^1H NMR spectrum of TetraEG-C6- α -hydroxy acid	199
Appendix A 51. ^{13}C NMR spectrum of TetraEG-C6- α -hydroxy acid.....	200

Appendix A 52. ^1H NMR spectrum of TetraEG-C6 dimer.....	201
Appendix A 53. ^{13}C NMR spectrum of TetraEG-C6 dimer	202
Appendix A 54. ^1H NMR spectrum of poly(MonoEG-C6)	203
Appendix A 55. ^1H NMR spectrum of poly(DiEG-C6).....	204
Appendix A 56. ^1H NMR spectrum of poly(TriEG-C6).....	205
Appendix A 57. ^1H NMR spectrum of poly(TetraEG-C6).....	206
Appendix A 58. ^1H NMR spectrum of propargyl- α -hydroxy ethyl ester.....	207
Appendix A 59. ^{13}C NMR spectrum of propargyl- α -hydroxy ethyl ester	208
Appendix A 60. ^1H NMR spectrum of propargyl- α -hydroxy acid.....	209
Appendix A 61. ^{13}C NMR spectrum of propargyl- α -hydroxy acid	210
Appendix A 62. ^1H NMR spectrum of propargyl glycolide	211
Appendix A 63. ^{13}C NMR spectrum of propargyl glycolide.....	212
Appendix A 64. ^1H NMR spectrum of poly(propargyl glycolide)	213
Appendix A 65. ^{13}C NMR spectrum of poly(propargyl glycolide).....	214
Appendix A 66. ^1H NMR spectrum of poly(propargyl glycolide) – <i>ran</i> - polylactide	215
Appendix A 67. ^{13}C NMR spectrum of poly(propargyl glycolide) – <i>ran</i> - polylactide	216
Appendix A 68. ^1H NMR spectrum of poly(propargyl glycolide) – <i>block</i> – polylactide.....	217
Appendix A 69. ^{13}C NMR spectrum of poly(propargyl glycolide) – <i>block</i> – polylactide.....	218
Appendix A 70. ^1H NMR spectrum of DiEG-grafted poly(propargyl glycolide) ..	219
Appendix A 71. ^1H NMR spectrum of 2-bromooctadecanoyl chloride	220
Appendix A 72. ^{13}C NMR spectrum of 2-bromooctadecanoyl chloride.....	221

Appendix A 73. ^1H NMR spectrum of TriEG-C6-C16 dimer	222
Appendix A 74. ^{13}C NMR spectrum of TriEG-C6-C16 dimer	223
Appendix A 75. ^1H NMR spectrum of TriEG-monobenzyl-ether-C6 bromide	224
Appendix A 76. ^{13}C NMR spectrum of TriEG-monobenzyl-ether-C6 bromide ...	225
Appendix A 77. ^1H NMR spectrum of TriEG-monobenzyl-ether-C6- α -hydroxy acid	226
Appendix A 78. ^{13}C NMR spectrum of TriEG-monobenzyl-ether-C6- α -hydroxy acid	227
Appendix A 79. ^1H NMR spectrum of TriEG-monobenzyl-ether-C6-C16 dimer	228
Appendix A 80. ^{13}C NMR spectrum of TriEG-monobenzyl-ether-C6-C16 dimer	229
Appendix A 81. ^1H NMR spectrum of poly(TriEG-monomethyl-ether-C6-C16) .	230
Appendix A 82. ^1H NMR spectrum of poly(TriEG-monobenzyl-ether-C6-C16) .	231
Appendix B 1. FT-IR spectrum of C6 dimer	233
Appendix B 2. FT-IR spectrum of C8 dimer	234
Appendix B 3. FT-IR spectrum of C10 dimer	235
Appendix B 4. FT-IR spectrum of C12 dimer	236
Appendix B 5. FT-IR spectrum of C14 dimer	237
Appendix B 6. FT-IR spectrum of C16 dimer	238
Appendix B 7. FT-IR spectrum of MonoEG-C6 dimer	239
Appendix B 8. FT-IR spectrum of DiEG-C6 dimer.....	240
Appendix B 9. FT-IR spectrum of TriEG-C6 dimer.....	241
Appendix B 10. FT-IR spectrum of TetraEG-C6 dimer.....	242
Appendix B 11. FT-IR spectrum of propargyl- α -hydroxy acid	243
Appendix B 12. FT-IR spectrum of propargyl glycolide	244

Appendix B 13. FT-IR spectrum of TriEG-monomethyl-ether-C6-C16 dimer245

Appendix B 14. FT-IR spectrum of TriEG-monobenzyl-ether-C6-C16 dimer246

Images in this dissertation are presented in color

List of Schemes

Scheme 1. Convergent approach toward triazole dendrimers by Hawker et al...	28
Scheme 2. Synthesis of amphiphilic dendrimer (Fokin, Sharpless, and Hawker et al.).....	29
Scheme 3. Preparation of block copolymers by combination of ATRP and Click Chemistry.....	30
Scheme 4. Synthesis and structure of dendronized linear polymers (Fréchet et al.).....	32
Scheme 5. Click functionalization of polymethacrylate	33
Scheme 6. synthesis functional poly(<i>p</i> -phenyleneethynylene)s	33
Scheme 7. Simultaneous click functionalization of terpolymer.....	34
Scheme 8. Preparation of chain-end functional polymers by Click Chemistry	35
Scheme 9. Click functionalization of aliphatic polyesters	35
Scheme 10. structure of mannose-functionalized dendrimer	37
Scheme 11. Synthesis of alkyl substituted lactide monomers.....	41
Scheme 12. Synthesis of PEO-grafted polylactides.....	81
Scheme 13. Synthetic route to propargyl glycolide and its polymers	106
Scheme 14. Synthesis of amphiphilic lactide monomers	132

List of Tables

Table 1. Properties of alkyl comb polylactides	49
Table 2. X-ray Diffraction Spacings (Å) of Comb-like PolyLactides.....	59
Table 3. properties of C14 and C16 copolymers.....	67
Table 4. Representative bulk polymerization results of PEO containing glycolides.	84
Table 5. Bulk polymerization results of propargyl glycolide.....	108

List of Abbreviations

BBA	4- <i>tert</i> -Butylbenzylalcohol
br	Broad
d	Doublet
dd	Doublet of doublet
DLS	Dynamic light scattering
DMA	Dynamic mechanical analysis
DMF	N,N-Dimethyl-formamide
DSC	Differential scanning calorimetry
GPC	Gel permeation chromatography
J	Coupling constant
LCST	Lower critical solution temperature
LS	Light scattering
m	Multiplet
M_n	Number average molecular weight
M_w	Weight average molecular weight
MS	Mass spectroscopy
NMR	Nuclear magnetic resonance
p	Pentet
PDI	Polydispersity index
PEO	Poly(ethylene oxide)
PEG	Poly(ethylene glycol)

PolyC6	Poly(hexylglycolide)
PolyC8	Poly(octylglycolide)
PolyC10	Poly(decylglycolide)
PolyC12	Poly(dodecylglycolide)
PolyC14	Poly(tetradecylglycolide)
PolyC16	Poly(hexadecylglycolide)
PPGL	Poly(propargyl glycolide)
q	Quartet
RT	Room temperature
s	singlet
Sn(Oct) ₂	Tin(II)-2-ethylhexanoate
t	Triplet
T_g	Glass transition temperature
T_m	Melting temperature
TGA	Thermal gravimetric analysis
THF	Tetrahydrofuran
UV-Vis	Ultraviolet-Visible
WAXS	Wide angle X-ray scattering

Chapter 1 Introduction

Structure and Properties of Comb-like Polymers

Comb-like polymers with long, linear side chains in each repeat unit are a bridge between branched polymers and linear polymers. Comb polymers have attracted a great deal of attention because the nature of the side chains leads to dramatically different polymer properties.^{1,2} For example, comb-like polymers with linear alkyl side chains have lower melt and solution viscosities than linear polymers, and decreased glass transition temperatures. Because of these properties, comb-like polymers have found numerous applications such as pour-point depressants for lubricants, viscosity modifiers, or additives in petroleum products. The side chain crystalline character of these polymers has also led to applications as temperature-triggered release matrices for the delivery of agricultural insecticides and herbicides.³ In contrast to hydrophobic crystalline combs, some comb-like polymers with oligo(ethylene oxide) side chains are water soluble and exhibit lower critical solution temperature (LCST) behavior, making them attractive “smart” materials for biotechnology.

Alkyl Comb Polymers with flexible backbone

Poly(acrylate)s, poly(methacrylates), poly(acrylamides)

In 1944 Rehberg and Fisher reported poly(*n*-alkyl acrylates) (**1**), the first alkyl comb polymers.⁴ The “brittle points” of these poly(*n*-alkyl acrylates) decreased

with increasing side chain length up to poly(*n*-octyl acrylate), and then reversed as the chains became progressively longer. Later, the higher alkyl polyacrylates were identified as crystalline materials⁵ and the increase in brittle points was attributed to the higher melting points of polymers with longer alkyl side chains.⁶ Crystallographic studies of these polymers by X-ray diffraction revealed that the long alkyl side chains are hexagonally packed and that the arrangement of the

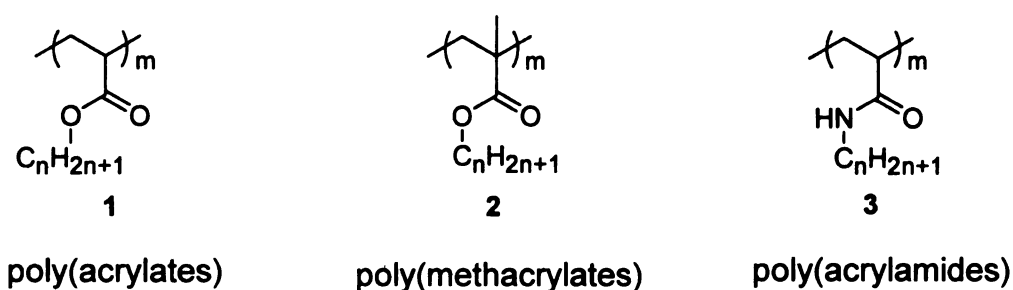


Figure 1. Chemical structures of comb-like poly(acrylates), poly(methacrylates), and poly(acrylamides)

side chain crystallites was independent of the stereoregularity of the polymer backbone.⁷⁻⁹ Furthermore, studies suggested that comb polymers form lamellar structures with amorphous regions formed by the polymer backbone and a portion of the side chains separated by sheets of side-chain crystallites. For poly(methacrylates) (2) and poly(acrylamides) (3), side chains of adjacent polymers intercalate to form the side-chain crystallites (Figure 2a),¹⁰ while in case of poly(acrylates), the crystallites are formed by the double layer packing of side chains pointing in opposite directions (Figure 2b).¹⁰ In both cases, the side chains are perpendicular to the polymer backbone. Systematic thermodynamic

studies of side-chain crystallization further concluded that, depending on the flexibility of the main-chain structure, about nine to twelve methylene groups in the side chain are in the amorphous state, and only the part of the side chain that extends beyond that limit participates in crystallization.¹⁰ These studies also showed that, in all cases, copolymers melt somewhere between the melting points of the two homopolymers. X-ray data suggested the side chains of the copolymers also packed into a hexagonal pattern.

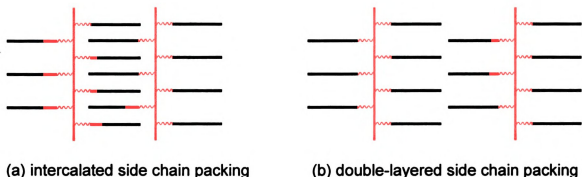


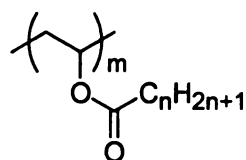
Figure 2. Possible side chain packing motifs for poly(acrylates) and poly(methacrylates) as proposed by Jordan et al.¹⁰

Because of the unique rheological properties result from the introduction of alkyl side chains, these polymers have long been used as viscosity index-improving and pour point-depressing additives in lubricating oils.¹¹⁻¹⁴ Side-chain crystallization has also lead to the formation of thermally reversible gels from dilute solutions of these comb-like polymers.¹⁵

Poly(vinyl ethers) and poly(vinyl esters)

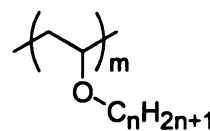
Swern and Jordan described the first side chain crystalline poly(vinyl esters) (4) as white wax-like solids.¹⁶ Later, the same team conducted a systematic

study of poly(vinyl esters) and concluded that their side chains are able to crystallize when the length of the chain exceeds twelve carbon atoms.¹⁷ However, no detailed structural data were available regarding the molecular packing. In the following years, X-ray diffraction revealed that they crystallized in hexagonal cells, regardless of the stereoregularity.¹⁸⁻²⁰ In addition, ten carbon atoms was the minimal length of side chain required for crystallization, again regardless of the stereoregularity of the backbone chains. Based on calorimetric data, Jordan *et al.* further concluded that, similar to poly(acrylates), a double-layered structure formed with only the outer part of the side chain included in the crystal lattice (**Figure 2b**).¹⁰ Although poly(vinyl alkyl ethers) (**5**) are also known to be capable of side chain crystallization, which has led to applications such as shape-memory materials,^{21,22} the structural data of this series are rather limited compared to poly(vinyl esters).



4

Poly(vinyl ester)s



5

poly(vinyl ether)s

Figure 3. Chemical structures of comb-like poly(vinyl ester)s and poly(vinyl ether)s

Poly(α -olefins), polyaldehydes, and poly(oxiranes)

A series of isotactic poly(α -olefins) (**6**) were studied by Turner-Jones using X-ray diffraction and the results lead to the conclusion that there must be at least

seven carbon atoms in the side chains for them to be crystallizable.²³ Depending on the thermal history of the sample, three different crystalline forms were observed.

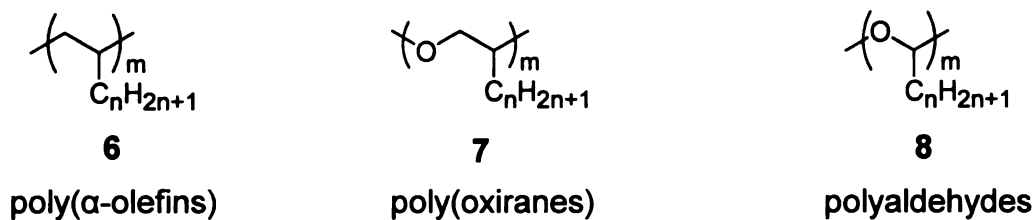


Figure 4. Chemical structures of comb-like poly(α -olefin)s, poly(oxiranes)s, and polyaldehydes

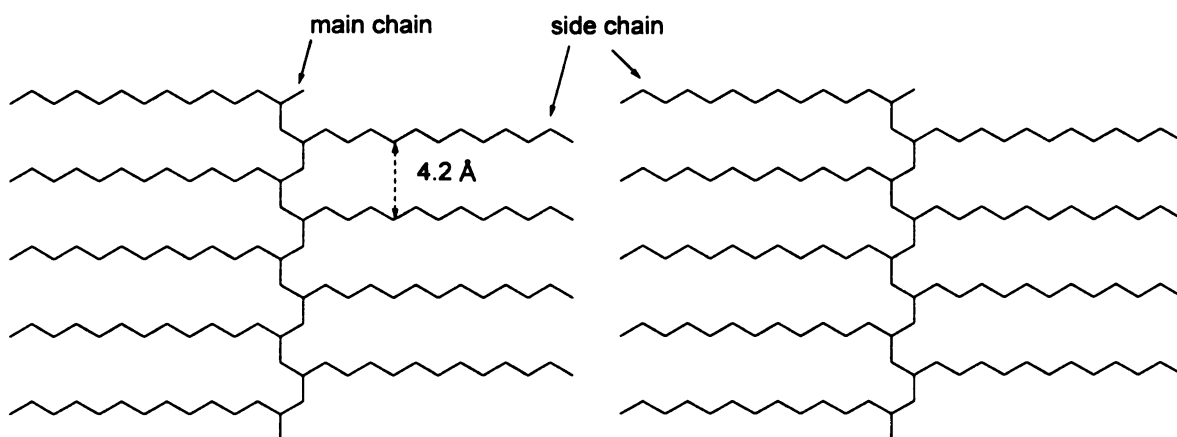


Figure 5. Packing of comb polymers with parallel main chains and fully extended side chains as proposed by Turner-Jones.²³

In a common crystalline form adopted by isotactic, side chain crystallizable polyolefins, the main chains align in planes with side chains fully extended on either side of the main chain axis and pack hexagonally (**Figure 5**). A second crystalline form is seen for polyolefins having more than twelve carbon atoms in the side chains, in which the side chains tilt $\sim 130^\circ$ relative to the axis defined by the main chain and pack in a double-layered structure. As shown in **Figure 6**,

three different side chain packing modes are possible for this crystalline form. Unlike other comb-like polymers, the isotactic backbone participates in the crystallization of the above mentioned crystalline forms. A third form was formed

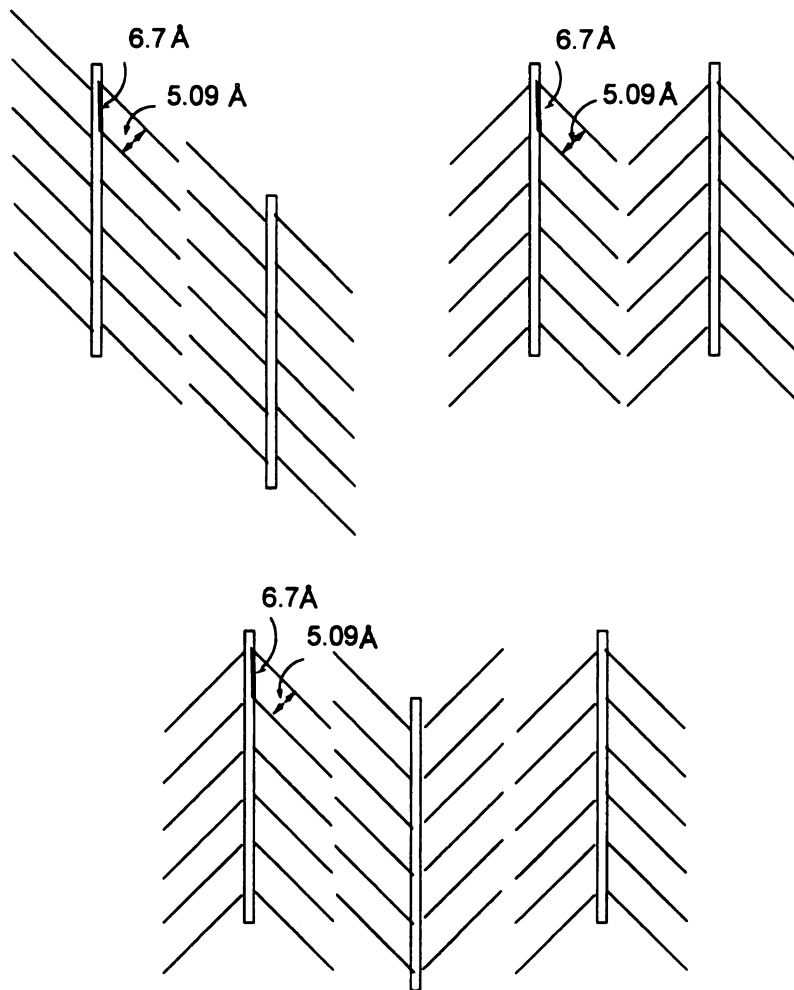


Figure 6. Possible packing arrangements for comb polymers with side chains tilted to main chain axis as proposed by Turner-Jones.²³

by efficient quenching from the melt. Only hexagonal side chain crystallites formed and no lamellar structure was observed.²⁴ Further study of isotactic polyolefins confirmed Turner-Jones's conclusions.²⁴⁻²⁷ In contrast, the structure of atactic polyolefins is characterized by highly disordered main chains and hexagonally packed side chains.²⁸ A calorimetric study of both isotactic and

atactic polyolefins carried out by Magagnini *et al.* suggested that the calorimetric properties of these comb polymers largely depend on the length of the side chains and are almost independent on the stereoregularity of the backbone.²⁸

The crystal structure of poly(oxiranes) (7) are very similar to those of poly(α -olefins). For atactic poly(octadecylethylene oxide), a single crystalline phase was observed, characterized by the efficient hexagonal packing of the side chains and main chains in regularly spaced, parallel planes perpendicular to the direction of the side chain. However, the side chains in the crystal structure of isotactic poly(octadecylethylene oxide) are oriented at 120° with respect to the plane defined by the main chain.^{29,30} The poly(oxirane) stereoregularity had a negligible influence on their enthalpies and entropies of fusion.²⁸

Vogel *et al.* proposed a supramolecular structure in which both main chain and side chains play important roles to explain the complex melting of polyaldehydes (8).³¹⁻³⁵ In this family of comb polymers, only six carbon atoms are necessary for the side chain to crystallize. The resulting polymers have two melting transitions, the lower typical of side chain crystallization and the higher due to melting of the backbone. Based on IR absorption bands, the authors concluded that the paraffinic side chains are arranged in a regular hexagonal structure within the tetragonal crystal lattice of the polymer.³² However, no detailed X-ray data have been reported for polyaldehydes.

Polystyrenes, poly(1,3-butadienes), and polyitaconates

Poly(*p*-alkyl styrenes) (9) were known as early as 1953.³⁶ For atactic polymers, thermal analysis suggested side chain crystallinity in polymers with

more than ten carbon atoms in the side chain.³⁶ The comparison between atactic and syndiotactic polystyrenes revealed that side chain crystallinity is strongly influenced by tacticity.³⁷ For example, the melting point of the side chains in atactic poly(*p-n*-dodecylstyrene) was reported to be around -30 °C,³⁸ while that of syndiotactic poly(*p-n*-dodecylstyrene) was ~90 °C.³⁷ However, there has been

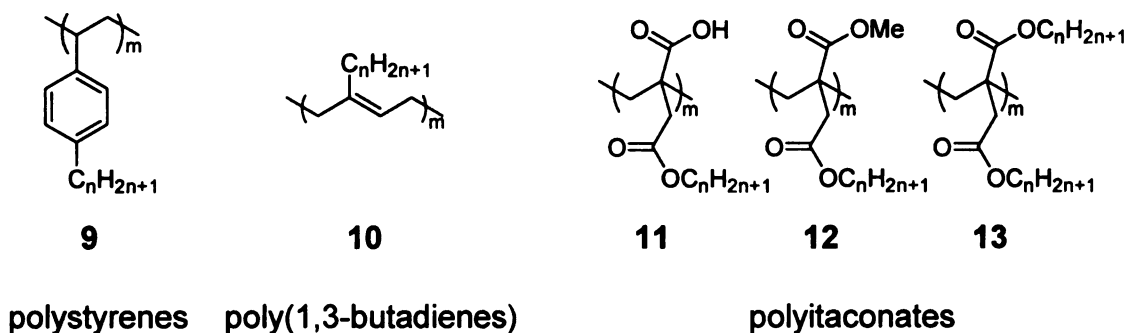


Figure 7. Chemical structures of comb-like polystyrenes, poly(1,3-butadiene)s, and polyitaconates

no detailed structural characterization for this series, resulting in incomplete information on supramolecular packing. Although thermal analysis suggest that side chain crystallization in poly(2-*n*-decyl-1,3-butadiene) is similar to polystyrenes,³⁹ no structural information is currently available for poly(1,3-butadienes) (10).

Because of their similarity to poly(alkyl acrylates) and poly(alkyl methacrylates), comb-like poly(itaconates) (11-13) have been extensively studied.⁴⁰⁻⁴⁸ When there are twelve or more carbon atoms in the side chain, the side chains of poly(mono *n*-alkyl itaconates) (11, 12) and poly(di *n*-alkyl itaconates) (13) crystallize.^{40,41,44} The crystalline side chains of poly(mono *n*-alkyl itaconates) melt at lower temperatures than the corresponding poly(di *n*-alkyl

itaconates).⁴⁴ X-ray data suggested that, like in most of the comb-like polymers, the side chains crystallized in hexagonal lattices.⁴⁴

Alkyl comb polymers with rigid backbone

Polypeptides

The alkyl comb polypeptides reported to date include poly(α ,L-aspartates) (**14**), poly(α ,L-glutamates) (**15**), poly(β ,L-aspartates) (**16**), and poly(γ -glutamates) (**17**). Their chemical structures are shown in **Figure 8**. Similar to poly((meth)acrylates), the linear alkyl side chain in these polypeptides is attached to the backbone through an ester bond. The first report on the solid state structure of comb-like poly(α -glutamates) appeared in 1978.⁴⁹ Watanabe *et al.* then systematically studied the supramolecular structure of comb-like polyglutamates by X-ray diffraction, differential scanning calorimetry (DSC), and dynamic mechanical analysis (DMA). Their data suggested that regardless of the

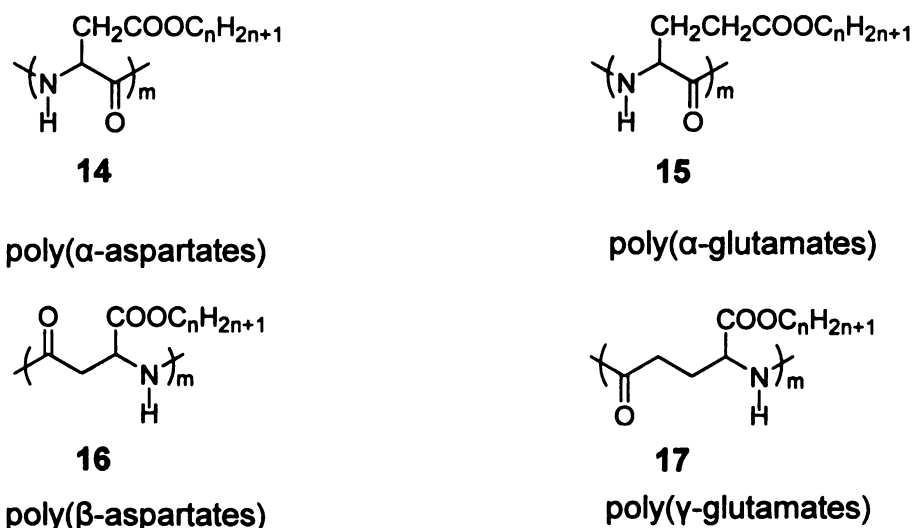


Figure 8. Chemical structures of comb-like polypeptides

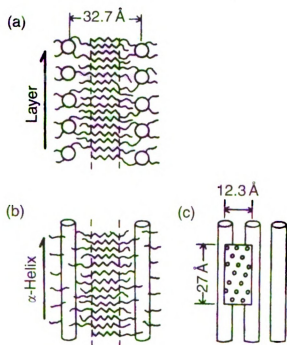


Figure 9. Model for the packing of poly(α -glutamates) at low temperatures (a) view parallel to the main chain axes; (b) view parallel to the side chain axis and perpendicular to the main chain axis; (c) view perpendicular to both the layer and the chain axis of the α -helices. (Reprinted with permission from *Macromolecules* 18:2141, 1985. Copyright 1985 American Chemical Society)

side chain length, the conformation of the main chain was an α -helix,^{50,51} and the side chain crystallized when its length exceeded ten carbon atoms. As a consequence of the side chain crystallization, the polymers formed a lamellar structure characteristic of comb-like polymers with the α -helices forced to align into sheets separated by side-chain crystallites. The X-ray data further suggested that the side chains are interdigitated and aligned perpendicular to the planes defined by the sheets of α -helices (**Figure 9**). Their conclusions were supported by dielectric measurements.⁵²

For comparison, poly(β -L-aspartates) were also systematically studied.^{53,54} This family of poly(β -peptides) are also helical and they closely follow the general behavior characteristic of poly(α -L-glutamates). The major difference is that the side chain crystallization requires at least twelve carbon atoms in the side chains instead of ten for poly(α -L-glutamates), likely due to the additional methylene spacer in the backbone. Three different phases were observed for these comb-like polypeptides as function of temperature. As schematically represented in **Figure 10**, when the temperature is below T_1 , the side chain melting temperature, the backbone helices are immobilized by the crystallized side chains. A cholesteric arrangement may form when the temperature is between T_1 and T_2 and temperature $> T_2$ can lead to the formation a nematic phase.

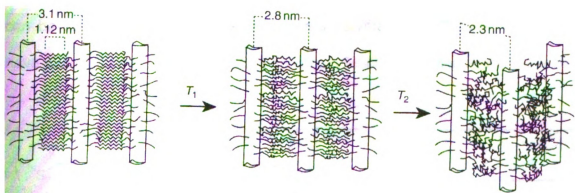


Figure 10. Schematic model illustrating the structural changes as function of temperature for side chain crystalline poly(β -aspartate)s. (Reprinted with permission from *Macromolecules* 28:5535, 1995. Copyright 1995 American Chemical Society)

Recently, comb-like poly(γ -glutamates) with different backbone stereoregularities were reported.^{55,56} Again, the layered structure characteristic of

comb-like polymers was observed regardless of the backbone stereoregularity. The additional methylene spacer in the backbone further increased the minimum side chain length for crystallization to fourteen carbon atoms and this minimum length was also independent of backbone regularity.

Poly(3-alkyl thiophene)s

Because of potential applications in light-emitting diodes, batteries, sensors, and electrochromic devices, polythiophenes have attracted a great deal of attention over the past two decades. Alkyl comb-like polythiophenes are particularly interesting because the introduction of flexible alkyl side chains leads to improved solubility, fusibility, and processability with retention of their stability and electrical conductivity.⁵⁷⁻⁶⁷ When there are twelve or more carbon atoms in the side chain, a first order transition associated with the side chain crystallization can be observed.^{59,60} Like other alkyl comb polymers, poly(3-alkyl thiophene)s have a lamellar structure, with alkyl side chains functioning as spacers between

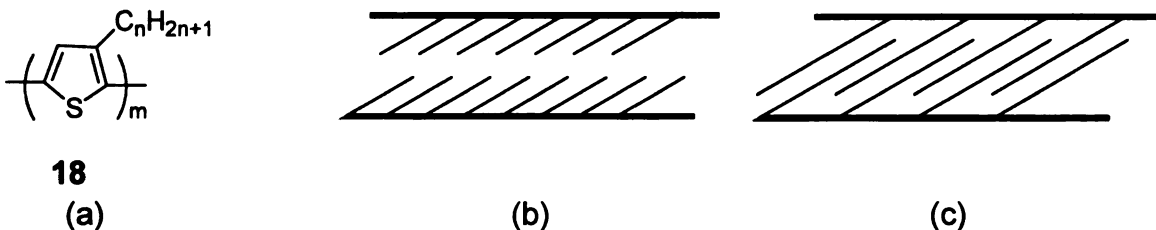


Figure 11. Chemical structure and proposed possible molecular packing of poly(3-alkyl thiophene)s

the stiff main chains. Depending on the thermal history, molecular weight, and regioregularity of the sample, the side chains can adopt several different packing

patterns. In the most common phase, the side chains are packed into a double-layered structure and are strongly tilted such that the side chains can pack into an approximately hexagonal lattice (**Figure 11b**).⁵⁸ A less common phase is characterized by the side chain interdigitation (**Figure 11c**),⁶¹ which can coexist with the double-layered phase.⁶⁵ The appearance of several other phases has also been reported, but the structural details are incomplete. Upon heating to a certain temperature range, a nematic mesophase has also been reported for polythiophenes with long alkyl side chains.^{58,61,65,67}

Stiff-chain polyesters, polyamides, and polyimides

Aromatic polyesters, polyamides, and polyimides are very attractive because of their unusual mechanical properties. However, like polythiophenes, their processability and solubility are limited by chain stiffness. The introduction of flexible alkyl side chains onto the stiff backbone has been proved to be an effective strategy for improving solubility and lowering melting temperatures.⁶⁸⁻⁸⁷ Shown in **Figure 12** and **Figure 13** are the chemical structures of these families of comb-like polymers that have been reported in the literature. The first comb-like aromatic polyester, the polyester of terephthalic acid and a 2-*n*-alkylhydroquinone (**19**), was reported by Lenz *et al.* in 1983. Its melting temperature decreased continuously with increasing side chain length, which eventually led to the appearance of liquid-crystalline phases over a conveniently accessible temperature range.⁸⁷ When the side chain length is more than twelve carbon atoms, mesophases characteristic of layered structures were observed. There also is evidence of side chain crystallization in these rigid-rod comb

polymers when the side chains are longer than twelve carbon atoms.^{68,72,73,77,78}

The detailed supramolecular packing depends on the substitution pattern in the polymer. Based on the available X-ray data, polymers that have substituents

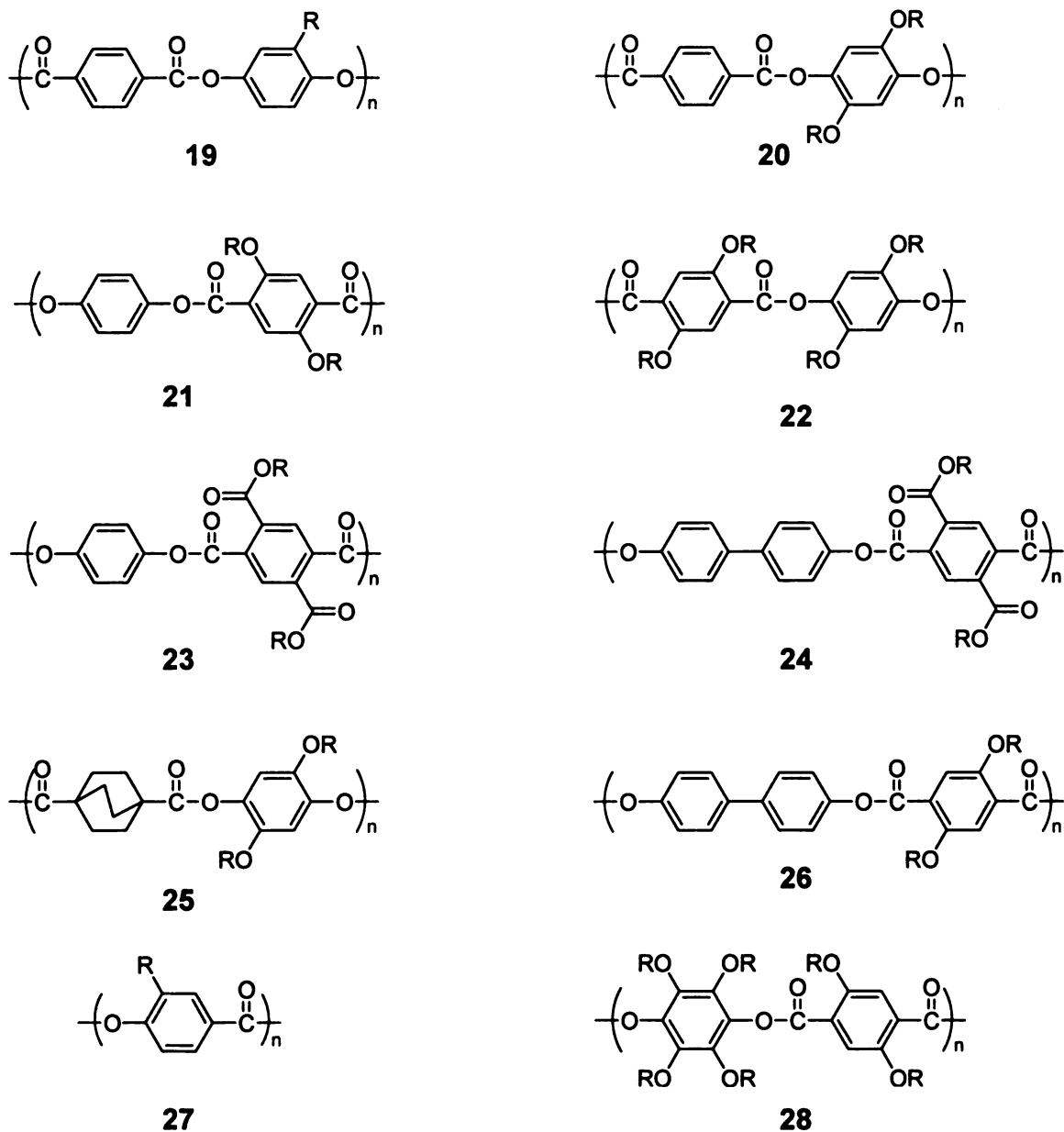


Figure 12. Chemical structures of comb-like rigid-rod polyesters, polyamides, and polyimides I (R represents linear alkyl groups)

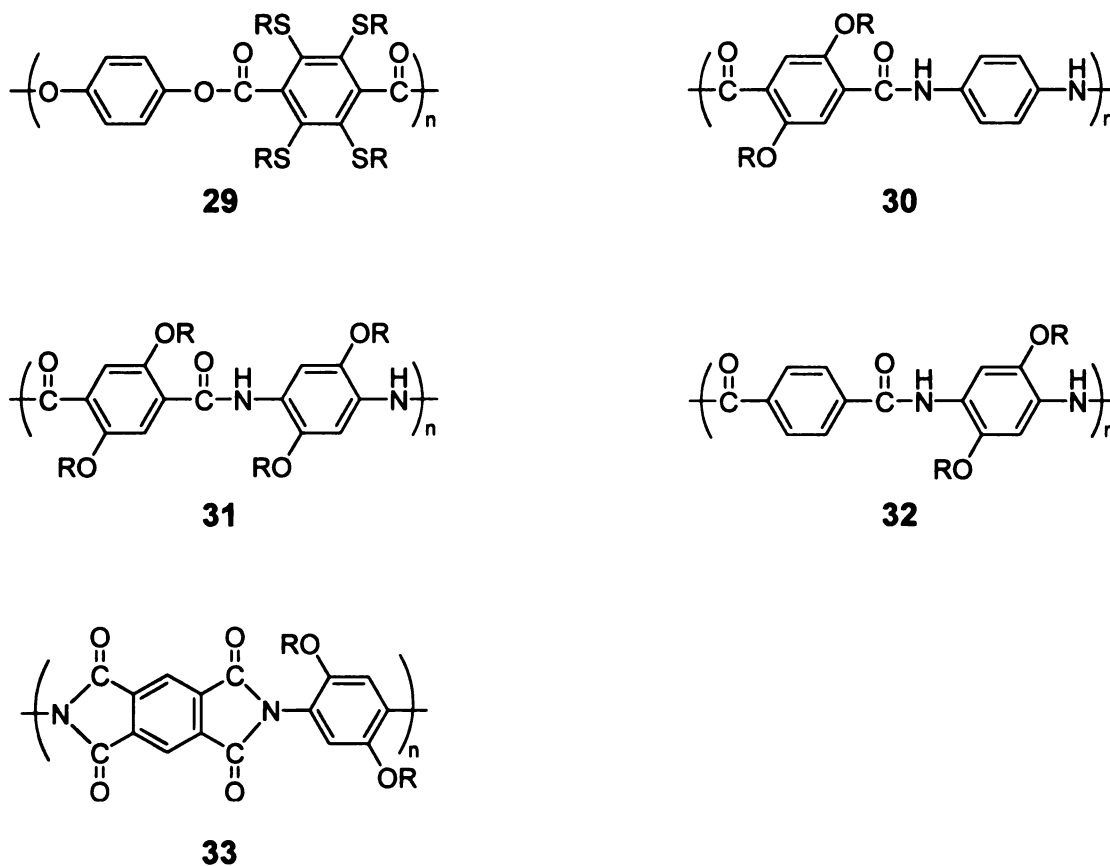


Figure 13. Chemical structures of comb-like rigid-rod polyesters, polyamides, and polyimides II (R represents linear alkyl groups)

limited to one phenyl ring in the repeat unit (20, 21, 23, 24, 25, 26, 29, 30, 32) pack into interdigitated layered structures with the side chains either perpendicular or tilted relative to the backbone plane.^{68,72,73,77,78} When both phenyl rings of the repeat unit are substituted as in case of polyamide 31 in Figure 13, a double-layer structure is formed.⁶⁸

Other stiff-chain alkyl comb polymers

There are several other stiff-chain alkyl comb polymers in addition to the examples cited above (Figure 14). Other examples include (hydroxypropyl)cellulose-based polymers (34),^{88,89} polydiacetylenes (35),⁹⁰ and

2-alkylbenzimidazole-based polymers (36).⁹¹ Like other alkyl comb polymers, both side chain crystallization and formation of a lamellar structure are observed once the side chain reaches a minimum length.

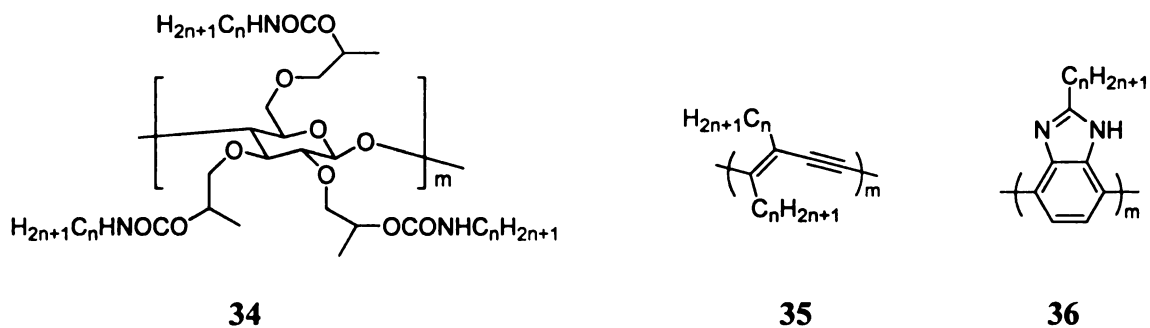


Figure 14. Chemical structures of several other alkyl comb-like polymers

PEG comb polymers

Because of its hydrophilicity, biocompatibility, and resistance to protein adsorption, poly(ethylene glycol) (PEG) based polymers have attracted a great deal of attention for industrial and biomedical applications.^{92,93} Comb-like polymers with PEG grafts are particularly interesting because these polymers can efficiently inhibit cell or protein adsorption even when the side chains are short PEG segments.^{94,95} Additionally, polymer properties can be easily tuned by changing the PEG segment length. However, the number of PEG comb polymers with well-defined structures are very limited, possibly due to the tedious synthetic procedures for the synthesis of exact length oligo(ethylene glycol)s.

Poly(vinyl ethers)

Shown in **Figure 15** are the chemical structures of well-defined PEG comb poly(vinyl ethers) terminated with either methyl or ethyl groups. Poly(vinyl ethers) with PEG pendant groups were known as early as 1950s⁹⁶ and were found to be water-soluble and show lower critical solution temperature (LCST) behavior.^{97,98} However, a systematic study of solution properties of these poly(vinyl ethers)



Figure 15. Chemical structures of PEG comb-like poly(vinyl ether)s

was not reported until 1992.⁹⁹ In their study, Kobayashi *et al.* found that LCST of poly(vinyl ethers) can be controlled either by the length of the PEG chain or the ω -alkyl group at the terminus of the chain. The LCST is also affected by the molecular weight and molecular weight distribution.⁹⁹ For the case of PEG chains terminated with an ω -methyl group (37), the LCST was 70, 82, and 100 °C for $n=1, 2,$ and $3,$ respectively. For an ω -ethyl group (38), the LCST was 20, 44, and 60 °C for $n=1, 2,$ and $3,$ respectively. The temperature range for the phase transition is only ~ 0.3 °C for polymers with narrow molecular weight distributions (PDI = 1.1) increasing to ~ 3 °C when PDI increased to ~ 3 .⁹⁹

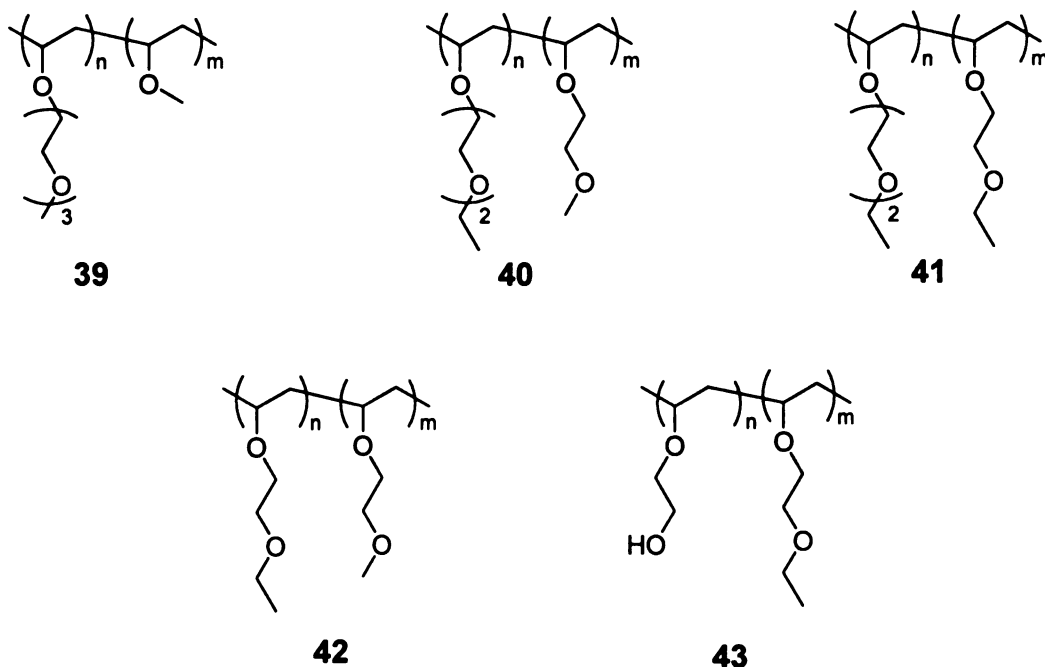


Figure 16. Chemical structures of PEG comb-like poly(vinyl ether)s block copolymers

Stimulated by the thermoresponsive properties of PEG comb poly(vinyl ethers), the block copolymers of poly(vinyl ethers) with PEG pendant groups were extensively studied during the last decade.¹⁰⁰⁻¹⁰⁸ Armes *et al.* prepared

diblock copolymers of methyl vinyl ether (MVE) and methyl triethylene glycol vinyl ether (MTEGVE) by living cationic polymerization (39).¹⁰⁸ The cloud points of poly(MVE) and poly(TTEGVE) are 8 and 83.5 °C, respectively. By simply changing the relative length of the individual blocks, the phase transition temperature of the block copolymer was tuned over the entire 18 – 80 °C range. Dynamic light scattering measurements showed that these block copolymers form micelles upon heating.

Related materials such as the block copolymer of ethyl diethylene glycol vinyl ether (EOEOVE) and methyl ethylene glycol vinyl ether (MOVE) (40), EOEOVE and ethyl ethylene glycol vinyl ether (EOVE) (41), EOVE and MOVE (42), and EOVE and ethylene glycol vinyl ether (HOVE) (43) were reported by Aoshima *et al.*^{102,104-107} The block copolymer EOEOVE₂₀₀-*b*-MOVE₄₀₀ is soluble in water at temperatures <40 °C. A 20 wt% solution of this block copolymer transformed to a transparent gel when warmed to 42-55 °C due to the phase transition of the EOEOVE₂₀₀ block. Further heating led to a clear solution and eventually polymer precipitation, because of the phase transition associated with MOVE₄₀₀ block. These materials were termed “double thermosensitive” materials.^{104,107} Further studies of EOEOVE-*b*-EOVE and MOVE-*b*-EOVE revealed similar phase transition behavior, and that the gelation temperature is determined by the phase transition temperature of the less hydrophilic block, which is easily tunable.^[107] In the case of EOVE-*b*-HOVE block copolymers, only a gelation temperature was observed above the LCST of the EOVE block because HOVE block is soluble in water over the entire temperature range.^{102,105,106}

Poly(methacrylates)

Polymethacrylates with pendant PEG groups have long been used as the polymeric component of polymer electrolytes.¹⁰⁹⁻¹¹² Smid *et al.* reported that the cloud points of polymethacrylates with an average of 4, 8, and 22 ethylene oxide



Figure 17. Chemical structures of comb-like PEG poly(methacrylate)s

repeat units in the side chain were 54.5, 83.5, and 102 °C respectively.¹¹³ However, the PEG chains of the oligo(ethylene glycol) methacrylates were polydisperse with a distribution of side chain length. The first linear water soluble PEG comb polymethacrylates with well-defined structures and at least two ethylene glycol units in the side chain (**44**) were not reported until 2003. Ishizone and coworkers synthesized poly(diethylene glycol methacrylate) and poly(triethylene glycol methacrylate) using living anionic polymerization.¹¹⁴ Both polymers were readily soluble in water at normal temperatures. The same group later reported the living anionic polymerization of diethylene glycol monomethyl ether methacrylate (PDEGMMA) and triethylene glycol monomethyl ether methacrylate (PTEGMMA) (**45**).¹¹⁵ Like the PEG comb poly(vinyl ethers), PDEGMMA and PTEGMMA showed very sharp and reversible phase transitions

at 26 and 52 °C respectively. Employing the thermoresponsive properties of PDEGMMA and PTEGMMA, Zhao *et al.* developed thermoresponsive hairy nanoparticles by using surface-initiated ATRP to grow PDEGMMA and PTEGMMA brushes from initiator-functionalized silica nanoparticles.¹¹⁶ Compared to analogous polymer solutions, the transition temperatures of polymer brushes were lower and the temperature range broader.

Polystyrenes

Like PEG comb polymethacrylates, polystyrenes with pendant PEG groups have been used in phase transfer catalysis¹¹⁷⁻¹¹⁹ and as polymer electrolytes.¹²⁰ As part of a study of their cation and anion binding properties, Smid *et al.* synthesized the first well-defined PEG comb polystyrenes with either one or two pendant PEG groups in each repeat unit.¹²¹ Some of these polymers strongly bound organic solutes such as picrate anions in aqueous solution. These polymers were reported to exhibit inverse temperature solubility in water but no detailed solution properties were reported at that time.¹²¹ Recently, Zhao *et al.*

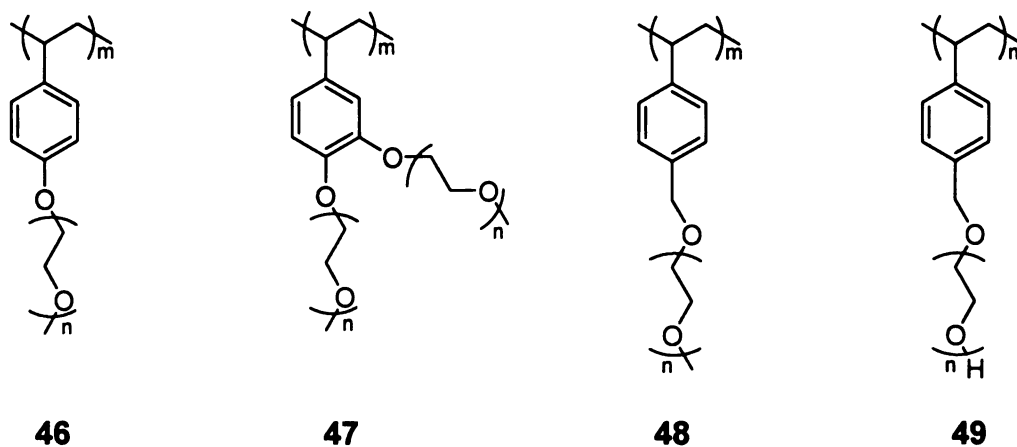


Figure 18. Chemical structure of comb-like PEG polystyrenes

reported the detailed aqueous solution properties of PEG comb polystyrenes synthesized by living radical polymerization.¹²² The reported polymers had three, four, and five ethylene oxide units in the pendant PEG group and the LCST for these polymers were 13, 39, and 55 °C respectively. They also showed that the cloud point of block copolymers can be easily tuned by changing the polymer composition, and that the experimental data agree well with theoretically calculated values.

PEG comb polystyrenes also are promising materials for applications in biotechnology. Results from the Sommerdijk group proved the biocompatibility of polystyrenes with pendant tetra(ethylene glycol) groups as well as its effectiveness in tuning cell proliferation rate, and suggested its potential application as a protective coating for *in vivo* sensors.⁹⁵ Through surface initiated living radical polymerization, Ober and coworkers reported PEG comb polystyrene brushes grafted to SiO_x surface.⁹⁴ This modified surface inhibited protein and cell adhesion better than surface assemblies with the same PEG length, suggesting potential applications in the fabrication of biological micro- and nanodevices.

PEG/Alkyl comb polymers

Because of a potentially broad range of applications, the synthesis and characterization of amphiphilic polymers has been one of the most popular research areas. Most amphiphilic synthetic polymers are block copolymers which undergo interesting self-assembly processes. A relatively new class of amphiphilic polymers is comb polymers with hydrophilic PEG groups and hydrophobic alkyl groups on the same polymer backbone. Their structure suggests interesting possibilities for self-assembly. However, only a few well-defined structures have been reported so far. McCullough *et al.* reported the

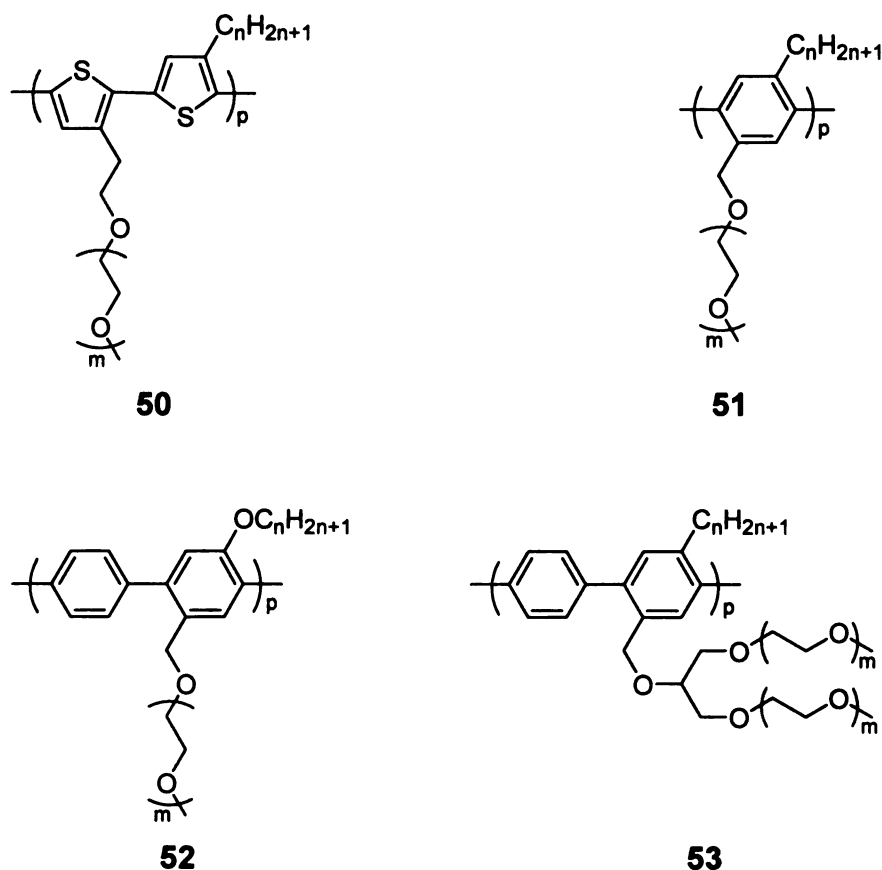
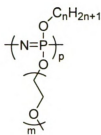


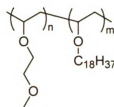
Figure 19. Chemical structures of PEG/alkyl comb polymers with well-defined structures

synthesis and self-assembly of regioregular, amphiphilic polythiophenes (**50**).¹²³ By using a self-assembly approach, ultrathin films of amphiphilic polythiophene were manipulated and processed on the nano- and micrometer scales. Three melting temperatures, assigned to the melting of tetraethylene glycol side chains (~5 °C), melting of dodecyl side chains (~55 °C), and melting of the backbone (~120 °C) were observed for amphiphilic polythiophenes having dodecyl and tetraethylene glycol monomethyl ether as substituents.¹²⁴ Amphiphilic poly(*p*-phenylene), with one linear alkyl side chain and one PEG side chain per repeat unit (**51**), self-organized into fibrous aggregates in micellar surfactant solutions.^{125,126} The synthesis of other PEG/alkyl-substituted amphiphilic polyphenylenes (**52** and **53**) was recently reported, but the bulk and solution properties of these polymers have not yet been studied.^{127,128}

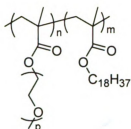
In addition to the well-defined amphiphilic comb polymers described above, amphiphilic combs with less well-defined structures have also been the topic of several recent publications. Allcock *et al.* synthesized poly(organophosphazenes) having roughly an equimolar mixture of PEG and alkyl groups (**54**).¹²⁹ With nine or more carbon atoms in the linear alkyl group, the polyphosphazene side chains crystallized, similar to the properties of alkyl comb polymers. Side chain crystallization in mixed-substituent comb polymers was exploited to prepare stimuli-responsive reversible physical networks. Reversible physical gels were obtained upon cooling aqueous solutions of poly(vinyl ether) (**55**) shown in **Figure 20** due to alkyl side chain crystallization.^{130,131} The copolymerization of poly(ethylene glycol) methyl ether methacrylate (PEOMA) with octadecyl



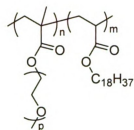
54



55



56



57

Figure 20. Chemical structures of PEG/alkyl comb polymers with ill-defined structures

methacrylate or acrylate (ODMA, ODA) also leads to amphiphilic comb polymers (56 and 57).¹³² Both the PEG and alkyl side chains are crystallizable. X-ray data suggests that the alkyl side chains in the copolymers are hexagonally packed, and that the PEG side chains are segregated from alkyl side chains and assembled on one side of the backbone. In the proposed structure, PEG side chains pack into a double-layer structure as shown in (Figure 21).

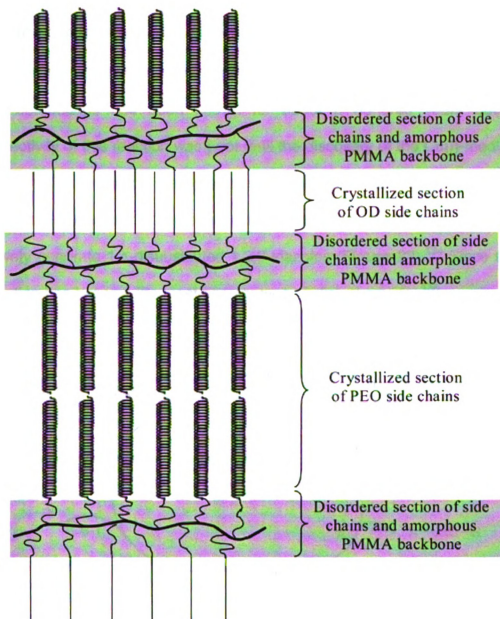


Figure 21. A proposed model for a hypothetical bilayer structure formed by the graft copolymers poly(PEOMA-*ran*-ODMA). (Reprinted with permission from Neugebauer D. *et al. Macromolecules* 39:584, 2006. Copyright 2006 American Chemical Society)

Application of click chemistry in polymer synthesis and functionalization

The Huisgen 1,3-dipolar cycloaddition of azides and terminal alkynes to form triazole compounds has been known for about a hundred years but the regioselectivity of this reaction was poor until the discovery of the Cu(I)-mediated variant.^{133,134} This reaction was proposed to start with the formation of Cu(I) acetylide, and according to theoretical calculations, follow a stepwise pathway to exclusively generate 1,4-disubstituted 1,2,3-triazoles (Figure 22).¹³⁴ Since then, this reaction has become the most popular type of click chemistry.¹³⁵

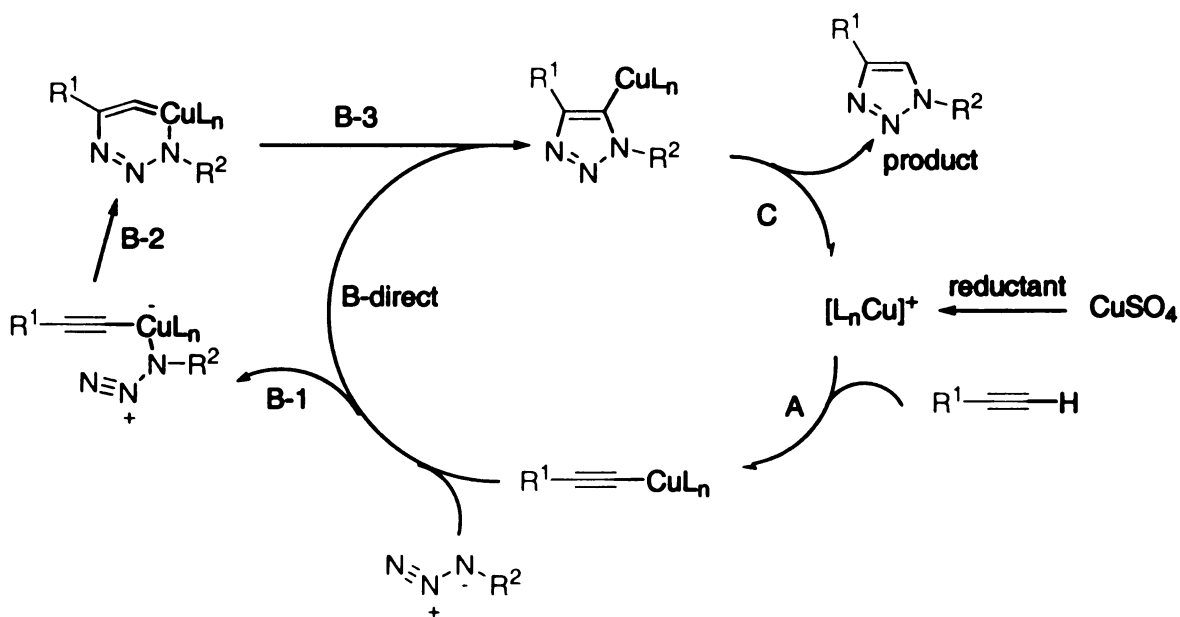
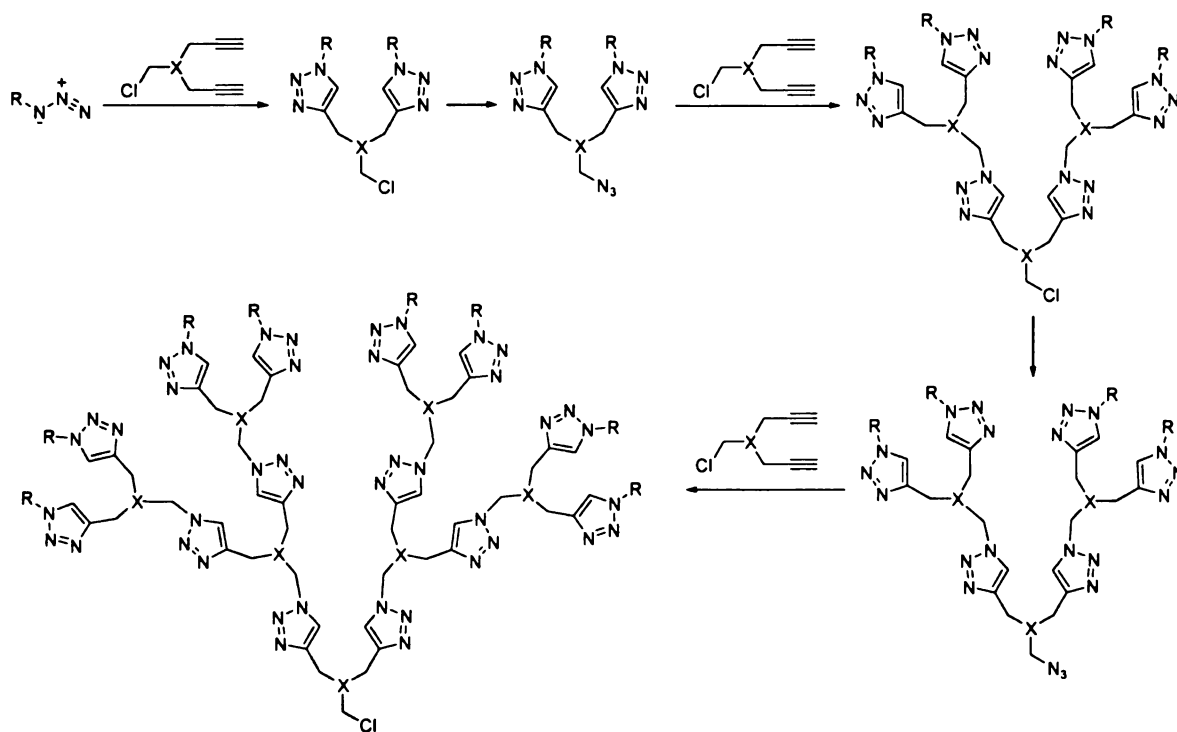


Figure 22. Mechanism of click chemistry proposed by Sharpless et al.¹³⁴

Because of its high selectivity, near-perfect reliability, nearly quantitative yields, and tolerance to a wide scope of functional groups and reaction conditions, click chemistry has been used as the key step in the synthesis or



Scheme 1. Convergent approach to triazole dendrimers by Hawker et al.¹³⁶

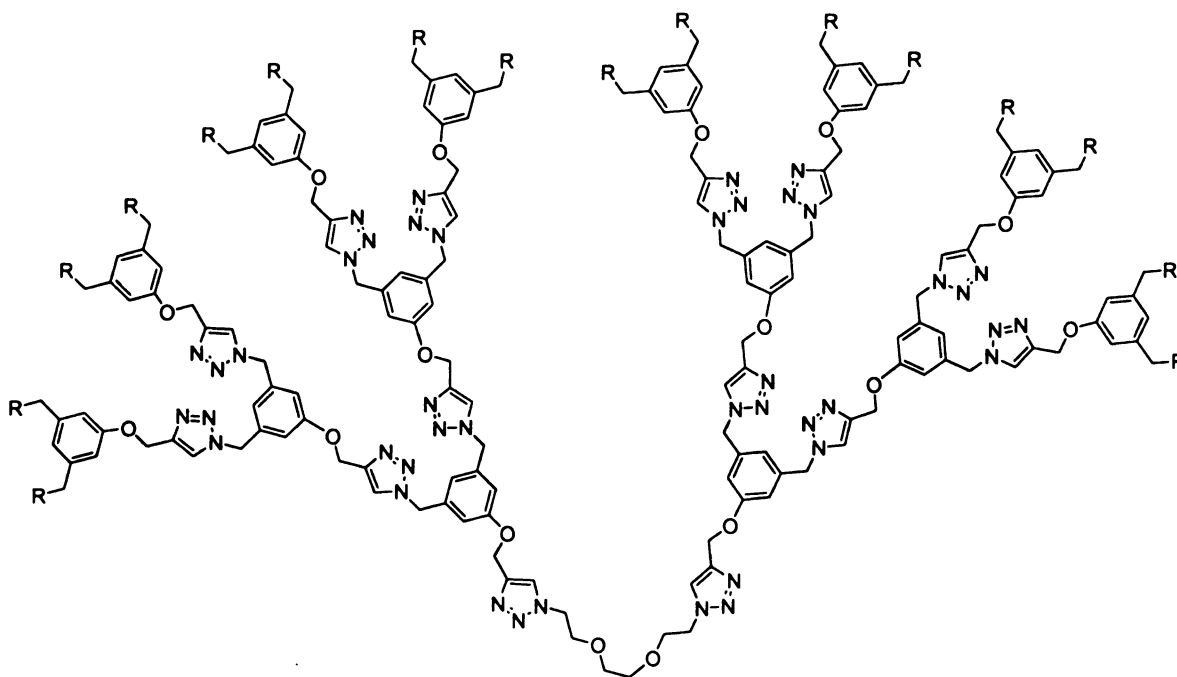
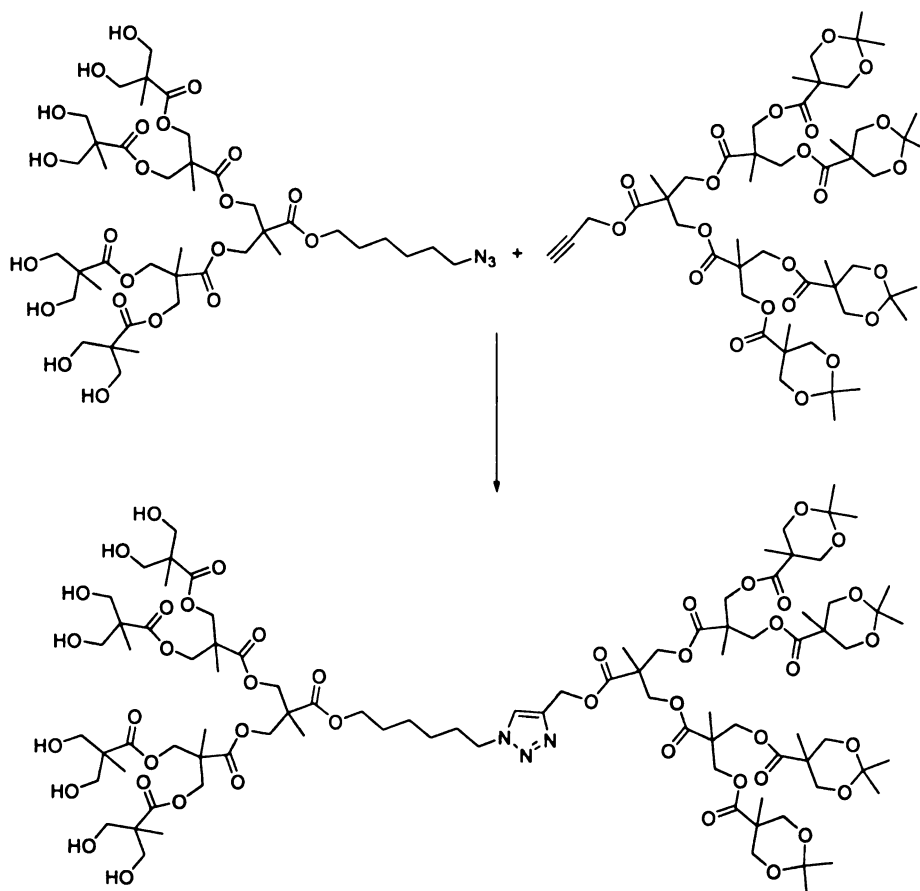


Figure 23. Structure of a divergent dendrimer synthesized by Hawker and Wooley et al.¹³⁷



Scheme 2. Synthesis of an amphiphilic dendrimer (Fokin, Sharpless et al.)¹³⁸

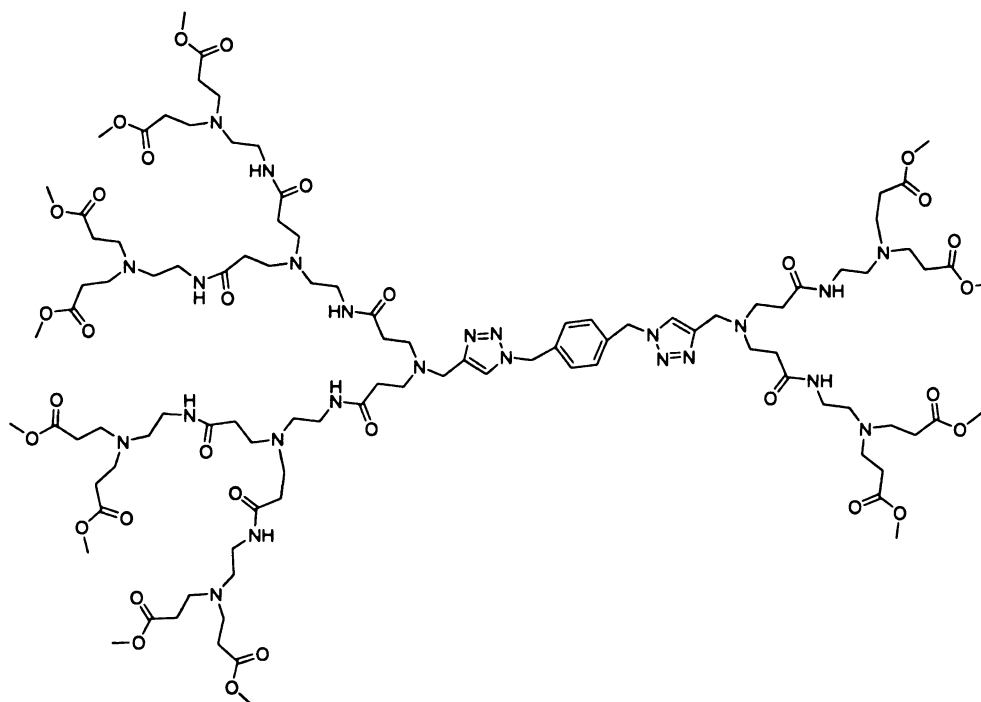
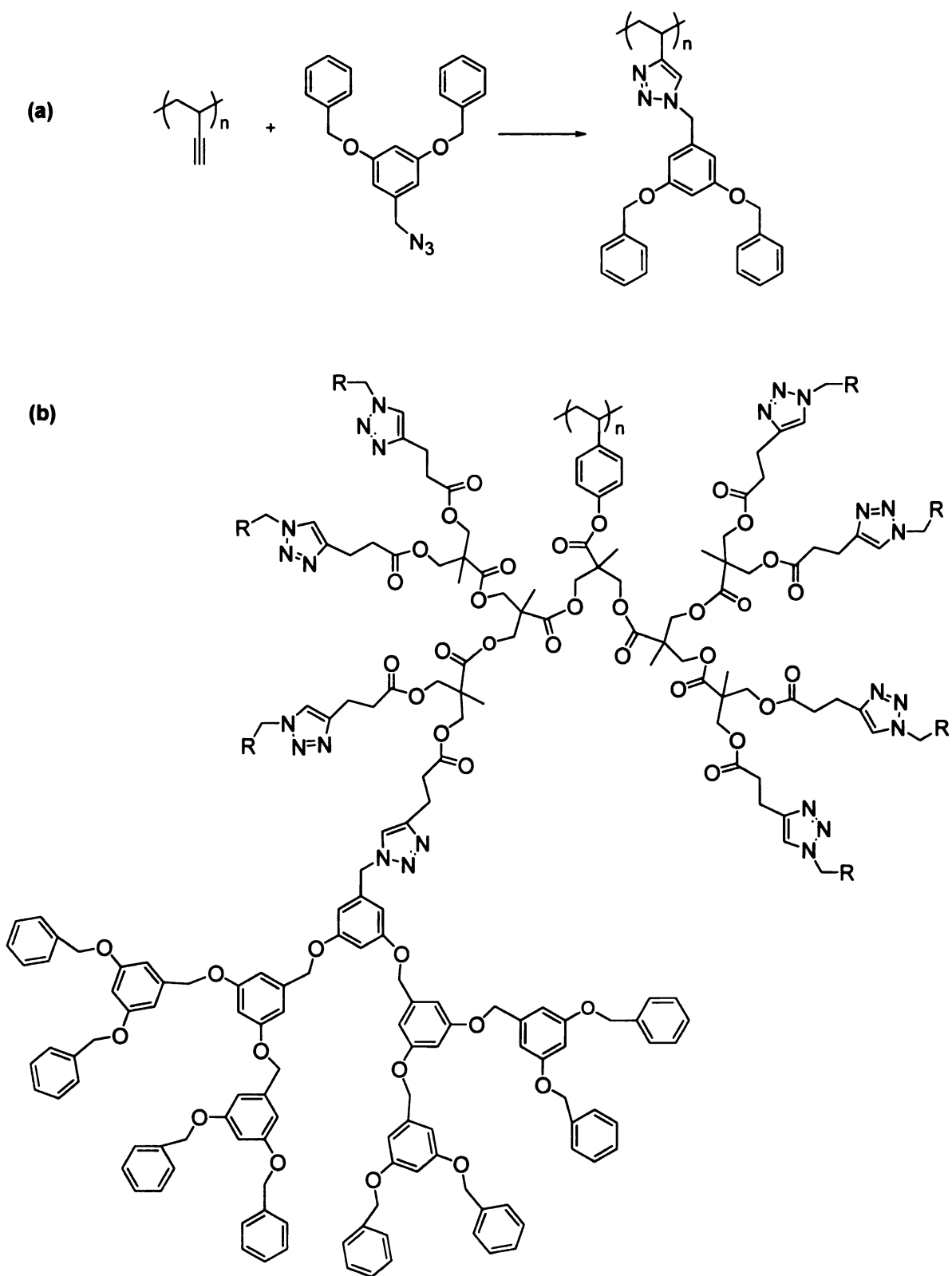


Figure 24. Structure of an unsymmetrical dendrimer synthesized by Lee et al.¹³⁹

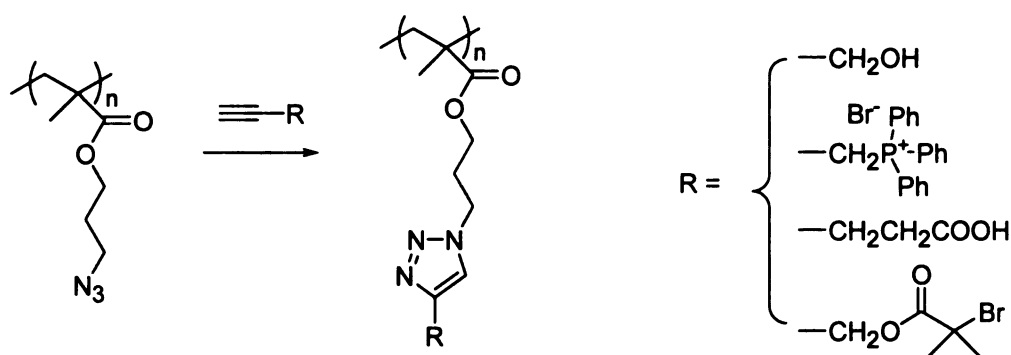
same strategy has been successfully utilized to synthesize unsymmetrical dendrimers such as those shown in **Figure 24**.¹³⁹

In addition to the synthesis of dendrimers, click chemistry is also very useful for the synthesis of other types of polymers. As shown in **Scheme 3a**, the click coupling of telechelic polystyrene prepared by ATRP yielded linear polystyrene containing ester bonds in the backbone¹⁴⁰ which renders the polymer partially biodegradable. A similar strategy is a versatile approach for the synthesis of various block copolymers from building block precursors prepared by ATRP (**Scheme 3b**).¹⁴¹

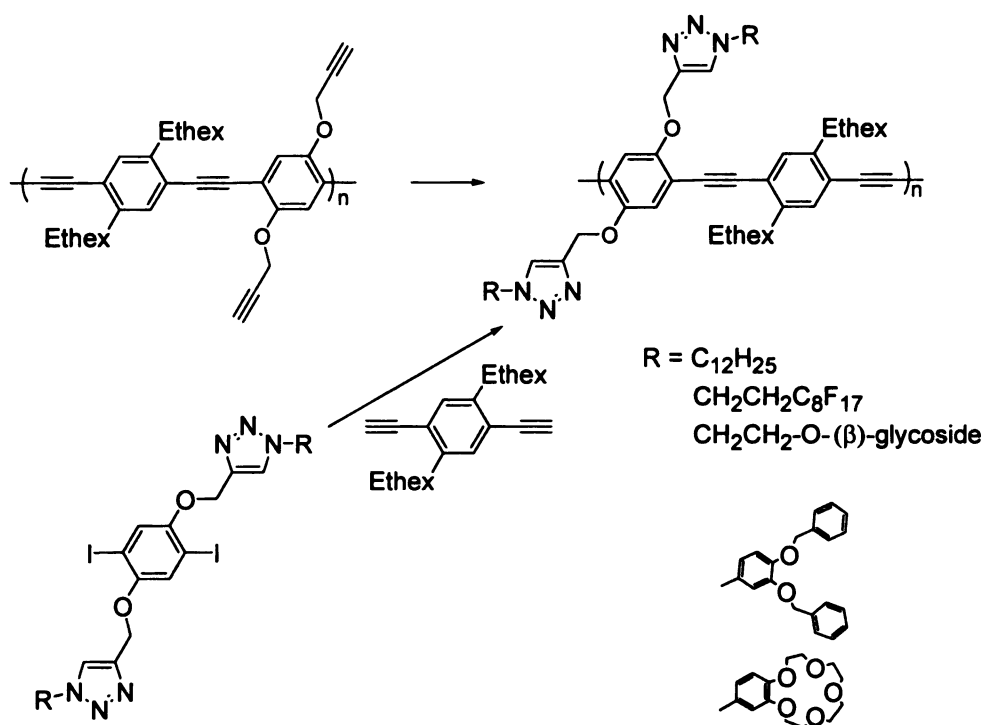
The advantages of click chemistry also provided polymer chemists with a powerful tool for attaching functional pendant groups onto various polymer backbones. Fréchet *et al.* reported the quantitative anchoring of dendrons onto the poly(vinylacetylene) backbone,¹⁴² fully covering the polymer backbone with Fréchet-type dendrons up to G3, and yielding dendronized linear polymers for nanoscale applications (**Scheme 4a**). In a related example, they started with acetylene functionalized bis(hydroxymethyl)propionic acid dendrons anchored to a linear poly(*p*-hydroxystyrene), and then used click chemistry to further elaborate the structure with Fréchet-type benzyl ether dendrons.¹⁴³ The resulting structure has the microstructure of a radial dendritic diblock copolymer and is shown in **Scheme 4b**, where the R groups correspond to benzyl ether dendrons. Matyjaszewski used click chemistry to introduce different side groups to poly(3-azidopropyl methacrylate), resulting in poly(methacrylates) with high degrees of functionalization (**Scheme 5**).¹⁴⁴ Functional poly(*p*-phenylene ethynylene)s were



Scheme 4. Synthesis and structure of dendronized linear polymers (Fréchet et al.)^{142,143}

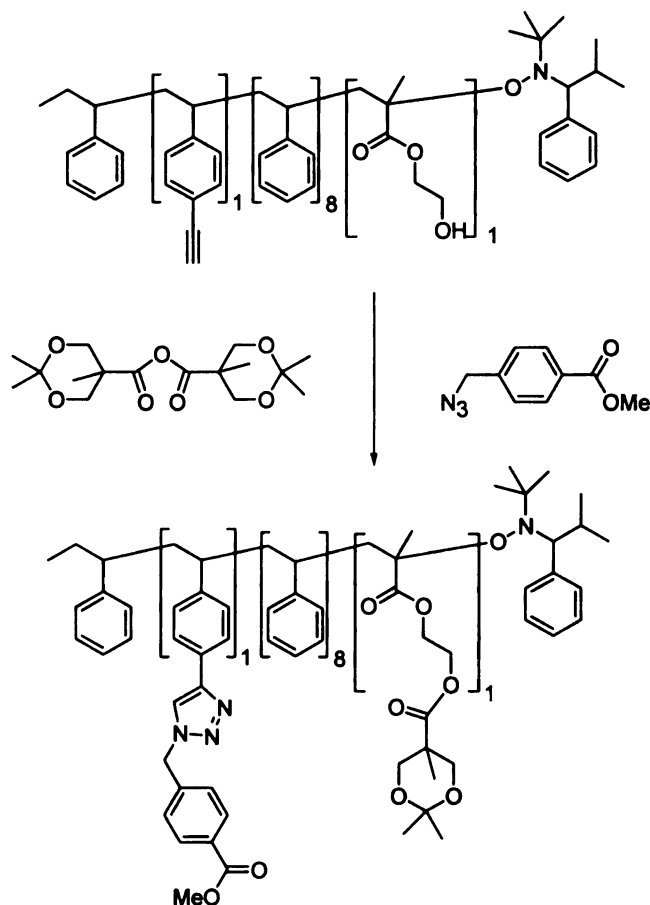


Scheme 5. Click functionalization of polymethacrylates¹⁴⁴



Scheme 6. Synthesis of functional poly(*p*-phenyleneethynylene)s.¹⁴⁵

synthesized by using click chemistry to introduce the side groups before and after polymerization to the conjugated polymer backbones (**Scheme 6**).¹⁴⁵ The high yield and specificity of click chemistry is compatible with the simultaneous introduction of various functional groups using other synthetic methods. For

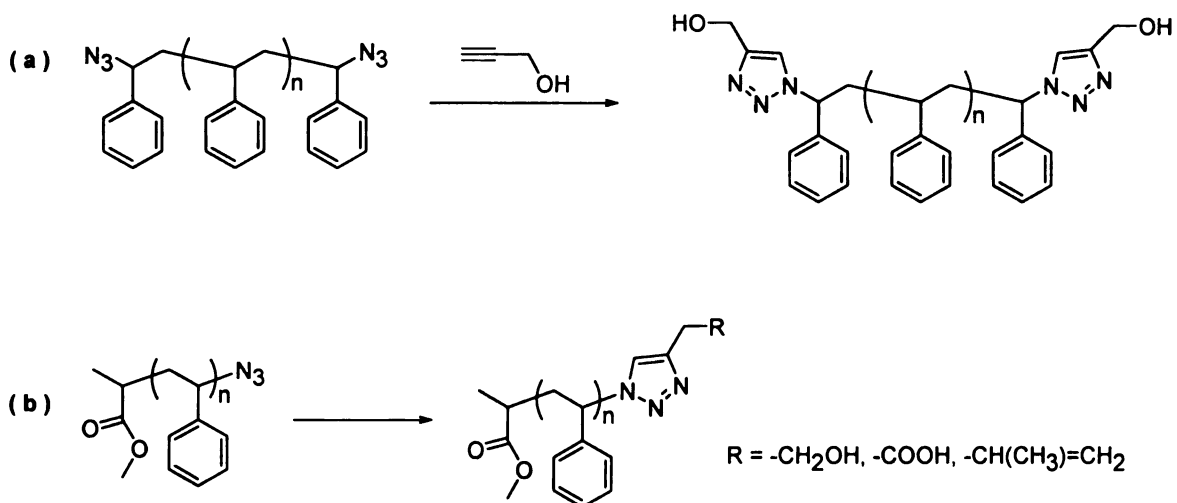


Scheme 7. Simultaneous click functionalization of terpolymer.¹⁴⁶

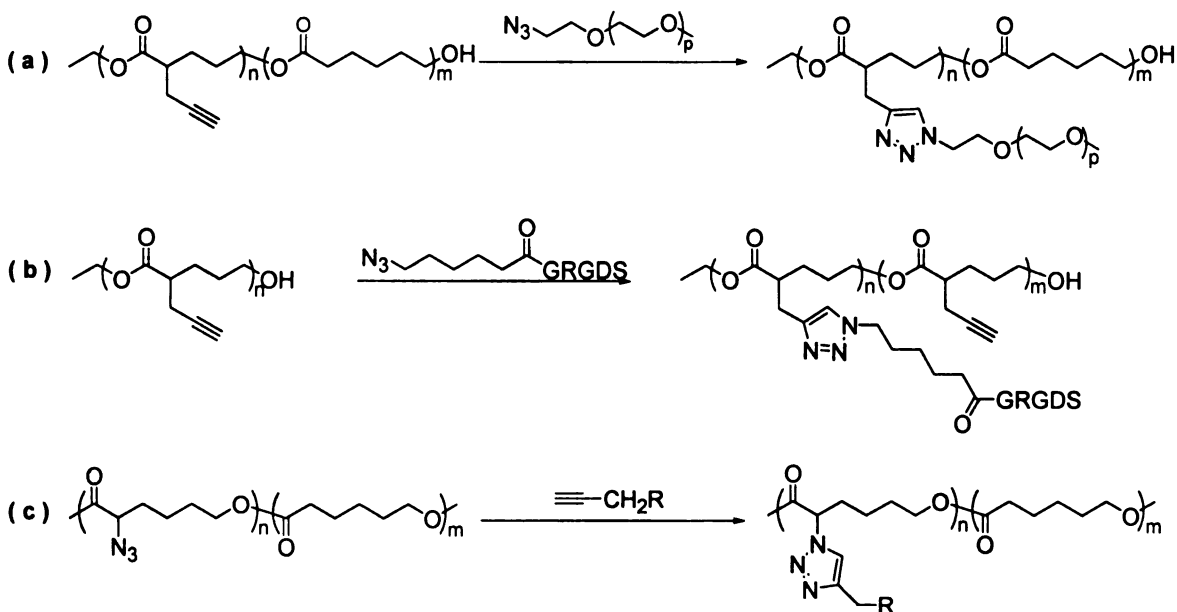
example, an 8:1:1 terpolymer of styrene, 4-(ethynyl)styrene, and 2-(hydroxyethyl)methacrylate was functionalized by combining click chemistry and alcoholysis of an anhydride to yield a difunctional polymer in a one-pot reaction (**Scheme 7**).¹⁴⁶

Click chemistry also is effective in the preparation of chain-end functional polymers (**Scheme 8**). An α,ω -dihydroxypolystyrene was prepared by combining click chemistry with a difunctional ATRP initiator for styrene polymerization.¹⁴⁷ Using similar strategies, olefins, and carboxyl groups were also attached to polystyrene chain ends.¹⁴⁸ Recently, Finn et al. extended the chain end click

functionalization methodology to the preparation of protein-glycopolymer conjugates, yielding useful materials for biotechnology.¹⁴⁹



Scheme 8. Preparation of chain-end functional polymers by click chemistry.^{147,148}

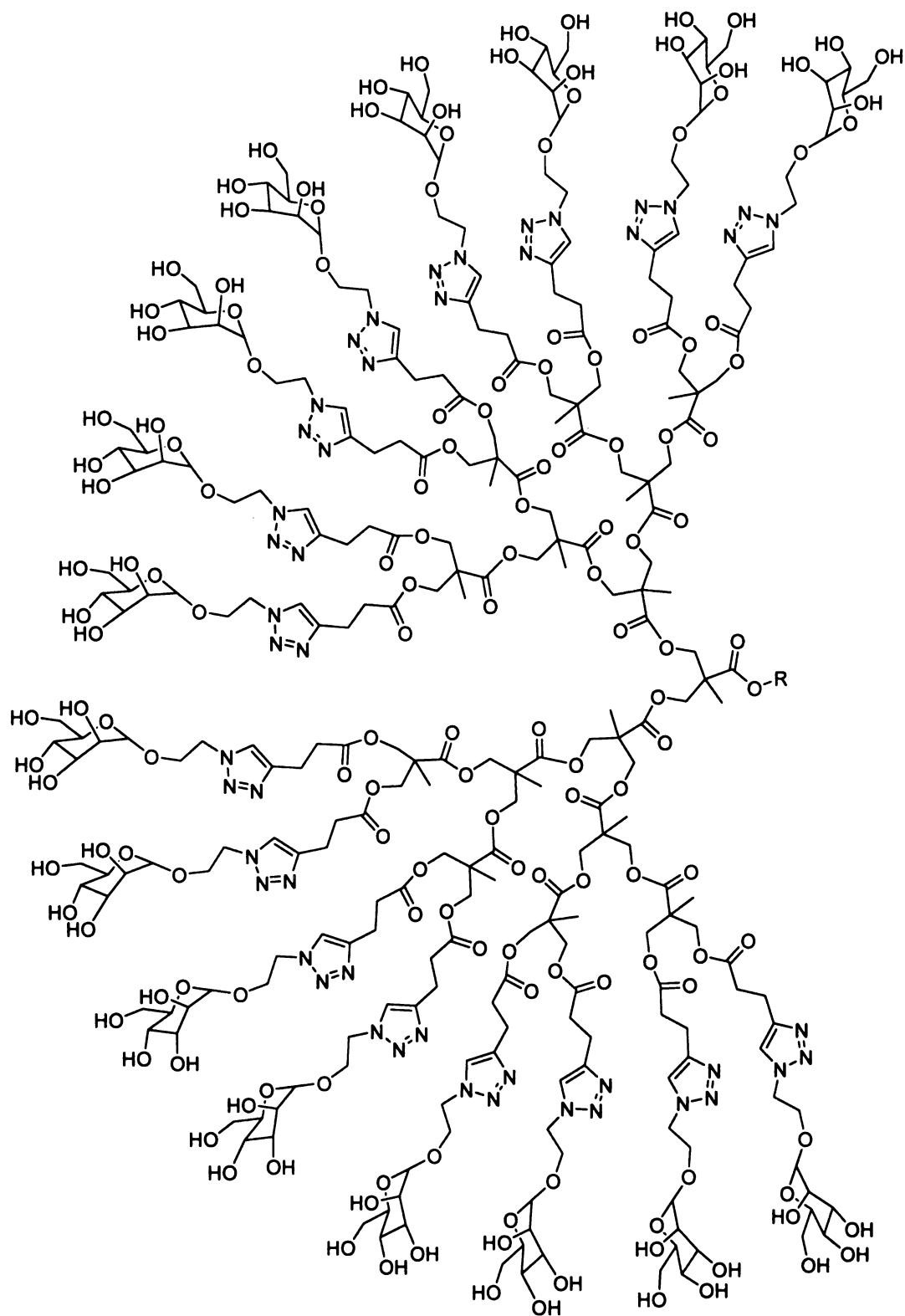


Scheme 9. Click functionalization of aliphatic polyesters.^{150,151}

Due to the chemical reactivity of the backbone in aliphatic polyesters, post-polymerization modification of polycaprolactones and polylactides is synthetically challenging because most of current synthetic transformations require conditions that cause degradation. Click chemistry is a general and efficient approach to aliphatic polyester functionalization, allowing introduction of functional groups such as PEG, peptide, tertiary amines, and ammonium salts onto a single polyester backbone without significant backbone degradation (**Scheme 9**).^{150,151}

Despite of the demanding requirements needed for dendrimer functionalization, click chemistry provides a versatile and efficient approach for introducing carbohydrates,^{138,152} peptides,¹⁵³ azo-dyes, and other functional moieties¹⁵⁴ on acetylene or azide functionalized dendrimers. Shown in **Scheme 10** is the structure of a mannose-functionalized poly(2,2-bis(hydroxymethyl)propionic acid) dendrimer, which due to the functional group tolerance of click chemistry, required no protection and deprotection steps.

Click chemistry also has played important role in the synthesis and modification of cross-linked polymeric materials. One such example is cross-linked polymeric adhesives synthesized from polyvalent azide and alkyne building blocks, that owe their adhesiveness to the strong affinity of triazoles for metal ions and surfaces.¹⁵⁵ More recently examples from Hawker and Wooley groups showed shell cross-linked nanoparticles can be generated from the reaction between alkynyl shell-functionalized block copolymer micelles and polyvalent azides. The cross-linker provided sites for chemical modification and further attachment of biologically important moieties to nanoparticles.¹⁵⁶



Scheme 10. Structure of a mannose-functionalized dendrimer.¹⁵²

Furthermore, the selective introduction of click-reactive groups in either the hydrophobic or hydrophilic domains of amphiphilic core-shell nanomaterials enabled regioselective functionalization within nanostructures.¹⁵⁷

Chapter 2 Alkyl Comb Polylactides

Introduction

The physical properties of polymers are dramatically altered when short chains are grafted to the polymer backbone. Comb polymers, the most studied member of this family, typically have one chain attached to the polymer per repeat unit and are readily available by the polymerization of macromonomers or from elaboration of acrylates, methacrylates or similar monomers.¹ More recently, the advent of controlled radical polymerizations led to numerous examples where comb polymers were synthesized by initiating polymerization from the side chains of polymers.¹⁵⁸⁻¹⁶³ One reason for the extensive interest in comb polymers is that the nature of the chains attached to the polymer backbone leads to dramatically different rheological properties. For example, comb polymethacrylates that have linear alkyl chains as the teeth tend to have lower melt and solution viscosities as well as decreased glass transition temperatures due to screening of backbone chain-chain interactions by the teeth.¹⁶⁴⁻¹⁶⁶ These same polymers may crystallize if the alkyl chain is sufficiently long.¹⁰ An important early application of comb polymers was to decrease the low temperature viscosity of motor oils,^{164,167} and more recently, comb polymers have been examined for many applications including ionic conductors,^{168,169} membranes for separations,¹⁷⁰ rendering rigid polymers soluble, and orienting macromolecules.^{50,57,75,171}

We are interested in preparing derivatives of polylactide where the methyl group in the polylactide structure is substituted or replaced to provide a polymer that has properties different from those that can be obtained from polylactide itself. Previous approaches to modifying the physical properties of polylactides include copolymerization,¹⁷² the preparation of block copolymers,^{173,174} and the manipulation of the polylactide stereochemistry.¹⁷⁵ In the context of the comb polymers studied to date, we should be able to realize analogous changes in physical properties in polylactide combs while retaining the degradability of the polylactide backbone. Our initial target is the preparation of a polylactide comb with long chain alkyl groups as the teeth. The degradability of polylactide plus the structural analogy of a comb with long chain alkyl teeth to biological membranes suggests potential applications in tissue engineering. In addition, the tendency of combs having linear alkyl chains to crystallize suggests a strategy for achieving crystallinity in polylactides that is independent of the stereochemistry of the backbone. Since the melting points in known alkyl combs typically range from ~30 - ~70 °C, it may be possible to design novel materials for drug delivery applications that exhibit significant changes in permeability within the physiologically relevant range of temperatures.

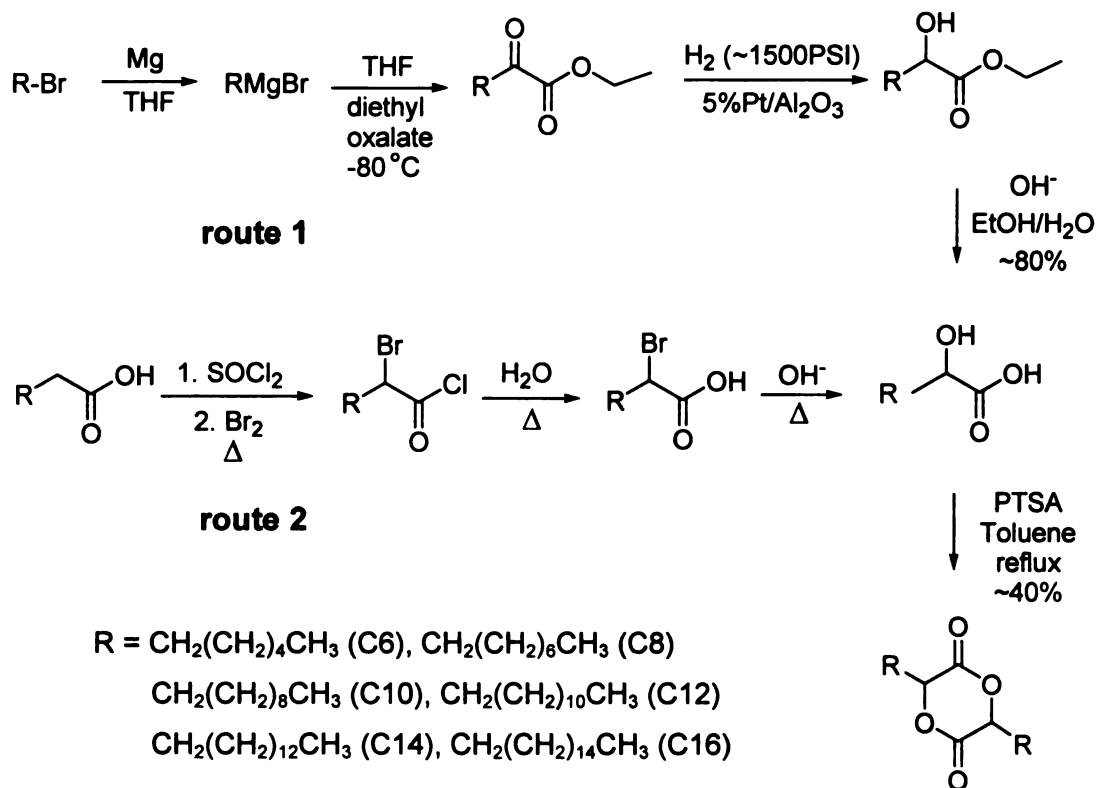
Since lactic acid derivatives are structural homologues of lactic acid, much of the chemistry developed for the preparation of polylactides is applicable to substituted lactides. We previously reported several substituted polylactides¹⁷⁶⁻¹⁷⁸ and as a further example of this approach, we describe in this chapter the preparation and characterization of comb-like polylactides. Our synthetic

approach to the α -hydroxy acids needed in the synthesis of comb poly lactides is based on the reaction of alkyl Grignards with diethyl oxalate. While not “green”, this approach enables preparation of quantities of materials suitable for investigating the properties of these new polymers. We note that the α -hydroxy acids also are available by α -hydroxylation of long chain fatty acids obtained from naturally occurring fats and oils.

Results and Discussion

Monomer Synthesis

Scheme 11 shows the synthetic routes to the six monomers described in this chapter. We refer to the monomers as glycolides rather than lactide derivatives



Scheme 11. Synthesis of alkyl-substituted glycolide monomers

since common names based on glycolide as the base structure clearly describe the length of the alkyl chain. Two synthetic approaches to substituted glycolide monomers were employed. In **route 1**, the reaction of alkyl Grignard reagents with diethyl oxalate at low temperature provided the corresponding α -keto esters.¹⁷⁹ The crude products were obtained in >90% yields, with no detectable contamination from addition of a second Grignard equivalent to the substrate. Catalytic hydrogenation of the crude keto ester at 1500 psig using Pt on carbon yielded the α -hydroxy ester, but since purification of the ester proved difficult, the crude α -hydroxy ester was hydrolyzed and isolated as the α -hydroxy acid. Crystallization of the acid three times from hexane gave white crystals in an overall yield of 68-84% from diethyl oxalate. In **route 2**, the reaction of fatty acids with thionyl chloride and bromine generated the corresponding α -bromoacyl chlorides.¹⁸⁰ Without further purification, the crude products were hydrolyzed and isolated as the α -hydroxy acids. Three crystallizations from petroleum ether gave the acids as white crystals in an overall yield of ~70% from the fatty acids. Some of the α -hydroxy acids were isolated or prepared earlier and the limited physical data reported in the literature match the data for our compounds.

Dimerization of the α -hydroxy acids in refluxing toluene using *p*-toluenesulfonic acid as a catalyst yielded a mixture of the *R,S* and *R,R/S,S* diastereomers in ~45% yield. The byproducts primarily consisted of linear oligomers which could in principle be recycled or thermally cracked to yield additional monomer. A representative ¹H NMR, that of hexadecyl glycolide, is shown in **Figure 25**. The methine protons of the 3,6-disubstituted glycolide ring

Bulk Polymerizations

Compared to lactide, glycolide monomers having substituents larger than methyl would be expected to polymerize more slowly due to the added steric bulk of the substituent. For a homologous series of *n*-alkyl-substituted monomers, only those methylenes close to the glycolide ring should influence the ring opening step and glycolides with alkyl chains beyond a critical number of methylenes should polymerize at the same rate. We tested this notion by measuring the polymerization kinetics for each of the monomers at 130 °C, using the polymerization of lactide under identical conditions as a control. The data were collected from bulk polymerizations run in sealed tubes using *t*-butylbenzyl alcohol as the initiator and Sn(2-ethylhexanoate)₂ as the catalyst. Since having pure and scrupulously dry monomer is a key to high molecular weights, low polydispersities, and repeatable kinetics, the monomer was crystallized several times and dried overnight under vacuum before used.

Ring-opening polymerizations of lactides are typically first-order in monomer¹⁸¹ and can be expressed as

$$R_p = -d[M]/dt = k_p[M][cat] \quad (1)$$

where [M] and [cat] are the concentration of monomer and catalyst respectively and k_p is the rate constant for propagation. Integration of (1) and assuming the catalyst concentration is constant provides (2)

$$-\ln([M]_t / [M]_0) = k_p[cat]_0 t \quad (2)$$

where the subscripts 0 and t refer to initial concentrations and at time = t. Data from such a polymerization can be linearized by plotting $-\ln([M]_t / [M]_0)$ vs time. Lactide polymerizations run to high conversions (or low monomer concentrations) often deviate from linearity due to the reversibility of the polymerization. Eventually polymerization ceases due to the establishment of an equilibrium between the propagation and depropagation steps, leaving an equilibrium monomer concentration $[M]_e$ unpolymerized.¹⁷⁶ To simplify evaluation of experimental data, equation 2 can be modified to account for effects of equilibrium polymerization by subtracting $[M]_e$ from $[M]_0$, giving eq 3.

$$-\ln\left(\frac{[M]_t - [M]_e}{[M]_0 - [M]_e}\right) = k_p[\text{cat}]_0 t \quad (3)$$

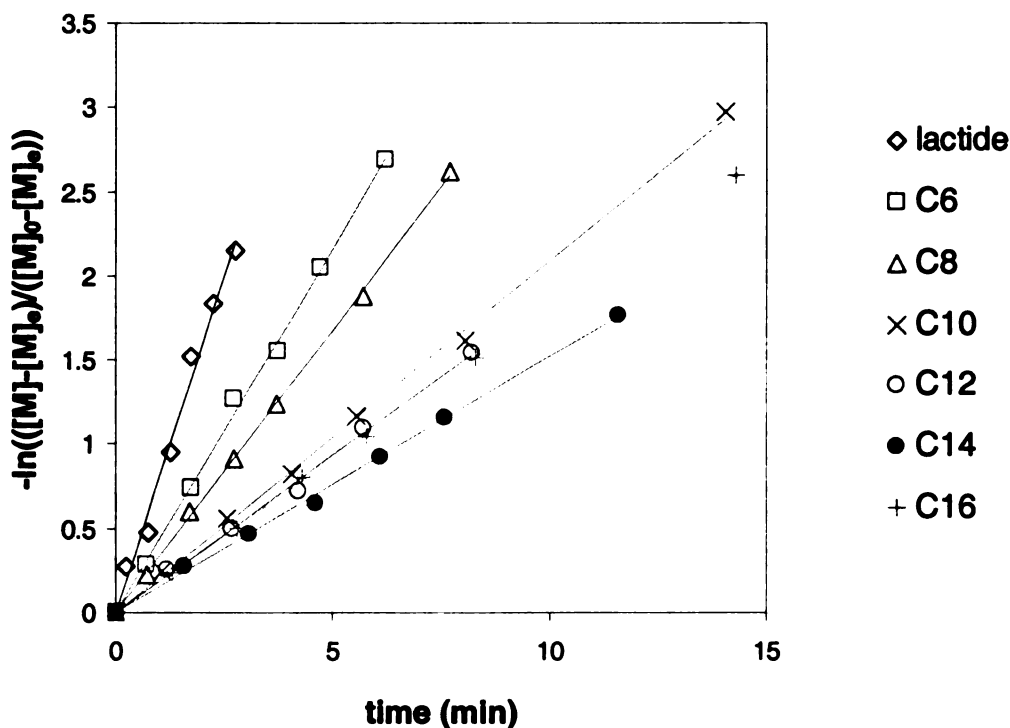


Figure 26. Bulk polymerization kinetics of substituted glycolides. Polymerization conditions: 130 °C, $[\text{Sn}(2\text{-ethylhexanoate})_2]/[\text{tert-butylbenzyl alcohol}] = 1$, $[\text{monomer}]/[\text{catalyst}] = 50$. Each data point is the average of three independent runs and corrected for equilibrium.

Kinetic data for the polymerization of lactide and alkyl-substituted glycolides are shown in **Figure 26**. Plots of $-\ln\left(\frac{[M]_t - [M]_e}{[M]_0 - [M]_e}\right)$ versus t should be linear, which are the experimental results as shown in **Figure 26**. Polymerization and depolymerization reactions under the same conditions show that all of the

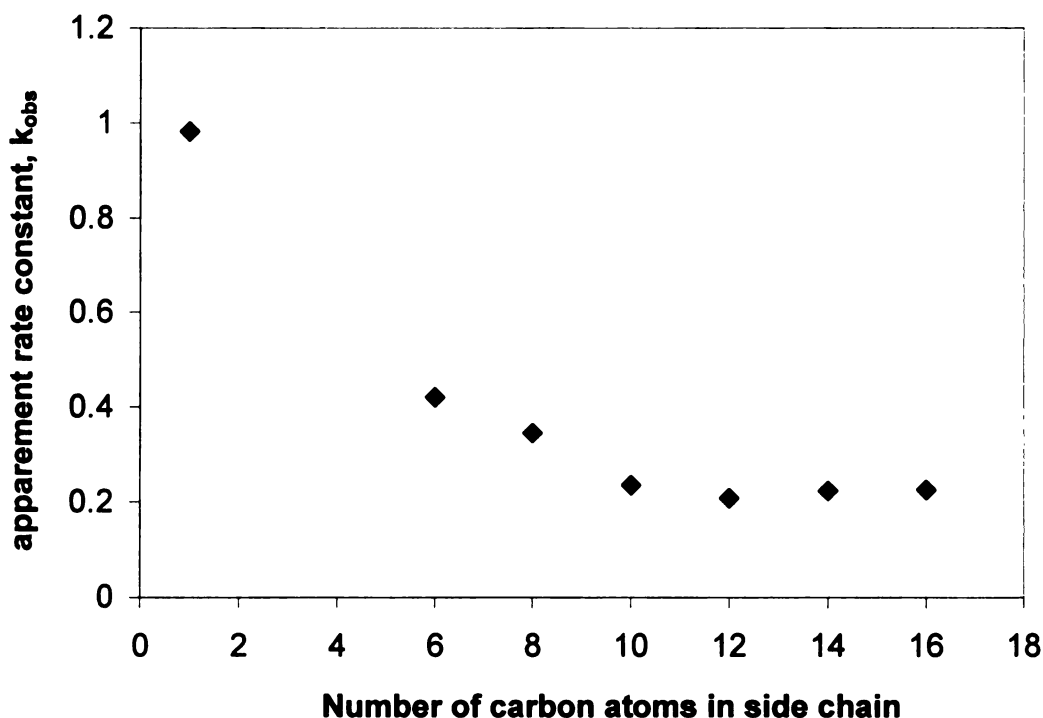


Figure 27. Relationship between apparent rate constant and the length of side chains for bulk polymerization of substituted glycolides.

lactides have similar equilibrium monomer concentrations (~ 1.4 mol% based on NMR). These results indicate that bulk polymerizations of the alkyl substituted lactides follow the same kinetic pattern as lactide and that ring-opening polymerization of glycolides substituted with linear alkyl groups is facile. The apparent rate constant values ($k_p[cat]$) were extracted from the slopes of the plots and then plotted as a function of the length of the side chain (**Figure 27**).

We found that the apparent rate constant decreases until the side chain length reaches ten methylene groups and then remained constant. However, the polymerization rates are not necessarily directly related to the length of the side chains. Since the monomer:initiator:catalyst ratios are constant, the side chains act as a diluent in these melt polymerizations and both the catalyst and monomer concentrations decrease with increasing side chain length; the trend in apparent polymerization rates is more likely the result of the combination of decreased catalyst and monomer concentrations and increased steric effects.

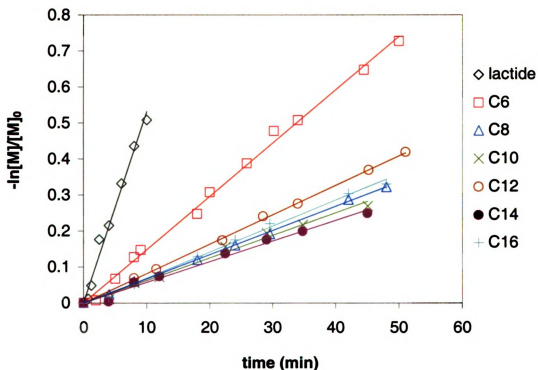


Figure 28. Solution polymerization kinetics of substituted glycolides. Polymerization conditions: 90 °C in toluene, $[\text{Sn}(2\text{-ethylhexanoate})_2]/[\text{tert-butylbenzyl alcohol}] = 1$, $[\text{monomer}]/[\text{catalyst}] = 100$. Each data set corresponds to a single kinetics run.

Solution Polymerizations

We further studied the polymerization kinetics by carrying out solution polymerizations in toluene at 90 °C with an initial monomer concentration of 0.2 M and [monomer]:[catalyst]:[initiator] ratio of 100:1:1. Again, the polymerization

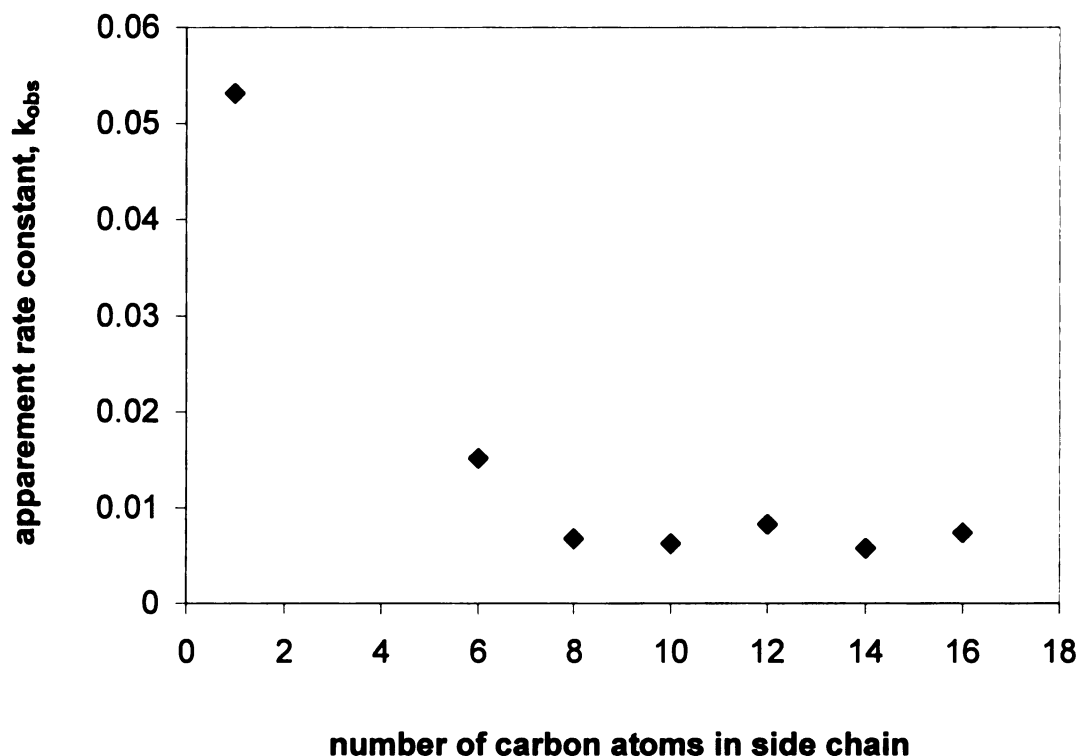


Figure 29. Relationship between apparent rate constant and the length of side chains for solution polymerization of substituted glycolides.

of lactide under identical conditions was used as a control. Solution polymerizations of glycolides should also follow first order kinetics described by eq. 2, and plots of $-\ln[M]_t / [M]_0$ vs t should be linear for low monomer conversions. The apparent rate constant values were again extracted from the slopes of the plots and plotted as a function of the length of side chain. As shown in **Figure 29**, the apparent rate constant decreased with increasing side

chain length, becoming constant at ≥ 8 carbon atoms in the side chain. However, since the solution data correspond to a single polymerization for each monomer, the differences in polymerization rates could have been complicated by trace amounts of impurities in the monomers. A more reliable way to compare the polymerization rates is to determine their reactivity ratios.

Homopolymer Properties

We determined the properties of the alkyl glycolide homopolymers using samples prepared by bulk polymerizations at 130 °C with the monomer to initiator ratio set at 200:1 (Table 1). These colorless polymers have molecular weights (M_n) between 55,000 and 70,000 g/mol and ranged from sticky liquids to waxy solids at room temperature. The polymers are soluble in common solvents such as toluene, THF and CH_2Cl_2 and were purified by washing with 2M HCl, and then precipitated from CH_2Cl_2 into 2-propanol and dried under vacuum.

Table 1. Properties of alkyl comb glycolides

Polymer	$M_n \times 10^{-3}$	PDI	T_g (°C) ^a	T_m (°C)	ΔH_m (cal/mol)	n_c ^b
polyC6	56.9	1.22	-37	~	~	~
polyC8	56.4	1.21	-46	~	~	~
polyC10	60.7	1.37	nd	-18	417	0.7
polyC12	67.7	1.28	nd	8	1676	2.9
polyC14	70.0	1.19	nd	28	2795	4.8
polyC16	55.9	1.13	nd	45	3912	6.7

a. nd indicates that the T_g was not detected. b. number of crystalline methylenes (see equation 5).

The polymer decomposition temperatures measured by thermal gravimetric analysis (TGA) estimate the limiting use temperatures of the polymers. As shown in **Figure 30**, the TGA profiles for all of the polymers are similar, with the onset for decomposition shifting to higher temperatures and the residue at 360 °C increasing as the length of the alkyl group increases. Alkyl substituted polyglycolides thermally decompose by depolymerizing to the volatile monomers, with some aldehydes formed by elimination reactions.¹⁷⁶ Consequently, the

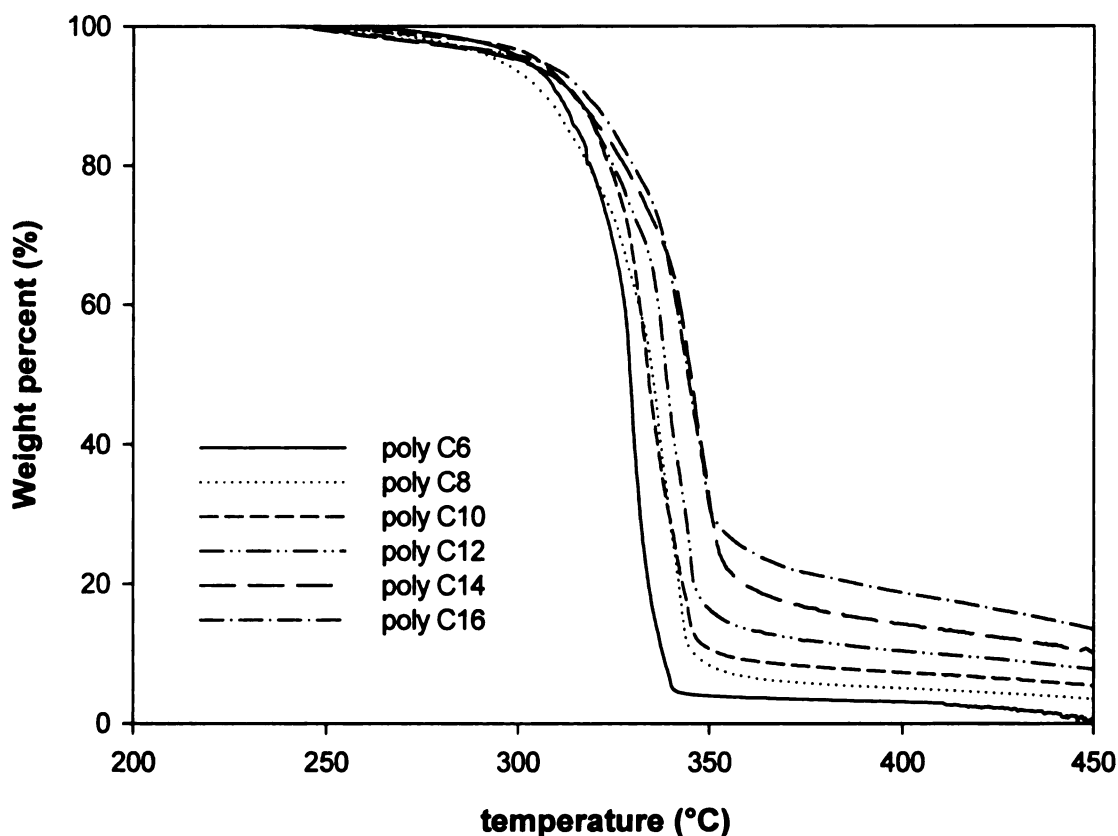


Figure 30. TGA results for substituted polyglycolides. (10 °C/min in air, no aging)

increase in residual mass percentage at 360 °C does not necessarily imply increased thermal stability for the polymers with longer side chains, but it more

likely is a char that reflects the increasing importance of reactions other than depolymerization as the monomer volatility decreases.

Differential scanning calorimetry (DSC) was used to measure the glass transition (T_g) and/or melting (T_m) temperatures for the polymers, and the results are displayed in **Figure 31**. When the substituted linear alkyl group is shorter

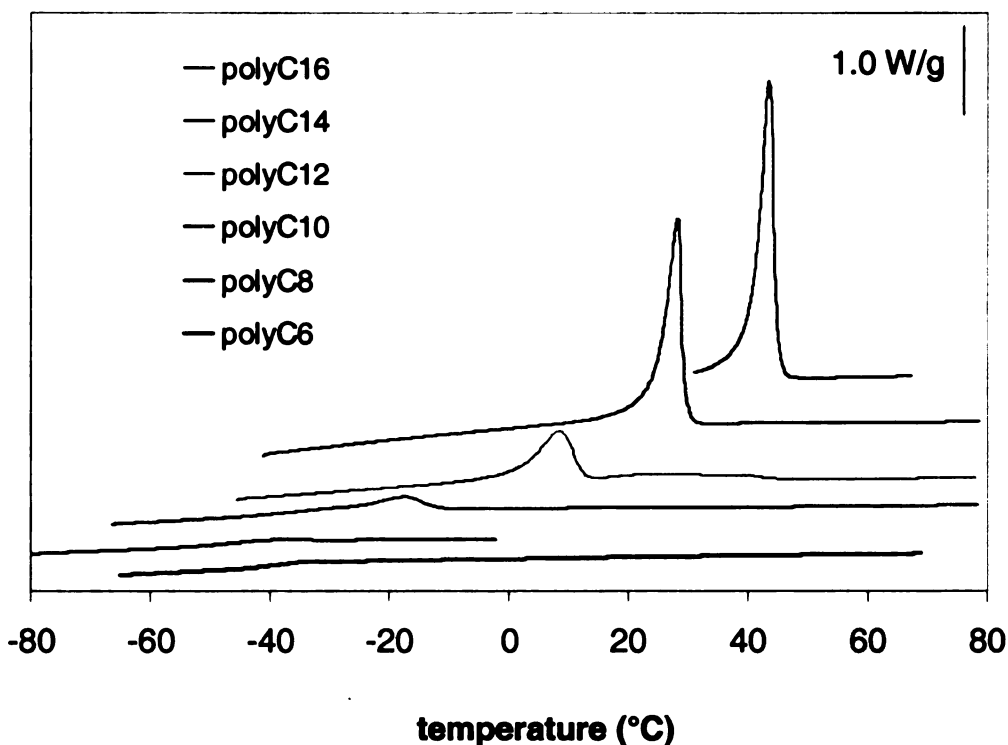


Figure 31. DSC scans for substituted polyglycolides. The data are second heating scans, taken after heating to 70 °C and flash cooled. Heating rate: 10 °C /min in N₂.

than decyl, the T_g decreased with increasing side chain length. In these cases the flexible pendant group is thought to reduce T_g by acting as an internal plasticizer, thereby lowering the frictional interaction between different main chains. After the alkyl group reached decyl, the glass transition was not detected by DSC. Instead, a first order transition corresponding to melting of the side

chain crystalites appeared with melting points ranging from $-18\text{ }^{\circ}\text{C}$ for polyC10 to $45\text{ }^{\circ}\text{C}$ for polyC16.

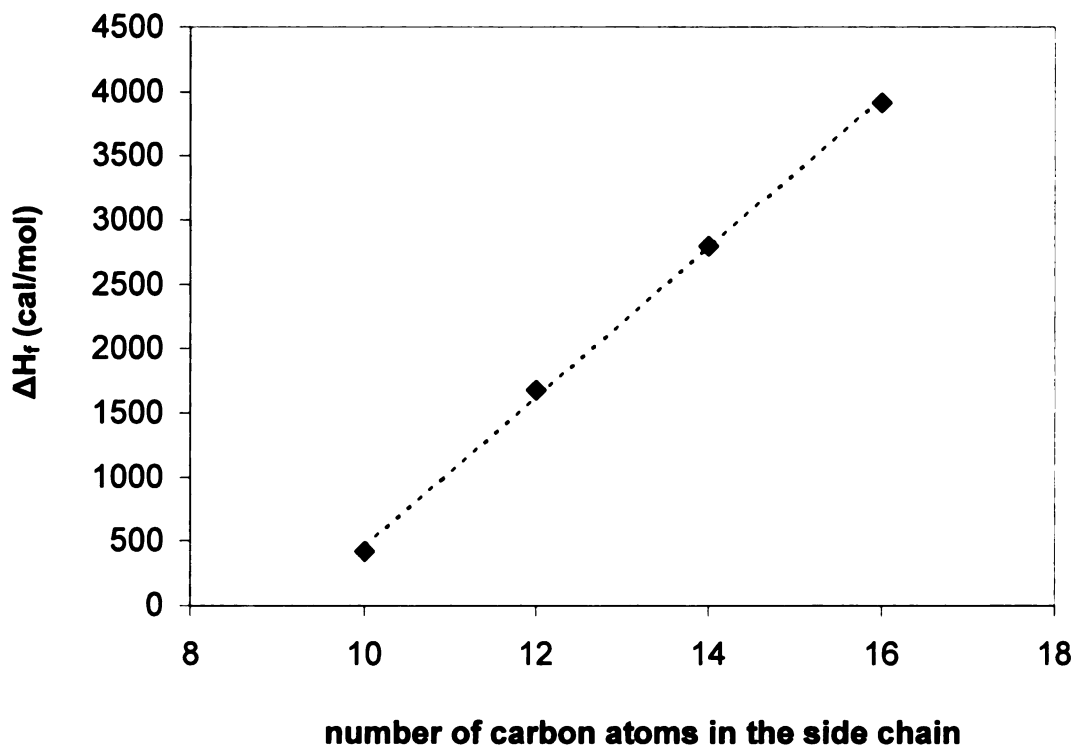


Figure 32. The relationship between ΔH_f and side chain length

The enthalpy of fusion (ΔH_f) for comb-like polymers bearing crystallizable linear alkyl side chains is indicative of the number of methylenes (n_c) participating in the paraffinic crystalline phase. Plotting ΔH_f as a function of the number of carbon atoms in the side chains (**Figure 32**) yields a straight line where the x-intercept is interpreted in the literature as the minimum number of side chain atoms required for side-chain crystallization of comb-like polymers.¹⁰

$$\Delta H_f = \Delta H_{fe} + nk \quad (4)$$

In equation 4, ΔH_{fe} is a constant representing the end methyl group's contribution to the enthalpy, and k is the average melting enthalpy for each crystallized

methylene group. The value of k extracted from the slope of the line in **Figure 32** is ~ 580 cal/mol CH₂, which is far from the 950-1000 cal/mol CH₂ reported for the rhombic-to-liquid transition of crystalline paraffins,¹⁰ but fairly close to the ~ 520 cal/mol CH₂ melting enthalpy measured for the crystalline alkyl side-chains in comb-like poly(D-glutamic acid esters).⁵⁶

Jordan *et al.*¹⁰ showed that each methylene in a crystalline side chain contributes a fixed enthalpy, and thus the number of crystalline CH₂ groups in a side chain, n_c , is given by the equation

$$n_c = \Delta H_f / k \quad (5)$$

Although equation 5 only allows a rough estimation of n_c due to the assumptions involved during its derivation, calculation of n_c is commonly used in studies of side chain crystallization.^{10,50,56} The n_c data listed in the last column of **Table 1** vary from 0.7 for polyC10 to 6.7 for polyC16, suggesting that ~ 9 methylene groups in the side chain are in a disordered state, and only those methylene groups beyond this limit participate in crystallization. The values of n_c in **Table 1** are close to those reported for flexible main chain polymers with linear alkyl side chains.¹⁰

To further elucidate the structure of flash-cooled comb-like polylactides, samples of polyC14 and polyC16 were melted, quickly transferred to a -40 °C freezer for eight minutes, and then their wide angle X-ray scattering (WAXS) profiles were recorded at room temperature. WAXS results for two independent runs of polyC14 and two independent runs of polyC16 are shown in **Figure 33**. Although the DSC melting points for both polyC14 runs are 28 °C, their diffraction patterns

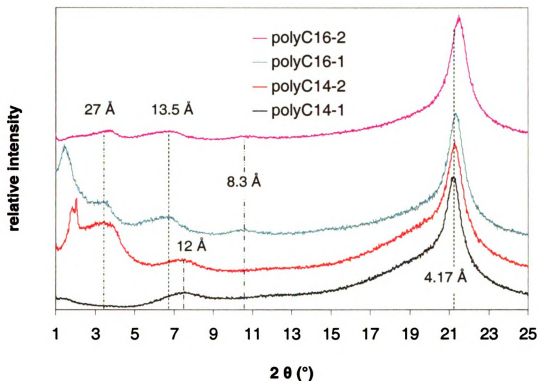


Figure 33. WAXS profiles of flash-cooled polyC14 and polyC16 (polyC14-1 and polyC14-2, polyC16-1 and polyC16-2 are two different runs from the same polyC14 and polyC16 sample, respectively.)

are only repeatable in the wide angle region, with a strong diffraction peak at $d = 4.17 \text{ \AA}$ and a broad, weak peak at $d = 12 \text{ \AA}$. Sample to sample variation in the WAXS data also is often seen for polyC16 as shown in **Figure 33**. According to current understanding of comb-like polymers, the peak at 4.17 \AA indicates a hexagonally crystallized paraffinic phase as has been reported for other comb-like polymers,^{9,56} while the poor reproducibility of the low angle X-ray data for both polyC14 and polyC16 indicates the absence of a well-defined layered structure.¹⁸² DSC analysis shows that both polyC12 and polyC10 crystallize, but we were unable to record WAXS profiles of flash-cooled samples of crystalline polyC12 and polyC10 due to their low melting points. Although the presence or

absence of a lamellar structure cannot be verified for these two polymers, we expect that the alkyl side chains in these two polymers are also hexagonally packed because of their structural similarity to polyC14 and polyC16.

As previously reported,^{9,50,56,89} a two-dimensional supramolecular structure consisting of a layered arrangement of alternating paraffinic and polymer backbone phases is commonly observed for comb-like polymers. Obviously the results obtained for flash-cooled comb-like polylactides do not necessarily lead to the same conclusion due to the irreproducible X-ray diffraction patterns in the low angle region. The appearance of hexagonal side chain crystallites and the lack of a layered structure was previously reported for quenched poly(α -olefin)s and was attributed to the formation of a phase in which backbone is highly disordered.^[23] Annealing experiments proved to be helpful in forming well-defined layered structures.

The DSC traces in **Figure 34** show the effect of annealing on polyC14. The melting temperature shifted from 28 °C to 37 °C after annealing the flash-cooled sample at 27 °C for 4 hours. Further annealing at 32 °C increased the melting point to 47 °C. The WAXS patterns of these polyC14 samples are shown in **Figure 35**. After annealing at 27 °C, an irreproducible low intensity broad peak in the low angle region disappeared and a strong sharp reflection appeared at 34.2 Å. Second and third order reflections (17.7 Å and 11.9 Å respectively) also appeared after annealing, with the third order reflection more intense. Enhancement in odd-order diffraction patterns has been observed in other comb-like polymers.^{77,89}

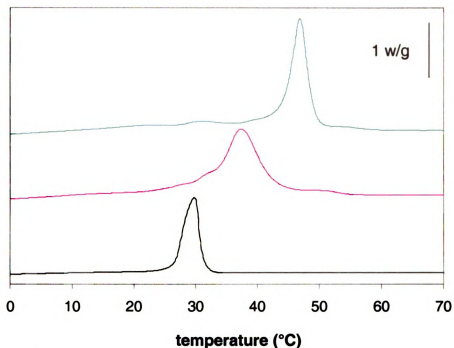


Figure 34. DSC traces of polyC14 samples with different thermal histories. First heating scan. 10 °C/min in N₂. (black line: flash cooled in freezer for 8 minutes; pink line: annealed at 27 °C for four hours; blue line: annealed 32 °C for six weeks)

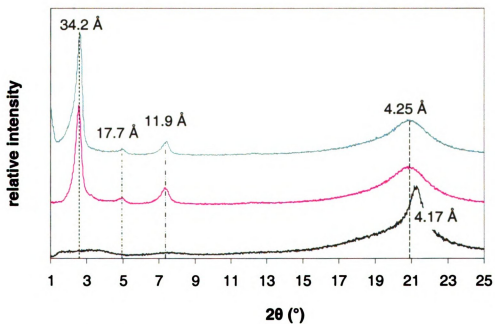


Figure 35. WAXS profiles of polyC14 samples with different thermal histories. (black line: flash cooled in freezer for 8 minutes; pink line: annealed at 27 °C for four hours; blue line: annealed 32 °C for six weeks)

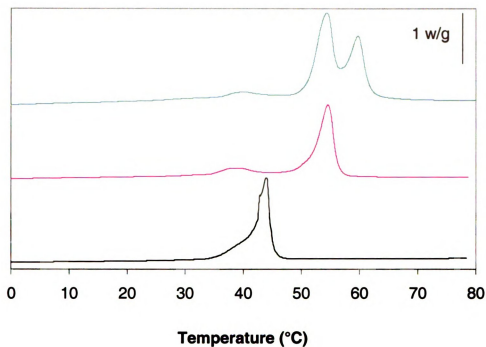


Figure 36. DSC traces of polyC16 samples with different thermal histories. First heating scan. 10 °C/min in N₂. (black line: annealed at room temperature for 12 hours; pink line: annealed at 45 °C for two weeks; blue line: annealed at 45 °C for two months)

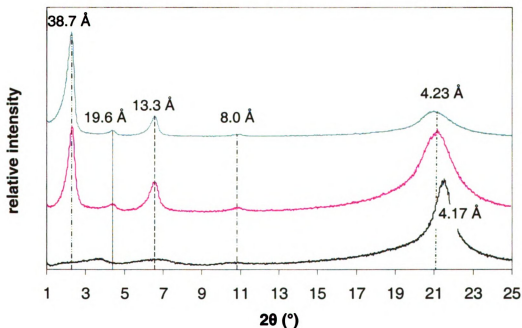


Figure 37. WAXS profiles of polyC16 samples with different thermal histories. (black line: annealed at room temperature for 12 hours; pink line: annealed at 45 °C for two weeks; blue line: annealed at 45 °C for two months)

Interestingly, the sharp diffraction peak at 4.17 Å seen in the flash-cooled sample broadens and shifts to 4.25 Å, which suggests looser packing of the alkyl chains in the annealed sample than in the flash-cooled sample. Although further annealing at 32 °C led to a 10 °C increase in the melting point, the X-ray patterns of both annealed polyC14 samples are almost identical with the only difference being a decrease in the relative intensity of the diffraction peak at 4.25 Å.

Annealing polyC16 at 45 °C first shifted the melting point from 45 °C to 55 °C and after further annealing, DSC detected a new melting transition at 60 °C (**Figure 36**). The effect of annealing on the WAXS profile is very similar to that seen for polyC14, with the peak in the wide angle region broadened and shifted from 4.17 Å to 4.23 Å (**Figure 37**). The broad weak reflection peaks in the low to medium angle region sharpened, with associated spacings of 38.7 Å, 19.6 Å, 13.3 Å, and 8.0 Å, indicating a well-defined lamellar structure.

PolyC12 and polyC10 were subjected to similar thermal treatments, and while DSC traces showed an increase in melting point, attempts to track changes in the WAXS profile failed due to the low melting points. It should be stressed that within experimental error, the enthalpy of melting for all crystalline samples remains constant during annealing, which suggests that according to equation 5, annealing does not appreciably increase the number of crystalline methylenes in side chains. This observation is helpful in understanding the broadening and shifting of the X-ray diffraction peak at ~4.2 Å. Since the observed ΔH is essentially constant, ΔS must increase for ΔG for this process to be negative. Since X-ray reflections in low angle region suggest the formation of a more

ordered two-dimensional structure, the side chain packing must disorder to compensate for the decrease in entropy.

Table 2. X-ray diffraction spacings (Å) of comb-like polyglycolides

polyC6	polyC8	polyC10		polyC12		polyC14	polyC16
		melt	annealed	melt	annealed		
13.6	16.2	18.9	26.8	21.1	30.5	34.2	38.7
					15.7	17.7	19.6
			9.1		10.5	11.9	13.3
						7.2	8.0
4.6	4.6	4.6	4.5	4.6	4.3	4.25	4.23

“melt” means the side chains are in disordered state; “annealed” means the side chains are crystalline.

Shown in **Figure 38** are the DSC traces from the first heating scan of annealed samples; the corresponding X-ray diffraction patterns taken at room temperature are shown in **Figure 39** and the spacings measured for the whole series are listed in **Table 2**. Because of the extremely slow annealing process, DSC scans of both polyC10 and polyC12 showed two melting temperatures even after being annealed at room temperature for a year. Apparently, an amorphous phase crystallizes as the samples are cooled to start the X-ray analysis, leading to two distinct melting transitions. The X-ray diffraction patterns of these samples are the result of diffraction from a minor side chain crystalline phase and substantial scattering from an ill-defined layered structure in which side chain is in disordered state, as seen from the broad peak at 18.6 Å for polyC10 and at 20.2 Å for polyC12.

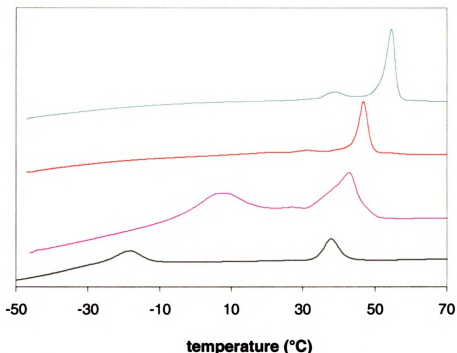


Figure 38. DSC traces (10 °C/min in N₂) of annealed alkyl comb polyglycolides. (black line: polyC10, annealed at room temperature for a year; pink line: polyC12, annealed at room temperature for a year; red line: polyC14, annealed at 32 °C for six weeks; blue line: polyC16, annealed at 45 °C for two weeks)

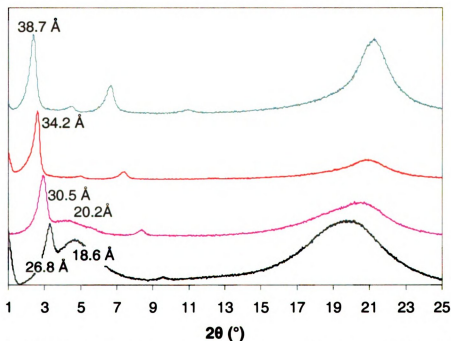


Figure 39. WAXS profiles of annealed alkyl comb polyglycolides. (black line: polyC10, annealed at room temperature for a year; pink line: polyC12, annealed at room temperature for a year; red line: polyC14, annealed at 32 °C for six weeks; blue line: polyC16, annealed at 45 °C for two weeks)

Diffraction from the crystalline phases can be readily interpreted as arising from a well-defined lamellar structure. The primary diffractions with associated spacings between 25 Å and 40 Å are due to the layer periodicity of the structure, whereas the reflections appearing at 4-4.6 Å are from the paraffinic phase. For polyC14 and polyC16, the ~4.2 Å spacing demonstrates unambiguously the formation of a hexagonally packed crystalline paraffinic phase. The broader reflection peaks with longer d spacings in this region in the case of polyC12 and polyC10 do not necessarily mean the side chains are packed in a different crystalline structure, but more likely results from the combination of a disordered paraffinic phase with an average spacing reported to be 4.5 Å⁵⁶ and a hexagonal paraffinic crystalline phase, as was expected by the DSC analysis and the broad diffraction peaks in low angle region.

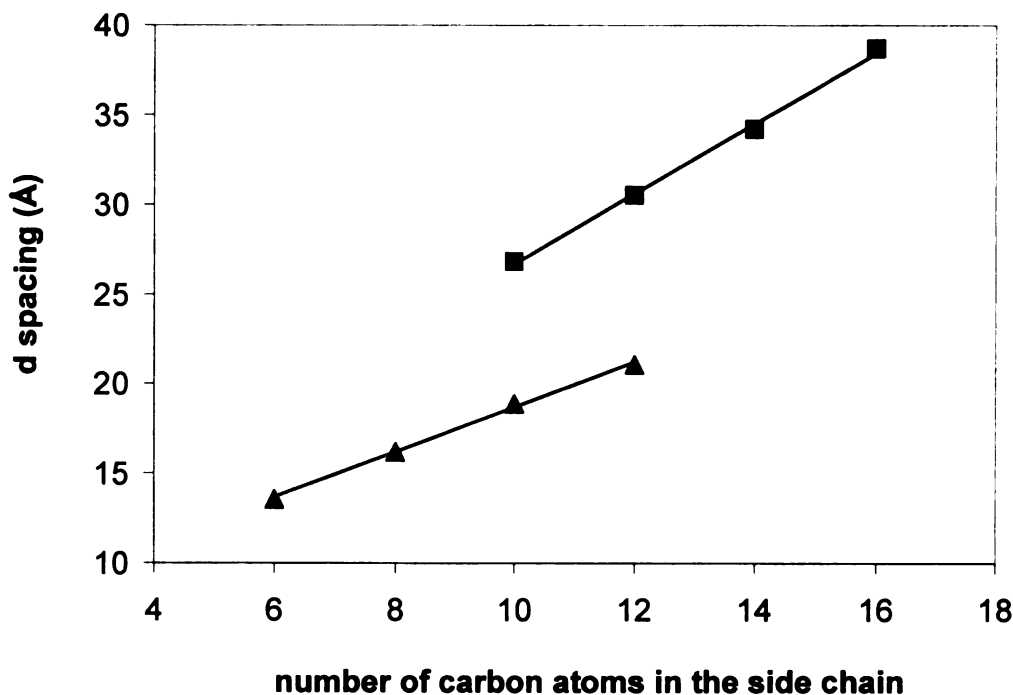


Figure 40. Evolution of d -spacings with side chain length. (■ crystalline polymer samples; ▲ melt polymer samples)

As seen in **Figure 40**, the periodicity of the layered structure seen in polyC10, polyC12, polyC14, and polyC16 increases linearly with n , giving a slope of 1.97 Å per carbon, very close to values observed for poly(4-alkylthiazole)s (2.0 Å per carbon) and poly(3-alkylthiophene)s (1.8 Å per carbon).¹⁸² Since this value is much greater than the theoretical value of 1.26 Å for each methylene in interdigitated side chains, the alkyl side chains of comb-like polylactides most likely are packed in a bilayer structure similar to that proposed by Wegner,⁷⁷ in which the side chains were tilted at an angle θ to the main chain (**Figure 41**). For the polymers described here, θ is $\sim 50^\circ$.

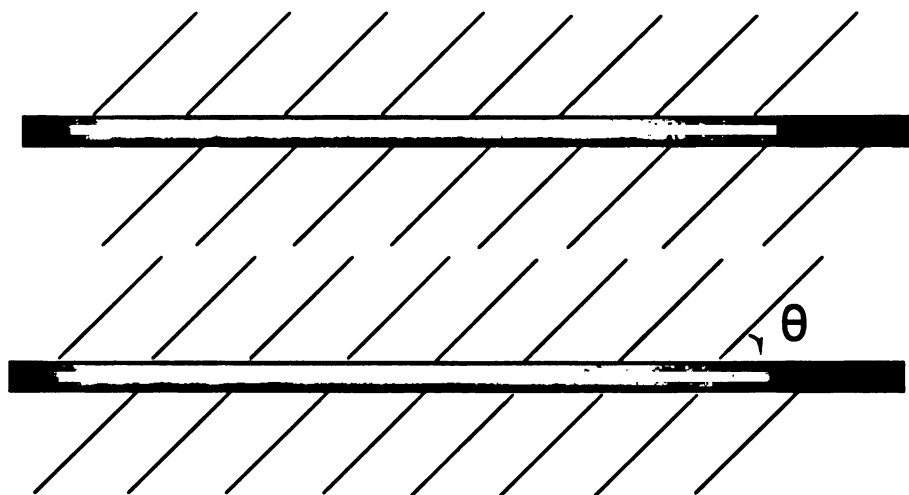


Figure 41. Proposed molecular packing of annealed alkyl comb polylactides

For comparison, the X-ray diffraction patterns of molten polyC6, polyC8, polyC10 and polyC12 were measured at room temperature (**Figure 42**). The broad reflection peak at ~ 4.6 Å in all four samples is consistent with a disordered paraffinic phase, as was expected by the DSC analysis. The broad primary reflections with associated d spacings between 10 and 25 Å and the absence of

higher order reflections suggests a poorly defined lamellar structure in the molten samples. From the plot of d as a function of n shown in **Figure 40**, we can see that the periodicity of the layered structure also increases linearly with n , but with a slope of 1.27 \AA per methylene unit. This value perfectly matches the theoretical value of 1.26 \AA per methylene expected for interdigitated side chains, and we conclude that above the melting point, the alkyl side chains are most likely perpendicular to the main chains and interdigitated.

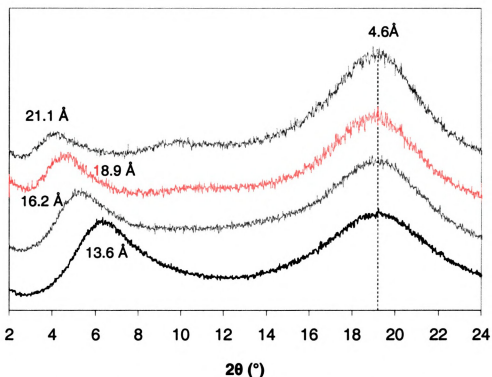


Figure 42. WAXS profiles of alkyl comb polyglycolides

Polymer Degradation

The temperature chosen for hydrolytic degradation experiments, $55 \text{ }^\circ\text{C}$, is higher than the glass transition temperature of each polymer, and higher than the

melting transition for all crystalline polymers. Measuring the degradation properties using this protocol should provide information about the intrinsic hydrolytic degradation rate without complications posed by crystallization or glassy phases. Shown in **Figure 43** is the evolution in molecular weight during degradation, where $M_n(0)$ and $M_n(t)$ are the initial and partially degraded number average molecular weights respectively. All of the polymers show an apparent induction time for degradation. Similar induction times were observed during the degradation of poly(phenyllactide),¹⁷⁷ lactic acid/mandelic acid¹⁸³ and lactic acid/phenyllactic acid copolymers. A plausible explanation is that initially the equilibrium concentration of water in pristine polymer samples is low, but hydrolysis renders the polymer increasingly hydrophilic and accelerates the degradation. Near the end of the experiment, all polymers appear to degrade slower. The likely reason is that the low molecular weight oligomers are soluble in the buffer solution and are not recovered during the experiment. Thus the molecular weights were overestimated.

To better evaluate the degradation rates, the molecular weight data were plotted according to random chain scission model as $(M_n(0)/M_n(t)-1)/P_n(0)$ vs. time,¹⁸⁴ where $P_n(0)$ is the initial degree of polymerization (**Figure 44**). All of the data sets were then shifted to the left by subtracting the induction time so that each data set passes through the origin. Surprisingly, all of the data sets yielded linear plots, and all data sets had roughly the same slope. These data show that while the gross physical properties of the polymers are dependant on the length of the alkyl side chain, their degradation rates (slope of the data) are remarkably

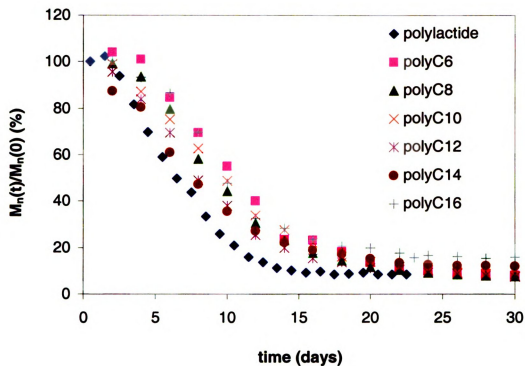


Figure 43. Molecular weight change of polyglycolides during hydrolytic degradation in pH = 7.4 phosphate buffer at 55 °C

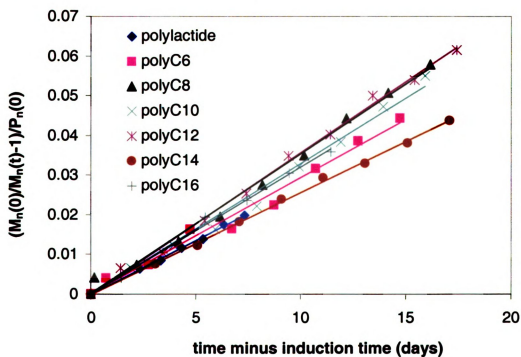


Figure 44. Molecular weight change of polyglycolides during hydrolytic degradation fitted to random chain scission model

similar to that of polylactide. Prior to the degradation experiment we thought that the longer alkyl side chains, being hydrophobic, might shield the polymer backbone decreasing the rate of hydrolysis. Clearly the length of the side chain appears to have only a minor effect on the degradation rate, and apparently the rubbery nature of each polymer ensures that the diffusion rate of water through these polymers is high enough that it is not rate limiting.

Alkyl Comb Copolymers

The melting points of poly(alkyl glycolide)s span a range including ambient to physiologically relevant temperatures. We prepared C16/C14 copolymers with different monomer loading ratios to assess physical properties expected for poly(alkyl glycolide) copolymers. The copolymers were prepared by melt copolymerization using conditions identical to those used to prepare the homopolymers. The polymerizations were run at 130 °C for two hours with a monomer/initiator ratio of 100 and reached $\geq 92\%$ conversions. GPC data showed that all of the copolymers have high molecular weights and narrow molecular weight distribution ($PDI < 1.2$) (**Table 3**). Both DSC and GPC results suggest a random distribution of monomer repeat units along the polymer backbone.

The DSC traces shown in **Figure 45** reveal a single melting transition for each copolymer, which was dependant on the monomer loading ratio and ranged from 29.4 °C for the C14 homopolymer to 45.7 °C for the C16 homopolymer. A similar relationship between melting temperature and polymer composition was previously reported for comb-like acrylate copolymers.¹⁰

Table 3. Properties of C14/C16 copolymers

mol% of C14 in the copolymer	$M_n \times 10^{-3}$	PDI	T_m (°C)
100	39.2	1.12	29
90	51.9	1.19	31
80	74.7	1.19	33
65	53.6	1.18	34
50	69.3	1.15	37
35	47.7	1.17	39
20	55.0	1.12	43
10	46.2	1.16	43
0	39.6	1.10	45

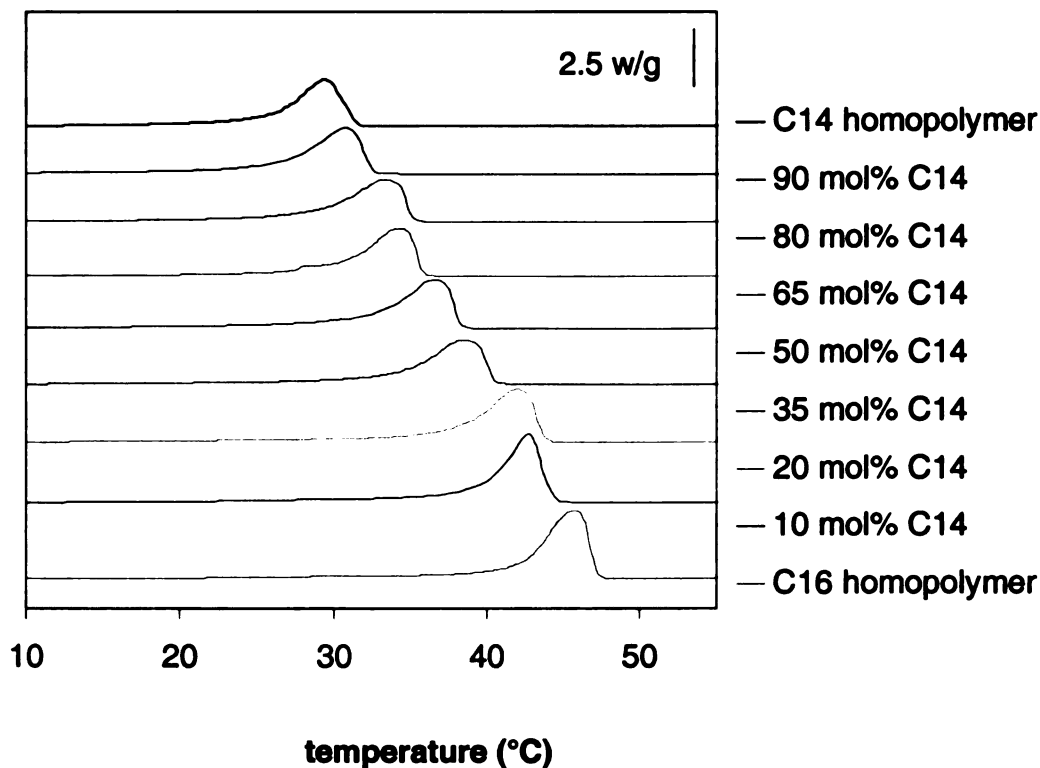


Figure 45. DSC heating scans of C14 and C16 random copolymers. Second heating scan, 10 °/min in N₂.

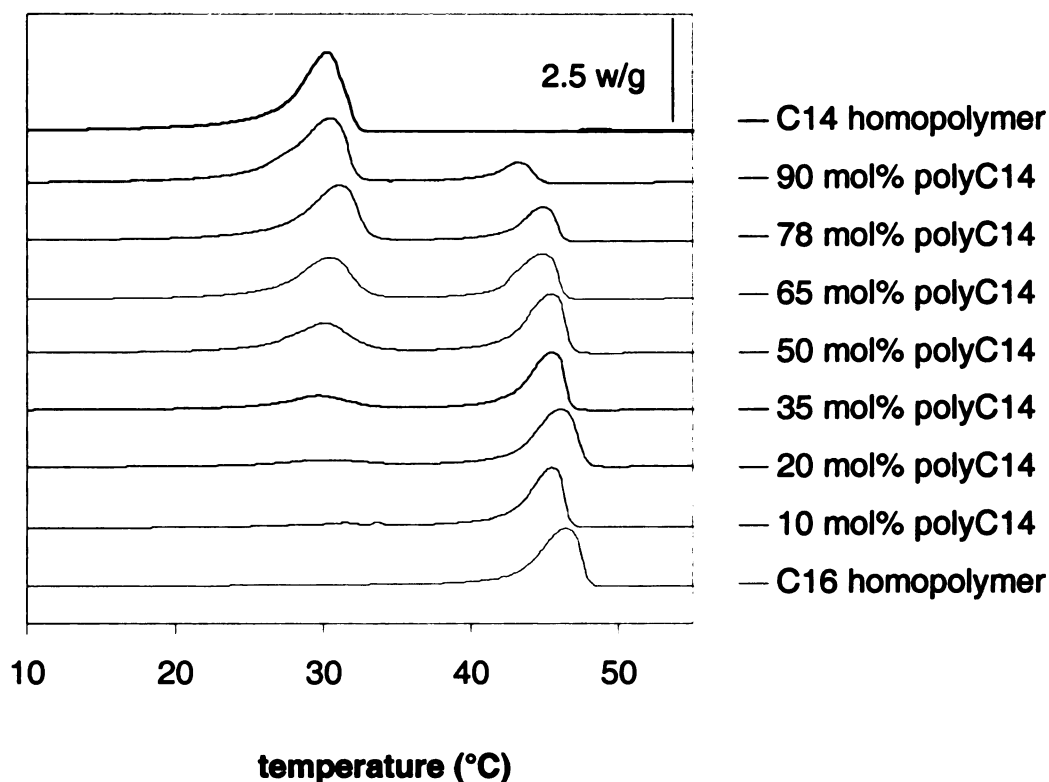


Figure 46. DSC heating traces of polyC14 and polyC16 blends. Second heating scan, 10 °C/min in N₂.

We carried out two experiments to rule out the formation of simple blends or blocky copolymers. We prepared polymer blends with compositions matching those used in the copolymerizations. The DSC traces of the blends (**Figure 46**) all show distinct melting points for polyC14 and polyC16 homopolymer phases, indicating the formation of two different crystalline phases in these blends. A C16/C14 block copolymer was prepared by sequential addition of C16 to C14. **Figure 47** shows two melting temperatures for the block copolymer, suggesting the formation of two different crystalline phases. Finally, the polymerization kinetics for the C16 and C14 monomers also support the conclusion that the copolymers are not blocky. Since the effect of the side chain length on

polymerization rates saturates at ≥ 8 chain atoms, the two carbon difference in the C14 and C16 side chains would not be expected to affect the rate at which the two monomers enter the polymer.

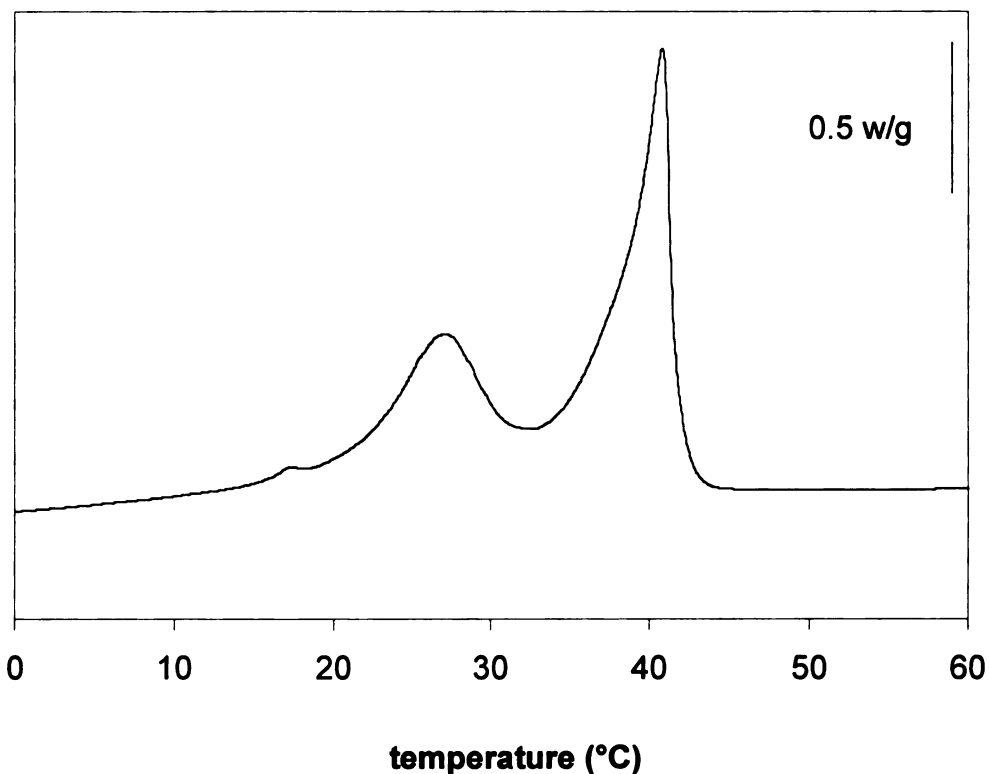


Figure 47. DSC heating scan of polyC16 – *block* - polyC14). Second heating scan, 10 °C/min in N₂.

Experimental Section

Unless otherwise specified, ACS reagent grade starting materials and solvents were used as received from commercial suppliers without further purification. THF was distilled from CaH₂ and sodium. ¹H NMR (300 MHz or 500 MHz) and ¹³C NMR (75 MHz or 125 MHz) spectra were recorded at room temperature in CDCl₃ using a Varian Gemini 300 or a Varian UnityPlus-500

spectrometer with chemical shifts referenced to residual proton signals from the solvent. Mass spectral analyses were carried out on a VG Trio-1 Benchtop GC-MS.

General procedure for the synthesis of α -hydroxy acids. The appropriate alkyl bromide (0.26 mol) was dissolved in anhydrous THF (250 mL) in a 1 L round bottom flask and stirred with magnesium turnings (9.4 g, 0.39 mol) at a temperature appropriate for forming the Grignard reagent (0 °C for hexyl bromide, 50 °C for hexadecyl bromide). After transferring the resulting Grignard reagent to an addition funnel, the solution was added dropwise under nitrogen to a 1-L three-neck round bottom flask containing a mechanically stirred solution of diethyl oxalate (29.5 g, 0.20 mol) in anhydrous THF (100 mL) at -80 °C.¹⁷⁹ The reaction mixture was stirred for an additional half hour at -80 °C, and then was quenched with 2M HCl (200 mL). The aqueous layer was extracted with ether or hexanes (for C16 and C14) (3 × 300 mL) and the combined organic layers were washed with saturated NaCl and dried over MgSO₄. Filtration and removal of the solvents by rotary evaporation gave a light brown oil. The oil was then poured into chilled (0 °C) methanol (300 mL), the mixture was filtered, and the methanol was removed by rotary evaporation to give a light brown oil. Without further purification, the crude ketoester was dissolved in acetic acid (250 mL) and 0.5 g of 5% Pt/Al₂O₃ was added. After hydrogenation at ~1500 psig for 5 days, the solids were removed by filtration, ether was added, and the acetic acid was removed by washing with water. The colorless oil was hydrolyzed in a refluxing mixture of 15 wt % solution of KOH in 70% aqueous ethanol (500 mL) for 2 days,

after which the mixture was neutralized with 2M HCl and extracted with CH₂Cl₂ (3 × 400 mL). The combined organic layers were dried over MgSO₄, and after filtration and removal of solvents by rotary evaporation, the crude α-hydroxy acid was recrystallized from hexanes three times.

2-Hydroxyoctanoic acid (1a) Isolated as white crystals, mp 67-69 °C (lit. 70 °C).¹⁸⁵ ¹H NMR: δ 4.23-4.27 (dd, 1H, *J* = 7.57 Hz, *J* = 4.15 Hz), 1.77-1.87 (m, 1H), 1.62-1.72 (m, 1H), 1.36-1.49 (br, 2H), 1.21-1.35 (br, 6H), 0.77-0.94 (t, 3H, *J* = 6.84 Hz). ¹³C NMR: δ 180.04, 70.28, 34.09, 31.58, 28.88, 24.66, 22.52, 14.00. MS (m/z): 161.4 (M+1).

2-Hydroxydecanoic acid (1b) Isolated as white crystals, mp 71-72 °C (lit. 70-72 °C).¹⁸⁶ ¹H NMR: δ 4.23-4.27 (dd, 1H, *J* = 7.57 Hz, *J* = 4.15 Hz), 1.77-1.86 (m, 1H), 1.62-1.71 (m, 1H), 1.35-1.48 (br, 2H), 1.18-1.34 (br, 10H), 0.78-0.91 (t, 3H, *J* = 6.84 Hz). ¹³C NMR: δ 180.01, 70.28, 34.09, 31.81, 29.36, 29.23, 29.19, 24.72, 22.62, 14.05. MS (m/z): 189.3 (M+1).

2-Hydroxydodecanoic acid (1c) Isolated as white crystals, mp 73-74 °C (lit. 73-74 °C).¹⁸⁷ ¹H NMR: δ 4.23-4.28 (dd, 1H, *J* = 7.57 Hz, *J* = 4.15 Hz), 1.78-1.87 (m, 1H), 1.62-1.72 (m, 1H), 1.37-1.49 (br, 2H), 1.18-1.35 (br, 14H), 0.78-0.91 (t, 3H, *J* = 6.84 Hz). ¹³C NMR: δ 180.10, 70.27, 34.14, 31.88, 29.57, 29.54, 29.42, 29.30, 29.24, 24.73, 22.66, 14.09. MS (m/z): 217.4 (M+1).

2-Hydroxytetradecanoic acid (1d) Isolated as white crystals, mp 81-82 °C (lit. 81.5-82 °C).¹⁸⁸ ¹H NMR: δ 4.19-4.31 (dd, 1H, *J* = 7.57 Hz, *J* = 4.15 Hz), 1.78-1.87 (m, 1H), 1.63-1.72 (m, 1H), 1.36-1.50 (br, 2H), 1.18-1.35 (br, 18H), 0.80-

0.89 (t, 3H, $J = 6.84$ Hz). ^{13}C NMR: δ 179.92, 70.26, 34.17, 31.91, 29.65, 29.63, 29.61, 29.54, 29.42, 29.34, 29.24, 24.72, 22.68, 14.11. MS (m/z): 245.4 (M+1).

2-Hydroxyhexadecanoic acid (1e) Isolated as white crystals, mp 87-88 °C (lit. 86.5-87 °C).¹⁸⁹ ^1H NMR: δ 4.03-4.09 (dd, 1H, $J = 7.57$ Hz, $J = 4.15$ Hz), 1.66-1.77 (m, 1H), 1.50-1.60 (m, 1H), 1.28-1.42 (br, 2H), 1.12-1.26 (br, 22H), 0.71-0.86 (t, 3H, $J = 6.84$ Hz). ^{13}C NMR: δ 176.66, 69.63, 33.85, 31.37, 29.14, 29.12, 29.11, 29.10, 29.06, 28.99, 28.87, 28.80, 24.44, 22.14, 13.64. MS (m/z): 273.5 (M+1).

2-Hydroxyoctadecanoic acid (1f) Isolated as white crystals, mp 89-90 °C (lit. 91-92 °C).¹⁸⁹ ^1H NMR: δ 4.22-4.28 (dd, 1H, $J = 7.57$ Hz, $J = 4.15$ Hz), 1.79-1.88 (m, 1H), 1.63-1.73 (m, 1H), 1.37-1.49 (br, 2H), 1.20-1.33 (br, 26H), 0.78-0.91 (t, 3H, $J = 6.84$ Hz). ^{13}C NMR: δ 176.99, 69.86, 34.07, 31.62, 29.39, 29.37, 29.35, 29.30, 29.23, 29.11, 29.05, 24.62, 22.39, 13.86. MS (m/z): 301.5 (M+1).

General procedure for the synthesis of substituted glycolides. The appropriate α -hydroxy acid (0.11 mol) was placed in a 2 L round bottom flask, along with 0.6 g *p*-toluenesulfonic acid and ~1600 mL of toluene. The solution was heated at reflux for 4 days, with the water removed azeotropically using a Barrett trap. After the toluene was removed by rotary evaporation, the residue was dissolved in 500 mL dichloromethane, washed with saturated NaHCO_3 (3 \times 300 mL) and dried over MgSO_4 . Removal of the dichloromethane gave the product as a light brown oil or solid which was purified by recrystallization three times from hexanes.

3,6-Dihexyl-1,4-dioxane-2,5-dione (2a). Hexylglycolide (5.9 g, 38% yield) was

isolated as white crystals mp 77-80 °C (lit. 78-80 °C).¹⁷⁶ ¹H NMR: δ 4.88 (dd, $J = 8.05$ Hz, $J = 4.88$ Hz), δ 4.83 (dd, $J = 7.81$ Hz, $J = 4.39$ Hz, 2H total for the signals at 4.88 and 4.83), 1.97-2.10 (m, 2H), 1.88-1.97 (m, 2H), 1.40-1.56 (br m, 4H), 1.22-1.36 (br m, 12H), 0.75-0.91 (t, 6H, $J = 6.84$ Hz). ¹³C NMR: δ 166.99, 165.84, 76.36, 75.56, 31.89, 31.41, 30.36, 30.06, 28.69, 28.52, 24.45, 24.28, 22.44, 22.41, 13.96, 13.93. MS (m/z): 285.2 (M+1).

3,6-Dioctyl-1,4-dioxane-2,5-dione (2b). Octylglycolide (8.8 g, 48% yield) was isolated as white crystals, mp 77-80.5 °C. ¹H NMR: δ 4.88 (dd, $J = 8.05$ Hz, $J = 4.88$ Hz), δ 4.83 (dd, $J = 7.81$ Hz, $J = 4.39$ Hz, 2H total for the signals at 4.88 and 4.83), 1.97-2.10 (m, 2H), 1.87-1.97 (m, 2H), 1.41-1.56 (br m, 4H), 1.19-1.36 (br m, 20H), 0.75-0.94 (t, 6H, $J = 6.84$ Hz). ¹³C NMR: δ 166.98, 165.85, 76.37, 75.58, 31.92, 31.76, 31.73, 30.08, 29.21, 29.17, 29.10, 29.06, 29.05, 28.88, 24.51, 24.34, 22.59, 22.57, 14.04. MS (m/z): 341.3 (M+1).

3,6-Didecyl-1,4-dioxane-2,5-dione (2c). Decylglycolide (9.1 g, 42%) was isolated as white crystals, mp 82-86 °C. ¹H NMR: δ 4.88 (dd, $J = 8.05$ Hz, $J = 4.88$ Hz), δ 4.83 (dd, $J = 7.81$ Hz, $J = 4.39$ Hz, 2H total for the signals at 4.88 and 4.83), 1.97-2.10 (m, 2H), 1.87-1.96 (m, 2H), 1.40-1.57 (br m, 4H), 1.18-1.36 (br m, 28H), 0.75-0.91 (t, 6H, $J = 6.84$ Hz). ¹³C NMR: δ 166.99, 165.84, 76.36, 75.56, 31.90, 31.83, 31.82, 30.06, 29.50, 29.47, 29.44, 29.40, 29.25, 29.23, 29.21, 29.05, 28.87, 24.51, 24.33, 22.61, 14.05. MS (m/z): 397.3 (M+1).

3,6-Didodecyl-1,4-dioxane-2,5-dione (2d). Dodecylglycolide (13.4 g 54% yield) was isolated as white crystals, mp 83-86 °C (lit. 82.5-83.5 °C).¹⁸⁸ ¹H NMR: δ 4.88 (dd, $J = 8.05$ Hz, $J = 4.88$ Hz), δ 4.83 (dd, $J = 7.81$ Hz, $J = 4.39$ Hz, 2H total

for the signals at 4.88 and 4.83), 1.97-2.10 (m, 2H), 1.87-1.97 (m, 2H), 1.41-1.56 (br m, 4H), 1.18-1.36 (br m, 36H), 0.78-0.92 (t, 6H, $J = 6.84$ Hz). ^{13}C NMR: δ 166.98, 165.85, 76.38, 75.58, 31.92, 31.87, 30.09, 29.61, 29.59, 29.56, 29.53, 29.46, 29.41, 29.31, 29.27, 29.23, 29.06, 28.89, 24.52, 24.35, 22.65, 14.08. MS (m/z): 453.4 (M+1).

3,6-Ditetradecyl-1,4-dioxane-2,5-dione (2e). Tetradecylglycolide (8.1 g, 29% yield) was isolated as white crystals, mp 87-89 °C (lit. 86-87 °C).¹⁸⁸ ^1H NMR: δ 4.88 (dd, $J = 8.05$ Hz, $J = 4.88$ Hz), δ 4.83 (dd, $J = 7.81$ Hz, $J = 4.39$ Hz, 2H total for the signals at 4.88 and 4.83), 1.98-2.11 (m, 2H), 1.88-1.97 (m, 2H), 1.41-1.55 (br m, 4H), 1.18-1.36 (br m, 44H), 0.77-0.90 (t, 6H, $J = 6.84$ Hz). ^{13}C NMR: δ 166.96, 165.86, 76.39, 75.60, 31.94, 31.90, 30.11, 29.66, 29.64, 29.62, 29.60, 29.58, 29.55, 29.47, 29.42, 29.34, 29.28, 29.24, 29.07, 28.90, 24.53, 24.36, 22.66, 14.10. MS (m/z): 509.4 (M+1).

3,6-Dihexadecyl-1,4-dioxane-2,5-dione (2f). Hexadecylglycolide (17.7 g 57% yield) was isolated as white crystals, mp 89-92 °C (88.5-90.5 °C).¹⁸⁸ ^1H NMR: δ 4.88 (dd, $J = 8.05$ Hz, $J = 4.88$ Hz), δ 4.83 (dd, $J = 7.81$ Hz, $J = 4.39$ Hz, 2H total for the signals at 4.88 and 4.83), 1.98-2.12 (m, 2H), 1.88-1.97 (m, 2H), 1.41-1.55 (br m, 4H), 1.20-1.37 (br m, 52H), 0.78-0.92 (t, 6H, $J = 6.84$ Hz). ^{13}C NMR: δ 166.96, 165.87, 76.40, 75.61, 31.95, 31.91, 30.12, 29.69, 29.67, 29.66, 29.64, 29.63, 29.61, 29.58, 29.56, 29.48, 29.43, 29.35, 29.28, 29.25, 29.08, 28.91, 24.54, 24.37, 22.68, 14.11. MS (m/z): 565.4 (M+1).

Bulk polymerization of substituted glycolides. Solvent free polymerizations were run in sealed tubes prepared from 3/8 in. diameter glass

tubing. A representative polymerization is described. Monomer (~150 mg) and a small magnetic stir bar were added to a tube and then the tube was connected to a vacuum line and evacuated at 12 mTorr for 12 hours. After backfilling with argon, a syringe was used to add anhydrous toluene solutions of Sn(2-ethylhexanoate)₂ and *t*-butylbenzyl alcohol (~0.02M) to give the desired monomer/catalyst/initiator ratio. After careful removal of the toluene under vacuum, the tube was flame-sealed under vacuum and immersed into a magnetically stirred oil bath at 130 °C. At the end of the polymerization, the tube was removed from the bath, cooled in ice water and opened. The contents of the tube were dissolved in dichloromethane. A portion of the solution was evacuated to dryness and analyzed by ¹H NMR to determine conversion. The remaining solution was washed with 2M HCl three times, followed by precipitation into cold 2-propanol multiple times to ensure the removal of residual catalyst and unreacted monomer. Typical polymer yields were > 60%. For kinetic runs, multiple tubes were prepared. For each data point, three tubes were removed from the heating bath at predetermined intervals, cooled in ice and opened, and the contents were analyzed by NMR for conversion. The data reported are averages of the three samples.

Solution polymerizations of substituted glycolides. Solution polymerizations were run in Schlenk flasks with magnetic stirring. The general procedure is as follows. The desired amount of glycolide was added to the flask, weighed, and held under vacuum (10 mTorr) overnight. Using a syringe, degassed anhydrous toluene, and catalyst and initiator solution in anhydrous

toluene were transferred into the Schlenk flask under argon ($[M] = 0.2M$, $[Cat]/[I] = 1$, $[M]/[I] = 100$). The polymerizations were heated with an oil bath controlled to $90 \pm 2^\circ$. At various times, a syringe was used to remove small volumes of the polymerization solutions and after the solvents were evaporated *in vacuo*, conversion was measured by NMR.

Hydrolytic degradation experiments. Polymer degradation experiments were carried out by placing ~25 mg of polymer in a test tube containing 15 mL of buffer solution (pH = 7.4). Taking care not to introduce air, the tube was inverted and sealed in a slightly larger second tube filled with buffer. The tubes were placed in a constant temperature bath at $55^\circ C$. At predetermined times, three tubes were removed from the bath and the degraded polymer was recovered by cooling the tip of the polymer-containing tube in dry ice to harden the polymer, and decanting the buffer. After drying under vacuum, the molecular weights were measured by GPC. The reported molecular weight data are the average of three samples.

Polymer characterization. The molecular weights of polymers were determined by gel permeation chromatography (GPC) at $35^\circ C$ using two PLgel 10μ mixed-B columns in series with THF as the eluting solvent at a flow rate of 1 mL/min. A Waters 2410 differential refractometer was used as the detector, and monodisperse polystyrene standards were used to calibrate the molecular weights. The concentration of polymer solutions used for GPC was 1 mg/mL. Differential scanning calorimeter (DSC) analyses of the polymers were obtained using a TA DSC Q100. Samples were run under a nitrogen atmosphere at a

heating rate of 10 °C/min, with the temperature calibrated with an indium standard. Thermogravimetric analyses (TGA) were run in air at a heating rate of 10 °C/min using a Perkin-Elmer TGA7. X-ray diffraction (WAXS) patterns were recorded using a Rigaku RTP 300 RC X-ray generator (Cu K α = 1.5418 Å) with a Rigaku diffractometer. Samples were obtained by heating bulk polylactides on a glass slide above the melting points to form a uniform film, followed by various thermal treatments.

Chapter 3 PEO-grafted Comb Poly lactides

Introduction

Thermoresponsive polymers that exhibit a lower critical solution temperature (LCST) at near-ambient temperatures have attracted a great deal of attention in the past two decades. One of the most studied systems is aqueous solutions of poly(*N*-isopropylacrylamide) which undergoes a rapid and reversible sol-gel transition when heated through its LCST.¹⁹⁰⁻¹⁹² Besides *N*-isopropylacrylamide and its copolymers, various polymers such as poly(methacrylate)s,¹¹⁵ poly(styrene)s,¹²² poly(phosphazene)s,¹⁹³⁻¹⁹⁶ poly(vinyl ether)s,^{104,107} and chitosan¹⁹⁷ have been reported to exhibit LCST behavior. Although their unique phase transition suggests potential applications in fields such as drug delivery systems,¹⁹⁷⁻¹⁹⁹ smart surfaces,²⁰⁰ bioseparations, and for controlling enzyme activity, the vast majority of LCST polymers are non-biodegradable, limiting their biomedical applications.

Lactide based polymers are an important class of degradable aliphatic polyesters. Due to their biodegradability and biocompatibility, poly lactides have long been used in medical applications as degradable sutures and implants, and are currently being developed for controlled drug delivery and degradable scaffolds for tissue engineering.²⁰¹⁻²⁰⁴ For these applications, it is important to have access to polymers that exhibit a broad range of physical properties. The properties of these polymers can typically be tailored by controlling of the stereochemistry of lactic acid precursors,^{175,205} manipulating their crystallinity, or

creating copolymers.^{173,206-208} Not surprisingly, there also is substantial interest in developing thermoresponsive polylactides. For example, thermoresponsive injectable drug-delivery systems were developed from thermoresponsive poly(ethylene oxide) and polylactide diblock and triblock copolymers (PEO-PLA and PEO-PLA-PEO).²⁰⁸ A disadvantage of such systems is that practical applications limit the allowable PEO block length and that manipulation of the transition temperature requires precise control over the length of lactide block. Furthermore, structural heterogeneity may lead to unpredictable degradation profiles, resulting in complicated drug release kinetics.

An alternative method for tailoring the thermoresponsive properties of polylactides is to replace the methyl group of the lactic acid repeat unit with different substituents and regulate polymer properties by the nature of the substituents. The effectiveness of this approach was proved by the successful synthesis of a various of substituted polylactides such as poly(phenyllactide),¹⁷⁷ polymandelide,¹⁷⁸ and alkyl substituted polylactides.¹⁷⁶

Recent reports have shown that introducing pendant oligo(ethylene oxide) groups onto a hydrophobic polymer backbone can lead to new water-soluble thermoresponsive polymers.^{104,107,115,122,193,194,196,197,209} For example, polymethacrylates that have two and three ethylene oxide units in the side chain exhibit LCSTs at 26 and 52 °C, respectively,¹¹⁵ and PEO-grafted polystyrene with three and four ethylene oxide units in the side chain shows LCST behavior at 13 and 39 °C, respectively.¹²² Additionally, the presence of PEO moieties can render the polymer resistant to protein adsorption, making them attractive biomaterials.⁹⁴

The few PEO-grafted polyesters^{94,150,151,210,211} reported to date all suffer from either a low grafting density, backbone degradation or a high polydispersity, and none has been shown to be thermoresponsive.

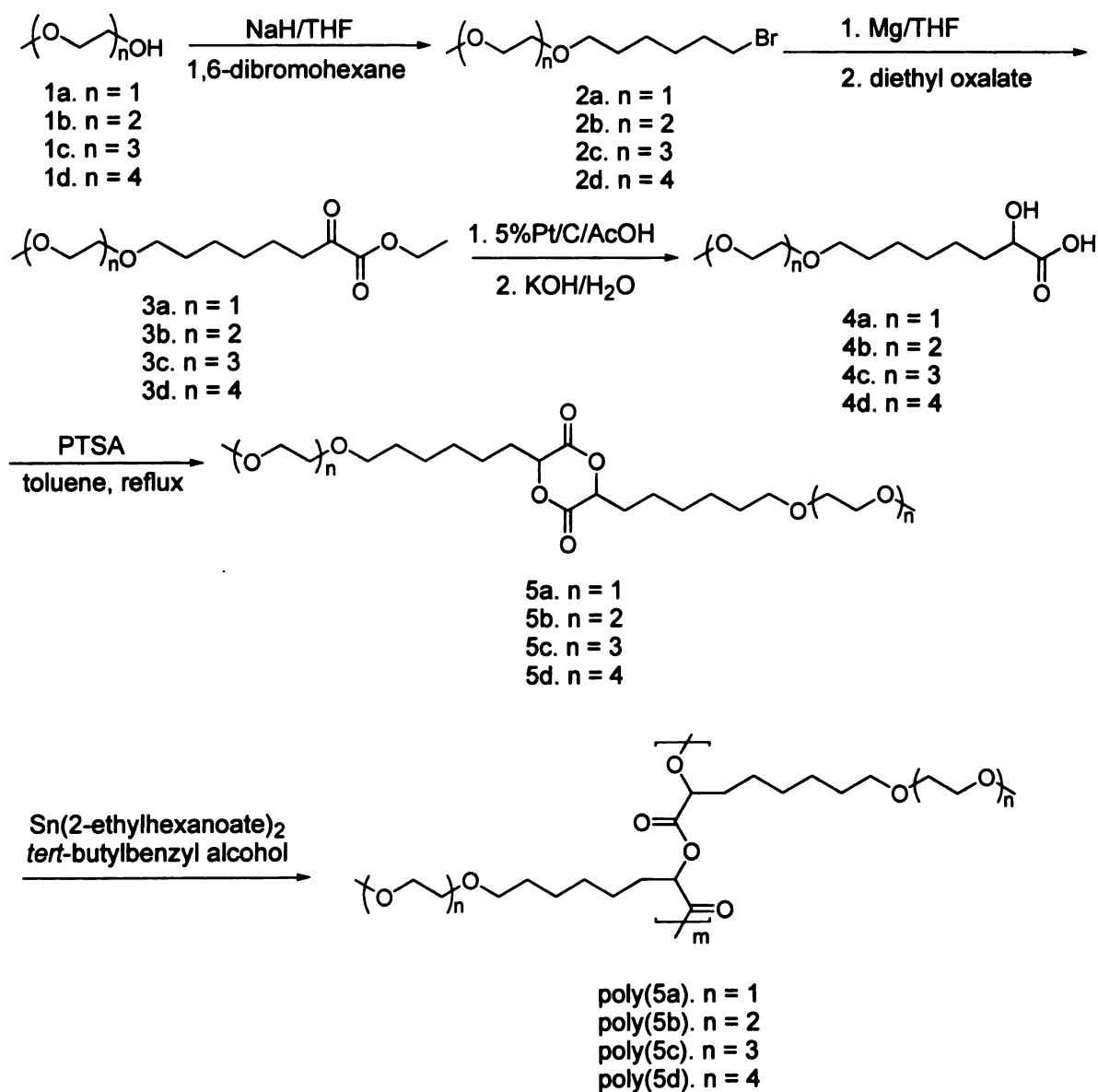
This chapter describes the synthesis and ring opening polymerization of lactide monomers that have been functionalized with exact length oligo(ethylene glycol) chains. The resulting PEO-grafted-poly lactides should have predictable degradation behavior because of their inherent structural homogeneity. These polymers are water-soluble and show LCST behavior, suggesting potential applications in biotechnology such as localized drug delivery.

Results and Discussion

Monomer synthesis

Scheme 12 shows the synthetic route to the four substituted glycolides described in this chapter. Our synthetic approach to all of the monomers follows the same pattern, the reaction of oligo(ethylene glycol) monomethyl ether with 1,6-dibromohexane to generate the corresponding oligo(ethylene glycol) monomethyl ether capped with hexyl bromides. The reaction of Grignard reagents generated from these functionalized oligo(ethylene glycol)s with diethyl oxalate at -78 °C provided the corresponding α -keto esters. Typically, the conversion of diethyl oxalate is >85%, with no detectable contamination from addition of a second Grignard equivalent to the substrate. Catalytic hydrogenation of the crude ketoesters at 1500 psig using Pt/C yielded the α -hydroxy esters, but since purification of the esters proved difficult, the crude α -

hydroxy esters were hydrolyzed and isolated as the α -hydroxy acids. To the best of our knowledge, none of the α -hydroxy acids were previously reported. Crystallization from ether at $-80\text{ }^{\circ}\text{C}$ and $-40\text{ }^{\circ}\text{C}$ gave the acids as colorless to light brown oils in overall yields of 41-80% based on diethyl oxalate. A representative ^1H NMR spectrum, that of compound **4b**, is shown in **Figure 48**.



Scheme 12. Synthesis of PEO-grafted polyglycolides

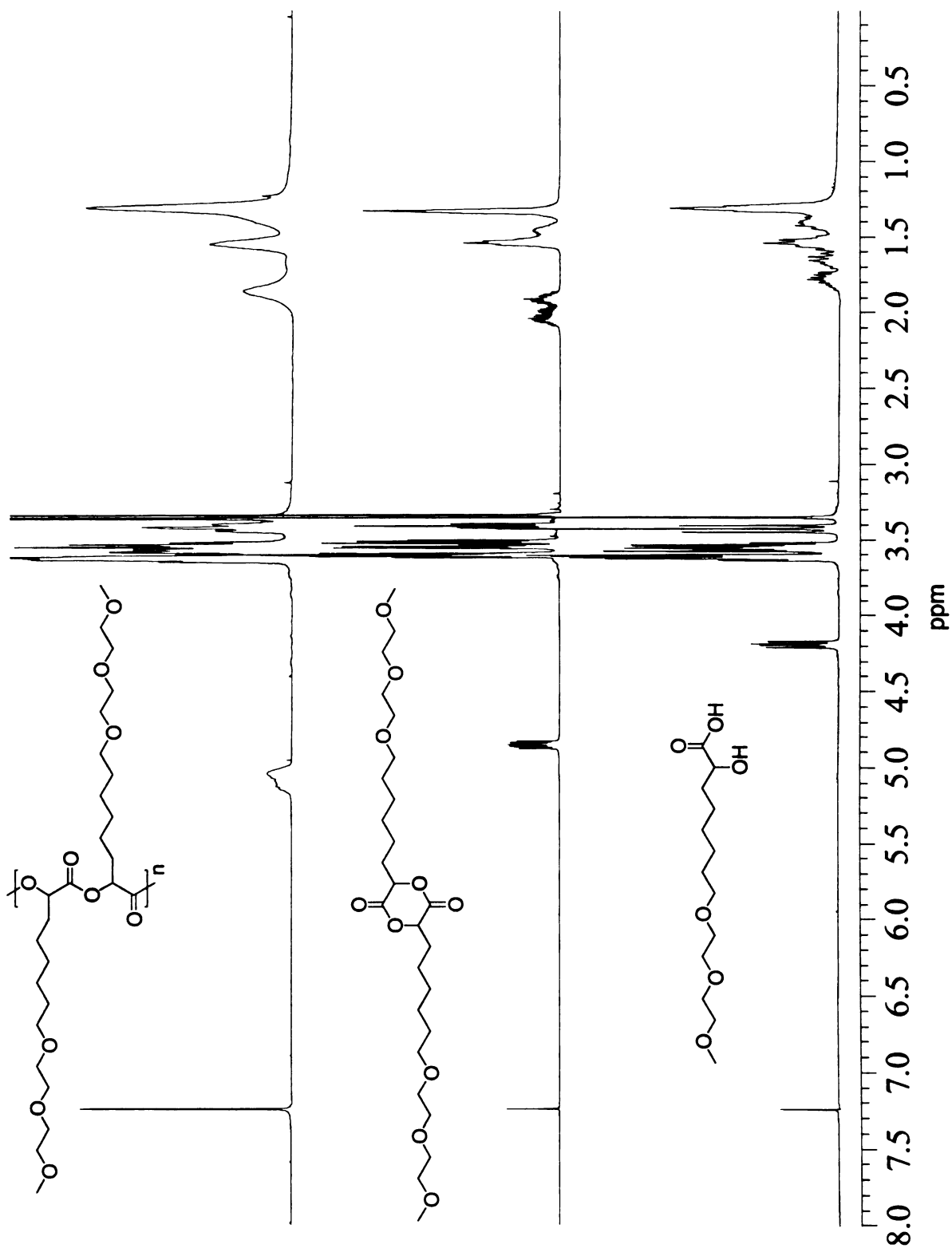


Figure 48. ¹H NMR spectra for 4b, 5b, and poly(5b).

The methine proton appears as doublet of doublets at 4.20 ppm and intense signals between 3.50 ppm and 3.65 ppm are characteristic of the methylene protons of the EO units. The methylene protons of the hexyl spacer adjacent to PEO segment appear as a triplet at 3.42 ppm and the ω -methoxy protons as a singlet at 3.35 ppm.

Dimerization of the α -hydroxy acids in refluxing toluene using *p*-toluenesulfonic acid as a catalyst yielded a mixture of the *R,S* and *R,R/S,S* diastereomers in ~45% yield before distillation. The major byproducts consisted of linear oligomers, which could in principle be recycled or thermally cracked to yield additional monomer. A representative ^1H NMR, that of compound **5b**, is shown in **Figure 48**. The methine protons of the 3,6-disubstituted glycolide ring appear as two sets of doublets of doublets centered at 4.88 and 4.83 ppm; integration of these two peaks in the ^1H NMR spectrum of crude product confirms the 1:1 ratio of the *meso* to *rac* diastereomers expected for the statistical coupling of a racemic mixture of hydroxy acids. Crystallization from ether significantly alters the diastereomeric ratio, favoring isolation of the *meso* diastereomer. Similar results were obtained for the other glycolides. We note that ^1H NMR also provides a convenient method for monitoring the polymerization reaction. As shown in **Figure 48** for glycolide **5b**, the methine peaks at 4.85 evolve into a broad peak at ~5.10 ppm during polymerization allowing straightforward calculation of the conversion of monomer to polymer.

Bulk polymerization

Bulk polymerizations of PEO-functionalized glycolides at 130 °C using *t*-butylbenzyl alcohol as the initiator and Sn(2-ethylhexanoate)₂ as the catalyst yielded PEO-grafted polylactides. The catalyst:monomer:initiator ratio for all polymerizations was 500:1:1. Since residual alcohol or water in monomer can also act as initiator and lead to lower than expected molecular weights, it is essential to have pure and dry monomers to obtain high molecular weight polymers. Because of the hydrophilic PEO segment in these PEO functionalized monomers, much more stringent purification and drying processes are required compared to hydrophobic glycolide monomers. All monomers were freshly distilled by K ugelrohr distillation after recrystallization and dried under vacuum at >100 °C before polymerization. (During K ugelrohr distillation, the monomer epimerized to a statistical mixture of diastereomers). The conversion of monomer to polymer was followed by ¹H NMR. The crude polymers were purified by dialysis against acetone and vacuum dried to give clear viscous liquids. Polymer molecular weights were measured by GPC in THF, and are reported relative to polystyrene standards.

Table 4. Bulk polymerization results for PEO functionalized glycolides.

Monomer	Time (hr)	Conversion (%) ^a	<i>M_n</i> (theo.) ^b	<i>M_n</i> ^c	PDI ^c
5a	4	97	209,500	148,500	1.28
5b	11	65	169,000	56,400	1.10
5c	20	73	221,900	59,800	1.16
5d	20	74	257,500	10,600	1.12

a. Measured by ¹H NMR; b. Corrected for conversion; c. Measured by GPC in THF using polystyrene standards for calibration

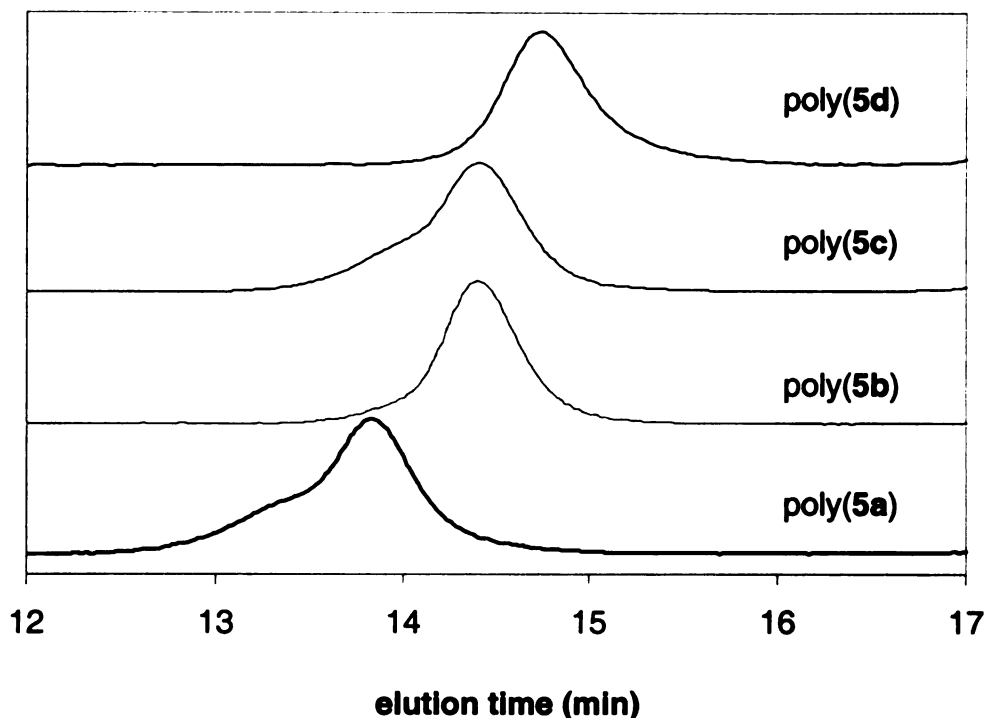


Figure 49. GPC traces of PEO-grafted polylactides

Typical polymerization results are listed in **Table 4** and the corresponding GPC traces are shown in **Figure 49**. The GPC molecular weights were lower than the theoretical values in all cases. Although low apparent molecular weights could be due to residual alcohol or water in the monomer, it is likely that the PEO segments in the side chains alter the hydrodynamic size of the polymer in THF leading to lower relative molecular weights. We also observed that multiple distillations of monomer or higher distillation temperatures generally led to slower polymerization rates and lower molecular weights, suggesting that thermal decomposition may introduce impurities into the monomer. The relative contributions of these effects and the origin of occasional shoulders seen on the high molecular weight side of GPC GPC traces (see the data for poly(5a) peak and poly(5c) in **Figure 49**) are unclear.

Polymer properties

The decomposition temperatures of polymers measured using TGA define the limiting use temperatures of the polymers. As shown in **Figure 50**, the TGA profiles for all polymers are similar, with the onset for decomposition at around

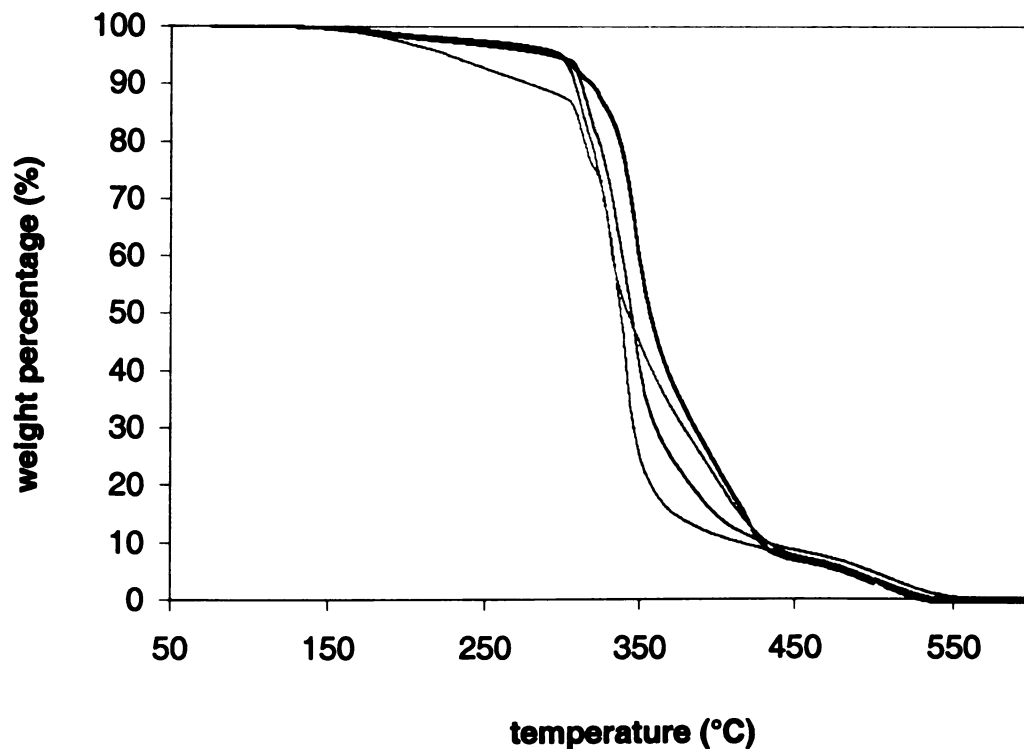


Figure 50. TGA of PEO-grafted polylactides (10 °C/min in air, samples were held at 135 °C for 30 min prior to run. Pink line: poly(5a); red line: poly(5b); black line: poly(5c); blue line: poly(5d))

300 °C. The weight loss at lower temperatures is most likely due to the loss of hydrogen bonded water because the weight loss depended on the length of time the sample was held at 135 °C prior to starting the run. The DSC scans displayed in **Figure 51** show no thermal transitions between -55 °C and 100 °C; the low

intensity and the consistency of the “peak” at ~ -15 °C suggests that it is a baseline fluctuation.

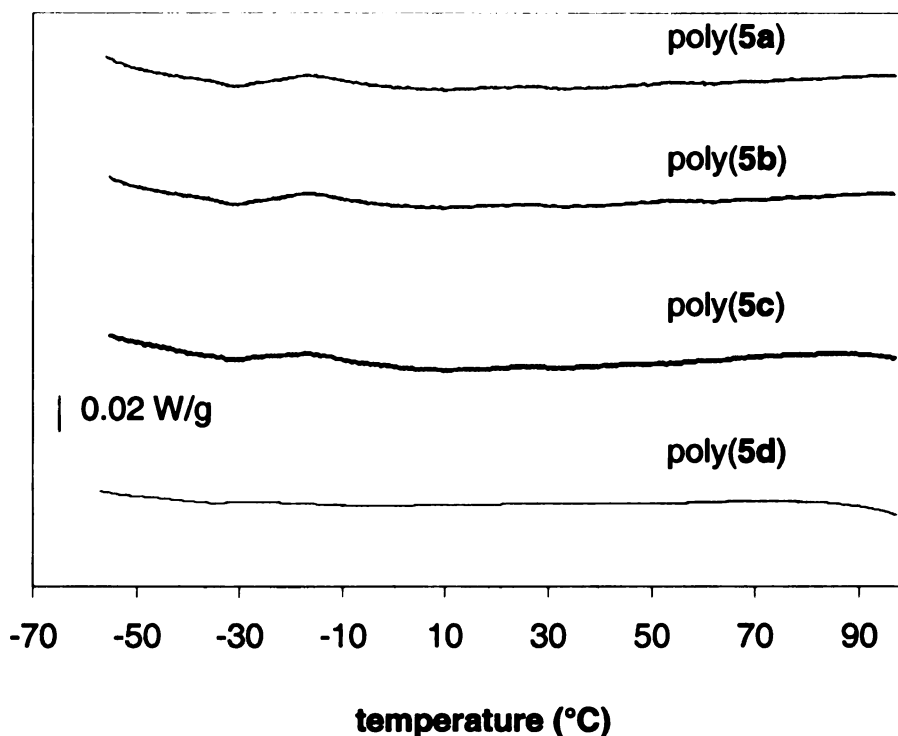


Figure 51. DSC traces of PEO-grafted poly lactides (second heating scan, 10 °C/min in N₂)

Aqueous solubility and solution properties of PEO-grafted poly lactides

Poly(5a) and poly(5b) are insoluble in water. Although hydration of the hydrophilic side chains preclude a precise measurement of the contact angle, the polymers are clearly more hydrophilic than poly(hexyl glycolide) (contact angles of 50-75° compared to 100°). Poly(5c) and poly(5d) are water soluble and form clear solutions at temperatures below their LCST. To determine the cloud points, we prepared aqueous solutions of poly(5c) ($M_{n, GPC} = 59,800$, PDI = 1.16) and poly(5d) ($M_{n, GPC} = 10,600$, PDI = 1.12) with a concentration of 15 mg/mL.

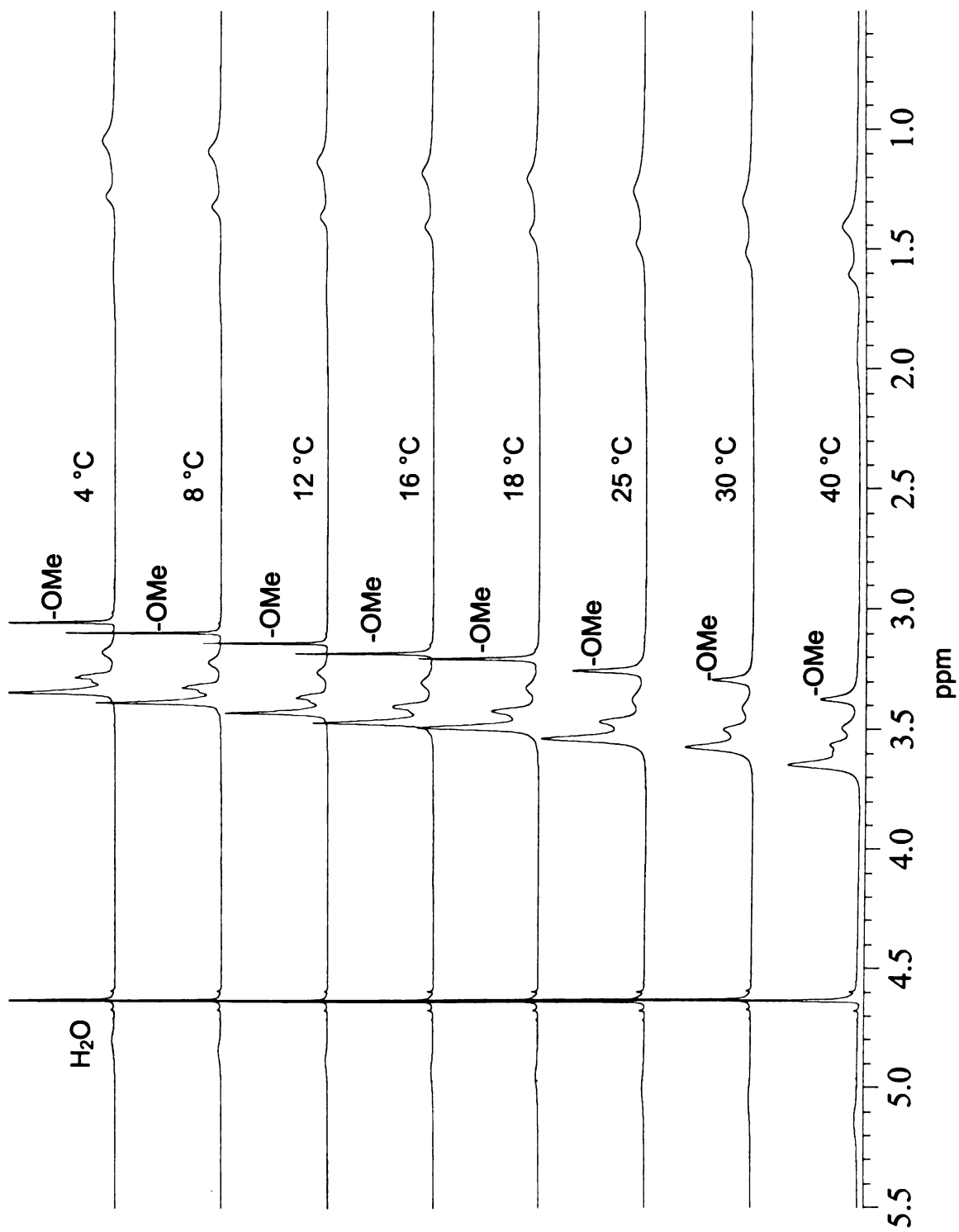


Figure 52. 500 MHz ¹H NMR spectra of poly(5c) ($M_n = 59,800$ g/mol, PDI = 1.16) in D₂O (15 mg/mL) at different temperatures.

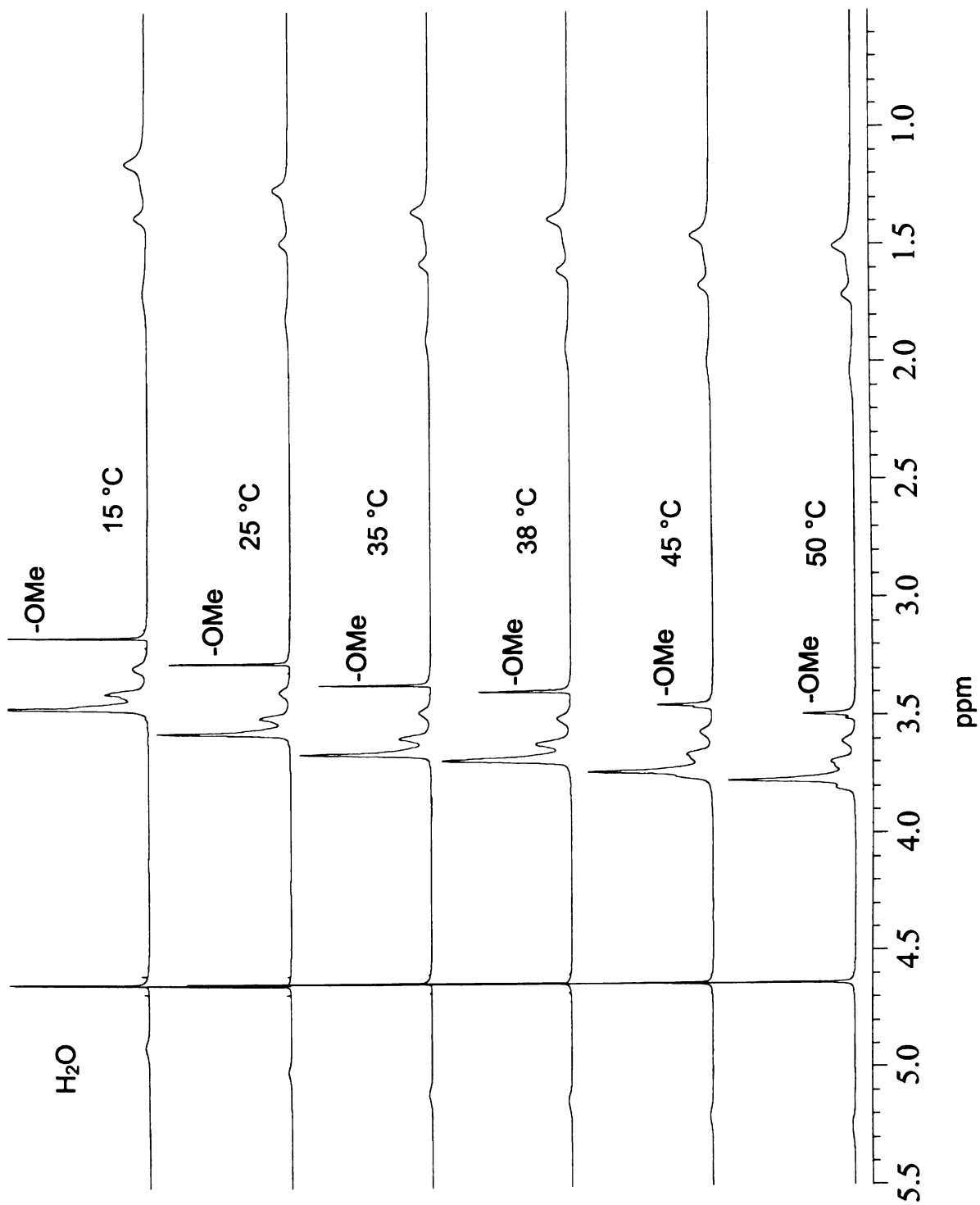


Figure 53. 500 MHz ¹H NMR spectra of poly(5d) ($M_n = 10,600$ g/mol, PDI = 1.12) in D₂O (15 mg/mL) at different temperatures.

Solutions of poly(**5c**) were transparent below 19 °C, and suddenly turned cloudy at 20 °C during the course of heating. After 24 hours at 25 °C, an obvious precipitate settled, but the precipitate re-dissolved when the solution was cooled. Similarly, solutions of poly(**5d**) exhibited a cloud point at 38 °C. Apparently, the cloud point increases with the length of oligo(ethylene glycol) group, as has been reported for other oligo(ethylene glycol)-grafted polymers.

We also used variable temperature ¹H NMR measurements to study the phase transitions of the two polymer solutions in D₂O. **Figure 52** and **Figure 53** show the ¹H NMR spectra of poly(**5c**) and poly(**5d**) solutions (15 mg/mL) at various temperatures, respectively. The height and position of water peak was used as an internal reference. When a solution of poly(**5c**) was heated from 4 °C to 18 °C, there were no visible changes in the height and shape of the proton signal from the terminal methoxy group. When heated to 25 °C, the peak broadened and the peak height noticeably decreased, indicating a phase transition from a soluble to an insoluble state somewhere between 18 °C and 25 °C, consistent with the cloud point measurements. For poly(**5d**), the height of the methoxy peak decreased and broadened between 35 °C to 45 °C, consistent with cloud point measurements that place the transition at 38 °C. The thermoresponsive behavior of the polymer solutions also can be monitored by variable temperature dynamic light scattering measurements. Shown in **Figure 54** are the DLS results for aqueous solutions of poly(**5c**) (3 mg/mL) at different temperatures. When the solutions were heated from 10 °C to 21 °C, the average hydrodynamic radius of the particles in the solution remained constant at ~5 nm.

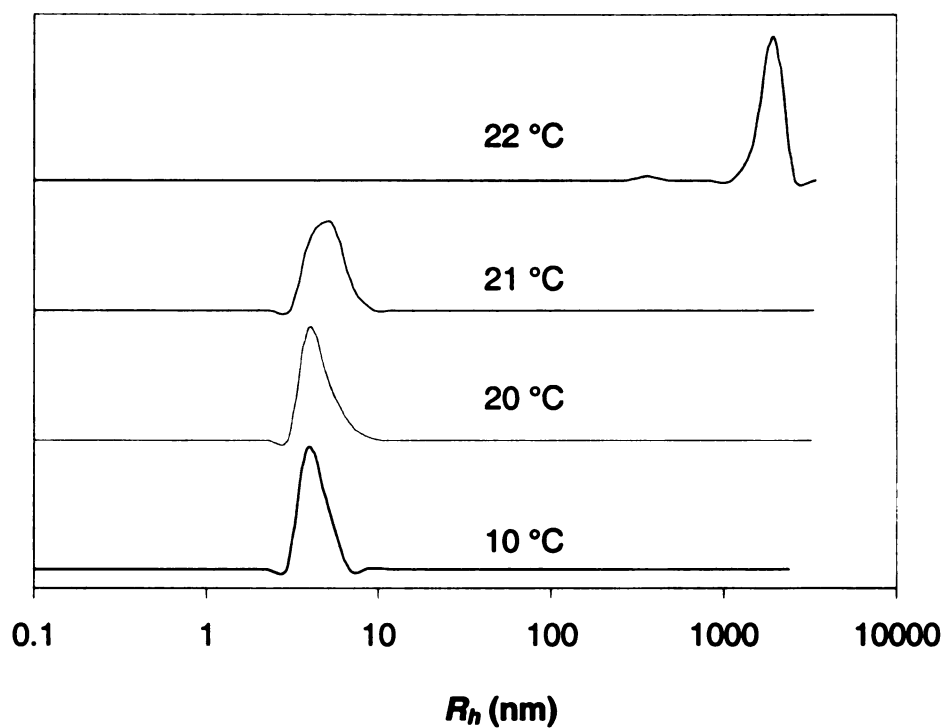


Figure 54. DLS results for poly(5c) ($M_n = 59,800$ g/mol, PDI = 1.16) in water (3 mg/mL) at different temperatures.

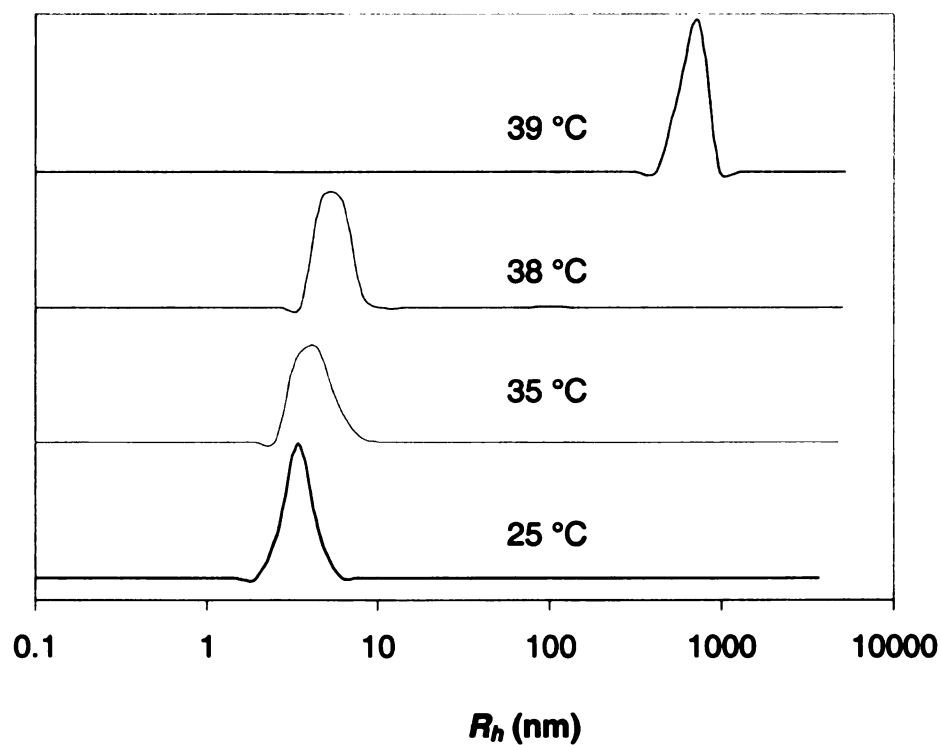


Figure 55. DLS results for poly(5d) ($M_n = 10,600$ g/mol, PDI = 1.12) in water (3 mg/mL) at different temperatures.

Further heating to 22 °C caused a drastic increase in the average hydrodynamic radius to hundreds of nanometers, and the variability of this value is consistent with polymer agglomeration. The DLS results for aqueous solutions of poly(5d) (3 mg/mL) are shown in **Figure 55**. Between 25 and 38 °C, the average hydrodynamic radius of the particles is essentially constant within experimental error. But heating the solution to 39 °C induces an increase in hydrodynamic radius to hundreds of nanometers, suggesting the polymer chains changed from a hydrated state to an agglomerated insoluble state.

Conclusions

We successfully synthesized a series of lactides that have one oligo(ethylene glycol) monomethyl ether chain per lactic acid residue. Their subsequent ring opening polymerization yielded high molecular weight PEO-grafted polylactides with narrow molecular weight distributions. Poly(5a) and poly(5b), having 1 and 2 PEO repeat units in the pendant chain, are hydrophilic but are not water soluble. Poly(5c) and poly(5d) are water-soluble, and we detected lower critical solution temperatures for both polymers. The cloud points of poly(5c) and poly(5d) in aqueous solutions were 20 °C and 37 °C respectively, which we confirmed by variable temperature ¹H NMR and DLS measurements.

Experimental Section

Materials. Ethylene glycol monomethyl ether (99%), di(ethylene glycol) monomethyl ether (99.6%), and tri(ethylene glycol) monomethyl ether (95%)

were purchased from Aldrich and distilled before use. 1,6-Dibromohexane (96%), NaH (60% dispersion in mineral oil), diethyl oxalate (99%) and 5 % platinum on activated carbon were obtained from Aldrich and used as received. Tetrahydrofuran (THF) was dried using an activated alumina column.

Characterization. The molecular weights of polymers were determined by gel permeation chromatography (GPC) at 35 °C using two PLgel 10 μ mixed-B columns in series with THF as the eluting solvent at a flow rate of 1 mL/min. A Waters 2410 differential refractometer was used as the detector, and monodisperse polystyrene standards were used to calibrate the molecular weights. The concentration of polymer solutions used for GPC was 1 mg / mL. Differential scanning calorimetry (DSC) analyses of the polymers were obtained using a TA DSC Q100. Samples were run under nitrogen at a heating rate of 10 °C/min, with the temperature calibrated using an indium standard. Thermogravimetric analyses (TGA) were run in air at a heating rate of 10 °C/min using a Perkin-Elmer TGA-7. ¹H NMR (300 or 500 MHz) and ¹³C NMR (75 or 125 MHz) spectra were acquired using either a Varian Gemini 300 spectrometer or a Varian UnityPlus-500 spectrometer with the residual proton signals from the CDCl₃ solvent used as the chemical shift standard. Mass spectral analyses were carried out on a VG Trio-1 Benchtop GC-MS. Variable temperature ¹H NMR (500 MHz) spectra were recorded on a thermoregulated Varian UnityPlus-500 spectrometer using polymer solutions in D₂O (D, 99.9%) with a concentration of 15 mg/mL. For each temperature, the solution was equilibrated for 20 min before acquiring the data. Variable temperature dynamic light scattering (DLS)

experiments were run on a temperature controlled Protein Solutions Dyna Pro-MS/X system. All samples were filtered through a 0.2 μm Whatman PTFE syringe filter. Samples were equilibrated in the instrument for 15 min at each temperature before taking the data used to calculate the hydrodynamic radius (R_h). The uniformity of the particle sizes was determined by a monomodal curve fit, which assumes a single particle size with a Gaussian distribution.

General synthetic procedure for PEO-functionalized hexyl bromides

The synthetic route to the desired monomers is summarized in **Scheme 12**. A general procedure is described here. A 2 L round bottom flask containing 600 mL of dry THF was cooled between $-25\text{ }^\circ\text{C}$ and $-35\text{ }^\circ\text{C}$ under a blanket of N_2 and charged with NaH (1.5 mol) and 1,6-dibromohexane (2.0 mol). The appropriate ethylene glycol monomethyl ether (1 mol) was dissolved in 500 mL dry THF and added dropwise into the stirred slurry over 5 hours. After the addition was complete, the mixture was stirred at $\sim -15\text{ }^\circ\text{C}$ for 24 hours and at $0\text{ }^\circ\text{C}$ for 2 days. The solids were removed by filtration, and the solvent was removed by rotary evaporation to give a light yellow oil, which was purified by fractional distillation.

1-Bromo-6-(2-methoxyethoxy)-hexane (2a). The distillate at $58\text{-}60\text{ }^\circ\text{C}$ (50 mTorr) was collected to give 151 g of **2a** (63%) as a colorless oil. ^1H NMR δ 3.53 (m, 2H), 3.49 (m, 2H), 3.42 (t, 2H, $J = 6.59\text{ Hz}$), 3.38 (t, 2H, $J = 6.84\text{ Hz}$), 3.34 (s, 3H), 1.84 (p, 2H), 1.59 (p, 2H), 1.38-1.46 (br m, 2H), 1.29-1.38 (br m, 2H). ^{13}C NMR δ 71.93, 71.20, 69.95, 58.97, 33.71, 32.65, 29.33, 27.90, 25.22.

1-Bromo-6-[2-(2-methoxyethoxy)-ethoxy]-hexane (2b). The distillate at 83-86 °C (30 mTorr) was collected to give 195 g of **2b** (69%) as a colorless oil. ^1H NMR δ 3.60 (m, 4H), 3.56 (m, 2H), 3.52 (m, 2H), 3.42 (t, 2H, $J = 6.59$ Hz), 3.36 (t, 2H, $J = 6.84$ Hz), 3.34 (s, 3H), 1.82 (p, 2H), 1.56 (p, 2H), 1.38-1.46 (br m, 2H), 1.30-1.38 (br m, 2H). ^{13}C NMR δ 71.94, 71.17, 70.63, 70.51, 70.08, 58.97, 33.75, 32.70, 29.40, 27.94, 25.27.

1-Bromo-6-[2-[2-(2-methoxyethoxy)-ethoxy]-ethoxy]-hexane (2c). The distillate at 108-112 °C (30 mTorr) was collected to give 213 g of **2c** (65%) as a colorless oil. ^1H NMR δ 3.61 (m, 8H), 3.51 (m, 4H), 3.41 (t, 2H, $J = 6.59$ Hz), 3.36 (t, 2H, $J = 6.84$ Hz), 3.33 (s, 3H), 1.82 (p, 2H), 1.54 (p, 2H), 1.37-1.45 (br m, 2H), 1.29-1.37 (br m, 2H). ^{13}C NMR δ 71.88, 71.11, 70.56, 70.53, 70.45, 70.04, 58.93, 33.70, 32.65, 29.36, 27.90, 25.23.

1-Bromo-6-(2-[2-[2-(2-methoxyethoxy)-ethoxy]-ethoxy]-ethoxy)-hexane (2d). After removal of excess 1,6-dibromohexane, the light brown residue was held under vacuum (10 mTorr) at 145 °C overnight and used without further purification because the attempts to distill this compound caused significant decomposition. ^1H NMR δ 3.57-3.64 (m, 16H), 3.48-3.55 (m, 5.5H), 3.39-3.43 (t, 2.7H, $J = 6.59$ Hz), 3.34-3.38 (t, 2.2H, $J = 6.84$ Hz), 3.32-3.34 (s, 3.8H), 1.77-1.85 (p, 2H), 1.50-1.59 (p, 2.6H), 1.37-1.45 (br m, 2.6H), 1.28-1.37 (br m, 2H). The integration of this compound was skewed due to contamination from by-products.

Synthesis of PEO monomethyl ether substituted α -hydroxy octanoic acids.

The appropriate bromide (0.5 mol) was dissolved in 600 mL dry THF and stirred with 24 g of magnesium turnings until the solution stopped boiling. The Grignard reagent was then added dropwise under nitrogen to a 2 L round bottom flask containing a stirred solution of diethyl oxalate (56 g, 0.38 mol) in dry THF (500 mL) at $-80\text{ }^{\circ}\text{C}$. The mixture was stirred for an additional hour at $-80\text{ }^{\circ}\text{C}$, and then was quenched by adding 300 mL 2M HCl into the reaction mixture. The water layer was extracted with ether ($5 \times 200\text{ mL}$) and the combined organic layers were dried over MgSO_4 . Filtration and removal of the solvents by rotary evaporation gave a light brown oil. After dissolving the oil in 500 mL ethanol and adding 1 g of 5% Pt/C and 15 g NaHCO_3 , the α -keto ester was hydrogenated at $\sim 1500\text{ psi}$. When ^1H NMR showed that the α -keto ester had fully reacted (disappearance of the triplet at 2.80 ppm), the solids were removed by filtration and the ethanol solution was concentrated by rotary evaporation to give a colorless oil. Saturated aqueous NaHCO_3 (1 L) was added and the mixture was heated to reflux for 3 days. When ^1H NMR showed the hydrolysis was complete (disappearance of the quartet at 4.30 ppm), the basic solution was continuously extracted with ether for 24 hours. The ether layer was discarded and the aqueous layer was acidified with concentrated HCl to $\sim \text{pH} = 1$. After continuous extraction with ether for 48 hours, the ether layer was dried over MgSO_4 , filtered, and evaporated to dryness to give the crude α -hydroxy acid. The final work up depended on the particular α -hydroxy acid as noted below.

2-Hydroxy-8-(2-methoxy ethoxy)-octanoic acid (4a). Three recrystallizations from ether at -40 °C followed by drying under vacuum (10 mTorr) at RT for 12 hours gave 71 g of **4a** (80%) as white crystals. ¹H NMR δ 4.21 (dd, 1H, *J* = 7.17 Hz, *J* = 4.39 Hz), 3.56 (m, 4H), 3.44 (t, 2H, *J* = 6.66 Hz), 3.37 (s, 3H), 1.80 (m, 1H), 1.67 (m, 1H), 1.56 (p, 2H), 1.24-1.50 (br m, 6H). ¹³C NMR δ 178.35, 71.89, 71.38, 70.06, 69.73, 58.88, 33.83, 29.27, 28.82, 25.69, 24.45.

2-Hydroxy-8-[2-(2-methoxy ethoxy)-ethoxy]-octanoic acid (4b). The crude product was recrystallized once from ether at -80 °C and twice from ether at -40 °C. The resulting colorless oil was then dried under vacuum (10 mTorr) at RT for 12 h to give 72 g of **4b** (67%) as a colorless oil at room temperature. ¹H NMR δ 4.20 (dd, 1H, *J* = 7.17 Hz, *J* = 4.39 Hz), 3.62 (m, 4H), 3.56 (m, 4H), 3.43 (t, 2H, *J* = 6.66 Hz), 3.35 (s, 3H), 1.78 (m, 1H), 1.66 (m, 1H), 1.55 (p, 2H), 1.24-1.48 (br m, 6H). ¹³C NMR δ 177.55, 71.68, 71.24, 70.34, 70.15, 69.96, 69.77, 58.75, 33.81, 29.12, 28.79, 25.61, 24.45.

2-Hydroxy-8-{2-[2-(2-methoxy ethoxy)-ethoxy]-ethoxy}-octanoic acid (4c). The crude product was recrystallized twice from ether at -80 °C and twice from ether at -40 °C. The colorless oil was dried under vacuum (10 mTorr) at room temperature for 12 h to give 76 g of **4c** (61%). ¹H NMR δ 4.20 (dd, 1H, *J* = 7.17 Hz, *J* = 4.39 Hz), 3.62 (m, 8H), 3.56 (m, 4H), 3.43 (t, 2H, *J* = 6.66 Hz), 3.35 (s, 3H), 1.78 (m, 1H), 1.66 (m, 1H), 1.55 (p, 2H), 1.24-1.48 (br m, 6H). ¹³C NMR δ 177.69, 71.77, 71.21, 70.44, 70.26, 69.97, 69.88, 33.83, 29.19, 28.78, 25.65, 24.47.

2-Hydroxy-8-(2-{2-[2-(2-methoxy ethoxy)-ethoxy]-ethoxy}-ethoxyl)-octanoic acid (4d). The crude product was recrystallized five times from ether at -80 °C. The light brown oil was dried under vacuum (10 mTorr) at room temperature for 12 h to give 57 g of **4c** (41%). ¹H NMR δ 4.20 (dd, 1H *J* = 7.08 Hz, *J* = 4.39 Hz), 3.62 (m, 12H), 3.56 (m, 4H), 3.43 (t, 2H, 2H, *J* = 6.59 Hz), 3.35 (s, 3H), 1.78 (m, 1H), 1.66 (m, 1H), 1.55 (p, 2H), 1.24-1.48 (br m, 6H). ¹³C NMR δ 177.37, 71.78, 71.21, 70.49, 70.43, 70.39, 70.26, 69.98, 69.91, 58.86, 33.84, 29.22, 28.79, 25.69, 24.46.

Synthesis of PEO monomethyl ether functionalized glycolides

The appropriate 2-hydroxy acid (0.1 mol) was placed in a 2 L round bottom flask, along with 1 g PTSA and ~1800 mL toluene. The solution was refluxed for 3 days, with the water removed azeotropically using a Barrett trap. After the toluene was removed by rotary evaporation, the residue was dissolved in 500 mL diethyl ether, washed with saturated NaHCO₃ and dried over MgSO₄. Filtration and removal of the ether gave the product as a light brown oil, which was purified by three recrystallizations from diethyl ether at low temperatures. These compounds are oils at room temperature.

3,6-Bis-[6-(2-methoxy-ethoxy)-hexyl]-[1,4]dioxane-2,5-dione (5a). The colorless oil was distilled (180 °C/3 mTorr) to give 9.6 g of **5a** (41%). ¹H NMR δ 4.88 (dd, *J* = 8.30 Hz, *J* = 4.88 Hz), δ 4.83 (dd, *J* = 7.69 Hz, *J* = 4.27 Hz, 1H total for the signals at 4.88 and 4.83), 3.52 (m, 4H), 3.40 (t, 2H, *J* = 6.66 Hz), 3.34 (s, 3H), 1.8-2.1 (br m, 2H), 1.4-1.6 (br m, 4H), 1.24-1.4 (br m, 4H). ¹³C NMR δ

166.87, 165.66, 76.24, 75.41, 71.87, 71.20, 71.15, 69.89, 58.93, 31.75, 29.87, 29.27, 28.74, 28.60, 25.65, 24.38, 24.18. Anal. Calcd. for C₂₂H₄₀O₈: C, 61.11; H, 9.26 Found: C, 60.80; H, 8.87. MS (m/z) 433.3 (M+1).

3,6-Bis-{6-[2-(2-methoxy-ethoxy)-ethoxy]-hexyl}-[1,4]dioxane-2,5-dione (5b).

The colorless oil was distilled (190 °C / 3 mTorr) to give 7.8 g of **5b** (28%). ¹H NMR δ 4.88 (dd, *J* = 8.30 Hz, *J* = 4.88 Hz), δ 4.83 (dd, *J* = 7.69 Hz, *J* = 4.27 Hz, 1H total for the signals at 4.88 and 4.83), 3.62 (m, 4H), 3.57 (m, 4H), 3.40 (t, 2H, *J* = 6.66 Hz), 3.34 (s, 3H), 1.9-2.2 (br m, 2H), 1.47-1.7 (br m, 4H), 1.3-1.47 (br m, 4H). ¹³C NMR δ 166.87, 165.69, 76.28, 75.46, 71.88, 71.18, 71.12, 70.57, 70.45, 70.01, 58.94, 31.80, 29.93, 29.33, 28.79, 28.65, 25.70, 24.43, 24.22. Anal. Calcd. for C₂₆H₄₈O₁₀: C, 60.00; H, 9.23 Found: C, 60.10; H, 9.60. MS (m/z) 521.1 (M+1).

3,6-Bis-(6-{2-[2-(2-methoxy-ethoxy)-ethoxy]-ethoxy}-hexyl)-[1,4]dioxane-2,5-dione (5c).

The colorless oil was distilled (210 °C / 3 mTorr) to give 6.9 g of **5c** (21%). ¹H NMR δ 4.88 (dd, *J* = 8.30 Hz, *J* = 4.88 Hz), δ 4.83 (dd, *J* = 7.69 Hz, *J* = 4.27 Hz, 1H total for the signals at 4.88 and 4.83), 3.62 (m, 8H), 3.57 (m, 4H), 3.40 (t, 2H, *J* = 6.66 Hz), 3.34 (s, 3H), 1.9-2.2 (br m, 2H), 1.47-1.7 (br m, 4H), 1.3-1.47 (br m, 4H). ¹³C NMR δ 166.84, 165.48, 76.05, 75.21, 71.64, 70.93, 70.88, 70.32, 70.29, 70.21, 69.80, 58.70, 31.54, 29.66, 29.15, 29.13, 28.61, 28.44, 25.51, 25.49, 24.21, 24.00. Anal. Calcd. for C₃₀H₅₆O₁₂: C, 59.21; H, 9.21 Found: C, 59.34; H, 9.60. MS (m/z) 609.4 (M+1).

3,6-Bis-[6-(2-[2-[2-(2-methoxy-ethoxy)-ethoxy]-ethoxy)-ethoxy]-hexyl]-

[1,4]dioxane-2,5-dione (5d). The light brown oil was distilled (238 °C / 3 mTorr) to give 5.2 g of **5d** (15%) as colorless oil. ¹H NMR δ 4.88 (dd, *J* = 8.30 Hz, *J* =

4.88 Hz), δ 4.83 (dd, $J = 7.69$ Hz, $J = 4.27$ Hz, 1H total for the signals at 4.88 and 4.83), 3.62 (m, 12H), 3.57 (m, 4H), 3.40 (t, 2H, $J = 6.66$ Hz), 3.34 (s, 3H), 1.9-2.2 (br m, 2H), 1.47-1.7 (br m, 4H), 1.3-1.47 (br m, 4H). ^{13}C NMR δ 166.90, 165.71, 76.31, 75.49, 71.88, 71.21, 71.16, 70.55, 70.52, 70.46, 70.03, 58.97, 31.84, 29.94, 29.38, 28.82, 28.69, 25.74, 24.46, 24.26. Anal. Calcd. for $\text{C}_{34}\text{H}_{64}\text{O}_{14}$: C, 58.62; H, 9.19 Found: C, 58.30; H, 9.25. MS (m/z) 697.4 (M+1).

Bulk Polymerization of PEO Functionalized Substituted Glycolides

Solvent free polymerizations were run in sealed tubes prepared from 3/8 in. diameter glass tubing. A representative polymerization is described. The desired amount of freshly distilled monomer and a small magnetic stir bar were added to the tube. The monomer was stirred and the tube was evacuated under vacuum (3 mTorr) for 12 hours at the desired temperature. After cooling to room temperature and back-filling with argon, a syringe was used to add toluene solutions of the catalyst ($\text{Sn}(\text{2-ethylhexanoate})_2$, 0.2 mol%) and initiator (*tert*-butylbenzyl alcohol, ~0.01 M). After careful removal of the toluene under vacuum, the tube was sealed under vacuum and immersed into an oil bath at 130 °C and stirred magnetically for the desired polymerization time. At the end of the polymerization, the tube was cooled in ice water and opened. A portion of the polymer was analyzed by NMR for conversion, and the remaining polymer was purified by dialysis (MWCO = 12-14,000) in acetone to give PEO-grafted polylactides.

Poly(5a). Monomer (2.24 g) was dried at 105 °C and polymerized for 4 h. The monomer conversion was 94%. After dialysis and removal of solvent by rotary evaporation, the residue was dried under vacuum (4 mTorr) at 70 °C overnight to give 1.86 g of Poly(5a) as a colorless viscous liquid (83%). ¹H NMR δ 5.01-5.23 (br, 1H), 3.53-3.64 (br, 4H), 3.44-3.52 (br. m, 2H), 3.39-3.43 (s, 3H), 1.82-2.03 (br, 2H), 1.55-1.70 (br, 2H), 1.28-1.53 (br, 6H). Anal. Calcd. for (C₂₂H₄₀O₈)_n: C, 61.11; H, 9.26 Found: C, 61.18; H, 9.33.

Poly(5b). The monomer (2.22 g) was dried at 115 °C and polymerized for 11 h. The monomer conversion was 95%. After dialysis and removal of solvent by rotary evaporation, the residue was dried overnight under vacuum (4 mTorr) at 70 °C to give Poly(5b) (1.72 g) as a colorless viscous liquid (77%). ¹H NMR δ 5.01-5.23 (br, 1H), 3.64-3.72 (br. m, 4H), 3.54-3.64 (br, 4H), 3.43-3.52 (br. m, 2H), 3.37-3.43 (s, 3H), 1.83-2.05 (br, 2H), 1.54-1.69 (br, 2H), 1.25-1.52 (br, 6H). Anal. Calcd. for (C₂₆H₄₈O₁₀)_n: C, 60.00; H, 9.23 Found: C, 59.83; H, 9.11.

Poly(5c). The monomer (1.90 g) was dried at 120 °C and polymerized for 15 h. The monomer conversion was 87%. After dialysis and removal of solvent by rotary evaporation, the residue was dried under vacuum (4 mTorr) at 70 °C overnight to give 1.40 g of Poly(5c) as a colorless viscous liquid (73%). ¹H NMR δ 5.01-5.24 (br, 1H), 3.63-3.74 (br. m, 8H), 3.54-3.63 (br, 4H), 3.42-3.51 (br. m, 2H), 3.38-3.42 (s, 3H), 1.79-2.05 (br, 2H), 1.53-1.69 (br, 2H), 1.25-1.53 (br, 6H). Anal. Calcd. for (C₃₀H₅₆O₁₂)_n: C, 59.21; H, 9.21 Found: C, 59.13; H, 9.06.

Poly(5d). The monomer (1.3 g) was dried at 130 °C and polymerized for 20 hrs. The monomer conversion was 74%. After dialysis and removal of solvent by

rotary evaporation, the residue was stirred under vacuum (4 mTorr) overnight to give 0.68 g of Poly(**5d**) as light yellow liquid (52%). $^1\text{H NMR } \delta$ 5.01-5.23 (br, 1H), 3.64-3.71 (br. m, 12H), 3.55-3.63 (br, 4H), 3.43-3.50 (br. m, 2H), 3.38-3.42 (s, 3H), 1.80-2.05 (br, 2H), 1.54-1.69 (br, 2H), 1.25-1.52 (br, 6H). Anal. Calcd. for $(\text{C}_{34}\text{H}_{64}\text{O}_{14})_n$: C, 58.62; H, 9.19 Found: C, 58.64; H, 9.08.

Chapter 4 Functionalization of Polylactides by “Click” Chemistry

Introduction

Aliphatic polyesters derived from lactide, glycolide and ϵ -caprolactone have been extensively studied for biomedical applications due to their biodegradability and biocompatibility. However, their range of applications is limited by their hydrophobic nature and the lack of chemical functionality along the polymer backbone to support further modification. Polyesters with pendant hydroxyl,^{210,212,213} carboxyl,²¹⁴ poly(ethylene oxide),^{150,151,210,211} allyl,^{215,216} and acetylene¹⁵⁰ functionalities have been synthesized using a variety of strategies including polymerization of functional monomers, post-polymerization modifications of polymers, or a combination of these two approaches. However, the functional monomer approach typically involves complex and tedious synthetic procedures, while careful control of conditions is required in the case of post-polymerization modification to avoid backbone degradation. In most cases, the chemical modifications are limited to a single class of functional groups. Having a single procedure that allows the introduction of a family of pendant functional groups onto a single polyester substrate polymer is highly desirable.

Because of its high selectivity, reliability, and tolerance to broad range of functional groups and reaction conditions, “click” chemistry, specifically the copper(I)-mediated 1,3-dipolar cycloaddition of azides and alkynes, is an excellent strategy for elaborating polymer architectures. “Click” chemistry has been used for the preparation of block copolymers,^{141,217} cross-linked

adhesives,¹⁵⁵ dendrimers,^{136-138,154} and for the introduction of pendant and terminal functional groups into various polymers including polyesters.^{144-148,150,151,157} The Emrick group first described the use of aqueous “click” chemistry to graft azide-terminated PEO and peptides onto polyesters containing pendant acetylene groups.¹⁵⁰ Later, Jérôme and coworkers found Emrick's conditions caused significant backbone degradation during functionalization,¹⁵¹ and using less severe conditions (THF as the solvent), they were able to introduce PEO, tertiary amines and ammonium salts onto caprolactone-based polyesters having pendant azides. However, in Jérôme's case, it is necessary to end-cap the terminal hydroxyl group of the polymer backbone to avoid significant backbone degradation when using lactide copolymers as substrates, and click reactions using CuI, the catalyst used by Jérôme, are known to cause more side reactions than *in situ* generated Cu(I).¹³⁴ It would be useful to have a simpler and more reliable protocol for click functionalization of polyesters, and especially polyesters wholly based on lactide monomers.

We are interested in tailoring the properties of polylactides through the synthesis and polymerization of substituted lactides. Over the years, this approach has led to the successful preparation of poly(phenyllactide),¹⁷⁷ polymandelide,¹⁷⁸ alkyl substituted polylactides,¹⁷⁶ allyl substituted polylactide,²¹⁶ PEO substituted polylactides, and alkyl/PEO substituted amphiphilic polylactides.²¹⁸ Stimulated by the versatility of post-polymerization modification of polyesters by click chemistry and the usefulness of having wholly lactide-based functional polymers, we synthesized and polymerized the acetylene-

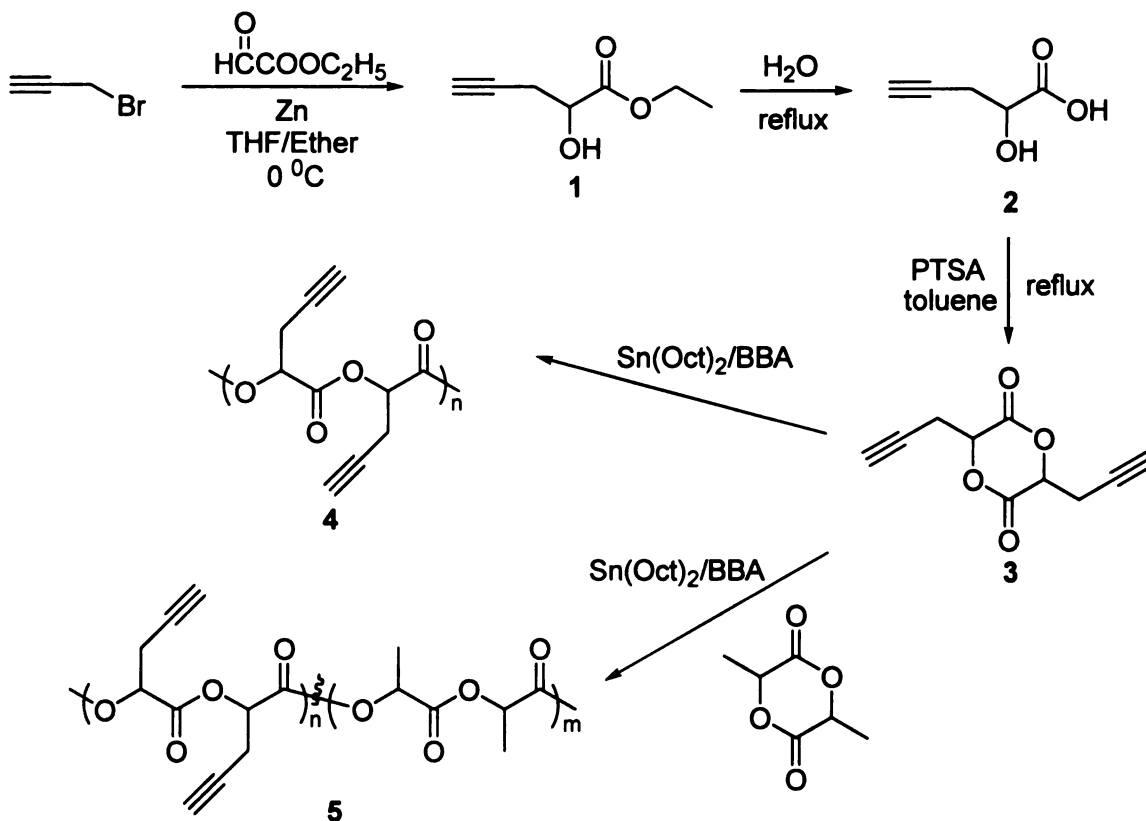
functionalized glycolide monomer, 3,6-dipropargyl-1,4-dioxane-2,5-dione (**3**). The subsequent polymerization of glycolide **3** provided the homopolymer of **3** as well as random and block copolymers with lactide that have pendant acetylene groups available for the attachment of functionality using click chemistry. The drawbacks encountered in Emrick's and Jérôme's conditions for click functionalization of polyesters were overcome by carrying out the reaction in DMF at room temperature in the presence of CuSO₄ and sodium ascorbate. The effectiveness of this protocol was demonstrated by the preparation of alkyl and PEO grafted polylactides

Results and Discussion

Monomer synthesis.

Scheme 13 shows the synthetic route to propargyl glycolide, an acetylene-functionalized monomer, and its polymers. The Reformatsky-type reaction of propargyl bromide with freshly distilled ethyl glyoxylate in the presence of activated zinc generated ethyl 2-hydroxy-3-butynoate in 51% yield.²¹⁹ The byproducts, most likely oligomers, were removed by eluting the crude product through silica gel using a 70:30 mixture of hexane/ethyl acetate. Hydrolysis of the ester in refluxing water yielded 2-hydroxy-3-butynoic acid in 84% yield. Hydrolysis under basic conditions resulted in lower yields due to side reactions.

Dimerization of 2-hydroxy-3-butynoic acid in refluxing toluene using *p*-toluenesulfonic acid as a catalyst yielded a mixture of the *meso* and *racemic*



Scheme 13. Synthetic route to propargyl glycolide and its polymers

diastereomers in 34% yield. The byproducts primarily consisted of linear oligomers which could in principle be recycled or thermally cracked to yield additional monomer. The 300 MHz ¹H NMR spectrum of propargyl glycolide is shown in **Figure 56**. The methine protons of the propargyl glycolide ring appear as a triplet at 5.29 ppm and a doublet of doublets at 5.05 ppm; integration confirms the 1:1 ratio of the *meso* (R,S) to *rac* (RR/SS) diastereomers expected for the statistical coupling of a racemic mixture of hydroxy acids. After recrystallization, the diastereomeric ratio was 2:3, favoring *rac*-propargyl glycolide.

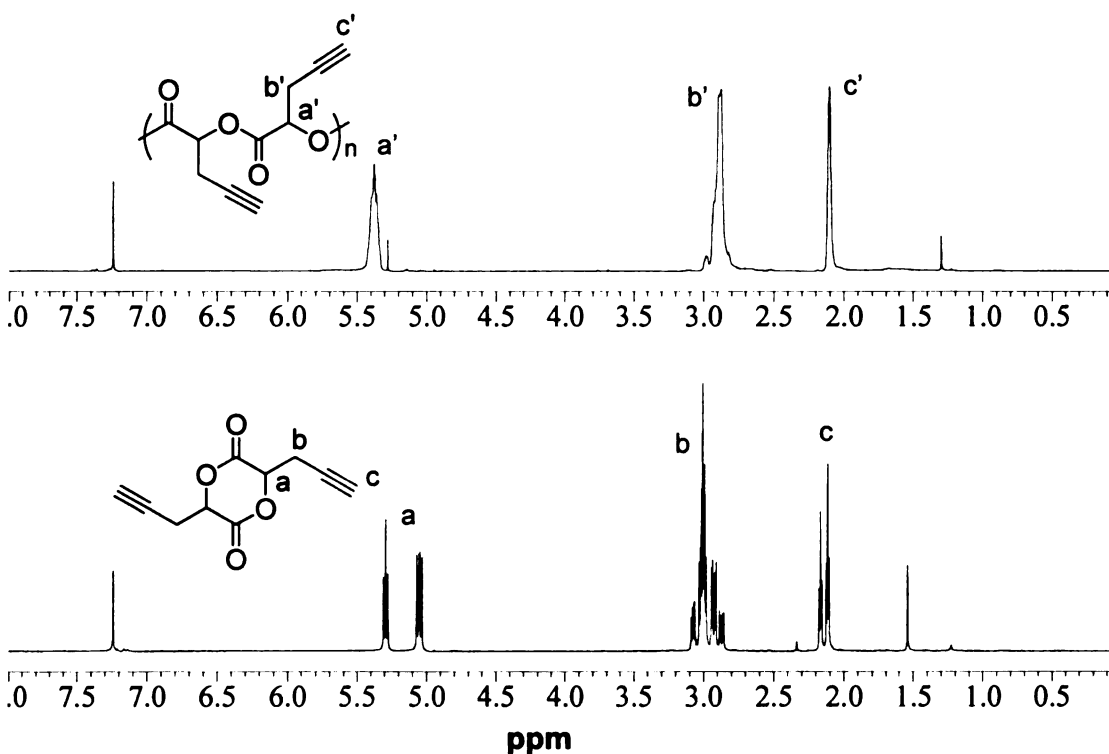


Figure 56. 300 MHz ^1H NMR spectra of propargyl glycolide and poly(propargyl glycolide)

Polymerization

Bulk polymerizations of propargyl glycolide at 130 °C catalyzed by $\text{Sn}(\text{2-ethylhexanoate})_2$ using *t*-butylbenzyl alcohol as the initiator yielded polymer 4. The catalyst to initiator ratio was 1:1 for all the polymerizations, and the monomer:initiator ratio ranged from 50:1 to 300:1. The increase in polymer molecular weight as a function of degree of polymerization (X_n) was monitored by gel permeation chromatography (GPC) in THF and calculated relative to polystyrene standards. The theoretical for each reaction, corrected for conversion, was calculated by ^1H NMR analyses of samples removed from the reaction mixture. We note that ^1H NMR provides a convenient method for

monitoring the polymerization reaction since as shown in **Figure 56**, the methine peaks at 5.05 and 5.29 ppm evolve into a broad peak at ~5.38 ppm during

Table 5. Bulk polymerization results for propargyl glycolide

[M]/[I]	Time (min)	Conversion (%) ^a	X_n ^b	M_n ^c (g/mol)	PDI ^c
50	10	85	43	9100	1.13
100	15	89	89	18500	1.21
150	25	91	136	28600	1.30
200	30	73	146	30500	1.31
250	55	78	195	38300	1.37
300	60	90	270	54600	1.38
300	75	94	280	56500	1.49

(a) Measured by ¹H NMR. (b) Corrected for conversion. (c) Measured by GPC in THF and calibrated using polystyrene standards.

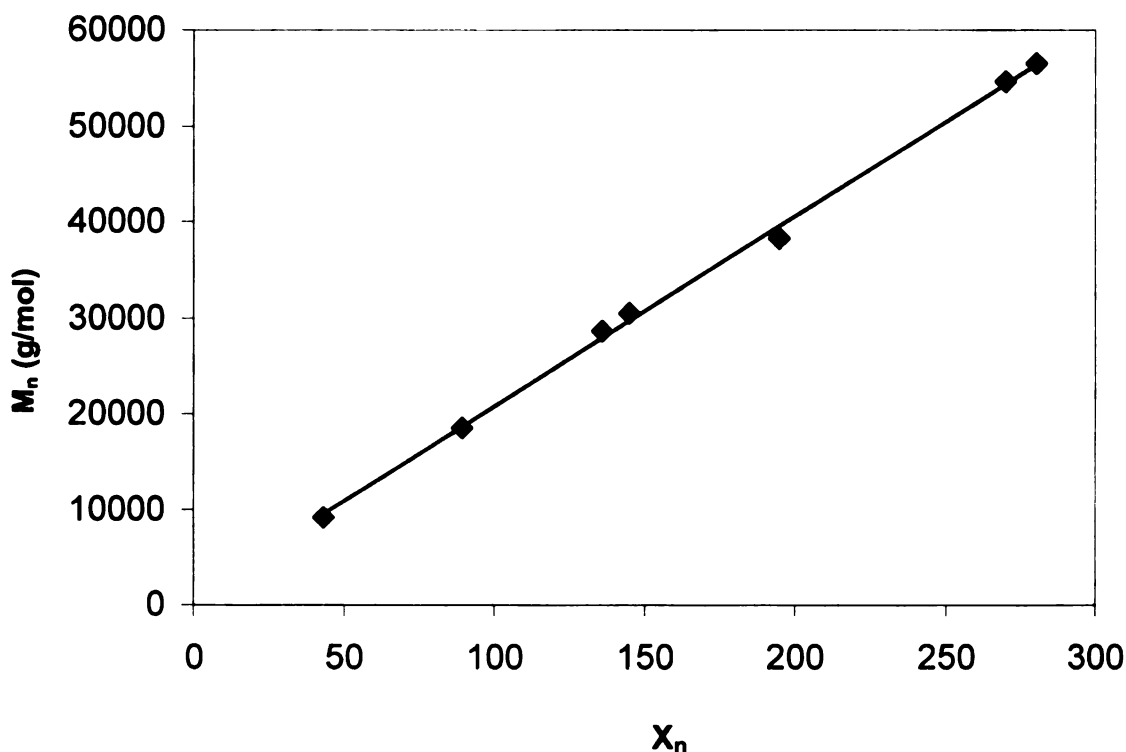


Figure 57. Relationship between M_n and X_n the degree of polymerization for the bulk polymerization of propargyl glycolide.

polymerization. Typical results for the bulk polymerization of propargyl glycolide are listed in **Table 5**. The molecular weights measured by GPC range from 9-60 kg/mol and are in good agreement with the theoretical values. The evolution of the molecular weight (measured by GPC) is plotted in **Figure 57** as a function of the expected number average degree of polymerization, X_n , corrected for conversion. The linear relationship and polydispersities of 1.2-1.5 are consistent with a reasonably controlled homopolymerization of propargyl glycolide.

Control over the number of pendant acetylene groups in a polymer can be achieved through copolymerization of propargyl glycolide and lactide. In a model copolymerization, we polymerized a mixture of *rac*-lactide and 8 mol% propargyl glycolide with the monomer to initiator ratio set to target an X_n of 300. The polymerization was run under the same conditions used for homopolymerization of propargyl glycolide. The incorporation of propargyl glycolide in the copolymer was 7.9%, calculated from integration of the ^1H NMR signals at δ 2.85 (methylene protons in pendant acetylene group) and the signal at δ 5.20 (methine proton in polymer backbone). The ^{13}C NMR spectrum of the copolymer is consistent with the propargyl glycolide being distributed throughout the polymer chains. Shown in **Figure 58** are spectra for the copolymer as well as polylactide and propargyl glycolide homopolymers. A comparison between the carbonyl regions showed the appearance of an additional peak at 168.92 ppm from the lactide repeat units and an ~ 0.2 ppm shift of the propargyl glycolide repeat units, suggesting that the propargyl glycolide units are not concentrated in “blocky” segments, but instead are distributed along the polymer backbone.

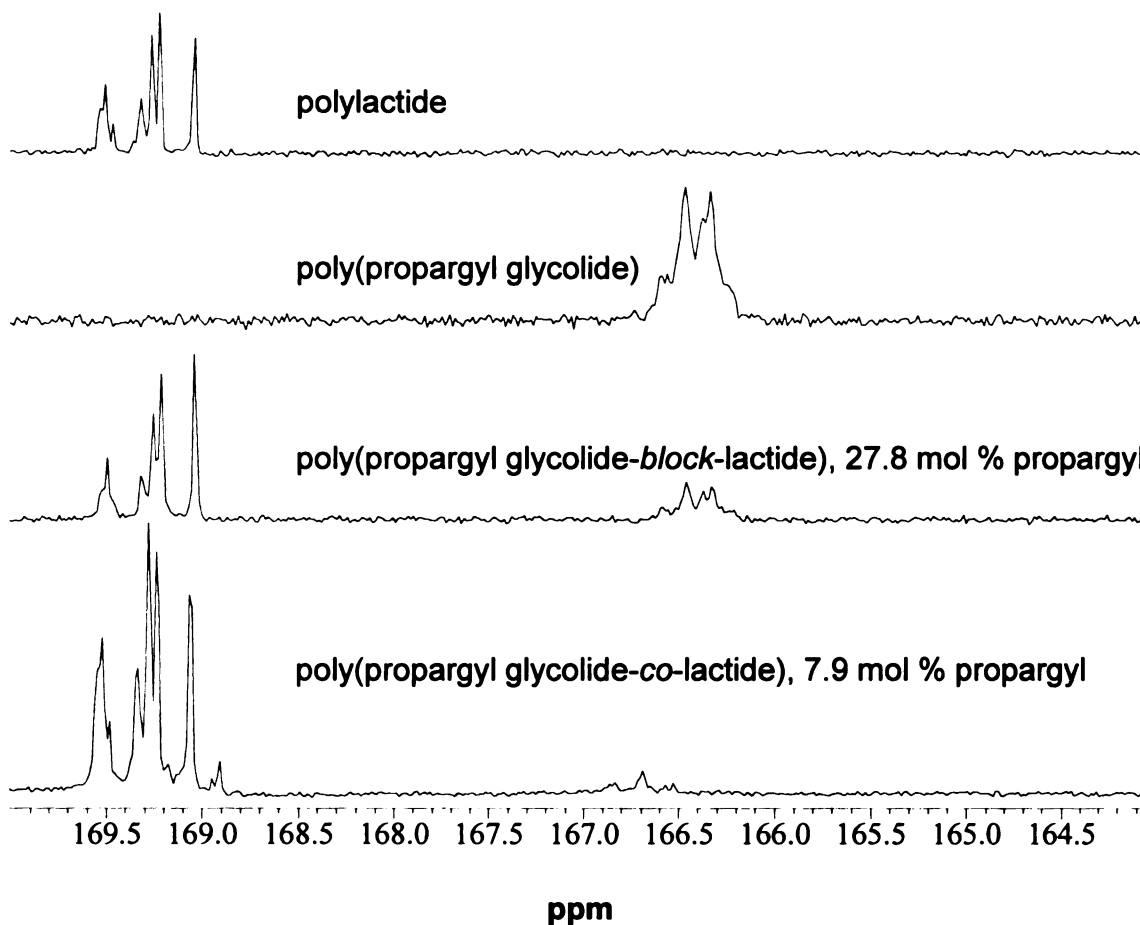


Figure 58. 75 MHz ^{13}C NMR carbonyl region of propargyl glycolide homopolymer, copolymers, and poly(lactide)

Poly(propargyl glycolide)(PPGL)-*block*-poly(lactide) was prepared by using scrupulously purified propargyl glycolide homopolymer as a macroinitiator ($X_n = 150$) and $\text{Sn}(2\text{-ethylhexanoate})_2$ as the catalyst for lactide polymerization ($[\text{I}]/[\text{Cat}] = 1$). The polymerization was carried out in THF at 70 °C to minimize transesterification. GPC traces show a shift of the peak molecular weight to shorter retention times, with slight broadening and a increase in the PDI, (**Figure 59**), both suggesting the formation of blocky architecture. The carbonyl regions in

the ^{13}C NMR spectrum of this copolymer directly correlate to the two homopolymers (Figure 58), which further confirms the blocky nature of this copolymer.

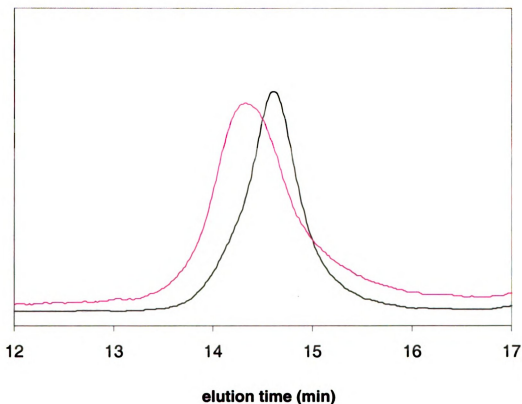


Figure 59. GPC traces of the PPGL macroinitiator, and PPGL-*block*-poly lactide. (black line: PPGL; pink line: PPGL-*block*-poly lactide)

“Click” functionalization

Alkyl-grafted poly lactides prepared by click chemistry. Errick *et al.* reported the click functionalization of pendant acetylenes incorporated into polycaprolactone. While the conditions for the reaction are somewhat aggressive, an aqueous solution of CuSO_4 and sodium ascorbate at $80\text{ }^\circ\text{C}$ or even higher temperatures for 10-12 hours,¹⁵⁰ they successfully modified

polycaprolactone without significant degradation. However, when poly(propargyl glycolide) (PPGL) ($M_{n, GPC} = 56\,500$, PDI = 1.49) was stirred in an acetone/water mixture at 50 °C for eight hours, GPC traces showed a significant reduction in M_n . This result was not surprising since the polylactide backbone is known to be more sensitive to degradation than polycaprolactone. Recently, Jérôme *et al.* reported the click functionalization of a copolymer prepared from an azide-functionalized caprolactone and lactide using milder conditions, CuI in THF at 35 °C.¹⁵¹ However, esterification of the terminal hydroxyl group was necessary to suppress backbone degradation, which complicated the synthetic procedure. In addition, the direct use of copper (I) salts in click reactions can reduce selectivity and lead to formation of undesired by-products.¹³⁴

We solved these problems by carrying out the “click” reaction in the presence of CuSO₄ and sodium ascorbate in DMF at room temperature. The low solubility of sodium ascorbate in DMF had no discernable effect on the reaction. The efficiency of the Huisgen 1,3-dipolar cycloaddition was demonstrated by grafting 1-azidodecane, synthesized by nucleophilic substitution of 1-bromodecane using sodium azide, onto PPGL. Thus, a propargyl glycolide polymer ($M_{n, GPC} = 35,500$, PDI = 1.44) was reacted with three equivalents of 1-azidodecane in the presence of 12 mol% sodium ascorbate and 5 mol% CuSO₄ (with respect to acetylene). ¹H NMR spectra taken after 2 hours showed that resonances at 2.85 ppm (-CH₂-CCH) and 2.05 ppm (-CH₂-CCH) had disappeared completely and a new peak appeared at 7.6 ppm (*H* of the triazole ring) indicating the quantitative formation of the triazole.

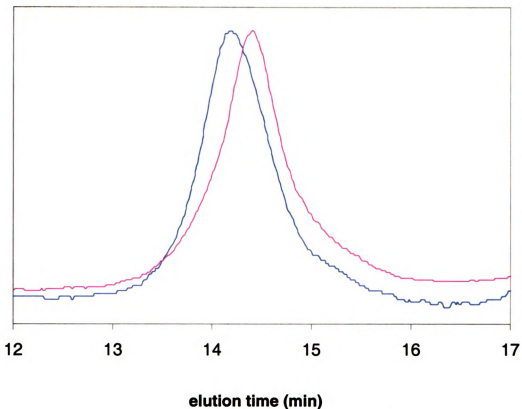


Figure 60. GPC traces of PPGL and C10-grafted PPGL. (pink line: PPGL; black line: C10-grafted PPGL)

The GPC results (**Figure 60**) of the resulting alkyl-grafted polymer ($M_{n, \text{GPC}} = 49,400$, $\text{PDI} = 1.41$) confirmed an increase in molecular weight, with the symmetry of the polymer peak and its molecular weight distribution unchanged. These experimental results confirm that no significant backbone degradation occurred during the “click” reaction of PPGL. To further confirm the stability of the backbone under these conditions, we treated PPGL ($M_{n, \text{GPC}} = 32,600$, $\text{PDI} = 1.45$) using the same experimental protocol (DMF, RT, 0.12 eq. sodium ascorbate, 0.05 eq. CuSO_4 , 2 h) but in the absence of 1-azidodecane. The GPC trace showed a slight decrease in molecular weight with the PDI unchanged ($M_{n, \text{GPC}} = 32\ 100$, $\text{PDI} = 1.44$) (**Figure 61**). Thus, “click” functionalization of PPGL

can be effected quantitatively in DMF at room temperature without significant backbone degradation by generating Cu(I) *in situ*. The formation of undesired by-products was minimized by the lower lower reaction temperature, and protection of the terminal hydroxyl group at the chain end was not necessary.

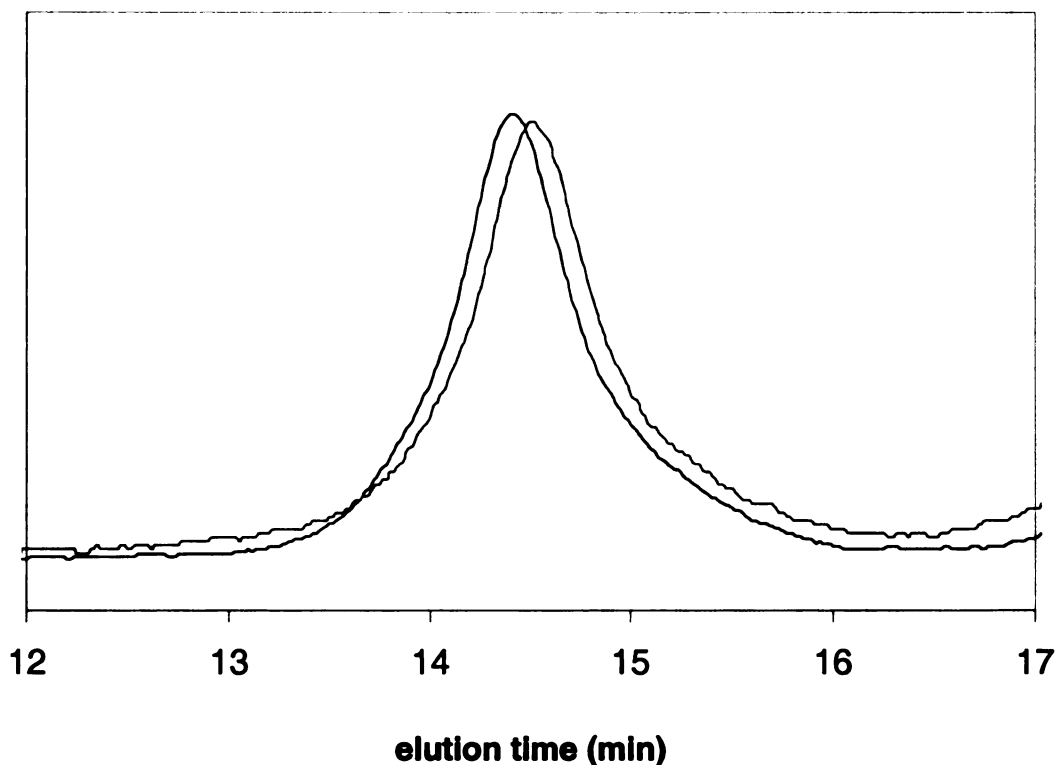


Figure 61. GPC traces from a control reaction where PPGL was exposed to click conditions, but without added azide. (black line: PPGL before the reaction; pink line: PPGL after the reaction)

PEG-grafted polylactide prepared by “click” chemistry. “Click” chemistry provides a simple route to analogs of the PEO-substituted polylactides described in Chapter 3. We selected a PEG-550 monomethyl ether as the pendant group because of its ready availability from commercial suppliers, and transformed it into the corresponding α,ω -PEG-550 monomethyl ether azide by tosylation of

PEG-550 monomethyl ether, followed by nucleophilic substitution using sodium azide. The azide group is easily identified by its IR absorption at 2105 cm^{-1} and by resonances for the methylene α to the azide at 3.38 ppm ($-\text{OCH}_2\text{CH}_2\text{N}_3$) in the ^1H NMR spectrum and at 50.5 ppm in the ^{13}C NMR spectrum. The “click” PEGylation of PPGL was performed under conditions identical to those described for grafting alkyl groups to PPGL (DMF, RT, 0.12 eq. sodium ascorbate, 0.05 eq. CuSO_4 , 3 eq. of azide, 2 h). Completion of the reaction was again confirmed by the disappearance of the ^1H NMR resonances at 2.85 ppm ($-\text{CH}_2\text{-CCH}$) and 2.05 ppm (CH_2CCH) and the appearance of a new resonance at 7.6 ppm (H of triazole). The crude product was purified by dialysis in acetone/water (1:1) mixture, and drying under vacuum gave the PEG-grafted polyglycolide as a water-soluble, viscous liquid tinted light green due to contamination by Cu(II).

Direct GPC analysis of this PEG-grafted polylactide proved to be problematic. When THF was used as solvent, we did not detect the polymer eluting from the column and we speculated that either the polymer and THF were iso-refractive, or that the polymer had adsorbed onto the column. We ran several control experiments to rule out backbone degradation during “click” PEGylation. We first subjected PPGL ($M_{n,\text{GPC}} = 32,600$, PDI = 1.45) to the same experimental conditions (DMF, RT, 0.12 eq. sodium ascorbate, 3 eq. of PEG azide, 2 h) but in the absence of CuSO_4 . GPC results for the recovered PPGL ($M_{n,\text{GPC}} = 32,200$, PDI = 1.44) showed no sign of backbone degradation. In a related experiment, a

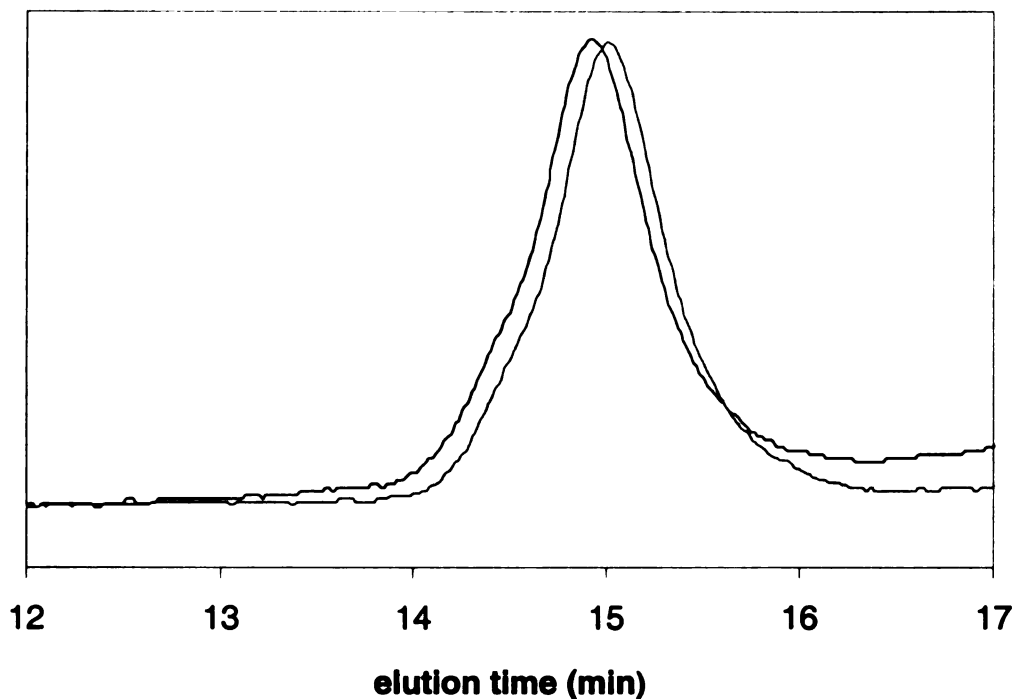


Figure 62. GPC traces of a polylactide sample exposed to “click” conditions. (black line: polylactide before the click reaction; pink line: polylactide after reaction)

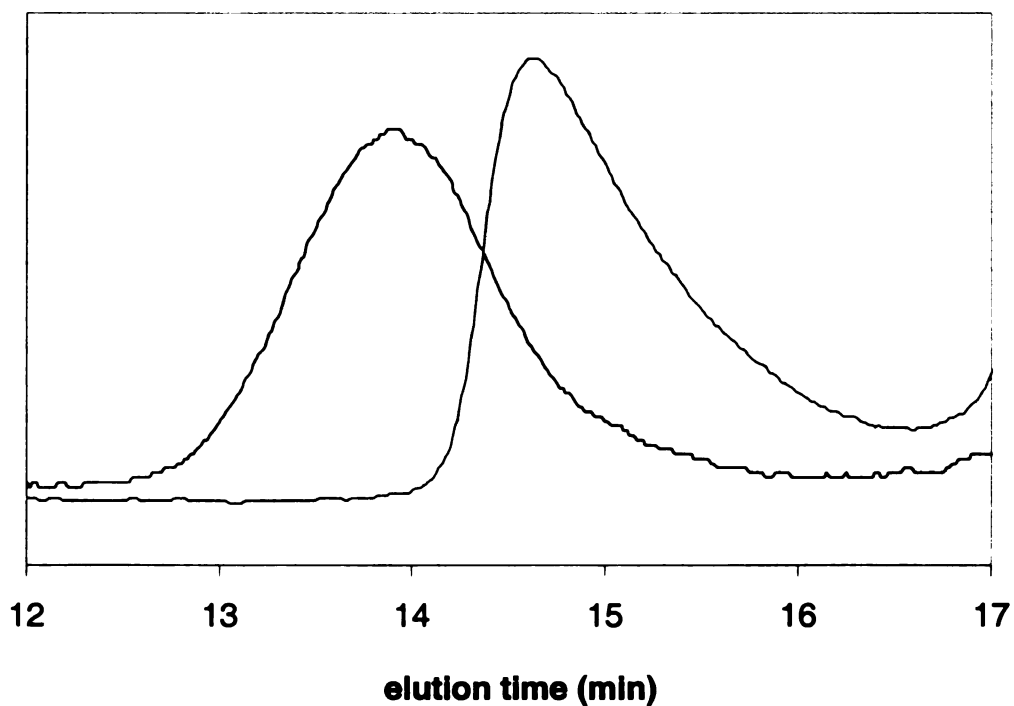


Figure 63. GPC traces for the poly(propargyl glycolide-co-lactide) click PEGylation. The concentration of propargyl glycolide in the copolymer was 7.9 mol %. (black line: copolymer before the click reaction; pink line: copolymer after click reaction)

mixture of PPGL ($M_{n, \text{GPC}} = 32,600$, PDI = 1.45) and polylactide ($M_{n, \text{GPC}} = 18,600$, PDI = 1.26) was subjected to the click PEGylation conditions. GPC results for the treated polylactide ($M_{n, \text{GPC}} = 18,300$, PDI = 1.26) (

Figure 62) again showed no loss in molecular weight.

The random copolymer of lactide with 7.9 mol% propargyl glycolide ($M_{n, \text{GPC}} = 63,600$, PDI = 1.66) was PEGylated under the identical experimental conditions. GPC analysis of this PEG-grafted copolymer shows a shift of the peak molecular weight to *longer* retention time than the starting copolymer (**Figure 63**), indicating a lower relative molecular weight ($M_{n, \text{GPC}} = 16,800$, PDI = 1.43). This result seems at odds with the results of previous control experiments that showed no change in molecular weight for polymers under click conditions, and we suspected the apparent decrease in molecular weight could be related to a decrease in the hydrodynamic radius of the polymer after PEGylation. Using light scattering, we characterized the starting copolymer ($M_{n, \text{LS}} = 83,200$, PDI = 1.20) and PEG-grafted copolymer ($M_{n, \text{LS}} = 156,000$, PDI = 1.21) which confirmed the stability of the polymer during “click” PEGylation. Thus, the combined results from these control experiments ruled out backbone degradation during the “click” PEGylation of propargyl glycolide homopolymer and copolymers, and also point to interesting solvent-induced changes in the size of the PEGylated polymer.

DiEG-grafted and DiEG/alkyl mixed-grafted polylactides and their thermoresponsive properties. 1-(2-Azidoethoxy)-2-(2-methoxyethoxy)ethane (DiEG-azide) was synthesized by the same procedure described for the synthesis of α, ω -PEG550 monomethyl ether azide. Recent reports demonstrate

that anchoring pendant oligo(ethylene glycol) groups onto hydrophobic polymer backbones can lead to water-soluble polymers that have lower critical solution temperatures (LCSTs) in an easily accessible temperature range, and that the LCST can be tuned by changing the PEG segment length.^{99,115,122} As described in Chapter 3, we found that the same design rule holds for polylactides. However, the synthesis of the thermoresponsive polylactides was rather difficult. Having devised a simple route to PPGL, click PEGylation of PPGL should provide easy access to thermoresponsive polylactides. From preliminary experiments using several oligo(ethylene glycol) azides, we found that the PEG-grafted polymer is water soluble (no cloud point) over the entire 0 to 100 °C range when there are three or more ethylene oxide units in the side chain. We did observe a cloud point for the DiEG-grafted polymer at ~ 80 °C, which is too high for biomedical applications.

Several strategies can be used to lower the LCST, including the introduction of additional methylene spacers between the azide group and the PEG segment, changing the ω -methyl group to a higher alkyl group, using shorter PEG segments, or by grafting a mixture of alkyl and DiEG groups to PPGL. To minimize the synthetic complexity, we adopted the mixture of DiEG/alkyl group strategy and carried out click chemistry using a 2:1 mixture of DiEG-azide and 1-azidodecane. By comparing the integration from δ 4.36-4.56 with δ 4.12-4.36 in the ^1H NMR spectrum of the grafted polymer, we concluded that ~48 % of the grafts were DiEG, which suggests that the click chemistry reaction rate for 1-

azidodecane is higher than for DiEG-azide. The resulting DiEG/alkyl mixed-grafted polylactide is still water-soluble at room temperature.

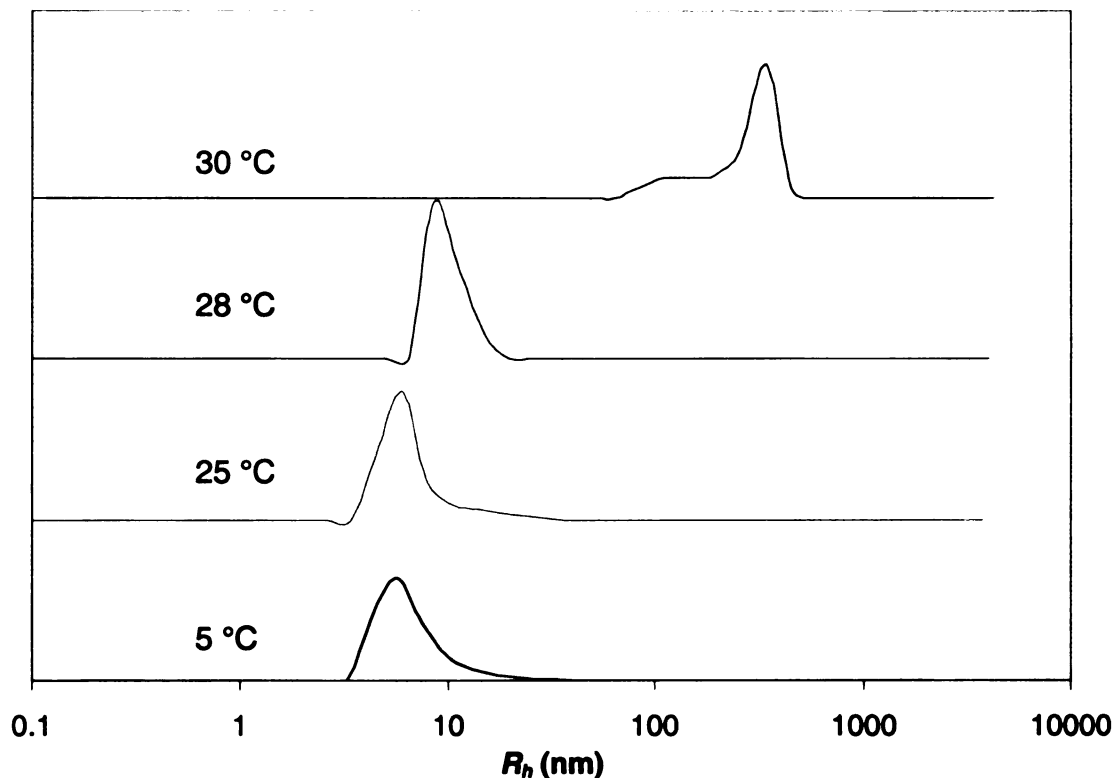


Figure 64. DLS of DiEG/alkyl-grafted PPGL (5 mg/mL in water)

To determine the cloud point, a 5 mg/mL solution of DiEG/alkyl grafted polylactide in water was prepared and filtered through a 0.2 μm PTFE syringe filter. The solution was transparent when the temperature was below 28 °C and turned into cloudy when heated to 31 °C. The thermoresponsive behavior of the polymer solution was also monitored by variable temperature dynamic light scattering measurements. Shown in **Figure 64** are the DLS results for a solution (5 mg/mL) of DiEG/alkyl grafted polylactide at different temperatures. When the solution was heated from 5 °C to 25 °C, the average hydrodynamic radius of

particles in the solution remained constant at ~5.5 nm. Upon further heating to 28 °C, the average hydrodynamic radius slightly increased to ~8 nm, and then dramatically increased to hundreds of nanometers at 30 °C. The magnitude of the hydrodynamic radius at >30 °C suggests a transition from a hydrated state to an agglomerated insoluble state.

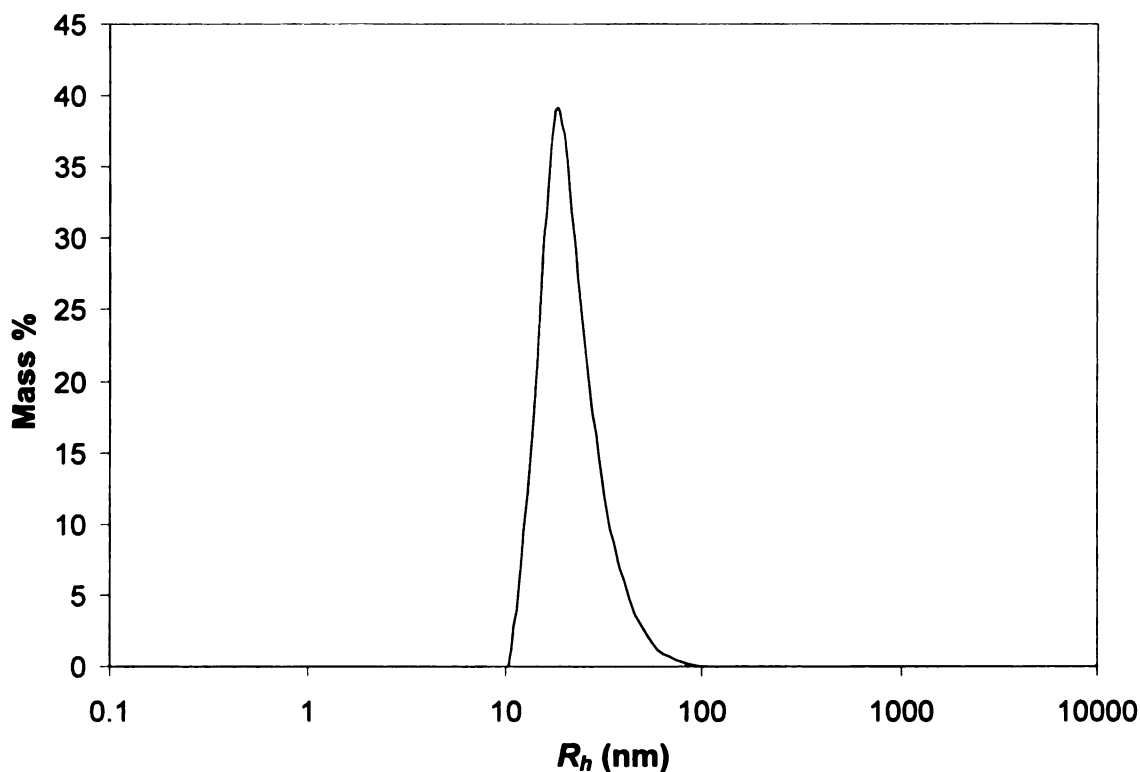


Figure 65. DLS of PEGylated PPGL-*block*-poly lactide in water

This approach to PEGylated polymers is easily extended to block copolymers. PPGL-*block*-PLA ($M_{n, GPC} = 38\ 000$, PDI = 1.44, 72 mol% lactide) was PEGylated using PEG-550 azide under the same experimental conditions as described before. The PEG-grafted PPGL-*block*-PLA was isolated as a green-tinted viscous liquid. The addition of an acetone solution of PEG-grafted PPGL-*block*-PLA to

magnetically stirred water followed by evaporation of acetone under reduced pressure resulted in a milky microemulsion. DLS measurement taken at room temperature for a 20 mg/mL solution (**Figure 65**) indicates the formation of polymeric micelles with an average hydrodynamic radius of 23 nm.

Conclusions

The synthesis of a propargyl glycolide **3** provides a convenient entry to “click” chemistry modification of polyglycolides. This functional monomer was homopolymerized in a controlled fashion to yield polyglycolide with pendant acetylene groups, and the preparation of random and block copolymers of **3** with lactide also was successful. Click reactions using these acetylene-containing polylactides with PEG550 azide provided PEG-grafted water soluble polylactides, PEG-grafted random copolymers, and new amphiphilic block copolymers. Grafting DiEG and DiEG/alkyl azide mixtures to poly(propargyl glycolide) (48% DiEG incorporated) provides water-soluble polymers which show lower critical solution temperatures. The approximate cloud points of DiEG and DiEG/alkyl grafted poly(propargyl glycolide) in aqueous solutions were 80 °C and 30 °C respectively, which were confirmed by variable temperature DLS measurements. The use of mild click reaction conditions avoided backbone degradation and eliminated the need to end-cap polylactides. Considering polylactide’s sensitivity to backbone degradation, this protocol should also be applicable to the click functionalization of other polyesters such as poly(caprolactone).

Experimental Section

Materials. Ethyl glyoxylate (Alfa Aesar, 50 wt % in toluene) was distilled before use. THF was dried by passage through a column of activated alumina. DMF was dried over activated 4Å molecular sieves. Zinc (Spectrum, 20 mesh) was treated with 2M HCl, and then washed sequentially with distilled water and absolute ethanol and dried under vacuum at 60 °C. Propargyl bromide (Alfa Aesar, 80 wt % in toluene), and all solvents were ACS reagent grade and used as received from commercial suppliers.

Characterization. Polymer molecular weight were determined by gel permeation chromatography (GPC) at 35 °C using two PLgel 10µ mixed-B columns in series, and THF as the eluting solvent at a flow rate of 1 mL/min. A Waters 2410 differential refractometer was used as the detector, and monodisperse polystyrene standards were used to calibrate the molecular weights. The concentration of polymer solutions used for GPC was 1mg/ mL. ¹H NMR (300 or 500 MHz) and ¹³C NMR (75 or 125 MHz) spectra were acquired in CDCl₃ using either a Varian Gemini 300 spectrometer or a Varian UnityPlus-500 spectrometer with the residual proton signals from the solvent used as the chemical shift standard. Mass spectral analyses were carried out on a VG Trio-1 Benchtop GC-MS. Dynamic light scattering (DLS) data were obtained using a temperature-controlled Protein Solutions Dyna Pro-MS/X system. All samples were filtered through a 0.2 µm Whatman PTFE syringe filter and allowed to equilibrate in the instrument for 15 min at 25 °C before measurements were taken that resulted in calculation of the hydrodynamic radius (R_h). The uniformity

of the particle sizes was determined by a monomodal curve fit, which assumes a single particle size with a Gaussian distribution.

Synthesis of 2-hydroxy-4-pentynoic acid ethyl ester (1). Propargyl bromide (~10 g) was added under a blanket of N₂ to a 3 L round bottom flask containing 350 mL anhydrous THF and Zn (230 g, 3.5 mol). The mixture was stirred at room temperature for 30 min and then cooled in an ice bath. A toluene solution of ethyl glyoxylate (51 wt %, determined by NMR, 473 g, 2.36 mol) and a toluene solution of propargyl bromide (80 wt %, 352 g, 2.36 mol) were combined with a mixture of 500 mL dry THF and 700 mL dry ether and added dropwise to the stirred slurry. After the addition was complete, the mixture was stirred at 0 °C overnight. The reaction mixture was then poured into a 4 L Erlenmeyer flask containing 1 L of ice-cold 3M HCl. After separation of organic layer, the aqueous layer was extracted with ether (3 x 300 mL) and the combined organic layers were dried over MgSO₄. Filtration and removal of the solvents by rotary evaporation gave a dark blue oil, which was purified by column chromatography using silica gel with EtOAc/hexanes (30/70) as the eluent. Vacuum distillation (50-55 °C/100 mTorr) gave 170 g of **1** as a colorless oil (51%). ¹H NMR δ 4.25 (m, 3H), 3.11 (d, 1H, *J* = 6.35 Hz), 2.65 (m, 2H), 2.03 (t, 1H, *J* = 2.68 Hz), 1.28 (t, 3H, *J* = 7.20 Hz). ¹³C NMR δ 172.99, 78.53, 71.25, 68.64, 62.11, 24.81, 14.13.

Synthesis of 2-hydroxy-4-pentynoic acid (2). Ester **1** (170 g) was added to 800 mL distilled water and heated to reflux for three days. After cooling to room temperature, the solution was acidified by the addition of 100 mL of concentrated

HCl and continuously extracted with ether for two days. The ether solution was diluted to 1.5 L with additional ether and dried over MgSO₄ for two hours. After filtration, the solution was concentrated by rotary evaporation and dried under vacuum to give a light brown solid, which was purified by recrystallization from CH₂Cl₂ at 0 °C, followed by sublimation at 58 °C and a second recrystallization from CH₂Cl₂ at 0 °C to give 115 g of **2** as white crystals (84%). ¹H NMR δ 4.42 (t, 1H, *J* = 5.00 Hz), 2.75 (m, 2H), 2.10 (t, 1H, *J* = 2.56 Hz). ¹³C NMR δ 177.28, 77.97, 71.96, 68.51, 24.66. MS (*m/z*) 115.3 (*M*+1), mp 61-63 °C.

Synthesis of 3,6-di-2-propynyl-1,4-dioxane-2,5-dione (3). 2-Hydroxy-4-pentynoic acid (**2**) (18 g) and *p*-toluenesulfonic acid monohydrate (1.5 g) were added to a 2 L round bottom flask charged with 1.8 L of toluene. The flask was heated to reflux for 3 days, and the water was removed azeotropically using a Barrett trap. After cooling to room temperature, the toluene was removed by rotary evaporation, and the residue was dissolved in 500 mL CH₂Cl₂, washed with saturated NaHCO₃ (3 x 150 mL) and dried over MgSO₄. Filtration and removal of the CH₂Cl₂ gave the product as a light brown solid which was washed with diethyl ether (3 x 50 mL), sublimed at 75 °C and recrystallized from toluene to give 6.1 g **3** as white crystals (34%). ¹H NMR δ 5.29 (t, *J* = 4.64 Hz), 5.05 (dd, *J* = 7.08 Hz, *J* = 4.39 Hz), (1H total for the signals at 5.29 and 5.05 ppm), 2.95 (m, 2H), 2.17 (t, *J* = 2.56 Hz), 2.11 (t, *J* = 2.69 Hz), (1H total for the signals at 2.17 and 2.11 ppm). ¹³C NMR δ 164.26, 163.44, 76.77, 76.67, 74.82, 74.15, 73.34, 72.02, 23.94, 21.24. Anal. Calcd. for C₁₀H₈O₄: C, 62.50; H, 4.17 Found: C, 62.80; H, 4.01. MS (*m/z*) 193.2 (*M*+1), mp 103-106 °C.

General procedure for bulk polymerizations. Monomer and a small magnetic stir bar were added to a bulb prepared from 3/8 in. diameter glass tubing. The tube was then held under vacuum (3 mTorr) for 12 hours at a room temperature and then filled with nitrogen. A syringe was used to add catalyst ($\text{Sn}(\text{2-ethylhexanoate})_2$) and initiator (BBA) solutions (~0.03 M in toluene) to the bulb, and after careful removal of the toluene under vacuum, the bulb was sealed under vacuum. Bulbs were immersed into an oil bath at 130 °C for the desired period of time, with the contents stirred magnetically. At the end of the polymerization, the bulb was removed from the bath, cooled in ice water and opened. A portion of the polymer was analyzed by NMR for conversion. The remaining polymer was dissolved in CH_2Cl_2 , precipitated from cold methanol five times and dried under vacuum (4 mTorr) at 40 °C for 24 hours.

Polymerization of propargyl glycolide. Propargyl glycolide (2.49 g) was polymerized for 25 min of a $[\text{M}]/[\text{I}] = 150$. The conversion of monomer to polymer calculated from ^1H NMR was 90.6%. Precipitation and drying under vacuum gave 2.16 g poly(propargyl glycolide) as a light brown solid (86.7%). ^1H NMR: δ 5.31-5.46 (br, 1H), 2.79-3.03 (br m, 2H), 2.01-2.18 (br, 1H). GPC (THF): $M_n = 28,600$ g/mol, PDI = 1.30.

Copolymerization of propargyl glycolide and *rac*-lactide. A mixture of propargyl glycolide (0.384 g, 2 mmol) and *rac*-lactide (3.394 g, 23.6 mmol) was polymerized for 50 min of a $[\text{M}]/[\text{I}] = 300$. Precipitation and drying under vacuum gave 3.59 g of the random copolymer as a white solid (95%). ^1H NMR: δ 5.03-5.39 (br m, 12.7H), 2.75-2.96 (br m, 2H), 1.97-2.11 (br, 1H), 1.43-1.65 (br m,

38.8H). GPC (THF, light scattering and refractive index detectors): $M_n = 8.32 \times 10^4$ g/mol, PDI = 1.20.

Preparation of PPGL-*block*-polylactide. PPGL (1.0 g, $M_{n, GPC} = 28,500$, PDI = 1.30) and lactide (5.0 g) were placed into a 25 mL Schlenk flask. The Schlenk flask was then sealed with a rubber septum and held under vacuum overnight to remove any residual water. The flask was then filled with nitrogen. After using a syringe to add 1.21 mL of a 0.0288 M solution of $\text{Sn}(\text{2-ethylhexanoate})_2$ in toluene and 8 mL of anhydrous THF, the flask was placed into an oil bath at 70 °C for 10 hours and the solution was stirred magnetically. At the end of the polymerization, the polymer was isolated by precipitation into cold methanol five times and dried under vacuum at 45 °C overnight to give 2.8 g of the block copolymer as a white solid. $^1\text{H NMR}$: δ 5.31-5.44 (br, 1H), 5.06-5.25 (br m, 2.6H), 2.80-3.02 (br m, 2H), 2.05-2.14 (br, 1H), 1.48-1.62 (br m, 8.1H). GPC (THF): $M_n = 38,000$ g/mol, PDI = 1.44.

General procedure for “click” functionalization. The desired amount of acetylene functionalized polymer and three equivalents of azide (with respect to acetylene groups) were dissolved in DMF in a Schlenk flask, and the solution was deoxygenated by three freeze-pump-thaw cycles. After the contents were refrozen, 5 mol % of $\text{CuSO}_4 \cdot 5\text{H}_2\text{O}$ crystals and 12 mol% of sodium ascorbate powder (with respect to acetylene group) were added to the frozen mixture under a nitrogen purge, and the flask was evacuated and backfilled with nitrogen. The mixture was then deoxygenated by three additional freeze-pump-thaw cycles, and then stirred at room temperature under nitrogen for 2 hours. At the end of the

reaction, the solids in the reaction mixture were removed by filtration and the polymer was isolated by dialysis (MWCO = 12-14,000) in acetone/water (1:1) mixture overnight and then dried under vacuum.

1-Azidodecane-grafted PPGL. PPGL (54 mg, $M_{n, GPC} = 35,500$ g/mol, PDI = 1.44) and 300 mg of 1-azidodecane were dissolved in 5 mL DMF for the click reaction. The decane-grafted PPGL was isolated as a light green solid (133 mg, 87%). GPC (THF): $M_{n, GPC} = 49,400$, PDI = 1.41.

PEG550-grafted PPGL. PPGL (100 mg) ($M_{n, GPC} = 35,500$ g/mol, PDI = 1.44) and PEG-550 azide (1.72 g) were dissolved in 10 mL DMF for the click reaction. PEG550-grafted PPGL was isolated as a light green viscous liquid (514 mg, 77%).

Poly(propargyl glycolide-co-lactide) grafted with PEG550. The copolymer (550 mg) and PEG-550 azide (990 mg) were dissolved in 20 mL DMF for the click reaction. The product was isolated as a light green rubbery solid (650 mg, 74 %). GPC (THF, light scattering): $M_n = 1.56 \times 10^5$ g/mol, PDI = 1.21.

DiEG-grafted PPGL PPGL (250 mg) ($M_{n, GPC} = 35,500$ g/mol, PDI = 1.44) and 1-(2-azidoethoxy)-2-(2-methoxyethoxy) ethane (1480 mg) were dissolved in 20 mL DMF for the click reaction. The DiEG-grafted PPGL was isolated as a light green elastomer (590 mg, 79%).

Alkyl/DiEG-grafted PPGL PPGL (122 mg) ($M_{n, GPC} = 35,500$ g/mol, PDI = 1.44), 1-(2-azidoethoxy)-2-(2-methoxyethoxy) ethane (480 mg, 2.6 mmol), and 1-azidodecane (240 mg, 1.3 mmol) were dissolved in 10 mL of DMF for the click reaction. The product was isolated as a light green elastomer (320 mg, 88%). ^1H

NMR: δ 7.36-7.78 (br, 1H), 5.22-5.56 (br, 1H), 4.36-4.56 (br, 1H), 4.12-4.36 (br, 1.1H), 3.73-3.91(br, 1H), 0.70-0.94 (br, 1.7H).

PEG550-grafted PPGL-*block*-polylactide. The block copolymer (300 mg) and PEG-550 azide (1.78 g, 3.2 mmol) were dissolved in 20 mL DMF for the reaction. The product was isolated as a light green viscous liquid (690 mg, 78 %).

Chapter 5 PEG/Alkyl-Grafted Comb Poly lactides

Introduction

Aliphatic polyesters such as polylactide (PLA), polyglycolide (PGA), and polycaprolactone (PCL) are of interest for medical and pharmaceutical applications due to their biodegradability and biocompatibility.²²⁰ Poly(ethylene glycol) (PEG) functionalized polyesters are of particular interest, because these polymers are amphiphilic and resistant to protein adsorption.^{221,222} PEG and polyester block copolymers such as PEG-PLA and PEG-PLA-PEG are being extensively investigated for drug delivery applications,^{208,220,223,224} however, the degradation profiles of these block copolymers are dependent on their compositional parameters and are typically irreproducible.²²³ Additionally, the structural heterogeneity of these block copolymers can also lead to increasing PLA/PEG ratios during degradation,^{225,226} which can change the protein resistant characteristics of particles and complicate drug release kinetics.

Trying to solve these problems, several groups have reported PEG-*grafted*-polyesters and argued that their inherent structural homogeneity should lead to predictable degradation behavior.^{210,211,227} However, these polymers often suffer from ill-defined chemical structures, low grafting densities, backbone degradation or high polydispersities. In some of these copolymers, the chemical nature of the linker between PEG grafts and polymer backbone can potentially cause compositional changes during degradation.

Structurally well-defined graft copolymers with hydrophilic PEG groups and hydrophobic alkyl groups on the same polymer backbone are a new family of amphiphilic polymers. Their structure suggests interesting possibilities for self-assembly. For example, ultrathin films of PEG/*alkyl-grafted*-polythiophene were manipulated and processed on the nano- and micrometer scales using a self-assembly approach,¹²³ PEG/*alkyl-grafted*-poly(*p*-phenylene) self-organized into fibrous aggregates in micellar surfactant solutions.^{125,126}

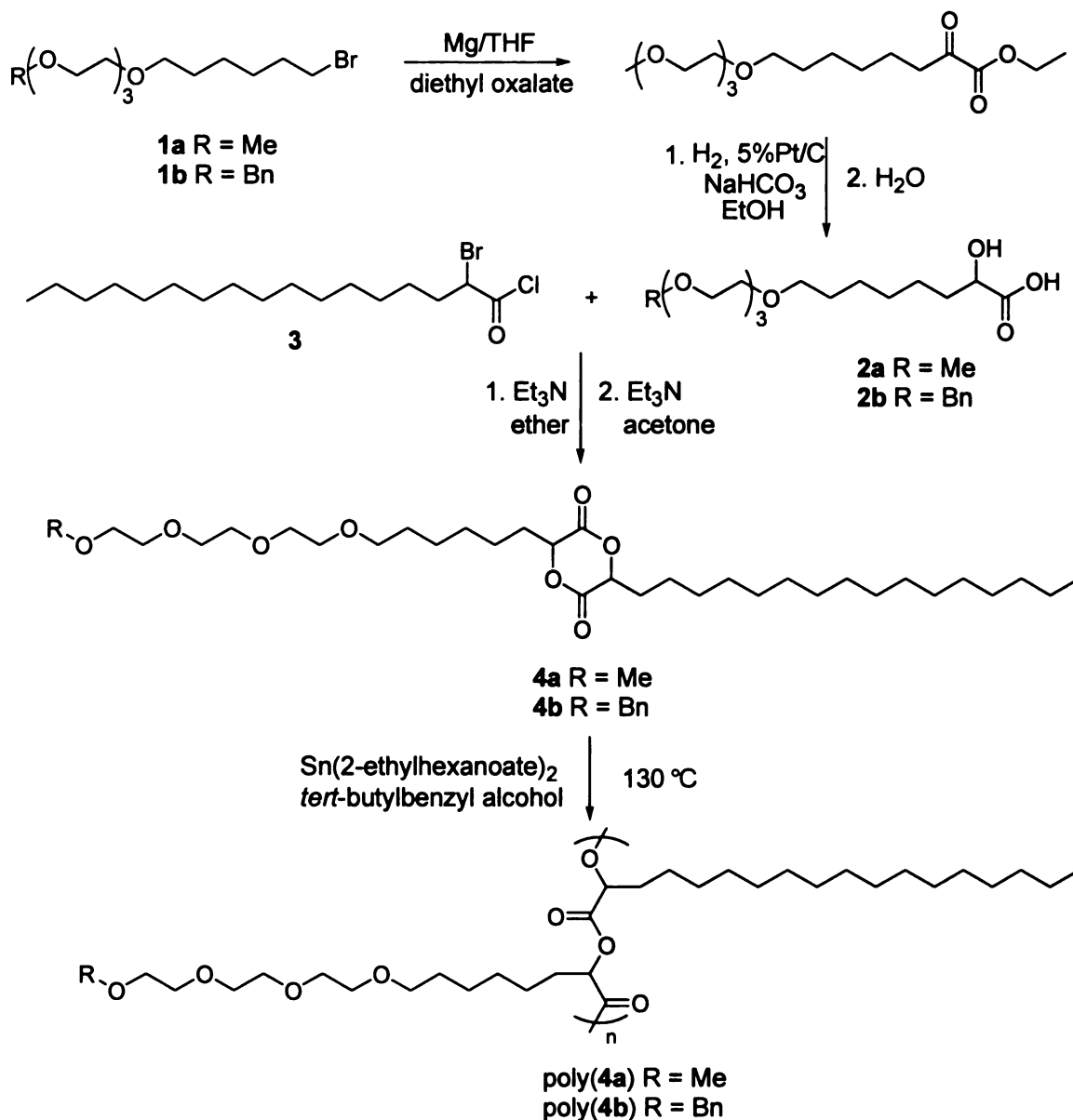
To avoid the problems encountered in existing PEG-*grafted*-polyesters and develop new amphiphilic biodegradable polymers, we synthesized asymmetric lactide monomers containing a PEG chain and linear alkyl group. Subsequent polymerizations of these monomers provided structurally homogeneous PEG/*alkyl-grafted* amphiphilic polyesters with high molecular weights. Similar to other PEG/*alkyl* grafted polymers, these new polyesters should have useful properties arising from self-assembly. Furthermore, the introduction of protected hydroxyl groups into the PEG grafts provides opportunities for further chemical modification after deprotection.

Results and Discussion

Scheme 14 shows the synthetic route to the two monomers described in this chapter. The reaction of tri(ethylene glycol) monomethyl ether or tri(ethylene glycol) monobenzyl ether with 1,6-dibromohexane generated the corresponding PEG functionalized hexyl bromide. The competing elimination reaction was minimized by conducting the reaction at approximately -25 °C. The reaction of Grignard reagents generated from these PEG functionalized hexyl bromides with diethyl oxalate at -78 °C provided the corresponding α -keto esters, with no detectable contamination from second addition of the Grignard reagent to the substrate. Catalytic hydrogenation of the crude keto esters at 1500 psig using Pt on carbon yielded the α -hydroxy esters, but since purification of the esters proved difficult, the crude α -hydroxy esters were hydrolyzed and isolated as the α -hydroxy acids. Crystallization of the acids from ether at low temperatures gave colorless to light brown oils in an overall yield of ~65 % from diethyl oxalate. The ^1H NMR spectra of both α -hydroxy acids are shown in **Figure 66**, with the most important spectral features being the methine protons, appearing as a doublet of doublets at 4.20 ppm, and the benzylic protons of compound **2b** at 4.51 ppm. To the best of our knowledge, neither α -hydroxy acid has been previously reported.

The reaction of α -hydroxy acids with 2-bromooctadecanoyl chloride^[180] (**3**) in the presence of base yielded linear dimers. But since their purification proved difficult, the crude linear dimers were directly cyclized in refluxing acetone in the presence of NEt_3 , yielding exclusively the *rac* diastereomer in low yield. The byproducts primarily consisted of linear oligomers, which in principle, could be

recycled. ^1H NMR spectra of both monomers are shown in **Figure 67**. The doublet of doublets at 4.83 ppm from the methine protons of the 3,6-disubstituted glycolide ring can be integrated to measure the conversion of polymerizations. Also prominent are the benzylic protons of compound **4b** at 4.51 ppm.



Scheme 14. Synthesis of amphiphilic glycolide monomers

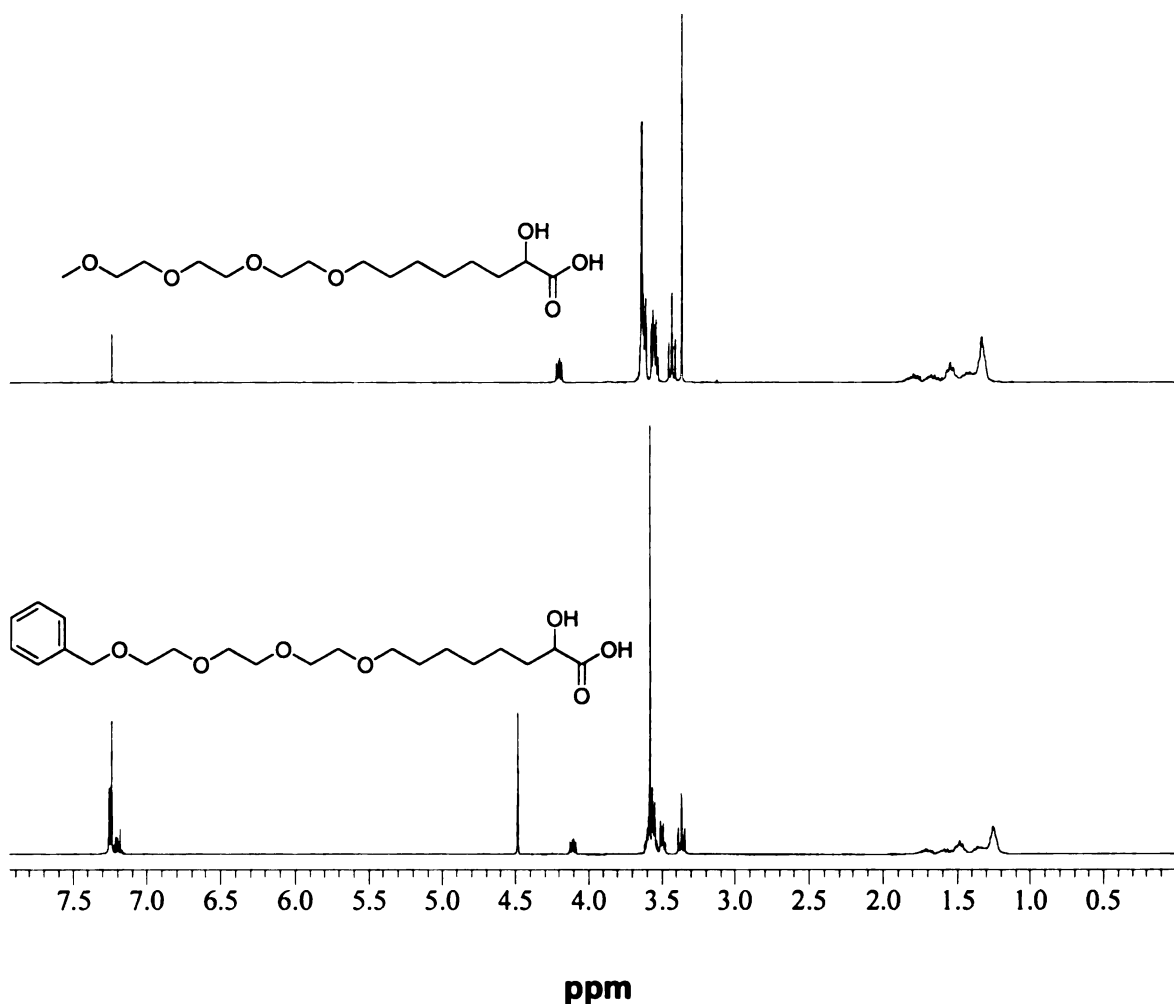


Figure 66. 300 MHz ^1H NMR spectra of PEG containing α -hydroxy acids

These new monomers were bulk polymerized at 130 °C using $\text{Sn}(\text{2-ethylhexanoate})_2$ as the catalyst and 4-*tert*-butyl benzyl alcohol as the initiator, yielding poly(**4a**) and poly(**4b**) (Scheme 14). The molar ratio of monomer, catalyst and initiator was 250:1:1. Since the data from chapter 2 show that substituted lactides generally polymerize slower than lactide, we used a 2 h reaction time and achieved over 90 % conversion of monomer to polymer. The ^1H NMR spectrum of poly(**4a**) (Figure 68) shows the expected peaks associated with alkyl and PEG side chains plus the methine protons of the polymer

backbone. The spectrum of poly(4b) (Figure 68) is similar, except that the resonance at 3.35 ppm from the terminal methoxy group in the PEG side chains was replaced by resonances at 4.54 ppm and 7.3 ppm for the benzyl group.

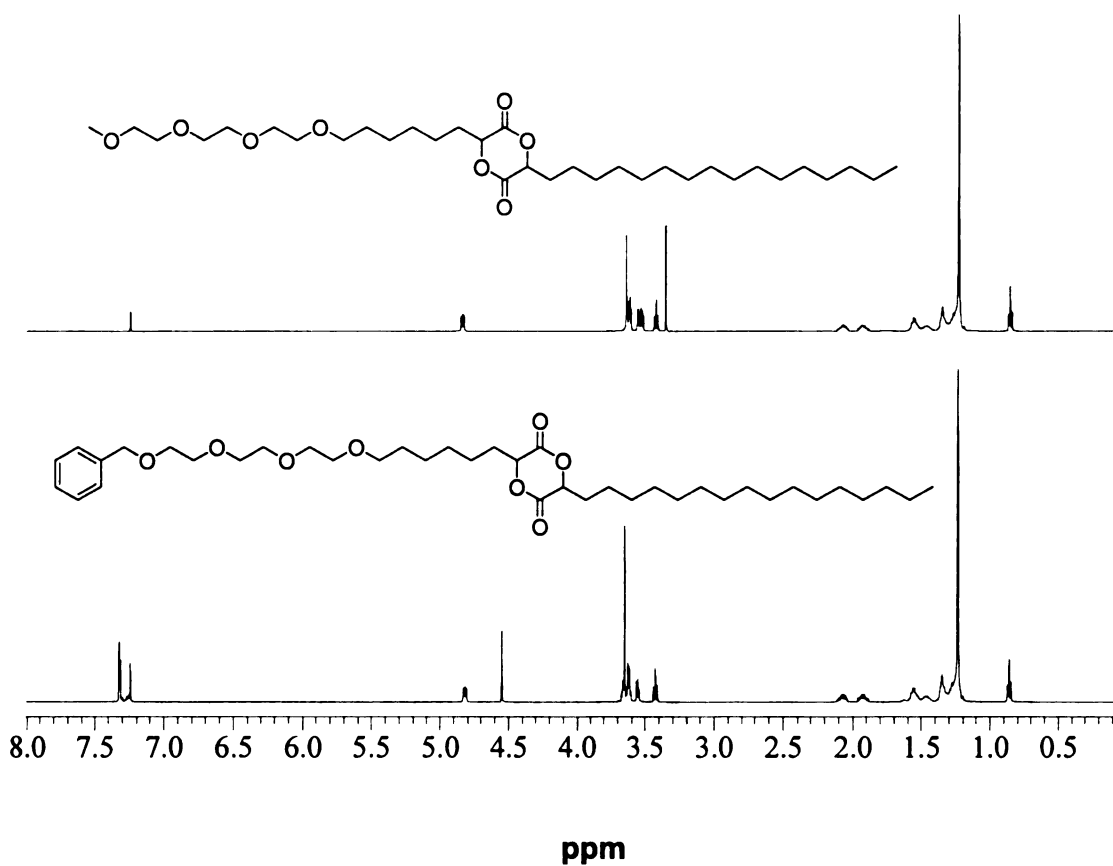


Figure 67. 500 MHz ¹H NMR spectra of amphiphilic glycolide monomers

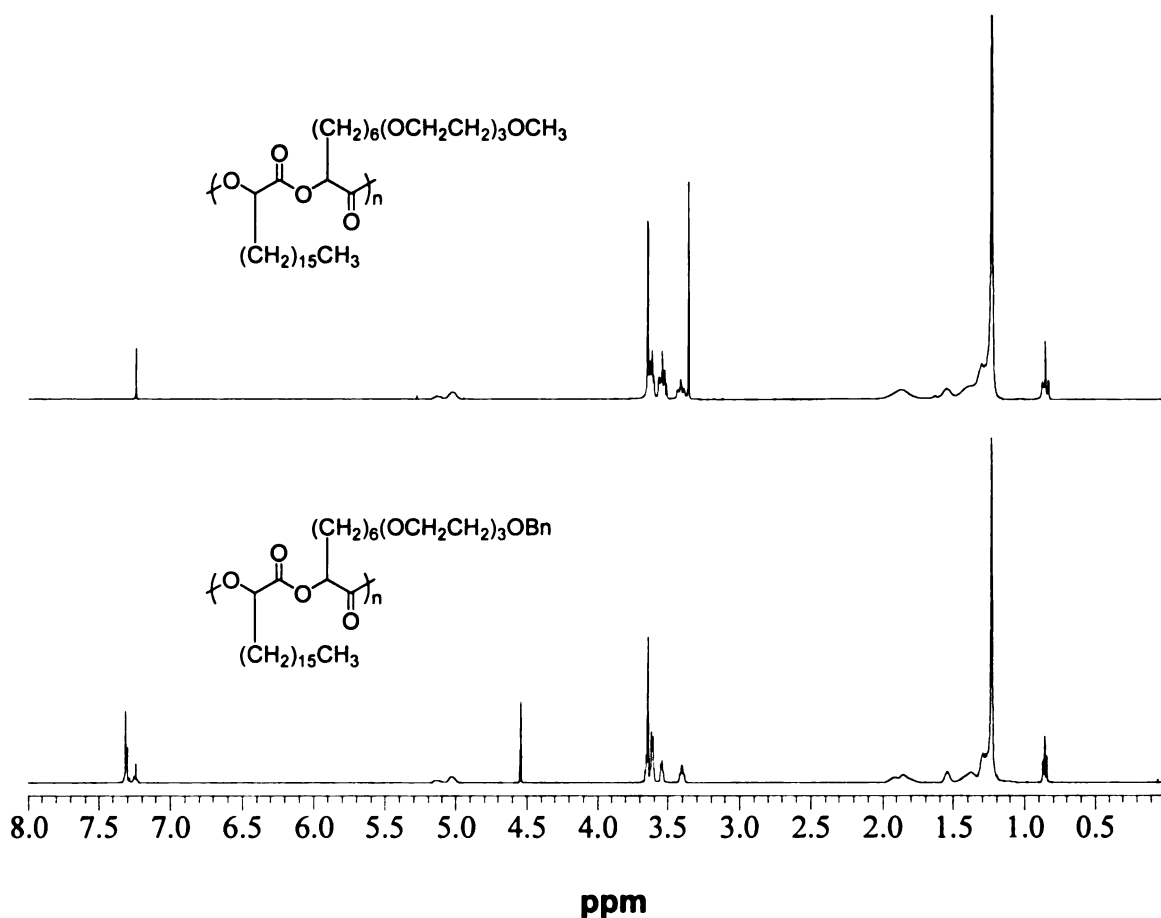


Figure 68. 500 MHz ^1H NMR spectra of amphiphilic polyglycolides

The GPC traces show that the molecular weight distributions of both polymers are somewhat bimodal (**Figure 69**). The origins of the high molecular weight shoulders seen in the GPC traces are not clear, but we note that the GPC traces of the PEG-containing polymers described in Chapter 3 also showed signs of bimodality. The molecular weight (M_n) of poly(4a) as measured by GPC (vs. polystyrene standards) was 132,000 g/mol which was in good agreement with the theoretical value (136,200 g/mol). The molecular weight of poly(4b) ($M_n = 146,000$ g/mol) was also in good agreement with the theoretical value (152,300 g/mol).

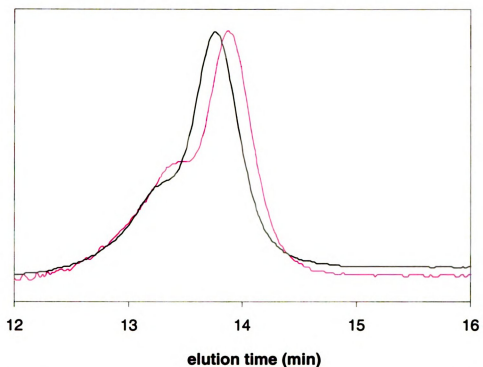


Figure 69. GPC traces of amphiphilic polyglycolides (pink line: poly(4a); black line: poly(4b))

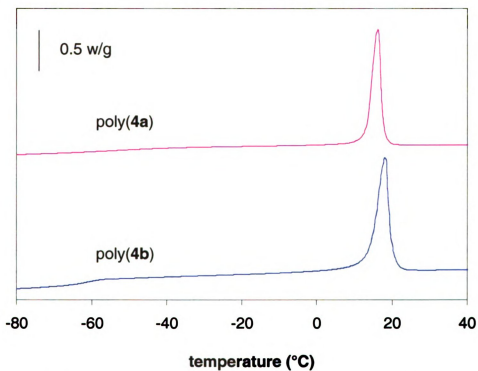


Figure 70. DSC heating traces of amphiphilic polylactides (second heating scan, 10 °C/min in N₂)

The DSC traces of both polymers showed a melt transition at $\sim 17^\circ\text{C}$, and a glass transition temperature (T_g) at $\sim -60^\circ\text{C}$ (Figure 70). Based on our results with alkyl-substituted polyglycolides, the melt transition can be associated with side chain crystallization. We also found that when the side chains are longer than 10 carbon atoms, they crystallize and the T_g from the backbone is not detectable using DSC. Thus we assign the glass transition temperature at $\sim -60^\circ\text{C}$ to the PEG segment in the side chain rather than from main chain, which was confirmed by comparing the DSC traces of the polymer and the corresponding monomer (not shown).

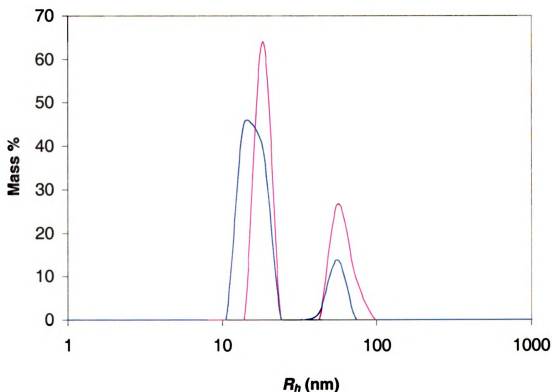


Figure 71. DLS of polymeric micelles and azobenzene loaded polymeric micelles (5 mg/mL in water, pink line: polymer only; black line: polymer + azobenzene)

Using the solvent displacement method, polymeric micelles encapsulating azobenzene can be prepared from polymer (4a) in aqueous media. Polymer (4a) and azobenzene were dissolved in acetone and the acetone solution was added drop-wise to stirred ice-cold water. Acetone was removed under vacuum to yield a stable homogenous microemulsion (polymer + dye) after filtration. Shown in **Figure 71** are the DLS results for the polymeric micelles, and azobenzene-loaded polymeric micelles. In both systems, there are two peaks corresponding to average hydrodynamic radii of ~20 nm and ~60 nm, respectively. The reason for the bimodal distribution in particle size is unclear, but it may be related to the bimodal molecular weight distribution seen in the GPC data.

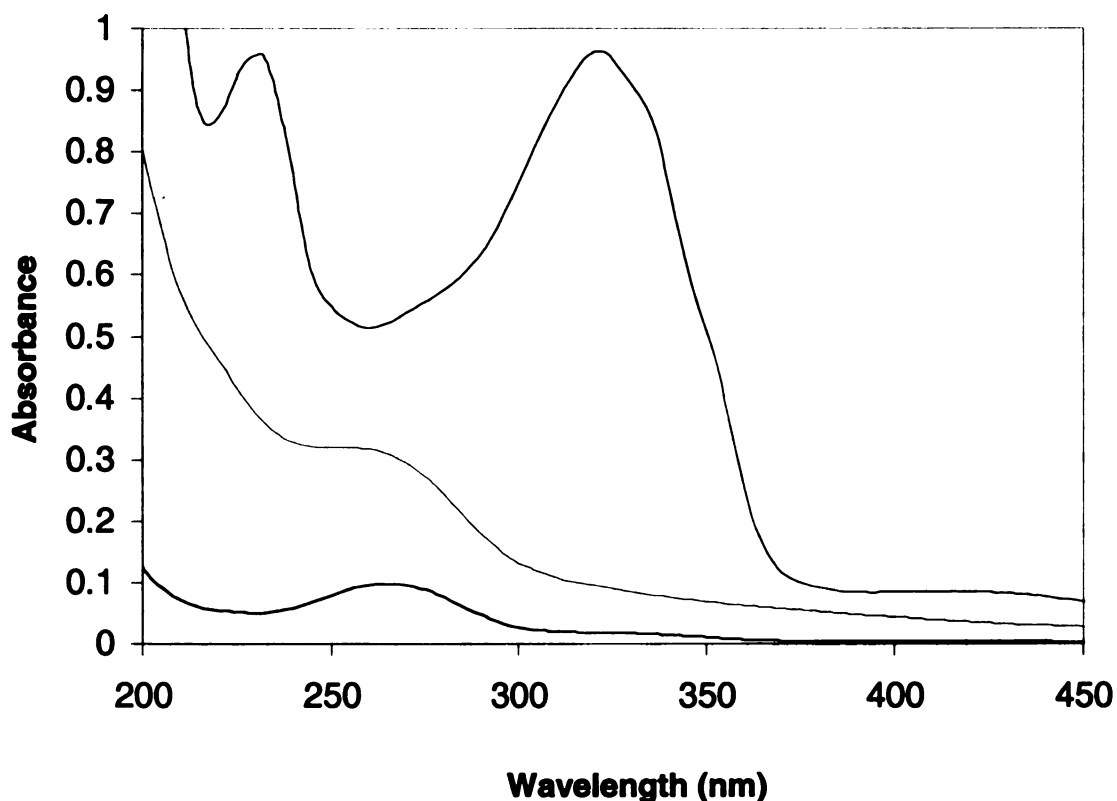


Figure 72. UV-vis spectra of polymeric micelles, azobenzene loaded polymeric micelles, and azobenzene in water. (black line: azobenzene; pink line: poly(4a); blue line: poly(4a) + azobenzene)

Shown in **Figure 72** are UV-Vis spectra of polymeric micelles, azobenzene loaded polymeric micelles, and azobenzene in water. The “azobenzene” spectrum shows only a small absorption peak at ~265 nm due to residual acetone and no absorption from azobenzene, which is completely insoluble in water. The spectrum of the polymeric micelles shows a weak absorption at ~ 260 nm from the ester group. In contrast, neither the peak from residual acetone nor the peak from the polyester backbone is visible in the spectrum of azobenzene loaded polymeric micelles. Instead, the spectrum is dominated by the characteristic absorption peaks of azobenzene at ~ 230 nm and ~320 nm. This simple experiment demonstrates the solubilization of otherwise water-insoluble azobenzene by poly(**4a**), thus suggesting the potential of related polymers as delivery vehicles for hydrophobic compounds.

Conclusions

PEG/alkyl substituted amphiphilic lactide monomers were synthesized by condensing a PEG-containing α -hydroxy acid with an alkyl-containing α -bromo acid chloride. The resulting AB substituted glycolide was isolated exclusively as the *rac* isomer. Subsequent ring-opening polymerization of the monomers using *tert*-butyl benzyl alcohol as initiator and Sn(2-ethylhexanoate)₂ as catalyst yielded novel amphiphilic polylactides capable of side chain crystallization due to their long linear alkyl side chain. The potential application of these new amphiphilic polylactides as drug delivery vehicles was demonstrated by encapsulation of azobenzene in the polymeric micelles using the solvent displacement method.

Experimental Section

Materials THF was dried by passing the solvent through a column of activated alumina. Compounds **1a** and **2a** were synthesized according to procedure described in Chapter 3. All other chemicals were used as received.

Characterization. The molecular weights of polymers were determined by gel permeation chromatography (GPC) at 35 °C using two PLgel 10 μ mixed-B columns in series with THF as the eluting solvent at a flow rate of 1 mL/min. A Waters 2410 differential refractometer was used as the detector, and monodisperse polystyrene standards were used to calibrate the molecular weights. The concentration of polymer solutions used for GPC was 1 mg/ mL. ¹H NMR (300 or 500 MHz) and ¹³C NMR (75 or 125 MHz) spectra were acquired in CDCl₃ using either a Varian Gemini 300 spectrometer or a Varian UnityPlus-500 spectrometer with the residual proton signals or carbon signals from the solvent used as the chemical shift standard. Mass spectral analyses were carried out on a VG Trio-1 Benchtop GC-MS. Dynamic light scattering (DLS) measurements were performed with a temperature-controlled Protein Solutions Dyna Pro-MS/X system. Samples were filtered through a 0.2 μ m Whatman PTFE syringe filter and allowed to equilibrate in the instrument for 15 min at 25 °C before taking measurements that resulted in calculation of the hydrodynamic radius (R_h).

2-Bromooctadecanoyl chloride (3). Stearic acid (142 g, 0.5 mol, recrystallized from ethanol) and SOCl₂ (140 mL, 1.9 mol) were placed into a 500 mL round bottom flask. The mixture was refluxed for 2 hours under nitrogen, and then

bromine (40 mL, 0.77 mol) was added dropwise to the solution. The mixture was refluxed under nitrogen overnight, and then the excess reagents were removed under vacuum at room temperature to give 187 g of **3** as a brown oil (98%). The product was used without further purification. ^1H NMR δ 4.44–4.52 (dd, 1H, $J = 7.61$ Hz, $J = 6.59$ Hz), 2.07–2.22 (m, 1H), 1.94–2.07 (m, 1H), 1.38–1.55 (br, 2H), 1.20–1.36 (br, 26H), 0.81–0.91 (t, 3H, $J = 6.73$ Hz). ^{13}C NMR δ 170.11, 54.14, 34.84, 31.93, 29.69, 29.66, 29.62, 29.54, 29.40, 29.36, 29.20, 28.72, 26.84, 22.68, 14.09.

2-Hydroxy-8-{2-[2-(2-methoxy ethoxy)-ethoxyl]-ethoxyl}-octanoic acid (2a).

Compound **1a** (164 g, 0.50 mol) was dissolved in dry THF (600 mL) and stirred with magnesium turnings (24 g, 1.0 mol) until the solution stopped boiling. The Grignard reagent was then added dropwise under nitrogen to a 2 L round bottom flask containing a stirred solution of diethyl oxalate (56 g, 0.38 mol) in dry THF (300 mL) at -80 °C. After the addition was complete, the mixture was stirred for an additional hour at -80 °C, and then quenched with 300 mL of 2M HCl. The water layer was extracted with ether (5×200 mL) and the combined organic layers were dried over MgSO_4 . Filtration and removal of the solvents by rotary evaporation gave the α -keto ester as a light brown oil. After dissolving the oil in ethanol (500 mL) and adding 1 g of 5% Pt/C and 15 g NaHCO_3 , the α -keto ester was hydrogenated at ~ 1500 psig H_2 . When ^1H NMR showed that the α -keto ester had been consumed (the disappearance of the triplet at 2.80 ppm), the solids were removed by filtration and the ethanol solution was concentrated by rotary evaporation to give a colorless oil. The oil was then dissolved in ether (500

mL) and continuously extracted with water for a week. Removal of water by rotary evaporation gave a light yellow oil, which was dissolved in diethyl ether (1000 mL) and dried over MgSO₄. Filtration, recrystallization from diethyl ether (once at -80 °C and twice at -45 °C), and removal of residual solvent under vacuum (20mTorr) at room temperature for 24 hours gave 76 g of compound **2a** as a colorless oil (61%). ¹H NMR δ 4.20 (dd, 1H), 3.62 (m, 8H), 3.56 (m, 4H), 3.43 (t, 2H), 3.35 (s, 3H), 1.78 (m, 1H), 1.66 (m, 1H), 1.55 (p, 2H), 1.24-1.48 (br m, 6H). ¹³C NMR δ 177.69, 71.77, 71.21, 70.44, 70.26, 69.97, 69.88, 33.83, 29.19, 28.78, 25.65, 24.47.

2-[2-(2-benzyloxyn ethoxy)-ethoxy]-ethanol. Benzyl chloride (165 g, 1.3 mol) was added to a 2 L round bottom flask that had been charged with tri(ethylene glycol) (975 g, 6.5 mol), NaOH (80 g, 2.0 mol) and water (80 mL). The mixture was heated at 110 °C for 36 hours, cooled to room temperature, and poured into 600 mL water. The water layer was continuously extracted with diethyl ether for 24 hours, and then the ether layer was dried over MgSO₄ and the solvent evaporated in vacuo. The residue was fractionally distilled under vacuum (122-126 °C/30 mTorr) to give 265 g of the benzyl-protected tri(ethylene glycol) as a colorless liquid (85%). ¹H NMR: δ 7.22-7.36 (m, 5H), 4.52-4.57 (s, 2H), 3.55-3.74 (m, 12H), 2.37-2.44 (s, 1H).

1-Bromo-6-{2-[2-(2-benzyloxy-ethoxy)-ethoxy]-ethoxy}-hexane (1b). A 3 L round bottom flask containing dry THF (1200 mL), NaH (42 g 1.75 mol), and 1,6-dibromohexane (900 g, 3.69 mol) was cooled to ~ -30 °C under a blanket of N₂. Tri(ethylene glycol) monobenzyl ether (210 g 0.87 mol) was dissolved in 600 mL

dry THF and added dropwise to the stirred slurry. After the addition was complete, the mixture was stirred at ~ -15 °C for 24 hours and at 0 °C for 2 days. The solids were removed by filtration, and the solvent was removed by rotary evaporation to give a light yellow oil, which was re-dissolved in 1000 mL hexane and washed with water (3 x 350 mL). The hexane layer was then dried over MgSO₄ and evaporated in vacuo. Removal of water and excess 1,6-dibromohexane under vacuum in a 120 °C oil bath gave 340 g of the product as a light brown oil (97%), which was used without further purification.

2-Hydroxy-8-{2-[2-(2-benzyloxy ethoxy)-ethoxy]-ethoxy}-octanoic acid (2b).

Compound **1b** (333 g, 0.83 mol) was dissolved in dry THF (1200 mL) and stirred with magnesium turnings (36 g, 2.0 mol) until the solution stopped boiling. The Grignard reagent was then added dropwise under nitrogen to a 2 L round bottom flask containing a stirred solution of diethyl oxalate (83 g, 0.57 mol) in dry THF (200 mL) at -80 °C. After the addition was complete, the mixture was stirred for an additional hour at -80 °C, and then was quenched with 300 mL of 3M HCl. The water layer was extracted with ether (2 x 200 mL) and the combined organic layers were dried over MgSO₄. Filtration and removal of the solvents by rotary evaporation gave the α-keto ester as a light brown oil. After dissolving the oil in ethanol (1000 mL) and adding 2 g of 5% Pt/C and 15 g NaHCO₃, the α-keto ester was hydrogenated at ~1500 psi. When ¹H NMR showed that the α-keto ester had been consumed (disappearance of the triplet at 2.80 ppm), the solids were removed by filtration and the ethanol solution was concentrated by rotary evaporation to give a colorless oil. The oil was then mixed with 1 L of 2M

aqueous NaOH solution. The mixture was heated at reflux for four days, cooled to room temperature, extracted with diethyl ether (3 × 200 mL, discarded), and acidified to pH ≈ 1 using concentrated HCl. The acidic solution was then extracted with ether (4 × 300 mL), and the combined ether layers were dried over MgSO₄. Filtration, recrystallization from diethyl ether (twice at -80 °C and twice at -45 °C) and removal of residual solvent under vacuum (20 mTorr) at room temperature for 24 hours gave 152 g of **2b** as a light yellow oil (67%). ¹H NMR δ 7.21-7.33 (m, 5H), 4.52-4.56 (s, 2H), 4.13-4.20 (dd, 1H), 3.58-3.68 (m, 10H), 3.51-3.58 (m, 2H), 3.38-3.46 (t, 2H), 1.70-1.86 (m, 1H), 1.59-1.70 (m, 1H), 1.48-1.59 (br m, 2H), 1.22-1.47 (br, 6H). ¹³C NMR δ 177.61, 137.92, 128.29, 127.73, 127.59, 73.12, 71.24, 70.47, 70.44, 70.40, 69.98, 69.88, 69.23, 33.80, 29.18, 28.75, 25.63, 24.41.

3-(6-{2-[2-(2-methoxy-ethoxy)-ethoxy]-ethoxy}-hexyl)-6-Hexadecyl-

[1,4]dioxane-2,5-dione (4a). NEt₃ (16.6 mL, 120 mmol) was added dropwise under nitrogen to a 0 °C solution of **2a** (10 g, 31 mmol) and **3** (19 g, 50 mmol) in diethyl ether (250 mL). After stirring at 0 °C for 5 hours, the mixture was washed with 2M HCl (2 × 100 mL) and dried over MgSO₄. After filtration and removal of solvent, the residual brown oil and NEt₃ (13.8 mL, 100 mmol) were dissolved in acetone (2500 mL) and refluxed for 16 hours. After removing the solvent by rotary evaporation, the residue was re-dissolved in diethyl ether (500 mL), washed with 0.5M HCl (3 × 200 mL), saturated NaHCO₃ (3 × 200 mL) and then dried over MgSO₄. Filtration and evaporation of the ether gave a brown oil, which was purified by column chromatography (silica gel, 3/1 hexanes/EtOAc),

recrystallized five times from hexanes at 5 °C, and dried under vacuum (15 mTorr) at room temperature overnight to give 2.2 g of **4a** as white crystals (12%). ¹H NMR δ 4.83 (dd, 2H, *J* = 7.69 Hz, *J* = 4.27 Hz), 3.62 (m, 8H), 3.53 (m, 4H), 3.42 (t, 2H, *J* = 6.71 Hz), 3.35 (s, 3H), 2.07 (m, 2H), 1.92 (m, 2H), 1.60-1.40 (br, 6H), 1.40-1.20 (br, 30H), 0.85 (t, 3H). ¹³C NMR δ 166.92, 75.61, 75.53, 71.92, 71.23, 70.61, 70.56, 70.50, 70.05, 59.00, 31.89, 30.10, 30.01, 29.66, 29.56, 29.46, 29.41, 29.33, 29.27, 29.07, 28.85, 25.77, 24.36, 24.29, 22.66, 14.09. Anal. Calcd. for C₃₃H₆₂O₈: C, 67.58; H, 10.58 Found: C, 67.98; H, 10.55. MS-EI (*m/z*) 587.3 (M+1), mp 51-55 °C.

3-(6-{2-[2-(2-benzyloxy-ethoxy)-ethoxy]-ethoxy}-hexyl)-6-Hexadecyl-[1,4]dioxane-2,5-dione (4b). NEt₃ (20 mL, 145 mmol) was added dropwise under nitrogen to a 0 °C solution of **2b** (20 g, 50 mmol) and **3** (30 g, 79 mmol) in diethyl ether (400 mL). After stirring at 0 °C for 5 hours, the mixture was washed with 2M HCl (2 × 200 mL) and water (2 × 200 mL) and dried over MgSO₄. After filtration and removal of solvent, the residual brown oil and NEt₃ (15 mL, 110 mmol) were dissolved in acetone (4000 mL) and refluxed for 16 hours. After removing the solvent by rotary evaporation, the residue was re-dissolved in diethyl ether (600 mL), washed with 0.5M HCl (3 × 200 mL) and saturated NaHCO₃ (3 × 200 mL) and dried over MgSO₄. After filtration and removal of the ether, the brown oil was purified by column chromatography (silica gel, 4/1 hexanes/EtOAc), recrystallized five times from hexanes at 5 °C, and dried under vacuum (15 mTorr) at room temperature overnight to give 3.2 g of **4b** as white crystals (9.7%). ¹H NMR δ 7.25-7.34 (m, 5H), 4.79-4.84 (dd, 2H, *J* = 7.81Hz, *J* =

4.39 Hz), 4.53-4.56 (s, 2H), 3.59-3.68 (m, 10H), 3.53-3.57 (m, 2H), 3.40-3.44 (t, 2H, $J = 6.71$ Hz), 2.03-2.12 (m, 2H), 1.87-1.97 (m, 2H), 1.41-1.59 (br, 6H), 1.20-1.40 (br, 30H), 0.82-0.88 (t, 3H). ^{13}C NMR δ 166.92, 138.27, 128.34, 127.72, 127.56, 75.61, 75.52, 73.21, 71.24, 70.65, 70.64, 70.63, 70.61, 70.08, 69.42, 31.90, 30.09, 30.00, 29.67, 29.65, 29.63, 29.62, 29.58, 29.47, 29.42, 29.34, 29.28, 29.07, 28.86, 25.78, 24.36, 24.29, 22.67, 14.11. Anal. Calcd. for $\text{C}_{39}\text{H}_{66}\text{O}_8$: C, 70.69; H, 9.97 Found: C, 70.97; H, 9.90. MS-EI (m/z) 663.5 ($M+1$), mp 51-53 °C.

General procedure for bulk polymerizations. The desired amount of monomer was loaded into a polymerization bulb prepared from 3/8 in. diameter glass tubing along with a magnetic stir bar. The bulb was connected to a vacuum line and the monomer was dried under vacuum (5 mTorr) at 105 °C for 18 hours. After cooling to room temperature, a syringe was used to add toluene solutions of catalyst ($\text{Sn}(\text{2-ethylhexanoate})_2$) and initiator (4-*tert*-butylbenzyl alcohol) (monomer:catalyst:initiator ratio = 250:1:1). The solvent was removed under vacuum, and the bulb was flame-sealed under vacuum and immersed in an oil bath at 130 °C for 2 hours. At the end of the polymerization, the tube was cooled in water, opened, and portions of the sample were removed for NMR and GPC analyses.

Poly(4a). Monomer **4a** was polymerized on a 704 mg scale. The monomer conversion determined by ^1H NMR was 93%, and the molecular weight (M_n) from GPC was 132,000 g/mol with a PDI of 1.30. The crude product was purified by

precipitation into cold methanol from CH₂Cl₂ five times and dried under vacuum at 50 °C overnight to give 430 mg of poly(**4a**) as a viscous liquid in 61% yield. NMR shows ~2% residual monomer in poly(**4a**) after precipitation. ¹H NMR δ 4.96-5.18 (br, 2H), 3.58-3.70 (br m, 8H), 3.49-3.58 (br m, 4H), 3.37-3.46 (br t, 2H), 3.33-3.37 (s, 3H), 1.72-2.04 (br, 4H), 1.48-1.62 (br, 2H), 1.14-1.48 (br, 34H), 0.80-0.92 (t, 3H).

Poly(4b). Monomer **4b** was polymerized on a 1.0 g scale. The monomer conversion determined by ¹H NMR was 92%, and the molecular weight (*M_n*) from GPC was 146,000 g/mol with a PDI of 1.31. The crude product was purified by precipitation into cold methanol from CH₂Cl₂ three times and dried under vacuum at 50 °C overnight to give 0.80 g of poly(**4b**) as a viscous liquid in 80% yield. ¹H NMR δ 7.21-7.34 (m, 5H), 4.94-5.18 (br, 2H), 4.50-4.58 (s, 2H), 3.63-3.70 (br m, 6H), 3.58-3.63 (br m, 4H), 3.50-3.57 (br, 2H), 3.36-3.44 (br, 2H), 1.70-2.01 (br, 4H), 1.49-1.62 (br, 2H), 1.09-1.49 (br, 34H), 0.78-0.91 (t, 3H).

Preparation of polymeric micelles. Polymer (5 mg) and azobenzene (5 mg) were dissolved in 1mL acetone, and then the acetone solution was added drop-wise over two minutes to 5 mL of ice-cold water (magnetically stirred) in a 25 mL Schlenk flask. The flask was then placed under a partial vacuum to remove the acetone. Floating particles were removed by filtration, giving a stable homogenous microemulsion (polymer + dye). For controls, the same procedure was used to prepare micelles free of azobenzene (polymer only) and azobenzene solutions free of polymer (dye only).

Appendicies

Appendix A. NMR Spectra

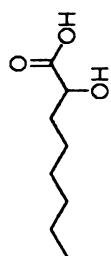
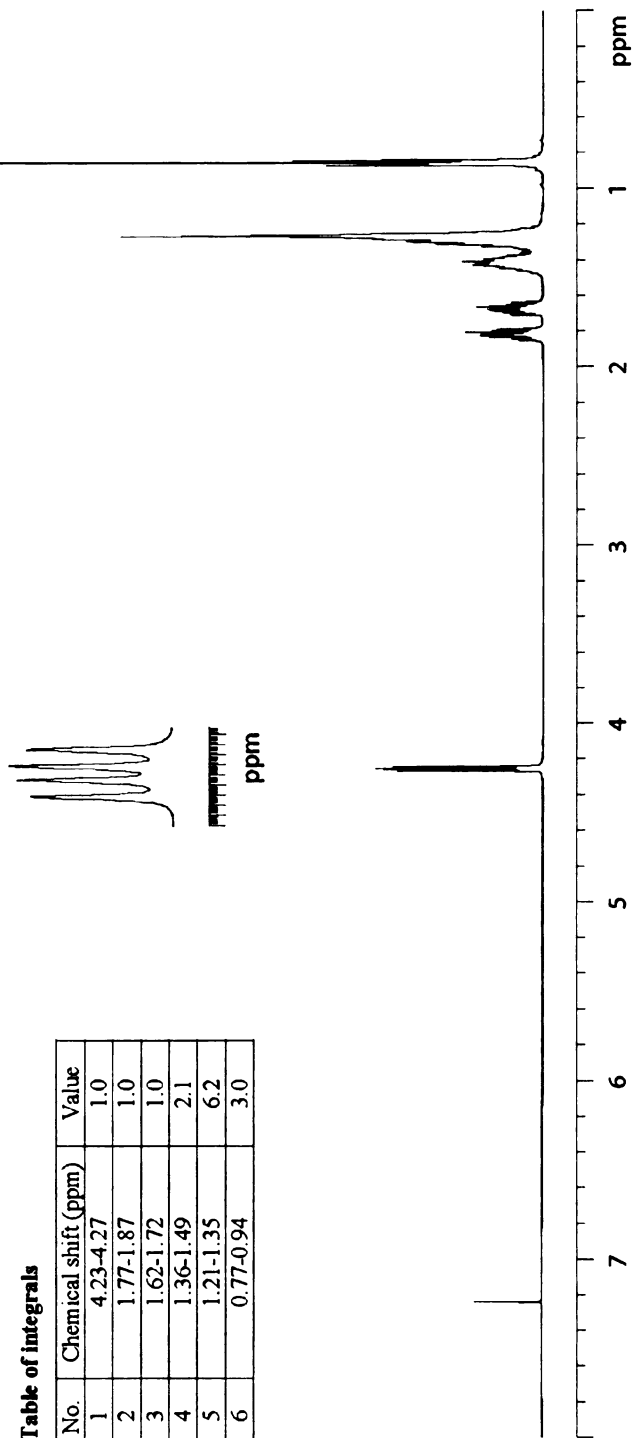


Table of integrals

No.	Chemical shift (ppm)	Value
1	4.23-4.27	1.0
2	1.77-1.87	1.0
3	1.62-1.72	1.0
4	1.36-1.49	2.1
5	1.21-1.35	6.2
6	0.77-0.94	3.0



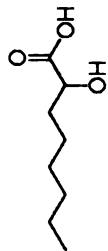
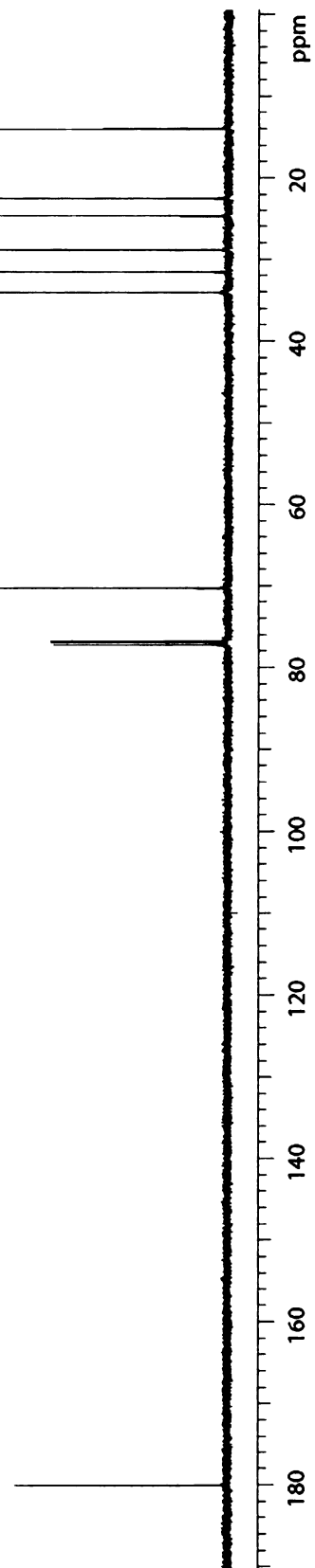


Table of peaks

No.	Chemical shift (ppm)	No.	Chemical shift (ppm)
1	180.04	5	28.88
2	70.28	6	24.66
3	34.09	7	22.52
4	31.58	8	14.00



Appendix A 2. ¹³C NMR spectrum of C6-α-hydroxy acid

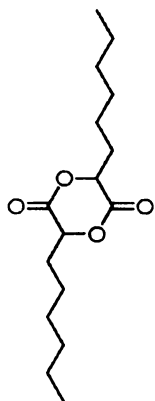
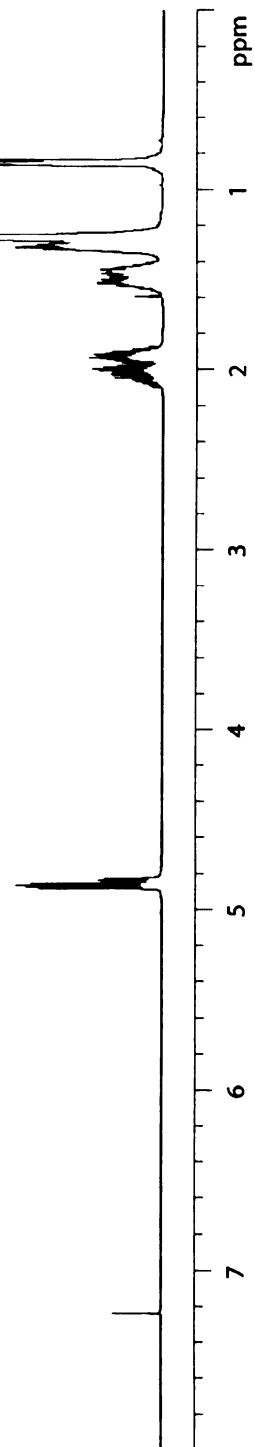
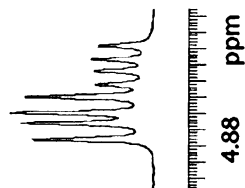


Table of Integrals

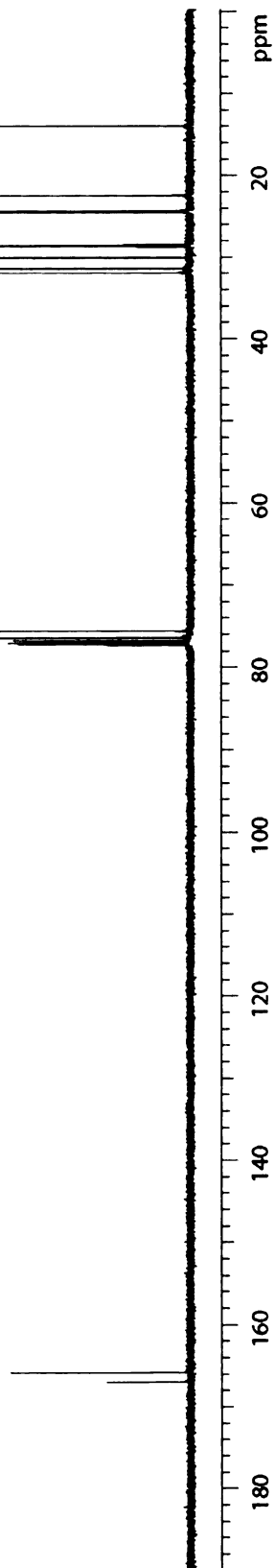
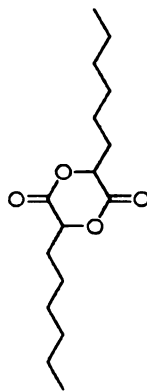
No.	Chemical shift (ppm)	Value
1	4.82-4.90	2.0
2	1.97-2.10	2.0
3	1.88-1.97	2.0
4	1.40-1.56	4.0
5	1.22-1.36	11.9
6	0.75-0.91	5.9



Appendix A 3. ¹H NMR spectrum of C6 dimer

Table of peaks

No.	Chemical shift (ppm)	No.	Chemical shift (ppm)
1	166.99	9	28.69
2	165.84	10	28.52
3	76.36	11	24.45
4	75.56	12	24.28
5	31.89	13	22.44
6	31.41	14	22.41
7	31.36	15	13.96
8	30.06	16	13.93



Appendix A 4. ^{13}C NMR spectrum of C6 dimer

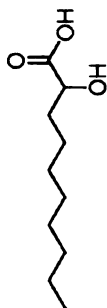
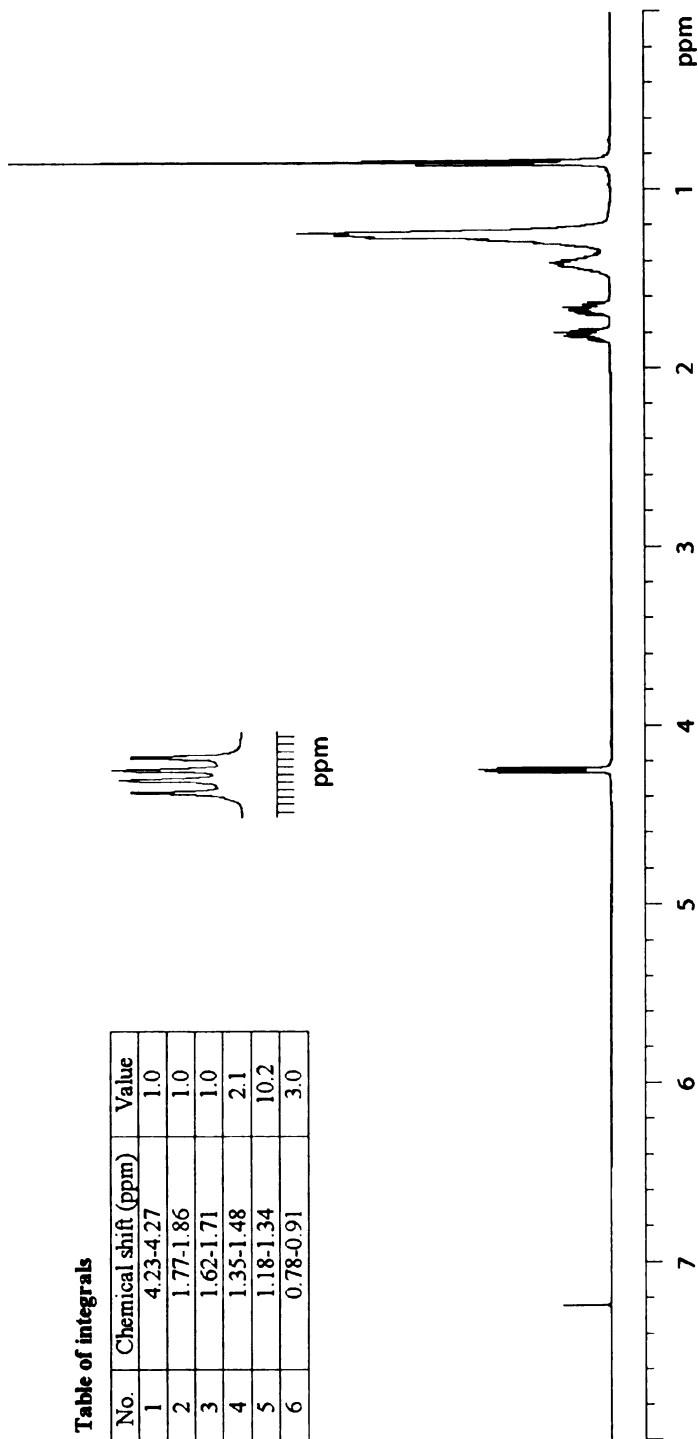


Table of integrals

No.	Chemical shift (ppm)	Value
1	4.23-4.27	1.0
2	1.77-1.86	1.0
3	1.62-1.71	1.0
4	1.35-1.48	2.1
5	1.18-1.34	10.2
6	0.78-0.91	3.0



Appendix A 5. ¹H NMR spectrum of C8-α-hydroxy acid

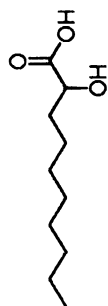
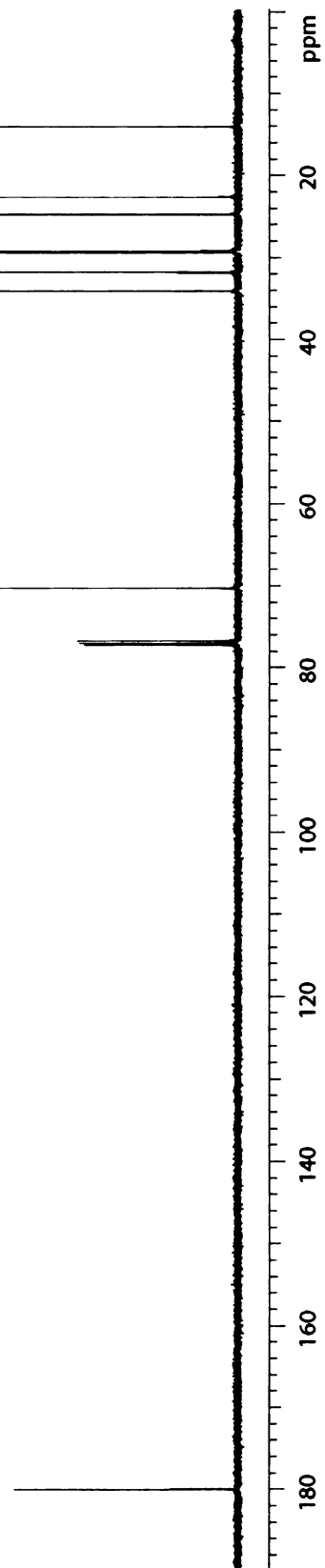


Table of peaks

No.	Chemical shift (ppm)	No.	Chemical shift (ppm)
1	180.01	6	29.23
2	70.28	7	29.19
3	34.09	8	24.72
4	31.81	9	22.62
5	29.36	10	14.05



Appendix A 6. ^{13}C NMR spectrum of C8- α -hydroxy acid

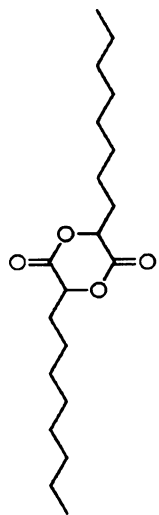
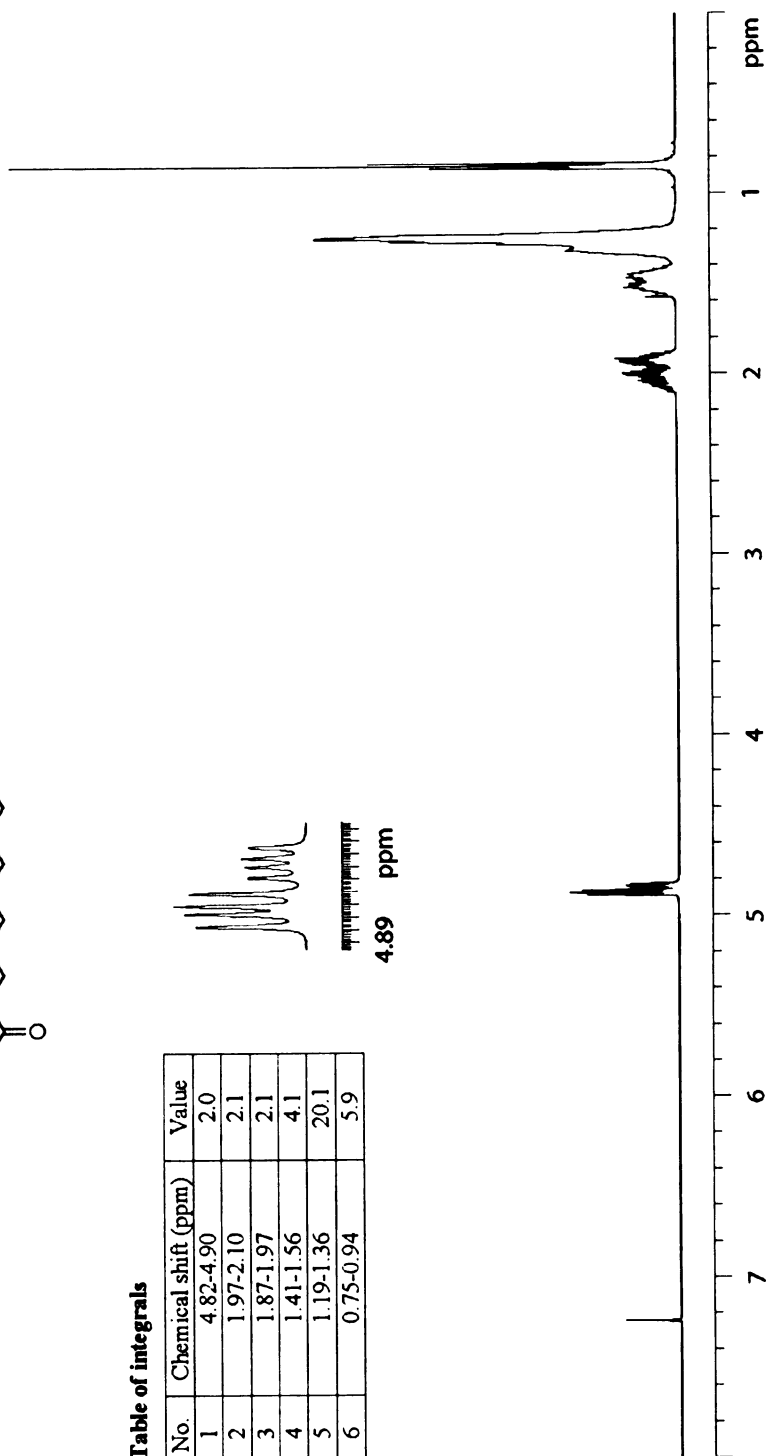


Table of integrals

No.	Chemical shift (ppm)	Value
1	4.82-4.90	2.0
2	1.97-2.10	2.1
3	1.87-1.97	2.1
4	1.41-1.56	4.1
5	1.19-1.36	20.1
6	0.75-0.94	5.9



4.89 ppm

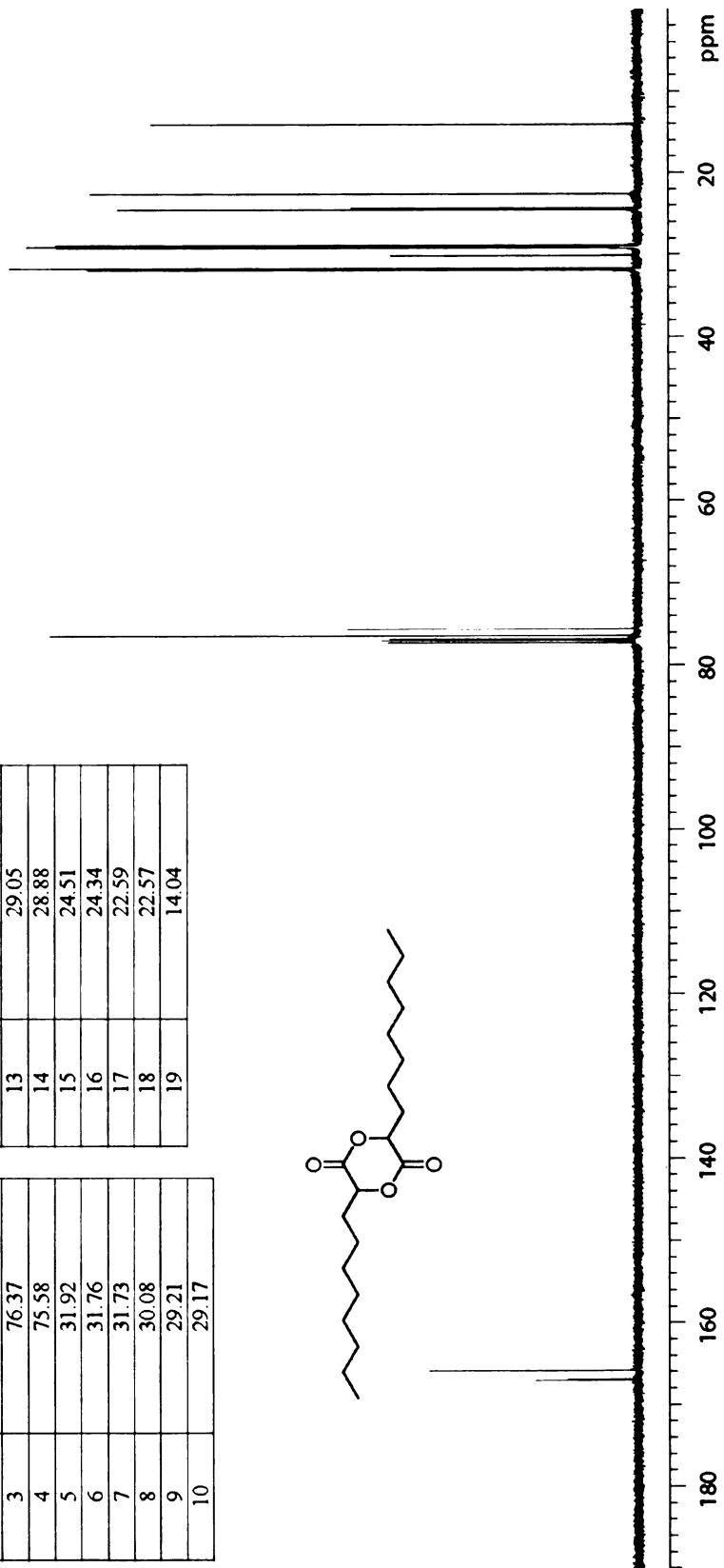
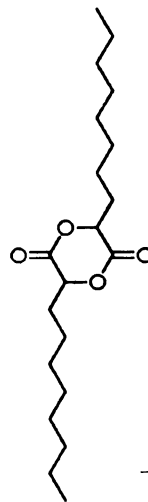


Appendix A 7. ¹H NMR spectrum of C8 dimer

Table of peaks

No.	Chemical shift (ppm)
1	166.98
2	165.85
3	76.37
4	75.58
5	31.92
6	31.76
7	31.73
8	30.08
9	29.21
10	29.17

No.	Chemical shift (ppm)
11	29.10
12	29.06
13	29.05
14	28.88
15	24.51
16	24.34
17	22.59
18	22.57
19	14.04



Appendix A 8. ¹³C NMR spectrum of C8 dimer

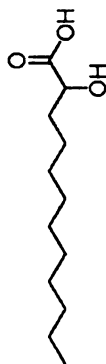
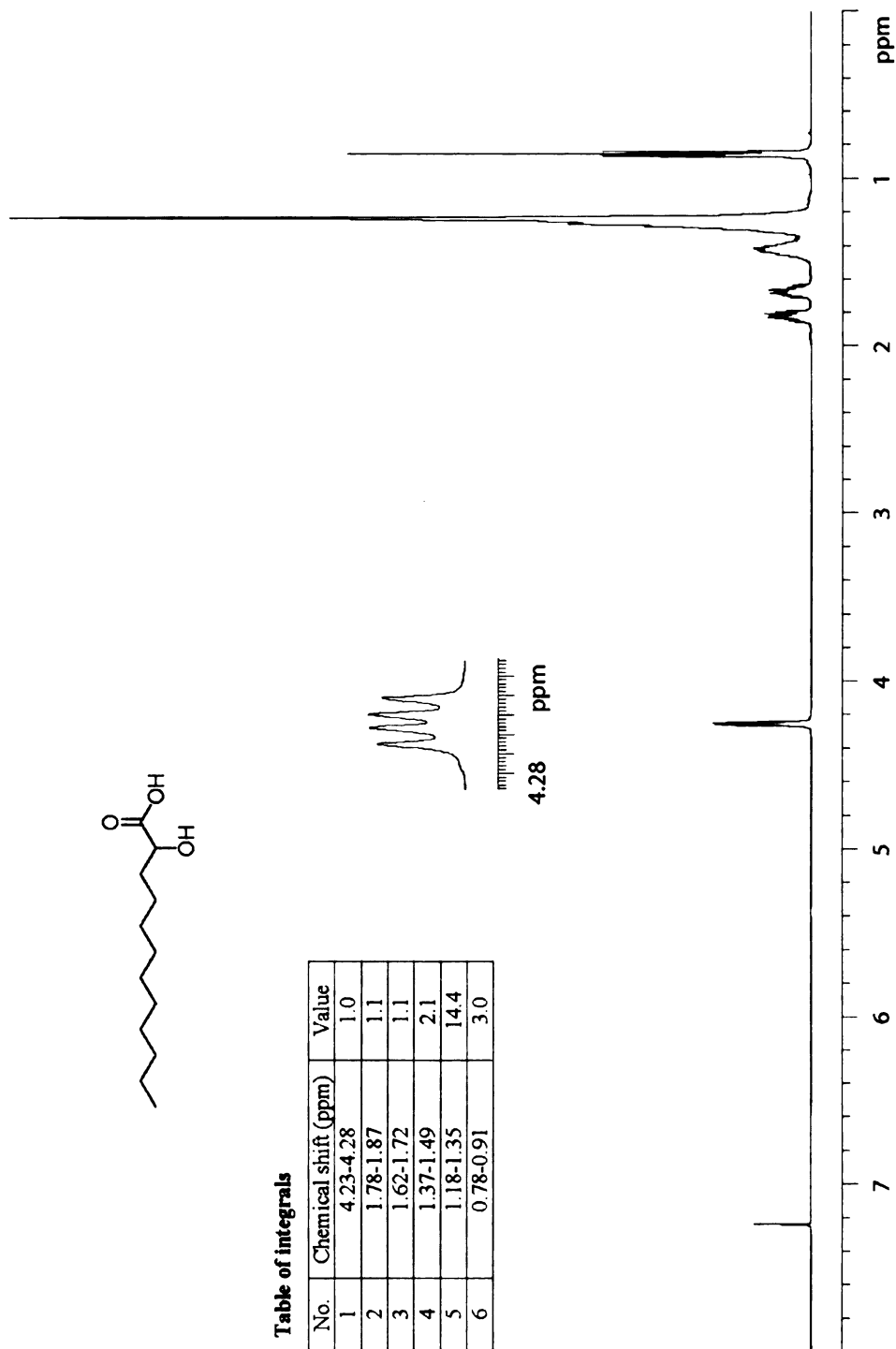
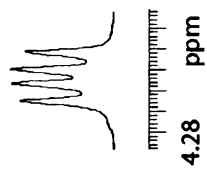


Table of integrals

No.	Chemical shift (ppm)	Value
1	4.23-4.28	1.0
2	1.78-1.87	1.1
3	1.62-1.72	1.1
4	1.37-1.49	2.1
5	1.18-1.35	14.4
6	0.78-0.91	3.0



Appendix A 9. ¹H NMR spectrum of C10 α-hydroxy acid

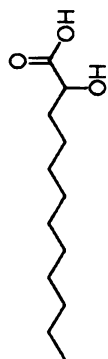
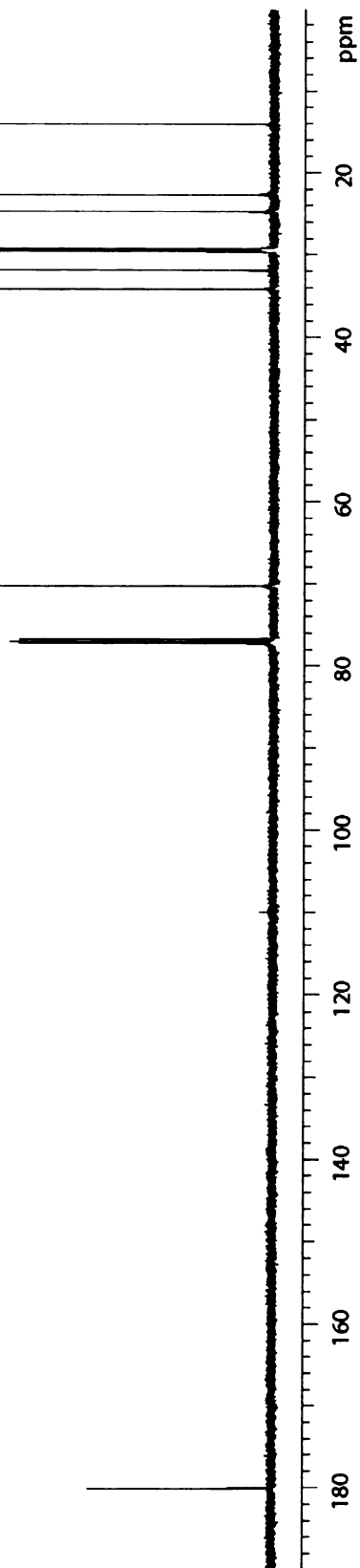


Table of peaks

No.	Chemical shift (ppm)	No.	Chemical shift (ppm)
1	180.10	7	29.42
2	70.27	8	29.30
3	34.14	9	29.24
4	31.88	10	24.73
5	29.57	11	22.66
6	29.54	12	14.09



Appendix A 10. ¹³C NMR spectrum of C10 α-hydroxy acid

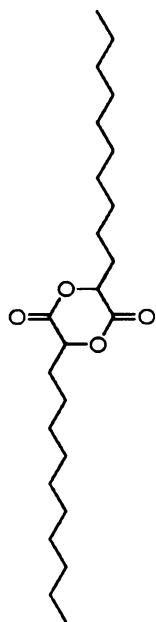
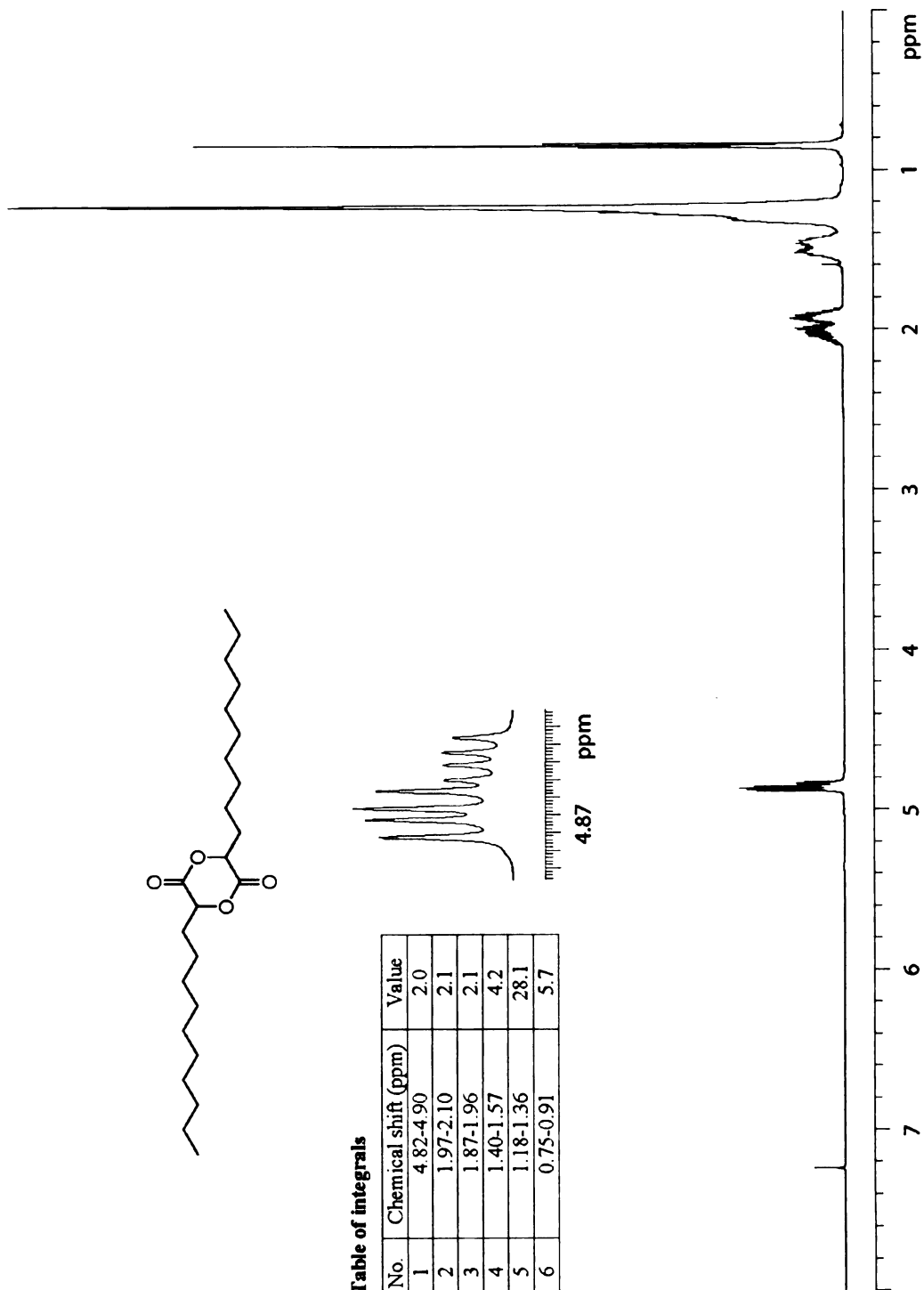
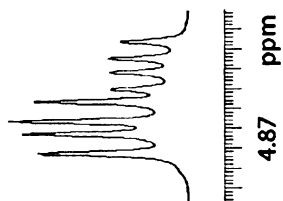


Table of integrals

No.	Chemical shift (ppm)	Value
1	4.82-4.90	2.0
2	1.97-2.10	2.1
3	1.87-1.96	2.1
4	1.40-1.57	4.2
5	1.18-1.36	28.1
6	0.75-0.91	5.7

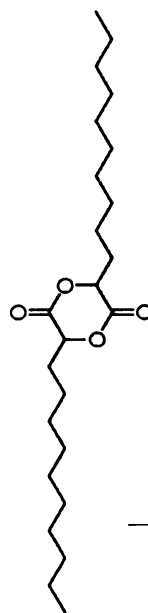


Appendix A 11. 1H NMR spectrum of C10 dimer

Table of peaks

No.	Chemical shift (ppm)
1	166.99
2	165.84
3	76.36
4	75.56
5	31.90
6	31.83
7	31.82
8	30.06
9	29.50
10	29.47
11	29.44

No.	Chemical shift (ppm)
12	29.40
13	29.25
14	29.23
15	29.21
16	29.05
17	28.87
18	24.51
19	24.33
20	22.61
21	14.05



ppm

20

40

60

80

100

120

140

160

180

Appendix A 12. ¹³C NMR spectrum of C10 dimer

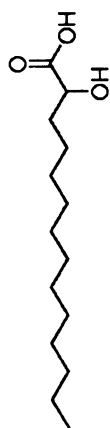
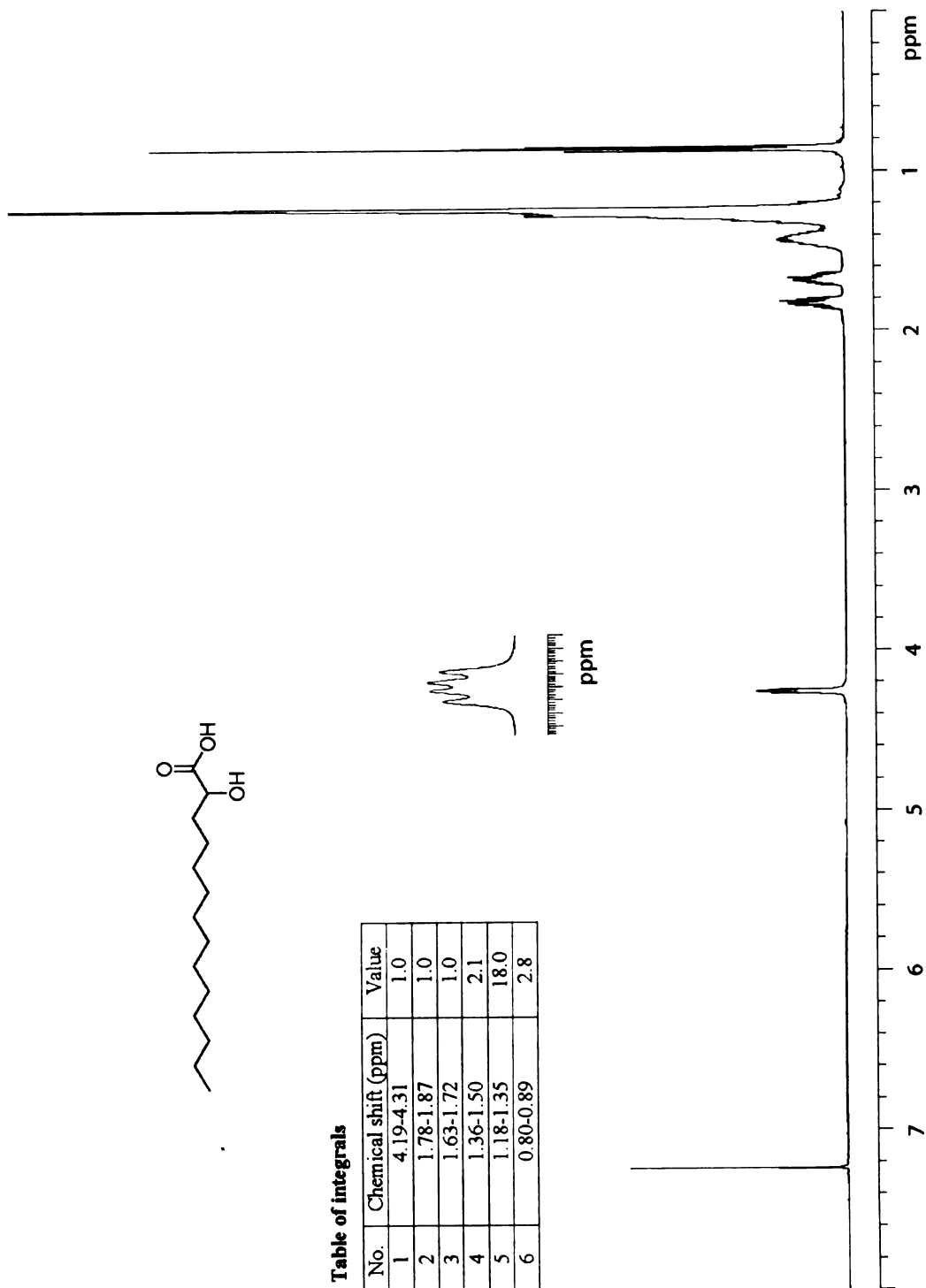


Table of integrals

No.	Chemical shift (ppm)	Value
1	4.19-4.31	1.0
2	1.78-1.87	1.0
3	1.63-1.72	1.0
4	1.36-1.50	2.1
5	1.18-1.35	18.0
6	0.80-0.89	2.8



Appendix A 13. ^1H NMR spectrum of C12 α -hydroxy acid

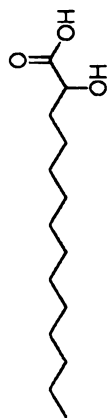
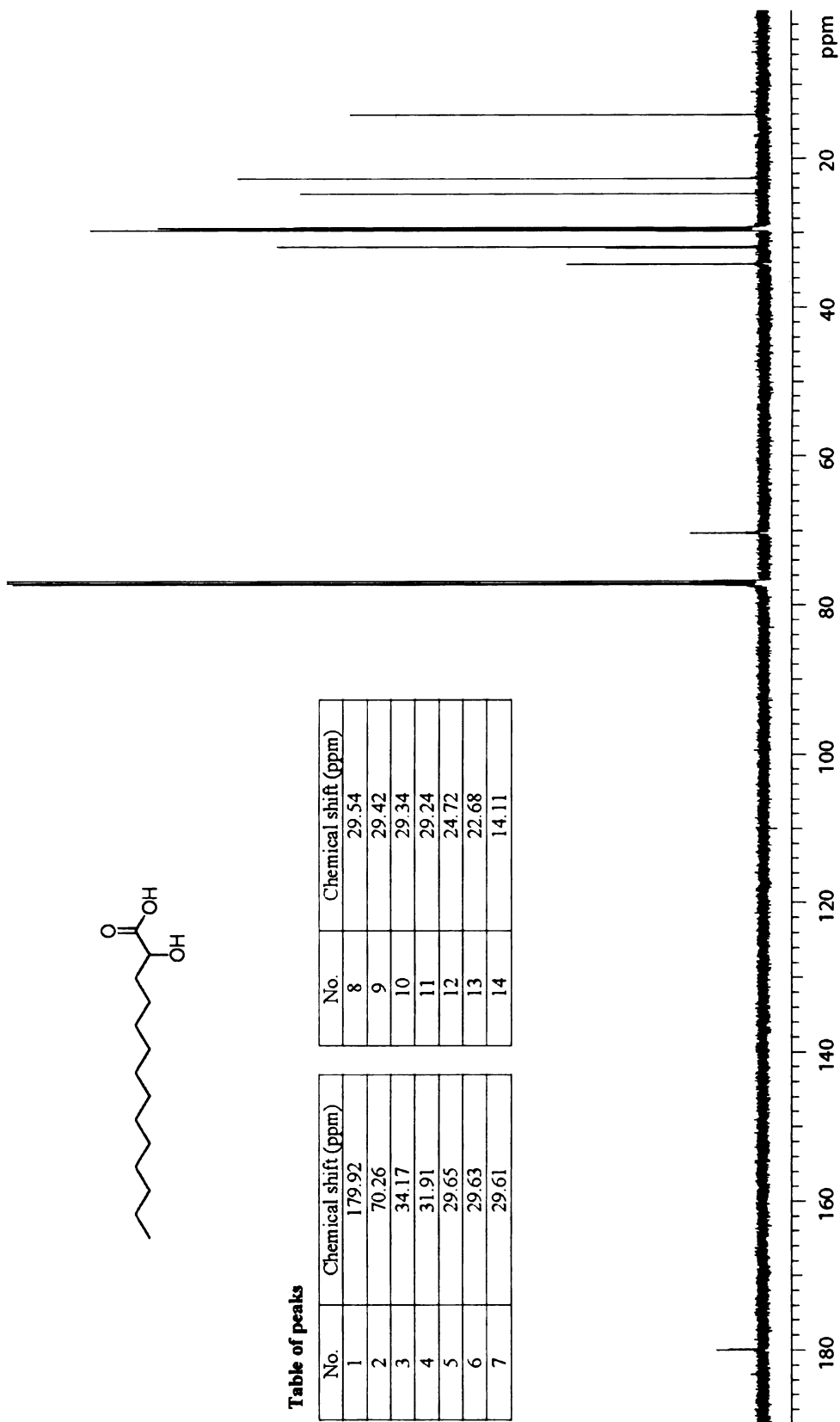


Table of peaks

No.	Chemical shift (ppm)	No.	Chemical shift (ppm)
1	179.92	8	29.54
2	70.26	9	29.42
3	34.17	10	29.34
4	31.91	11	29.24
5	29.65	12	24.72
6	29.63	13	22.68
7	29.61	14	14.11



Appendix A 14. ^{13}C NMR spectrum of C12 α -hydroxy acid

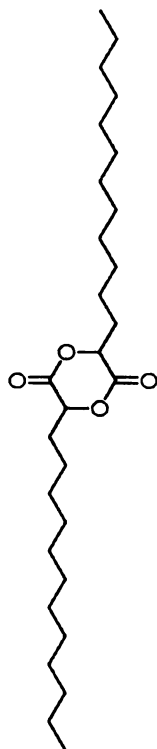
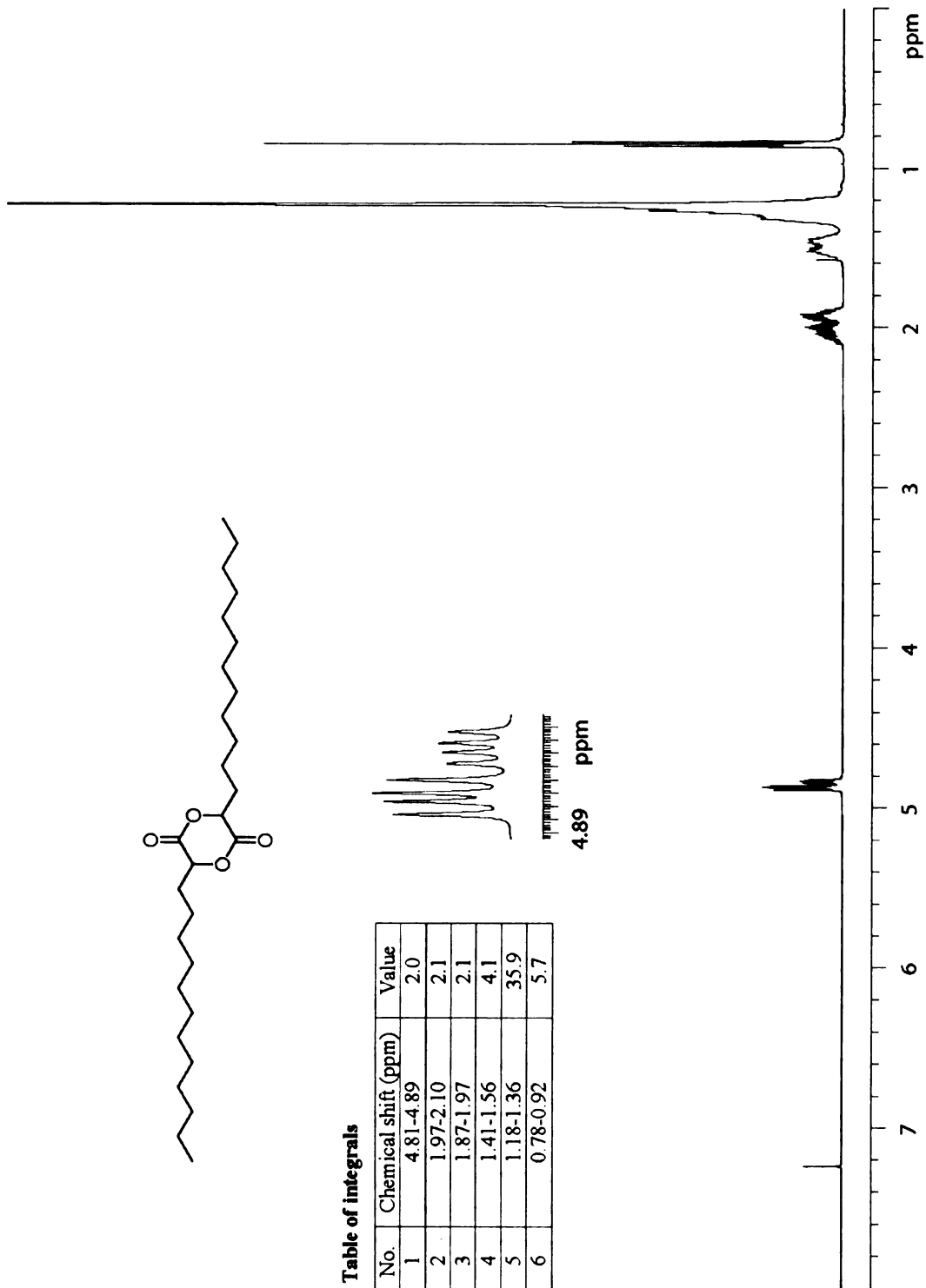
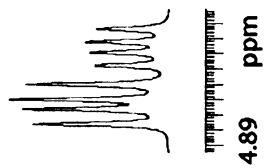


Table of integrals

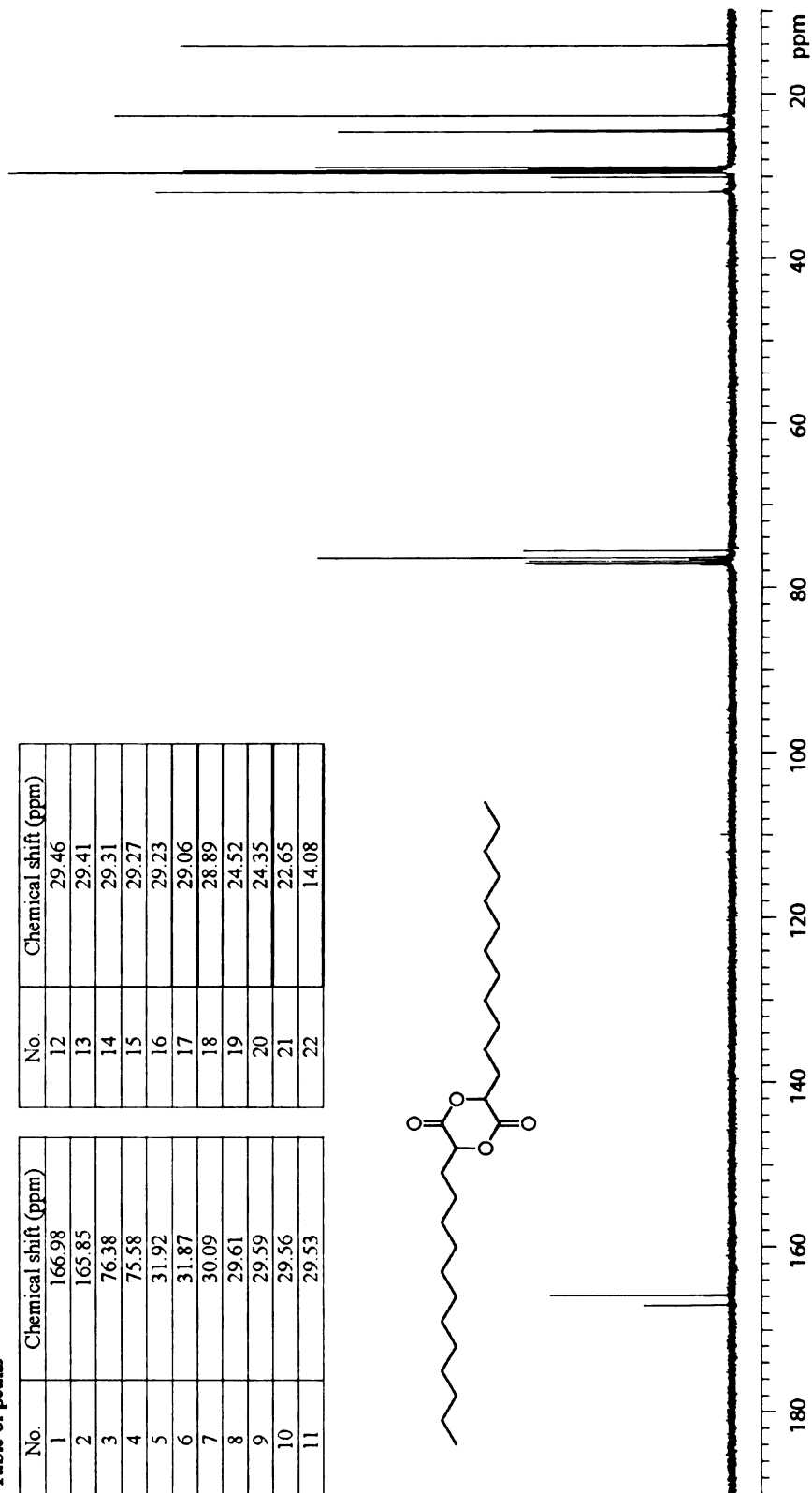
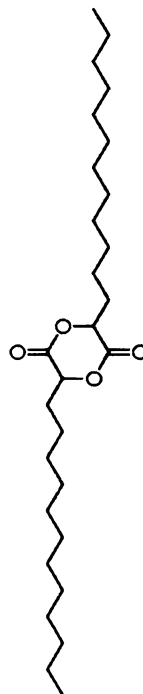
No.	Chemical shift (ppm)	Value
1	4.81-4.89	2.0
2	1.97-2.10	2.1
3	1.87-1.97	2.1
4	1.41-1.56	4.1
5	1.18-1.36	35.9
6	0.78-0.92	5.7



Appendix A 15. ¹H NMR spectrum of C12 dimer

Table of peaks

No.	Chemical shift (ppm)	No.	Chemical shift (ppm)
1	166.98	12	29.46
2	165.85	13	29.41
3	76.38	14	29.31
4	75.58	15	29.27
5	31.92	16	29.23
6	31.87	17	29.06
7	30.09	18	28.89
8	29.61	19	24.52
9	29.59	20	24.35
10	29.56	21	22.65
11	29.53	22	14.08



Appendix A 16. ¹³C NMR spectrum of C12 dimer

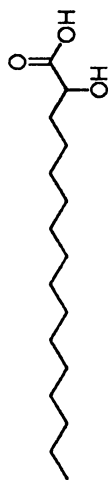
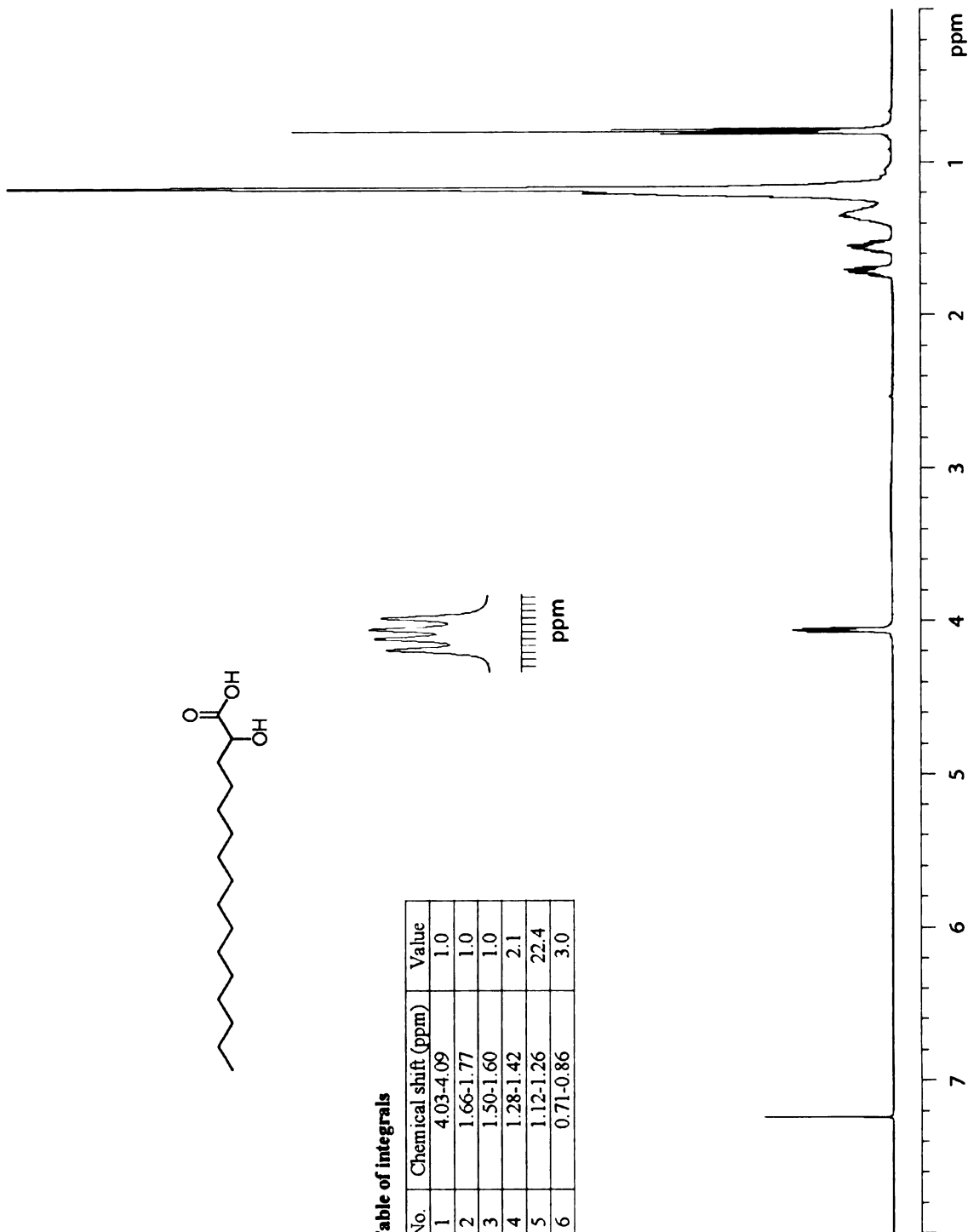


Table of integrals

No.	Chemical shift (ppm)	Value
1	4.03-4.09	1.0
2	1.66-1.77	1.0
3	1.50-1.60	1.0
4	1.28-1.42	2.1
5	1.12-1.26	22.4
6	0.71-0.86	3.0



Appendix A 17. ¹H NMR spectrum of C14 α-hydroxy acid

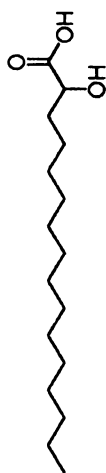
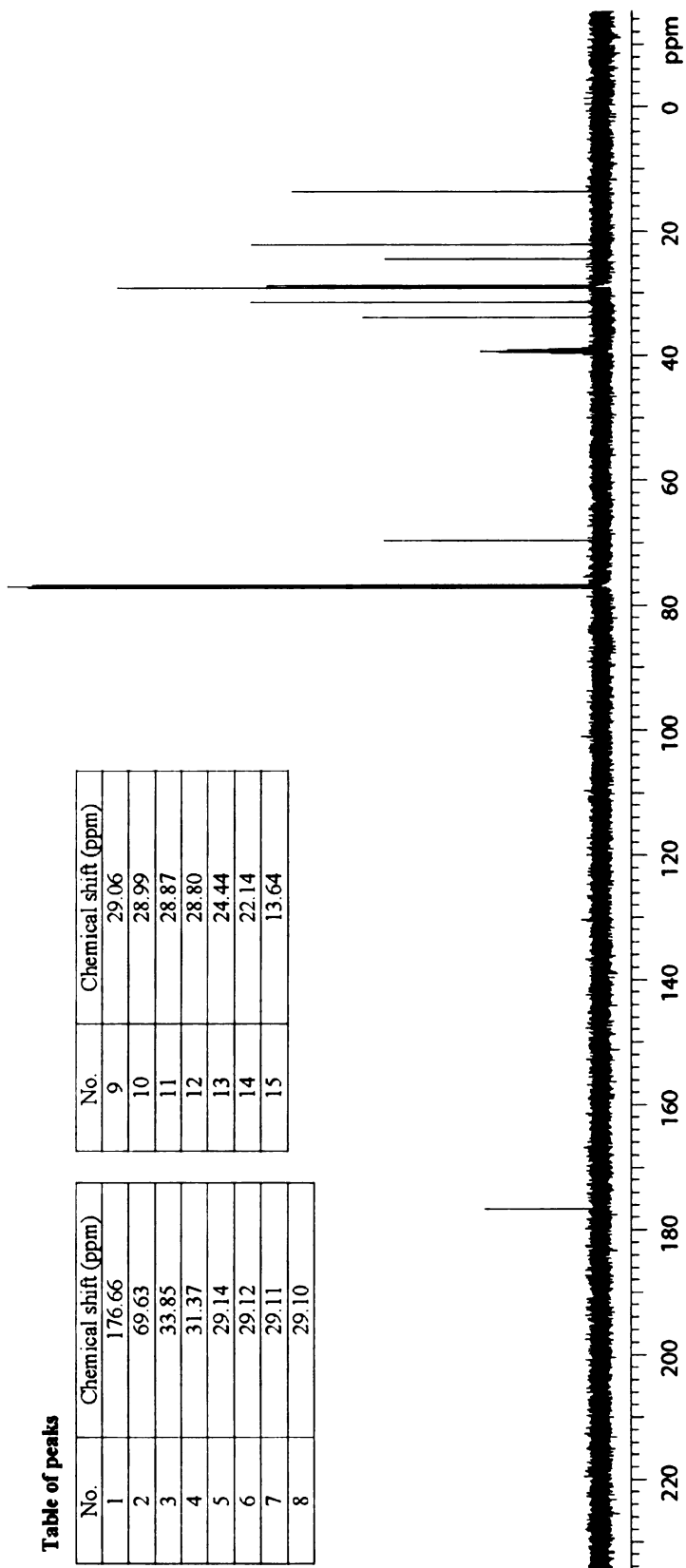


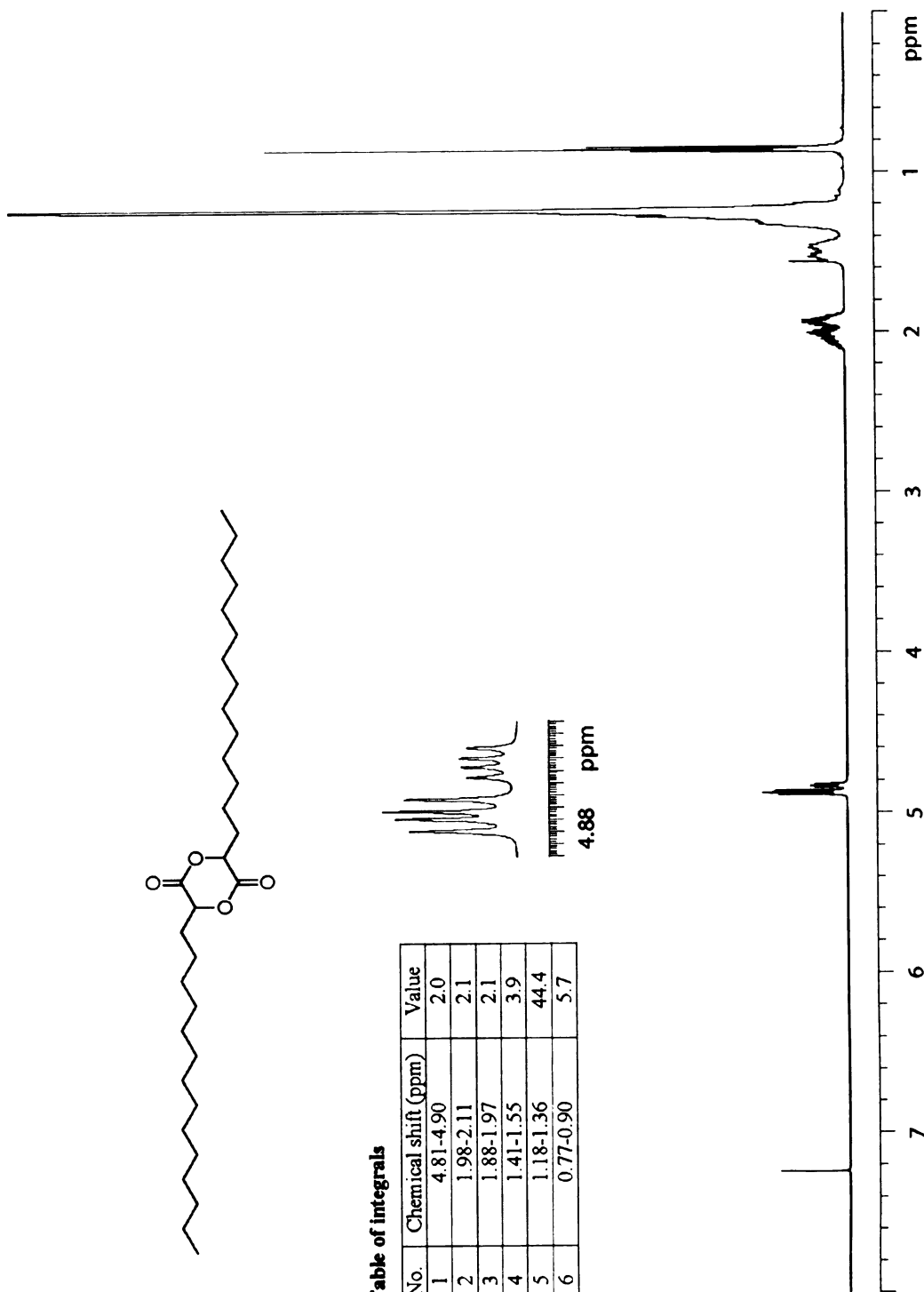
Table of peaks

No.	Chemical shift (ppm)
9	29.06
10	28.99
11	28.87
12	28.80
13	24.44
14	22.14
15	13.64

No.	Chemical shift (ppm)
1	176.66
2	69.63
3	33.85
4	31.37
5	29.14
6	29.12
7	29.11
8	29.10



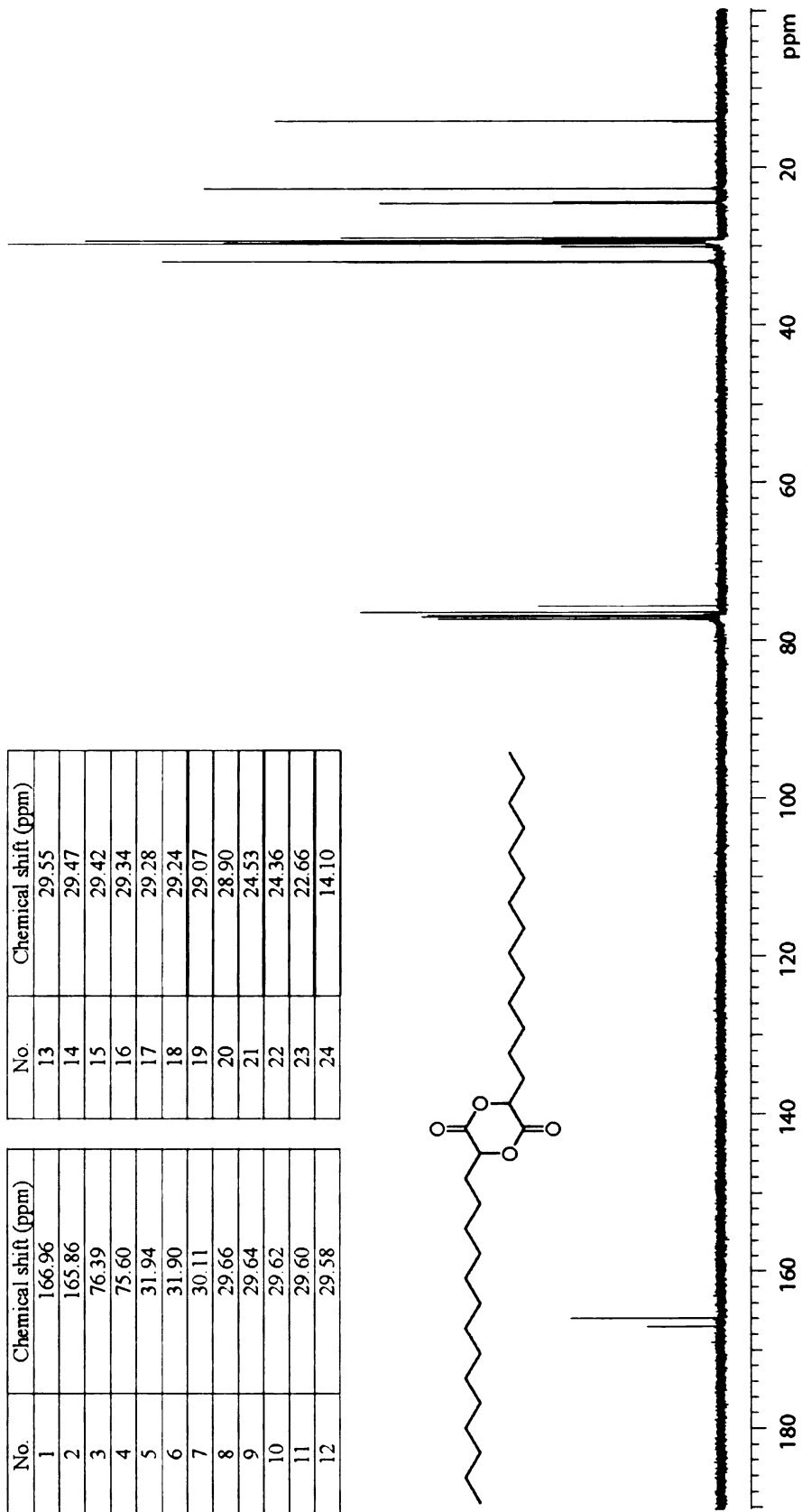
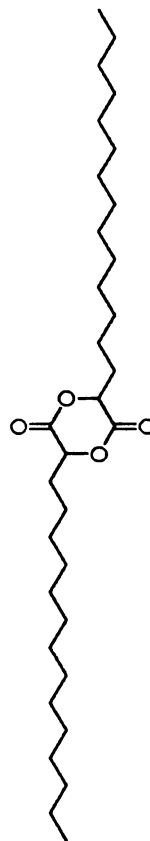
Appendix A 18. ^{13}C NMR spectrum of C14 α -hydroxy acid



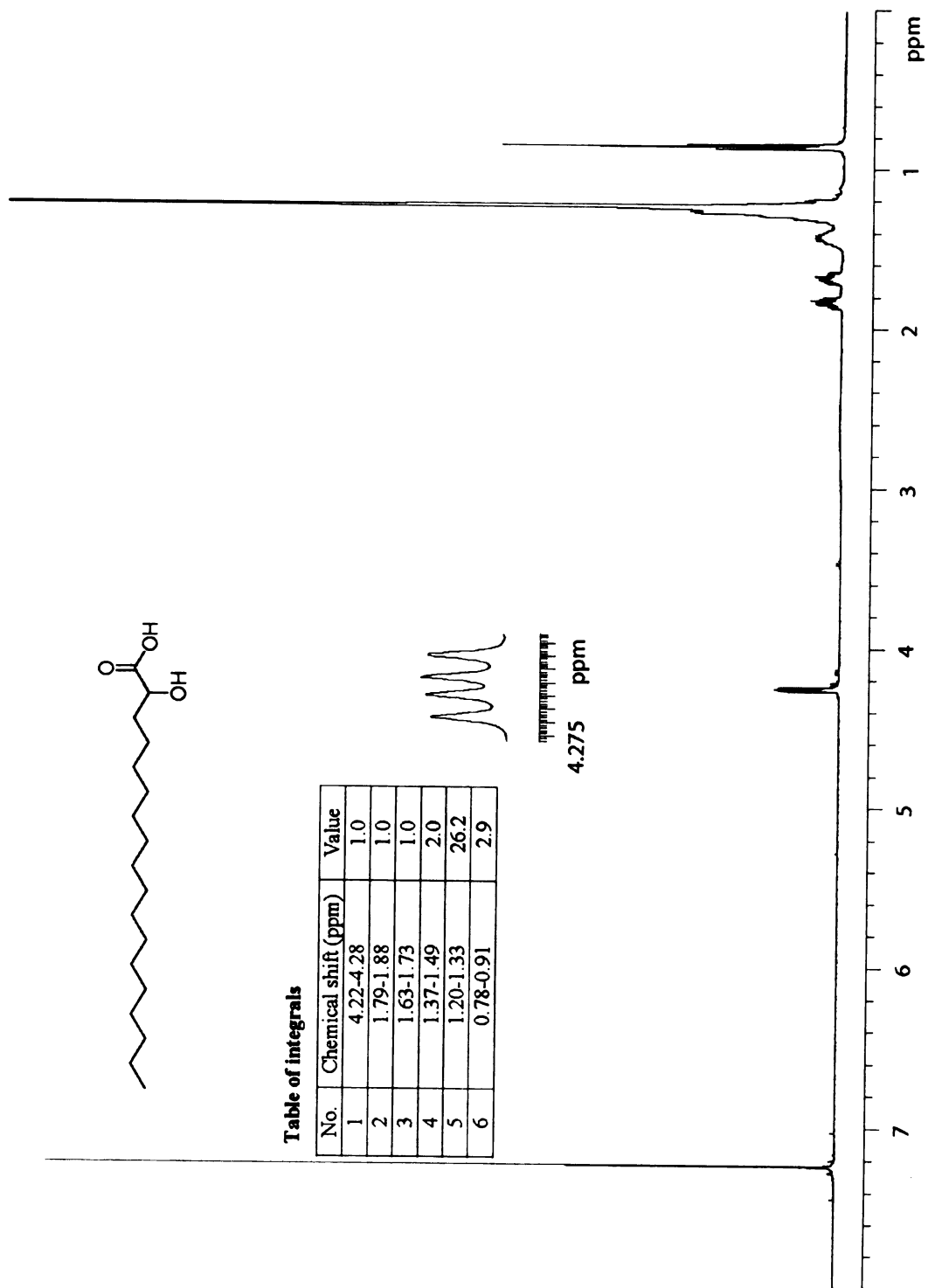
Appendix A 19. ¹H NMR spectrum of C14 dimer

Table of peaks

No.	Chemical shift (ppm)	No.	Chemical shift (ppm)
1	166.96	13	29.55
2	165.86	14	29.47
3	76.39	15	29.42
4	75.60	16	29.34
5	31.94	17	29.28
6	31.90	18	29.24
7	30.11	19	29.07
8	29.66	20	28.90
9	29.64	21	24.53
10	29.62	22	24.36
11	29.60	23	22.66
12	29.58	24	14.10



Appendix A 20. ¹³C NMR spectrum of C14 dimer



Appendix A 21. ^1H NMR spectrum of C16 α -hydroxy acid

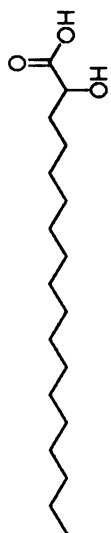
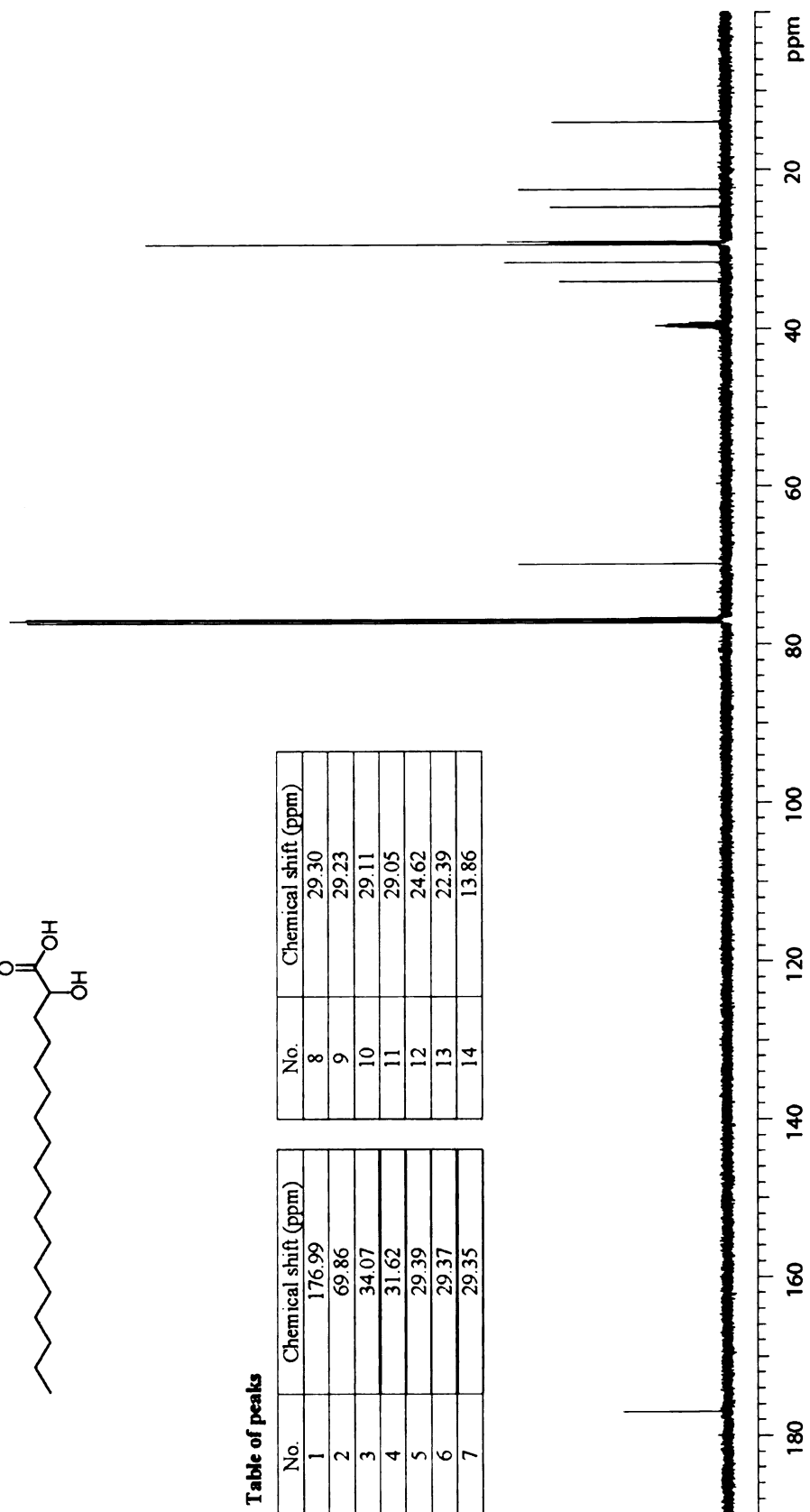


Table of peaks

No.	Chemical shift (ppm)
1	176.99
2	69.86
3	34.07
4	31.62
5	29.39
6	29.37
7	29.35

No.	Chemical shift (ppm)
8	29.30
9	29.23
10	29.11
11	29.05
12	24.62
13	22.39
14	13.86



Appendix A 22. ^{13}C NMR spectrum of C16 α -hydroxy acid

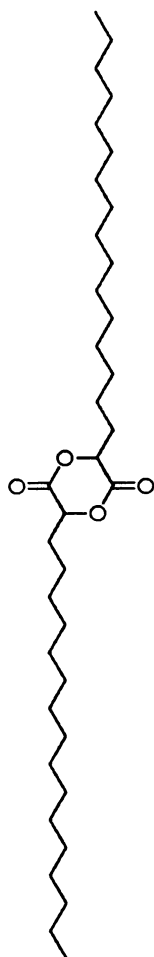
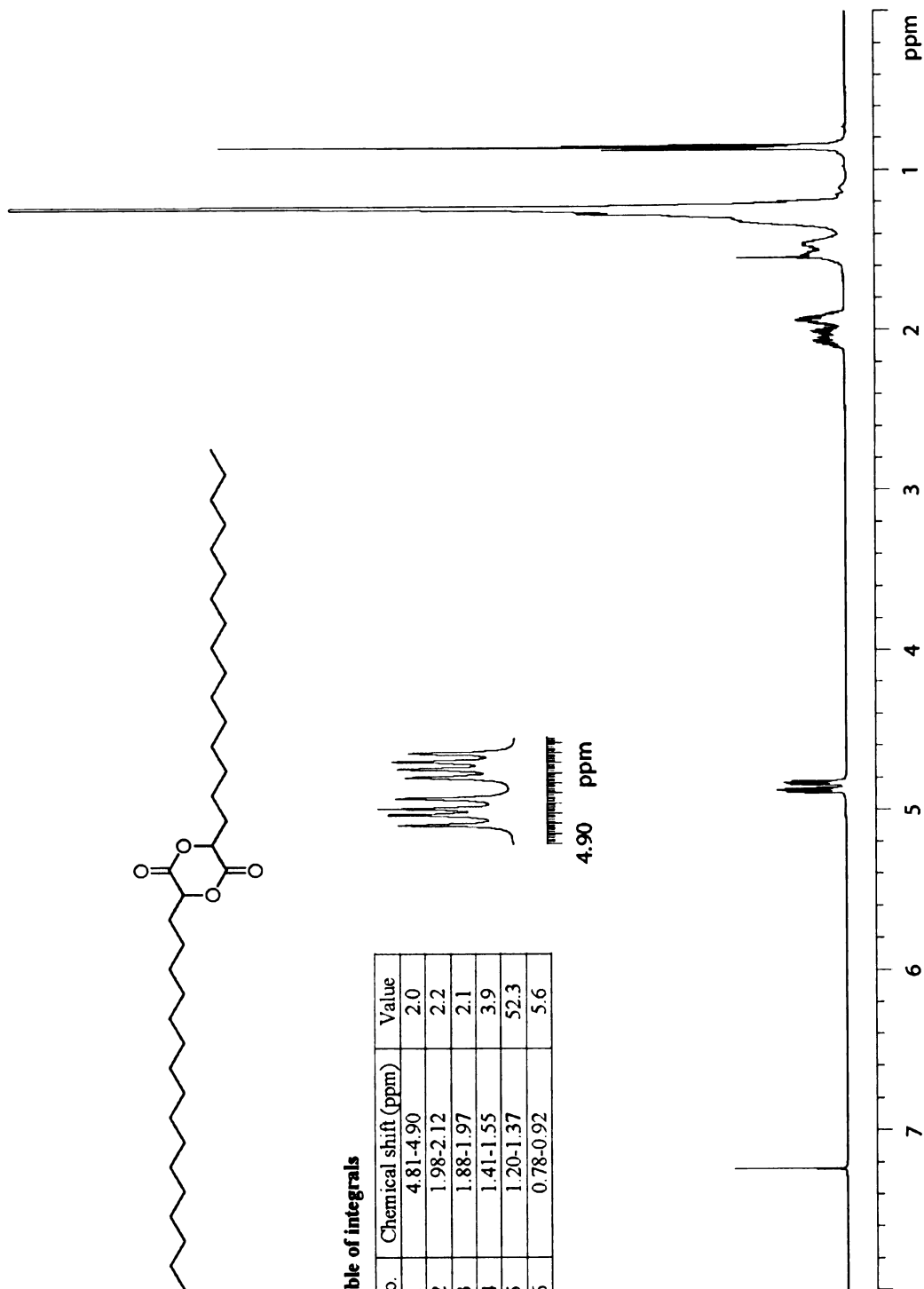
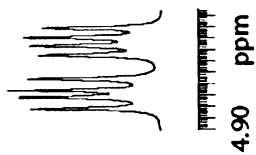


Table of integrals

No.	Chemical shift (ppm)	Value
1	4.81-4.90	2.0
2	1.98-2.12	2.2
3	1.88-1.97	2.1
4	1.41-1.55	3.9
5	1.20-1.37	52.3
6	0.78-0.92	5.6

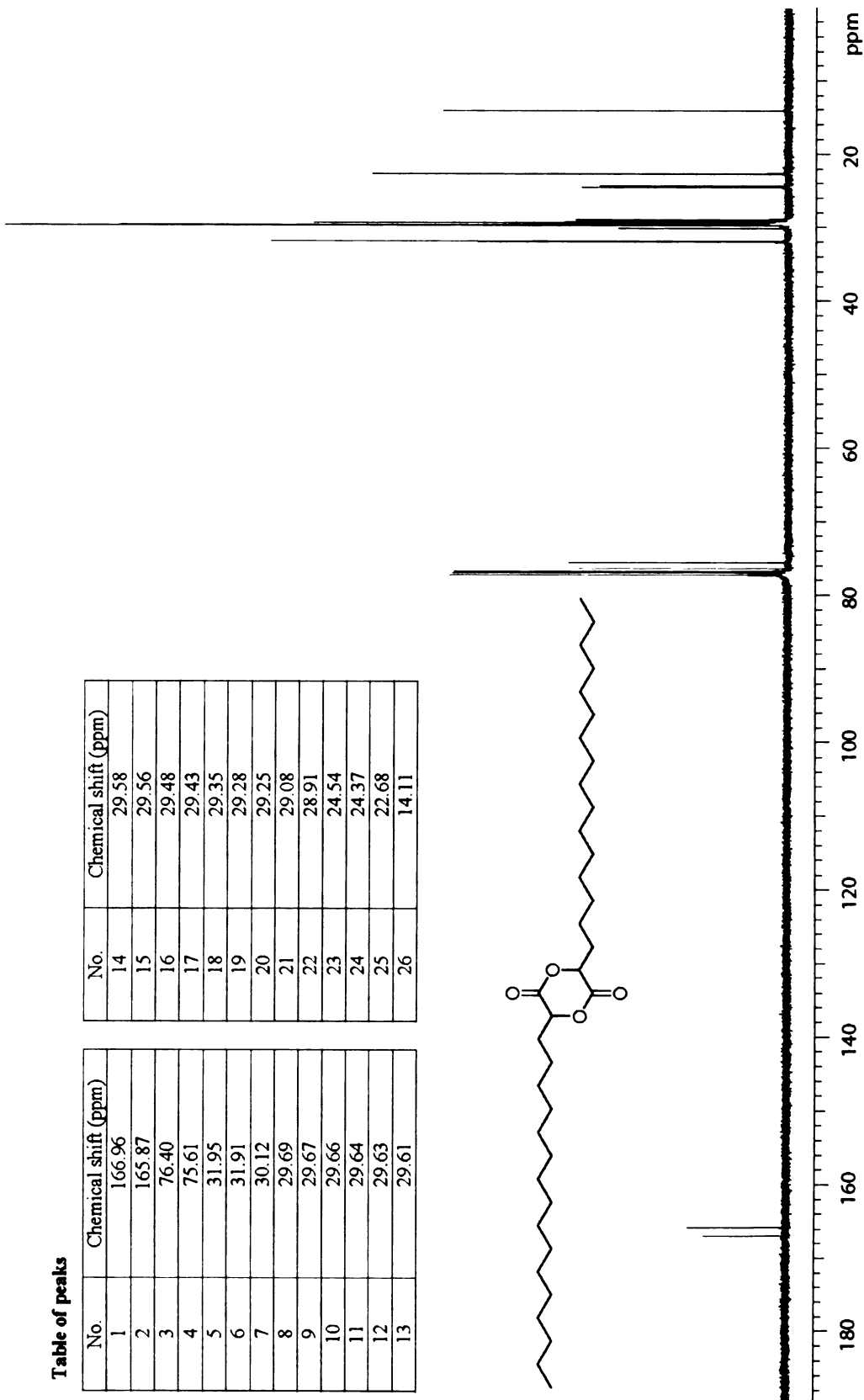
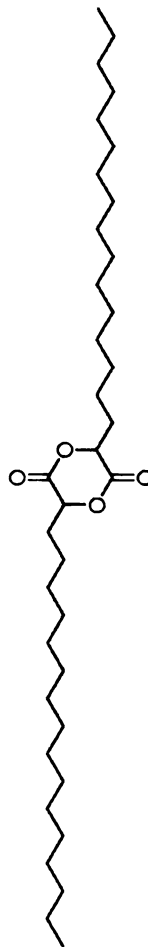


Appendix A 23. ¹H NMR spectrum of C16 dimer

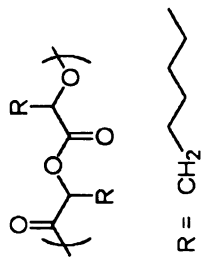
Table of peaks

No.	Chemical shift (ppm)
1	166.96
2	165.87
3	76.40
4	75.61
5	31.95
6	31.91
7	30.12
8	29.69
9	29.67
10	29.66
11	29.64
12	29.63
13	29.61

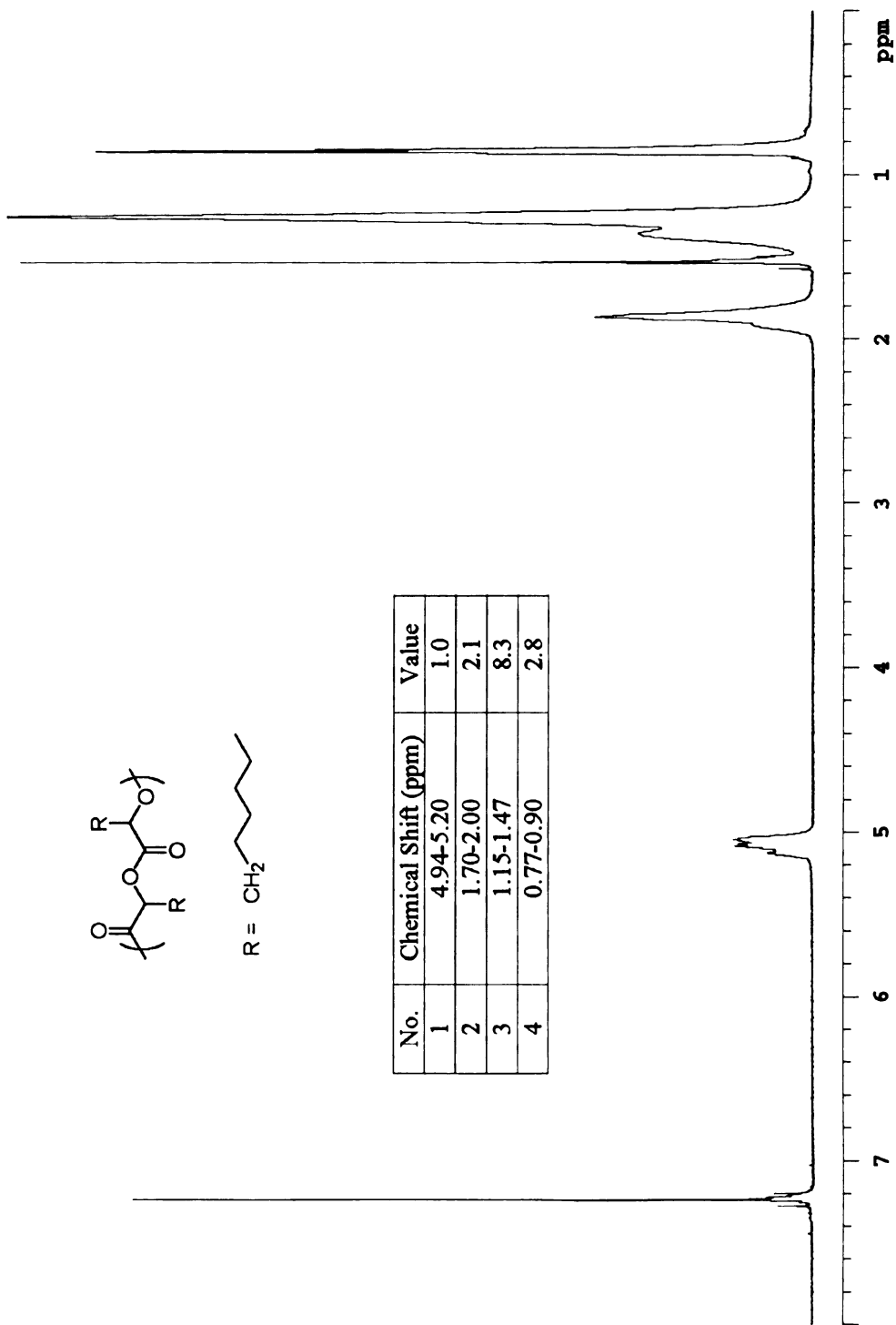
No.	Chemical shift (ppm)
14	29.58
15	29.56
16	29.48
17	29.43
18	29.35
19	29.28
20	29.25
21	29.08
22	28.91
23	24.54
24	24.37
25	22.68
26	14.11



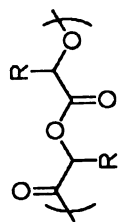
Appendix A 24. ¹³C NMR spectrum of C16 dimer



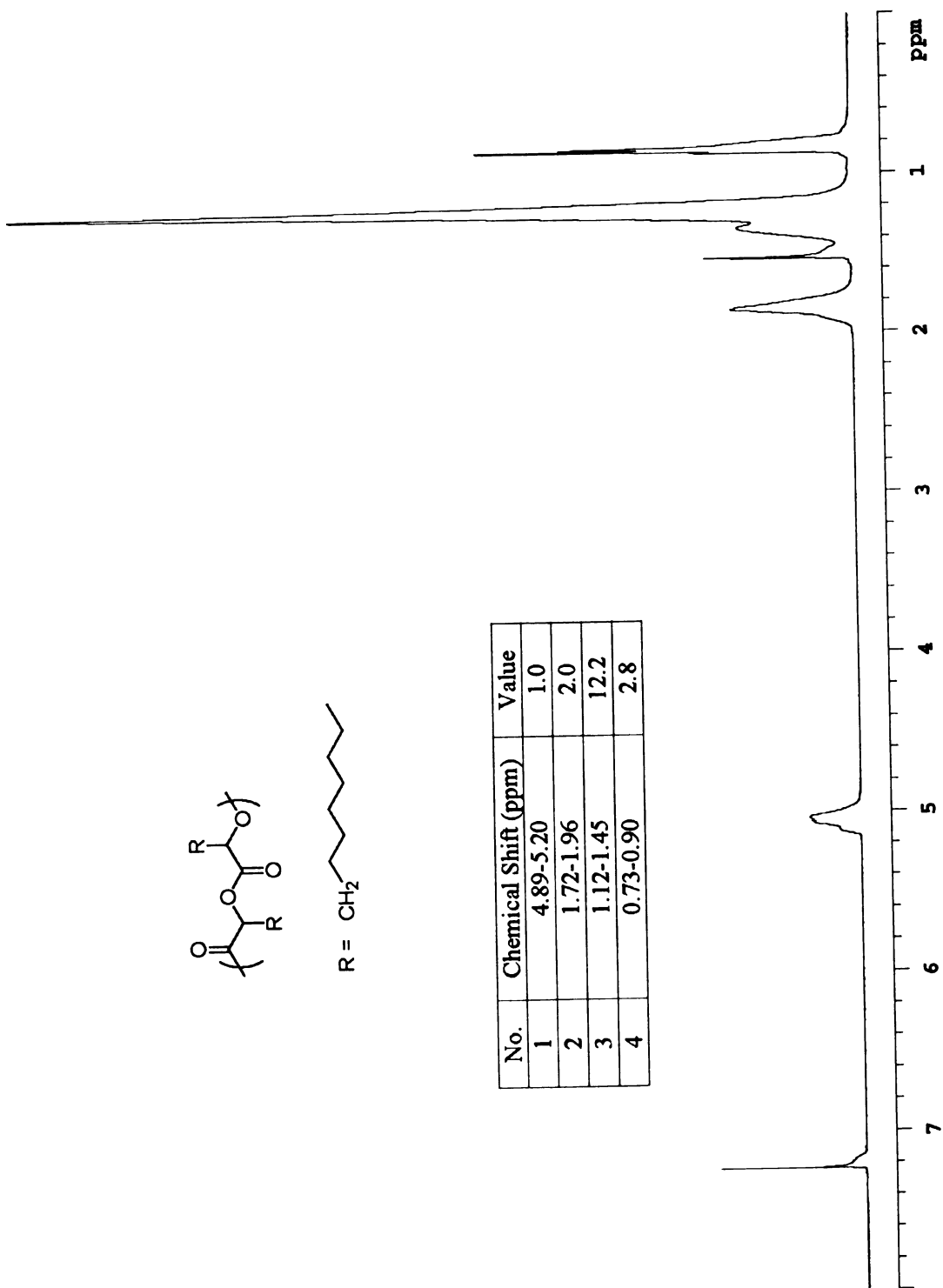
No.	Chemical Shift (ppm)	Value
1	4.94-5.20	1.0
2	1.70-2.00	2.1
3	1.15-1.47	8.3
4	0.77-0.90	2.8



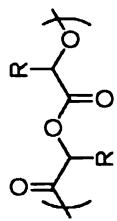
Appendix A 25. ^1H NMR spectrum of polyC6



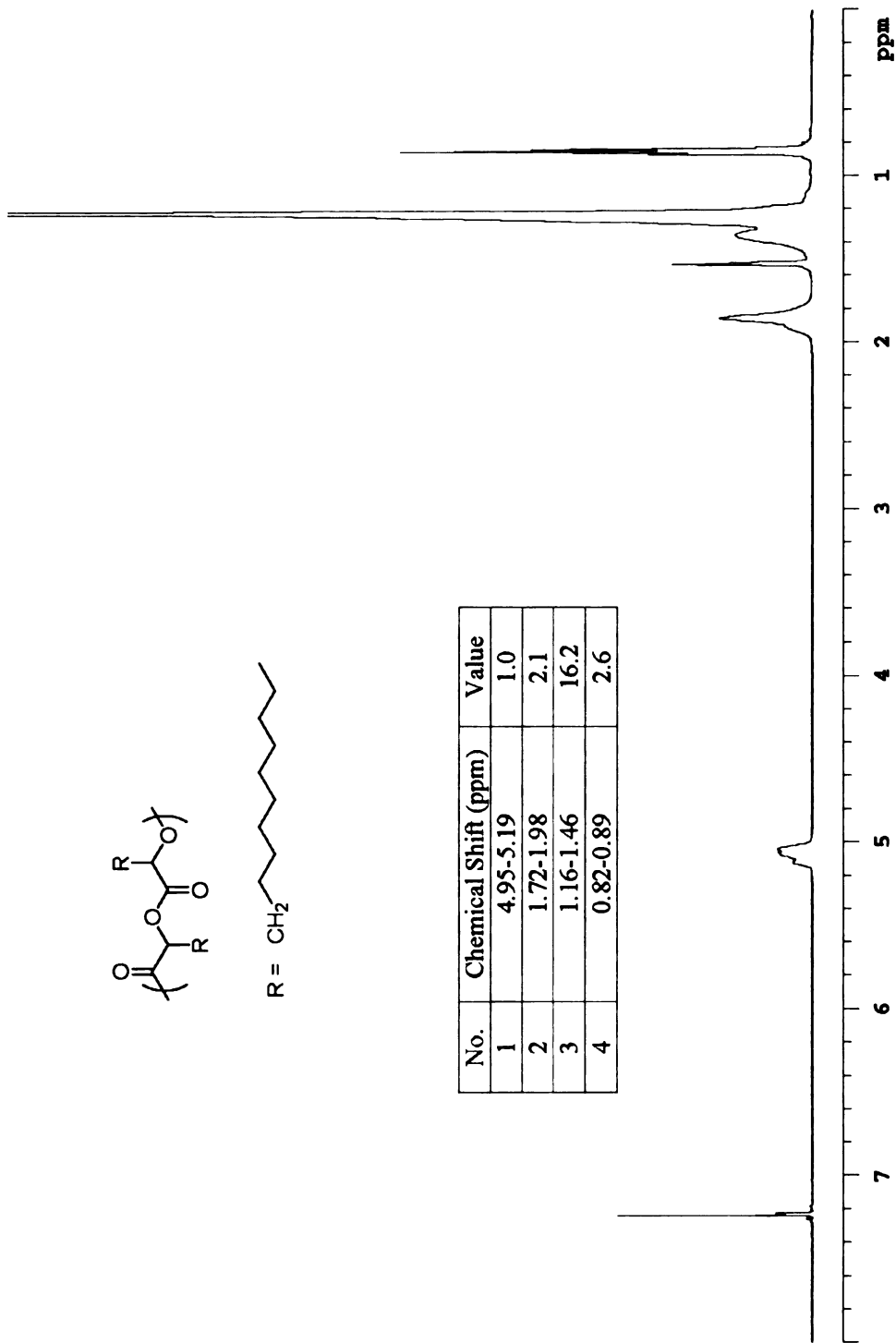
No.	Chemical Shift (ppm)	Value
1	4.89-5.20	1.0
2	1.72-1.96	2.0
3	1.12-1.45	12.2
4	0.73-0.90	2.8



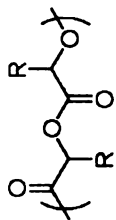
Appendix A 26. ^1H NMR spectrum of polyC8



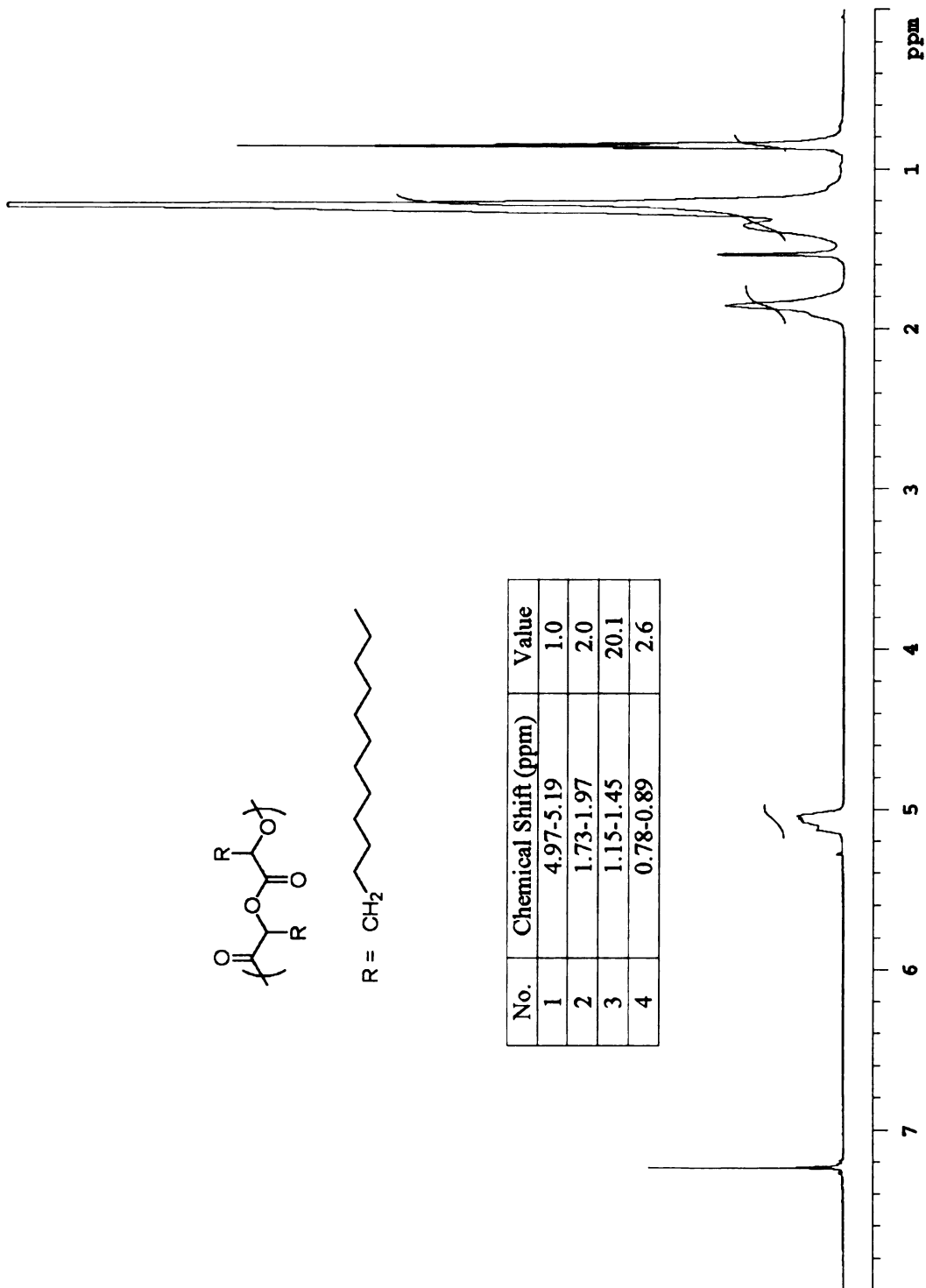
No.	Chemical Shift (ppm)	Value
1	4.95-5.19	1.0
2	1.72-1.98	2.1
3	1.16-1.46	16.2
4	0.82-0.89	2.6



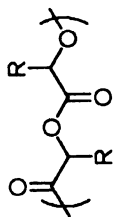
Appendix A 27. ¹H NMR spectrum of polyC10



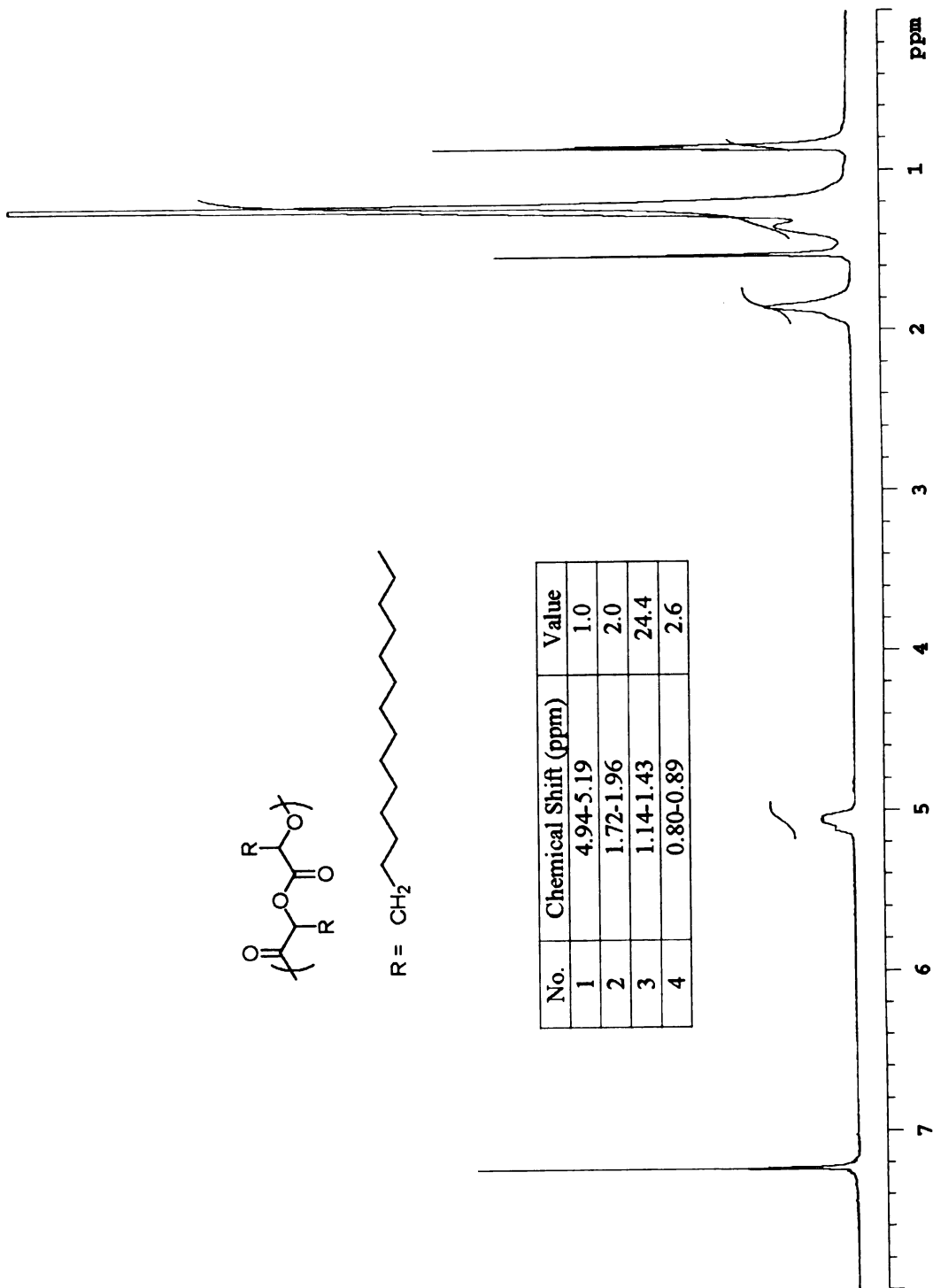
No.	Chemical Shift (ppm)	Value
1	4.97-5.19	1.0
2	1.73-1.97	2.0
3	1.15-1.45	20.1
4	0.78-0.89	2.6



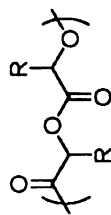
Appendix A 28. ¹H NMR spectrum of polyC12



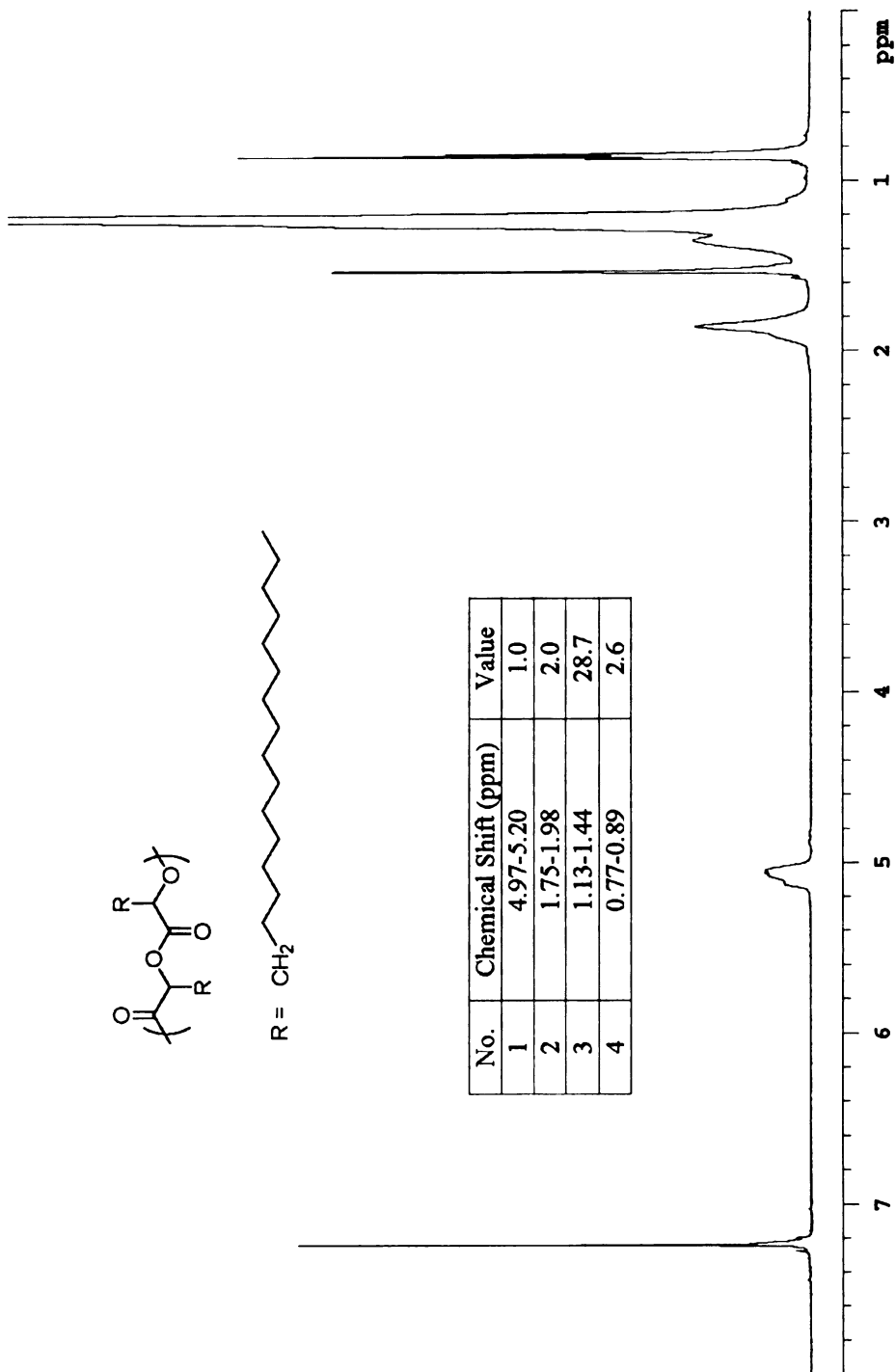
No.	Chemical Shift (ppm)	Value
1	4.94-5.19	1.0
2	1.72-1.96	2.0
3	1.14-1.43	24.4
4	0.80-0.89	2.6



Appendix A 29. ¹H NMR spectrum of polyC14



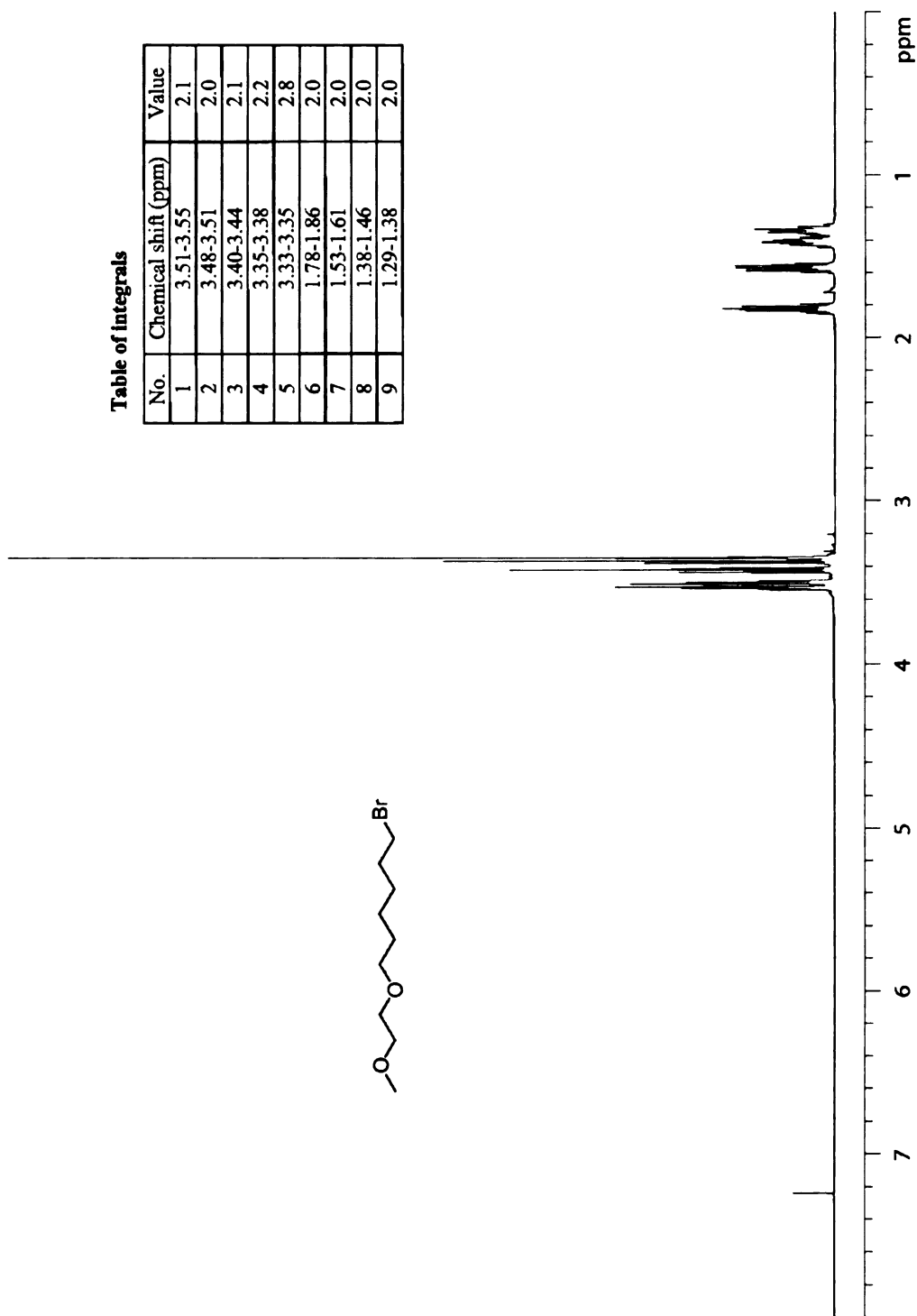
No.	Chemical Shift (ppm)	Value
1	4.97-5.20	1.0
2	1.75-1.98	2.0
3	1.13-1.44	28.7
4	0.77-0.89	2.6



Appendix A 30. ¹H NMR spectrum of polyC16

Table of Integrals

No.	Chemical shift (ppm)	Value
1	3.51-3.55	2.1
2	3.48-3.51	2.0
3	3.40-3.44	2.1
4	3.35-3.38	2.2
5	3.33-3.35	2.8
6	1.78-1.86	2.0
7	1.53-1.61	2.0
8	1.38-1.46	2.0
9	1.29-1.38	2.0



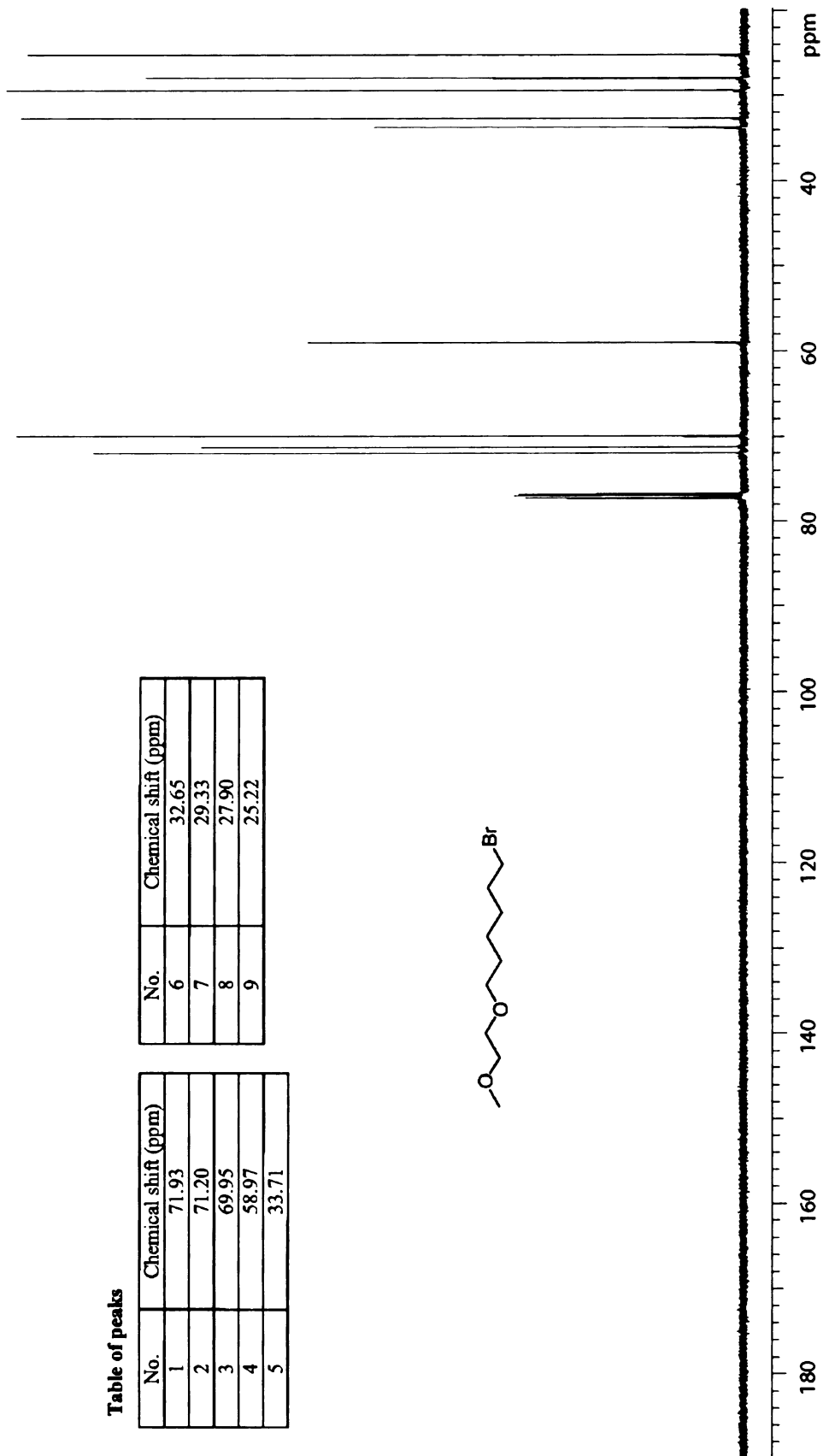
Appendix A 31. ¹H NMR spectrum of MonoEG-C6 bromide

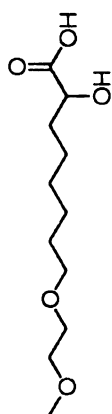
Appendix A 32. ¹³C NMR spectrum of MonoEG-C6 bromide

Table of peaks

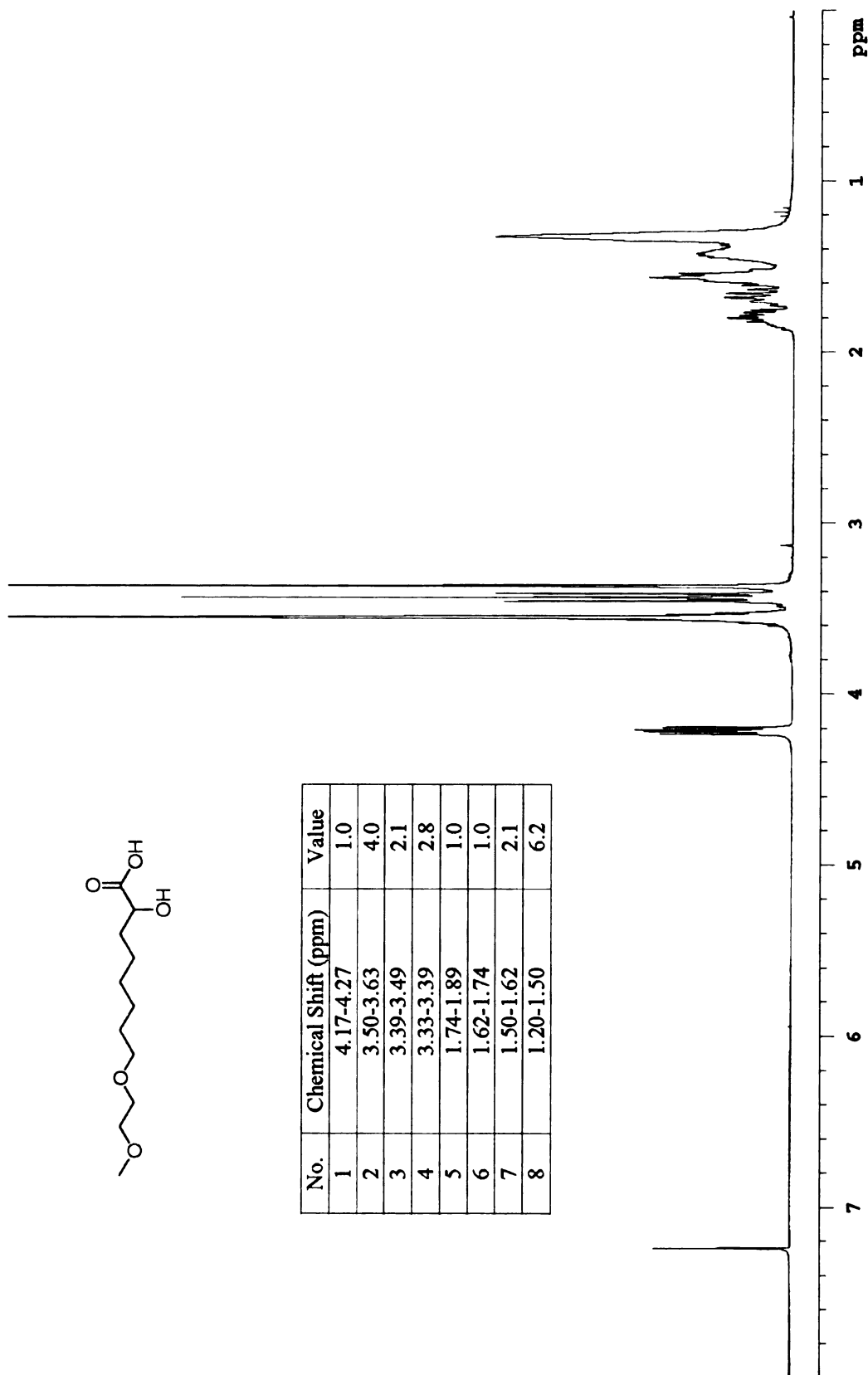
No.	Chemical shift (ppm)
1	71.93
2	71.20
3	69.95
4	58.97
5	33.71

No.	Chemical shift (ppm)
6	32.65
7	29.33
8	27.90
9	25.22





No.	Chemical Shift (ppm)	Value
1	4.17-4.27	1.0
2	3.50-3.63	4.0
3	3.39-3.49	2.1
4	3.33-3.39	2.8
5	1.74-1.89	1.0
6	1.62-1.74	1.0
7	1.50-1.62	2.1
8	1.20-1.50	6.2



Appendix A 33. ^1H NMR spectrum of MonoEG-C6- α -hydroxy acid

Appendix A 34. ¹³C NMR spectrum of MonoEG-C6- α -hydroxy acid

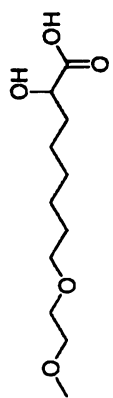
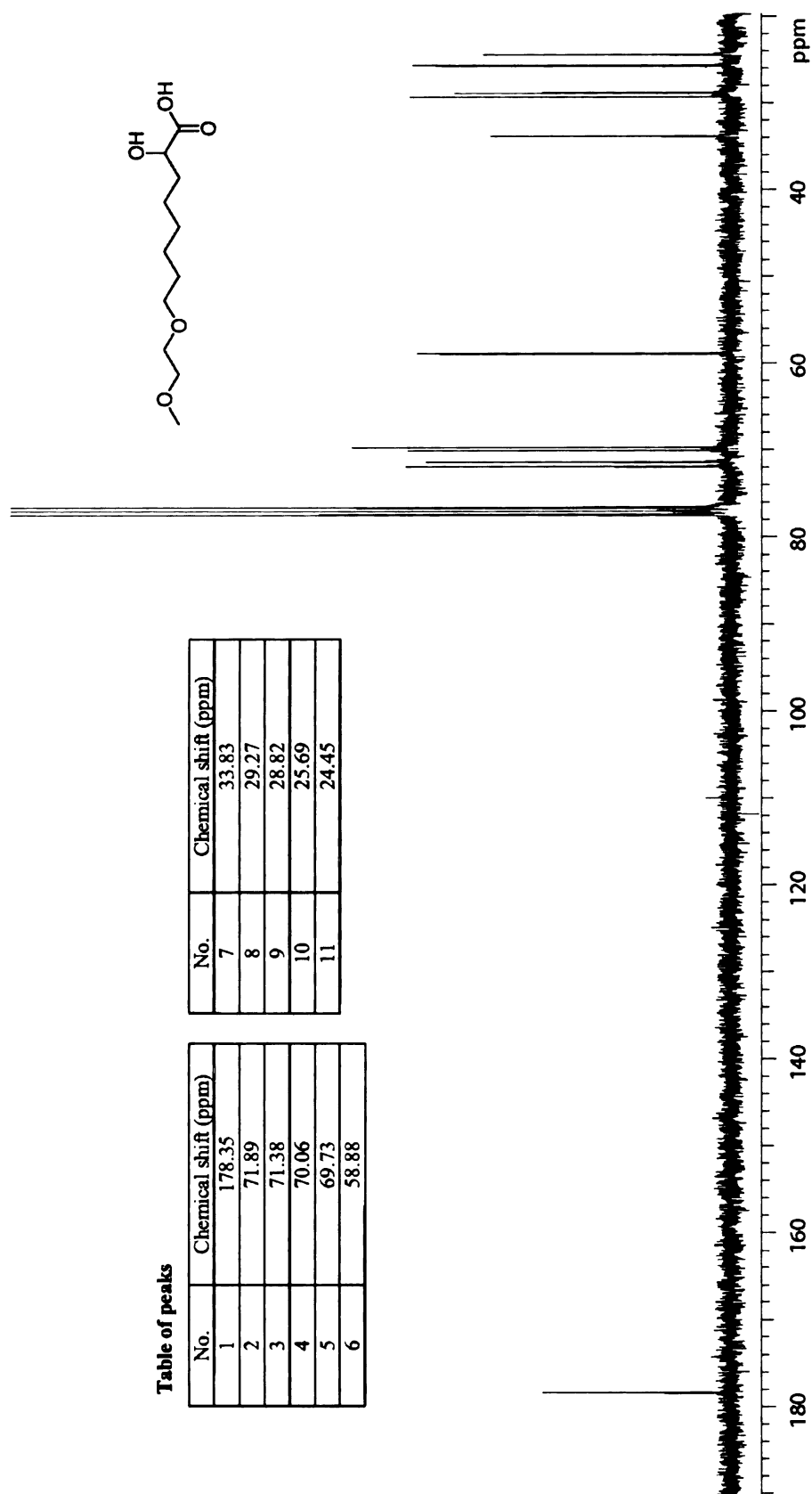


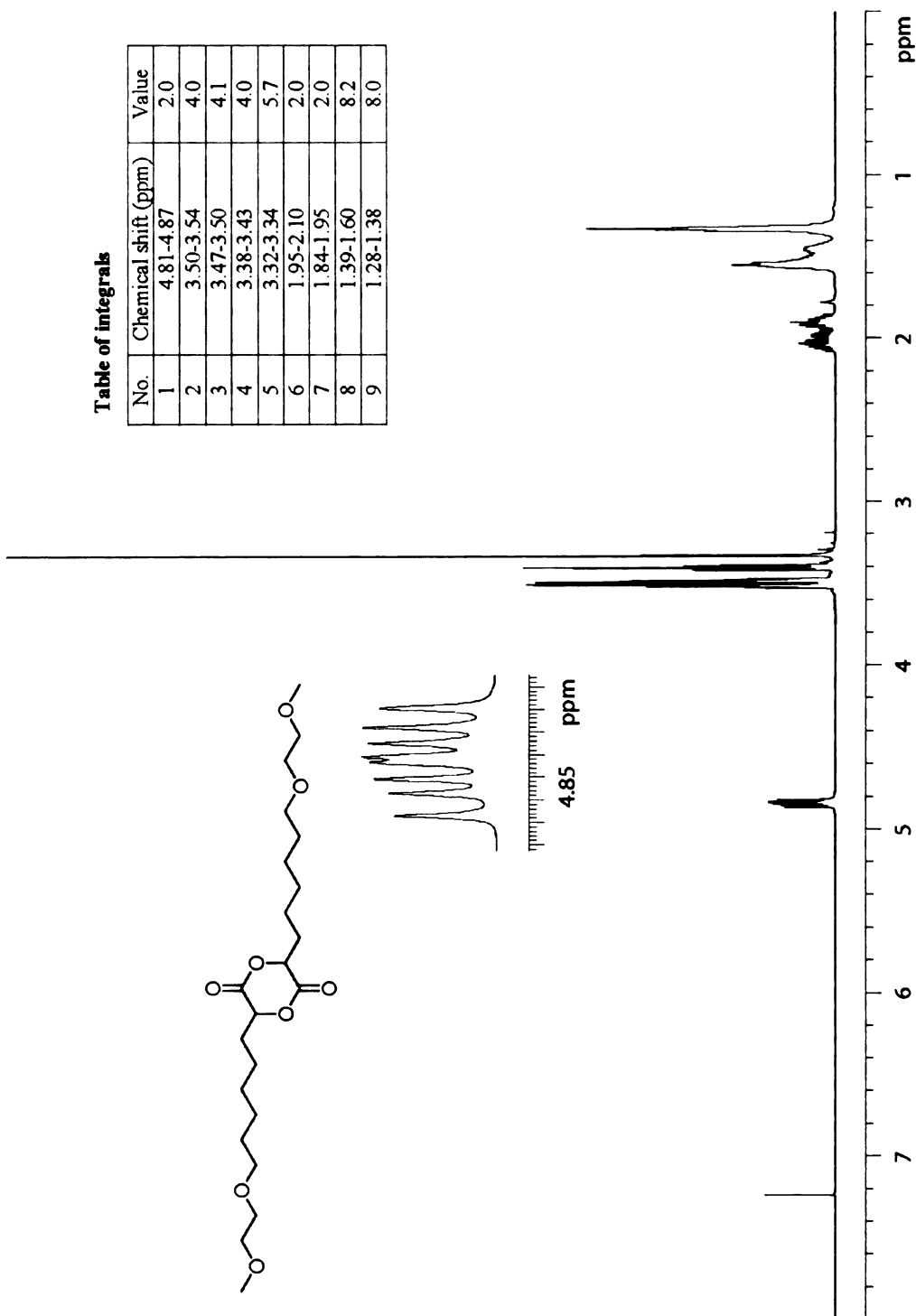
Table of peaks

No.	Chemical shift (ppm)
1	178.35
2	71.89
3	71.38
4	70.06
5	69.73
6	58.88

No.	Chemical shift (ppm)
7	33.83
8	29.27
9	28.82
10	25.69
11	24.45

Table of integrals

No.	Chemical shift (ppm)	Value
1	4.81-4.87	2.0
2	3.50-3.54	4.0
3	3.47-3.50	4.1
4	3.38-3.43	4.0
5	3.32-3.34	5.7
6	1.95-2.10	2.0
7	1.84-1.95	2.0
8	1.39-1.60	8.2
9	1.28-1.38	8.0

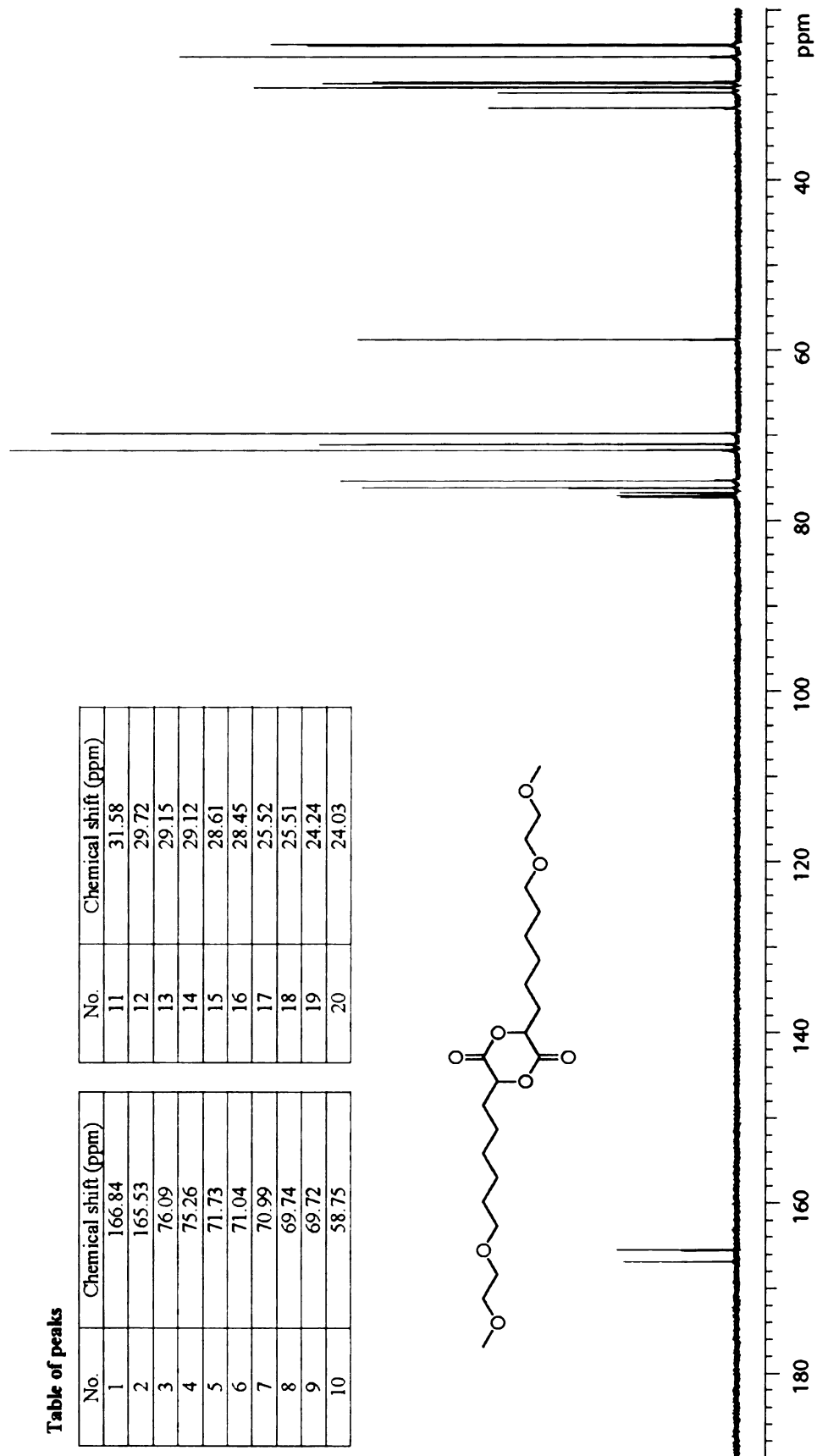
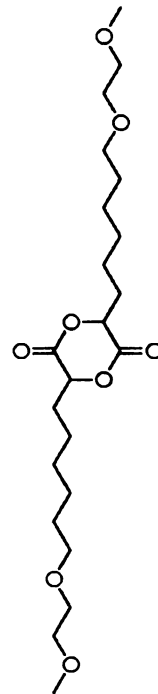


Appendix A 35. ¹H NMR spectrum of MonoEG-C6 dimer

Table of peaks

No.	Chemical shift (ppm)
1	166.84
2	165.53
3	76.09
4	75.26
5	71.73
6	71.04
7	70.99
8	69.74
9	69.72
10	58.75

No.	Chemical shift (ppm)
11	31.58
12	29.72
13	29.15
14	29.12
15	28.61
16	28.45
17	25.52
18	25.51
19	24.24
20	24.03

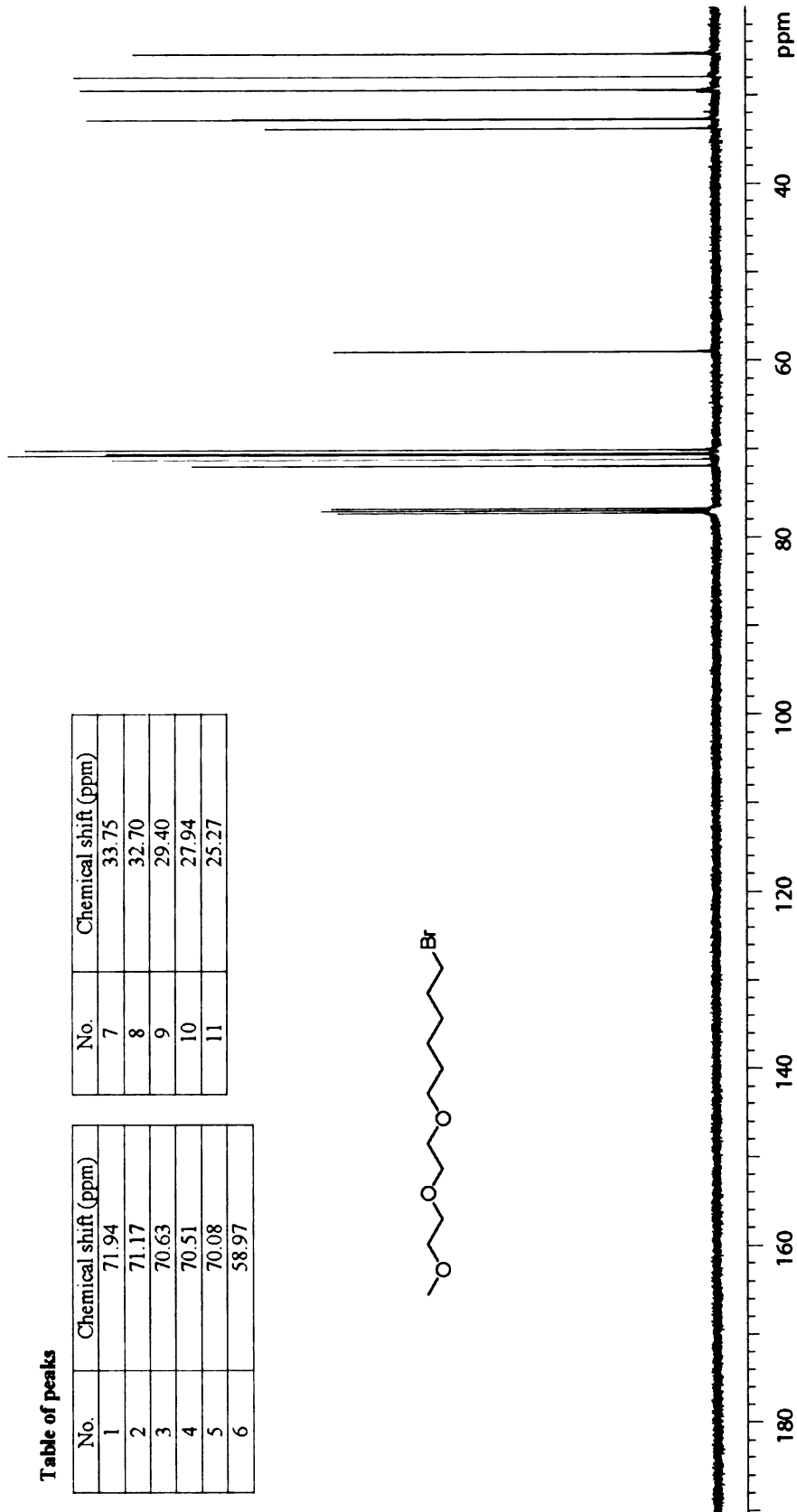


Appendix A 36. ¹³C NMR spectrum of MonoEG-C6 dimer

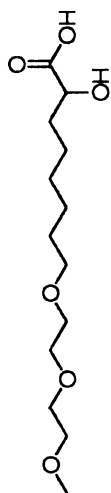
Table of peaks

No.	Chemical shift (ppm)
1	71.94
2	71.17
3	70.63
4	70.51
5	70.08
6	58.97

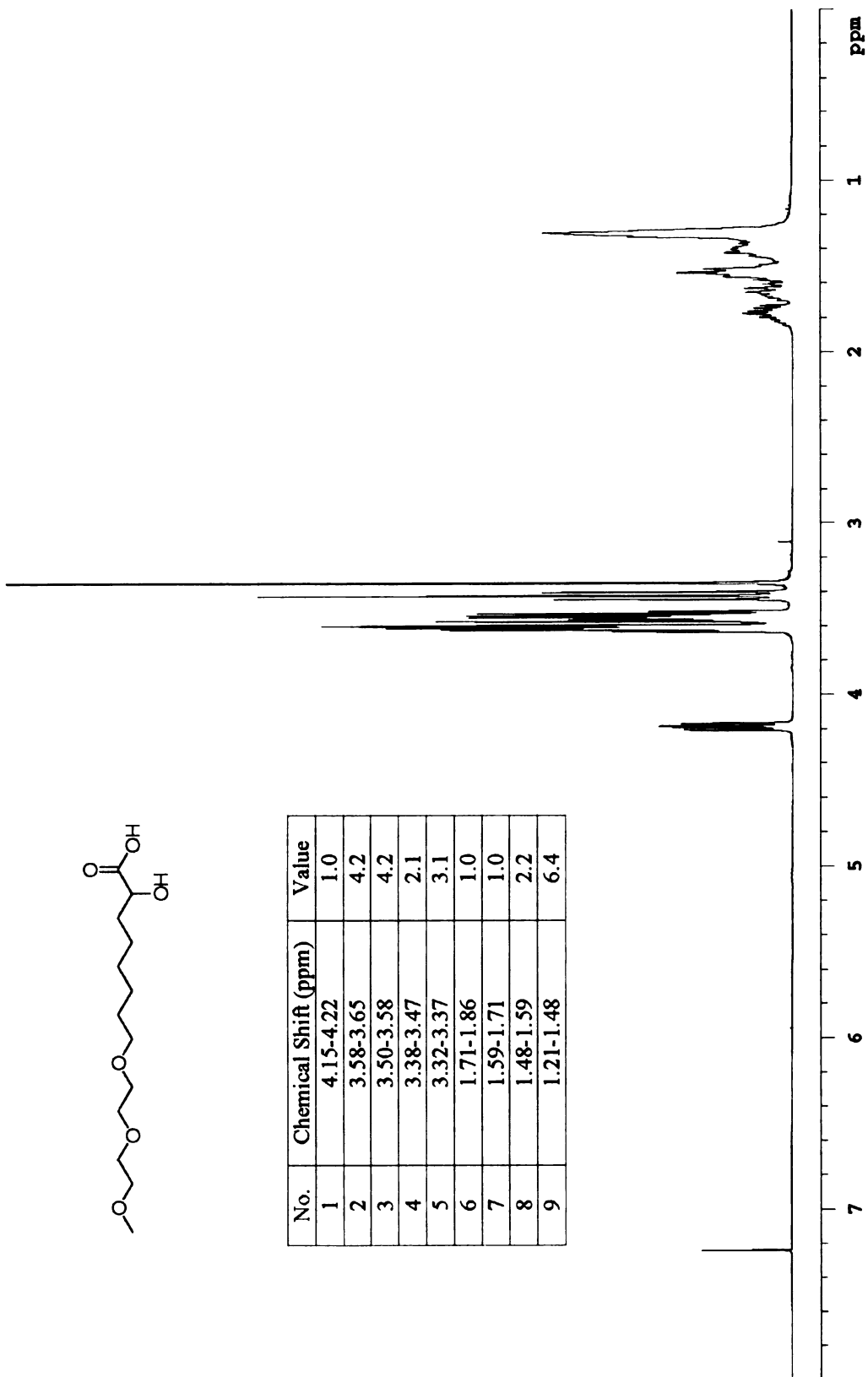
No.	Chemical shift (ppm)
7	33.75
8	32.70
9	29.40
10	27.94
11	25.27



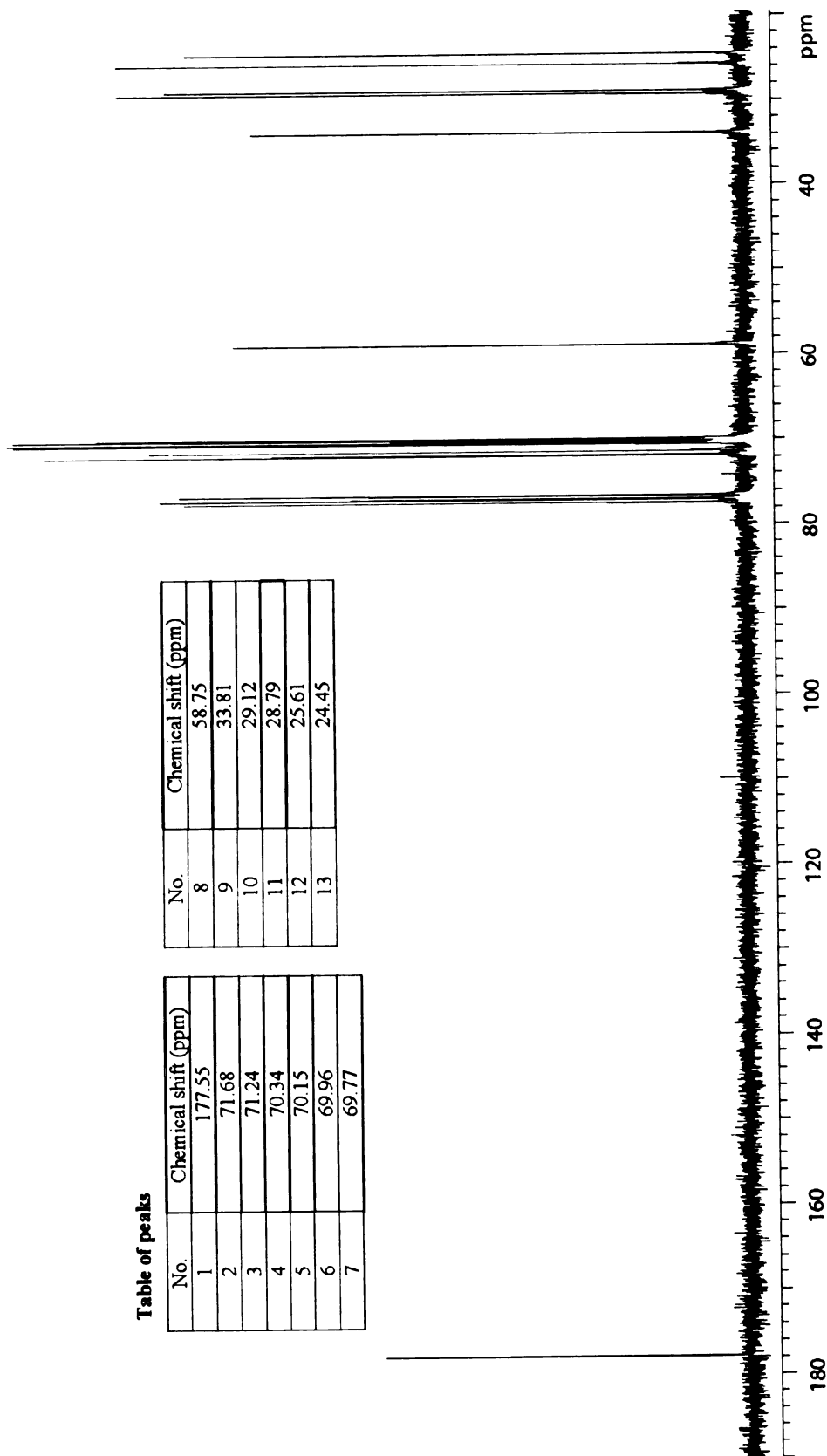
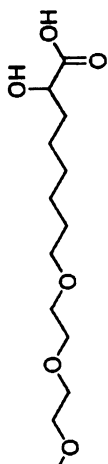
Appendix A 38. ^{13}C NMR spectrum of DiEG-C6 bromide



No.	Chemical Shift (ppm)	Value
1	4.15-4.22	1.0
2	3.58-3.65	4.2
3	3.50-3.58	4.2
4	3.38-3.47	2.1
5	3.32-3.37	3.1
6	1.71-1.86	1.0
7	1.59-1.71	1.0
8	1.48-1.59	2.2
9	1.21-1.48	6.4



Appendix A 39. ¹H NMR spectrum of DiEG-C6-α-hydroxy acid

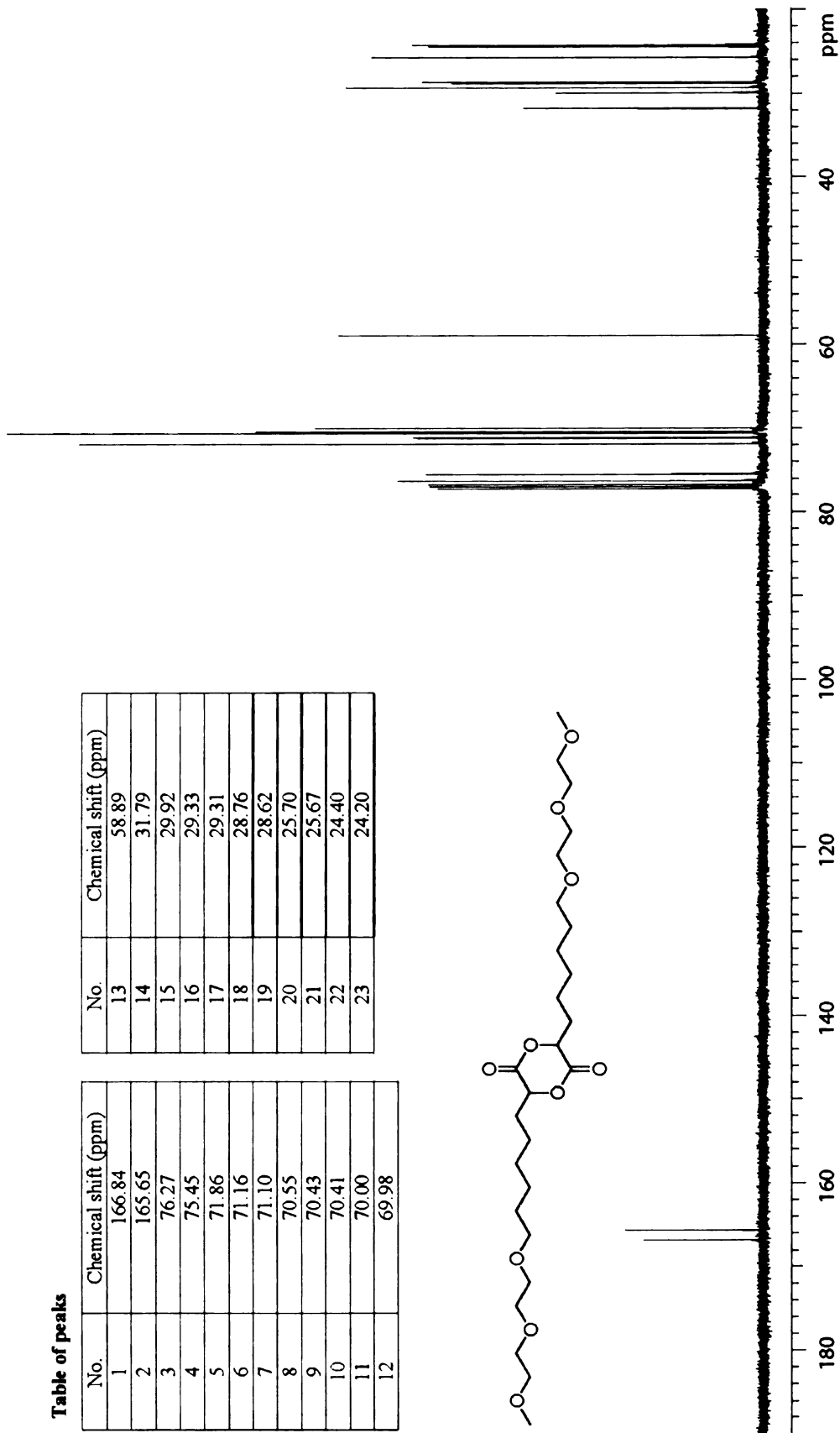
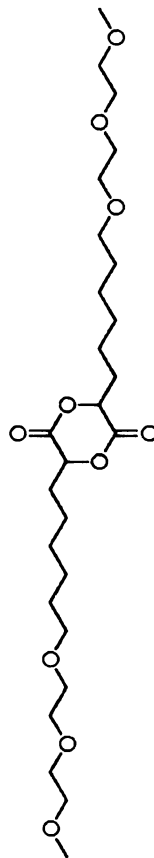


Appendix A 40. ¹³C NMR spectrum of DiEG-C6-α-hydroxy acid

Table of peaks

No.	Chemical shift (ppm)
1	166.84
2	165.65
3	76.27
4	75.45
5	71.86
6	71.16
7	71.10
8	70.55
9	70.43
10	70.41
11	70.00
12	69.98

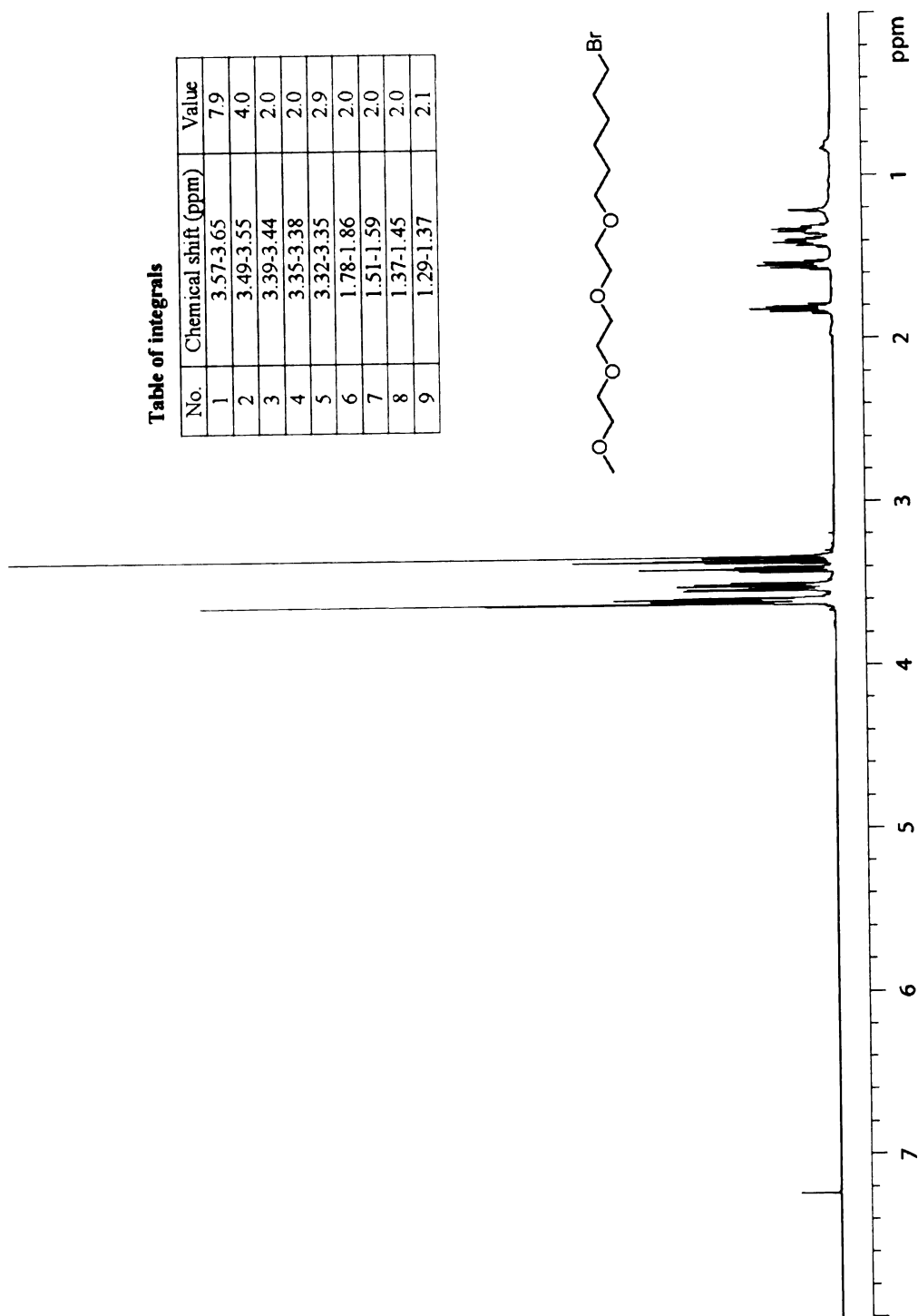
No.	Chemical shift (ppm)
13	58.89
14	31.79
15	29.92
16	29.33
17	29.31
18	28.76
19	28.62
20	25.70
21	25.67
22	24.40
23	24.20



Appendix A 42. ¹³C NMR spectrum of DiEG-C6-dimer

Table of integrals

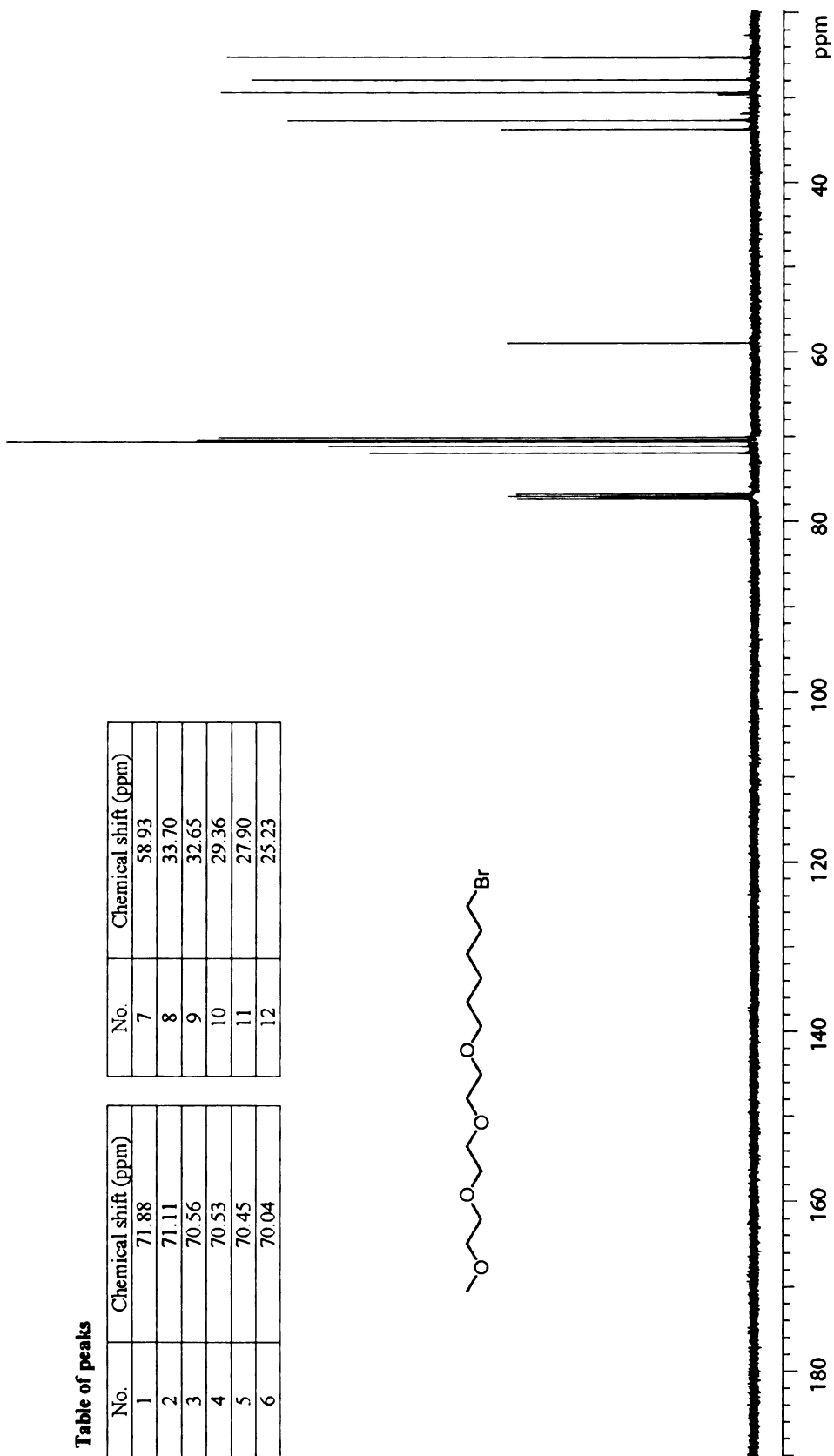
No.	Chemical shift (ppm)	Value
1	3.57-3.65	7.9
2	3.49-3.55	4.0
3	3.39-3.44	2.0
4	3.35-3.38	2.0
5	3.32-3.35	2.9
6	1.78-1.86	2.0
7	1.51-1.59	2.0
8	1.37-1.45	2.0
9	1.29-1.37	2.1



Appendix A 43. ¹H NMR spectrum of TriEG-C6 bromide

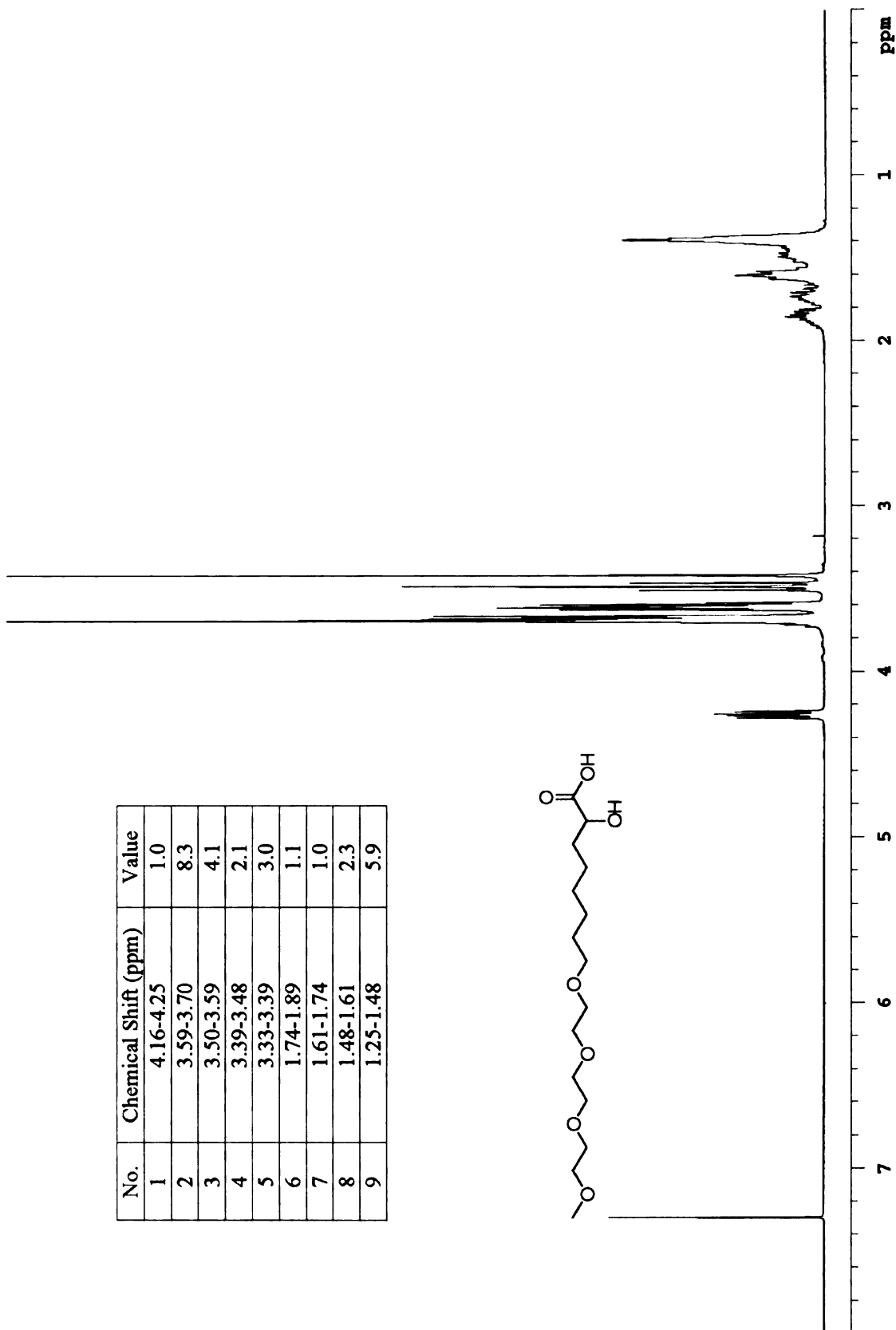
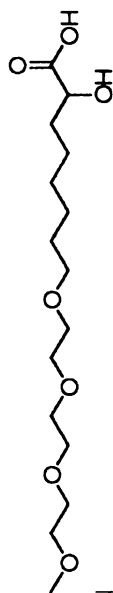
Table of peaks

No.	Chemical shift (ppm)	No.	Chemical shift (ppm)
1	71.88	7	58.93
2	71.11	8	33.70
3	70.56	9	32.65
4	70.53	10	29.36
5	70.45	11	27.90
6	70.04	12	25.23



Appendix A 44. ¹³C NMR spectrum of TriEG-C6 bromide

No.	Chemical Shift (ppm)	Value
1	4.16-4.25	1.0
2	3.59-3.70	8.3
3	3.50-3.59	4.1
4	3.39-3.48	2.1
5	3.33-3.39	3.0
6	1.74-1.89	1.1
7	1.61-1.74	1.0
8	1.48-1.61	2.3
9	1.25-1.48	5.9



Appendix A 45. ^1H NMR spectrum of TriEG-C6- α -hydroxy acid

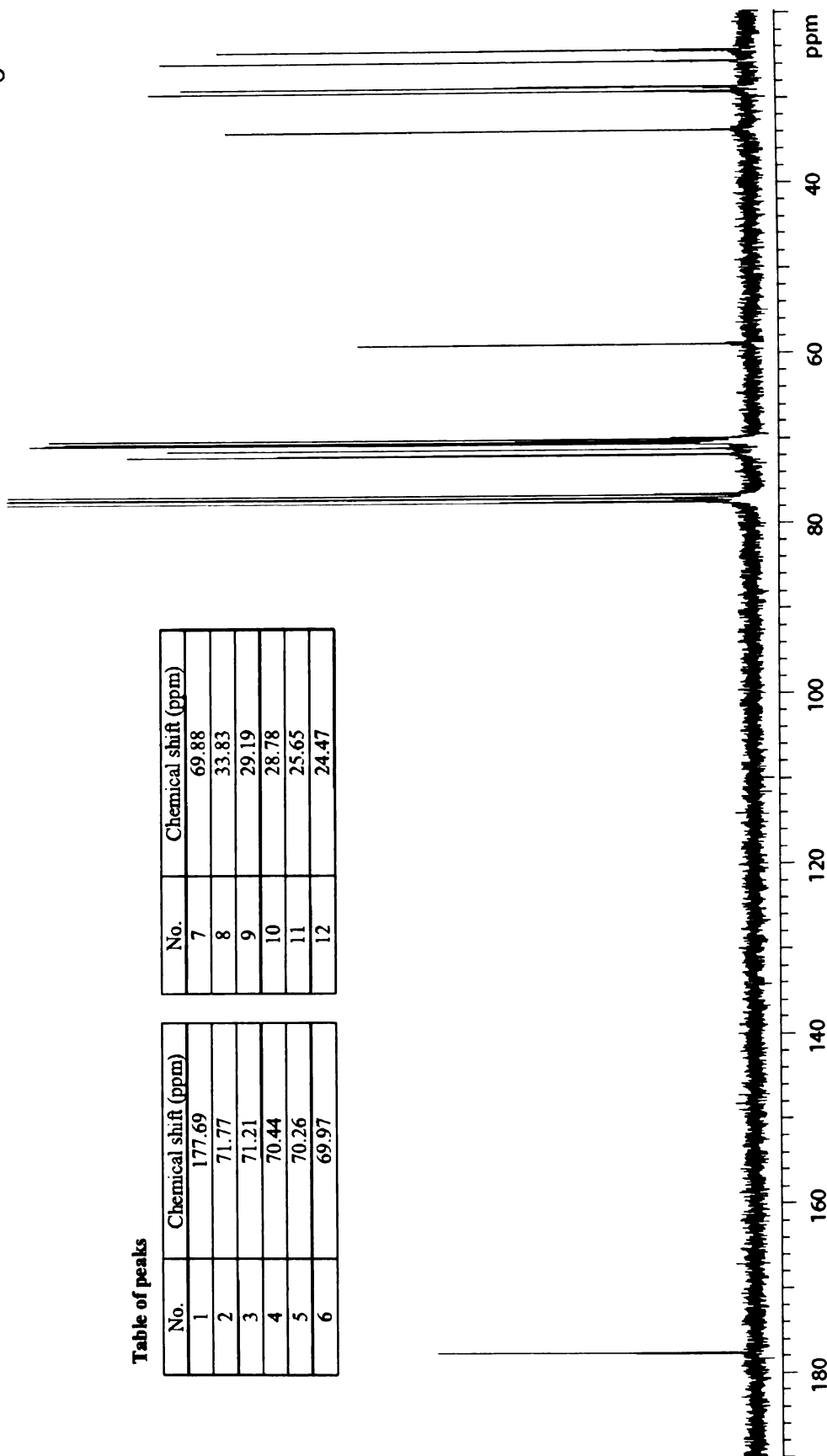
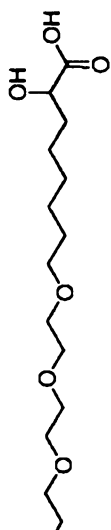


Table of peaks

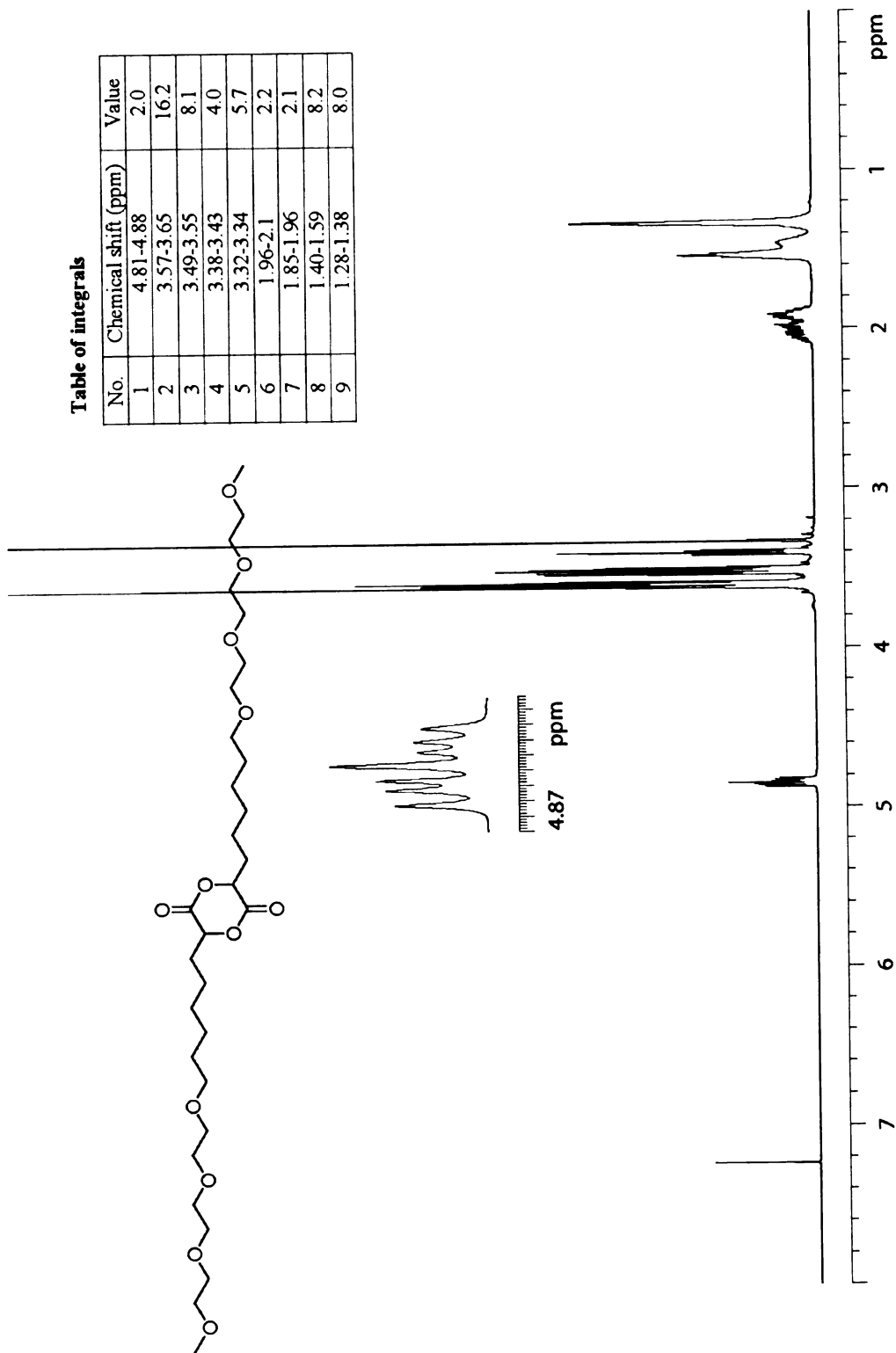
No.	Chemical shift (ppm)
1	177.69
2	71.77
3	71.21
4	70.44
5	70.26
6	69.97

No.	Chemical shift (ppm)
7	69.88
8	33.83
9	29.19
10	28.78
11	25.65
12	24.47

Appendix A 46. ¹³C NMR spectrum of TriEG-C6-α-hydroxy acid

Table of integrals

No.	Chemical shift (ppm)	Value
1	4.81-4.88	2.0
2	3.57-3.65	16.2
3	3.49-3.55	8.1
4	3.38-3.43	4.0
5	3.32-3.34	5.7
6	1.96-2.1	2.2
7	1.85-1.96	2.1
8	1.40-1.59	8.2
9	1.28-1.38	8.0

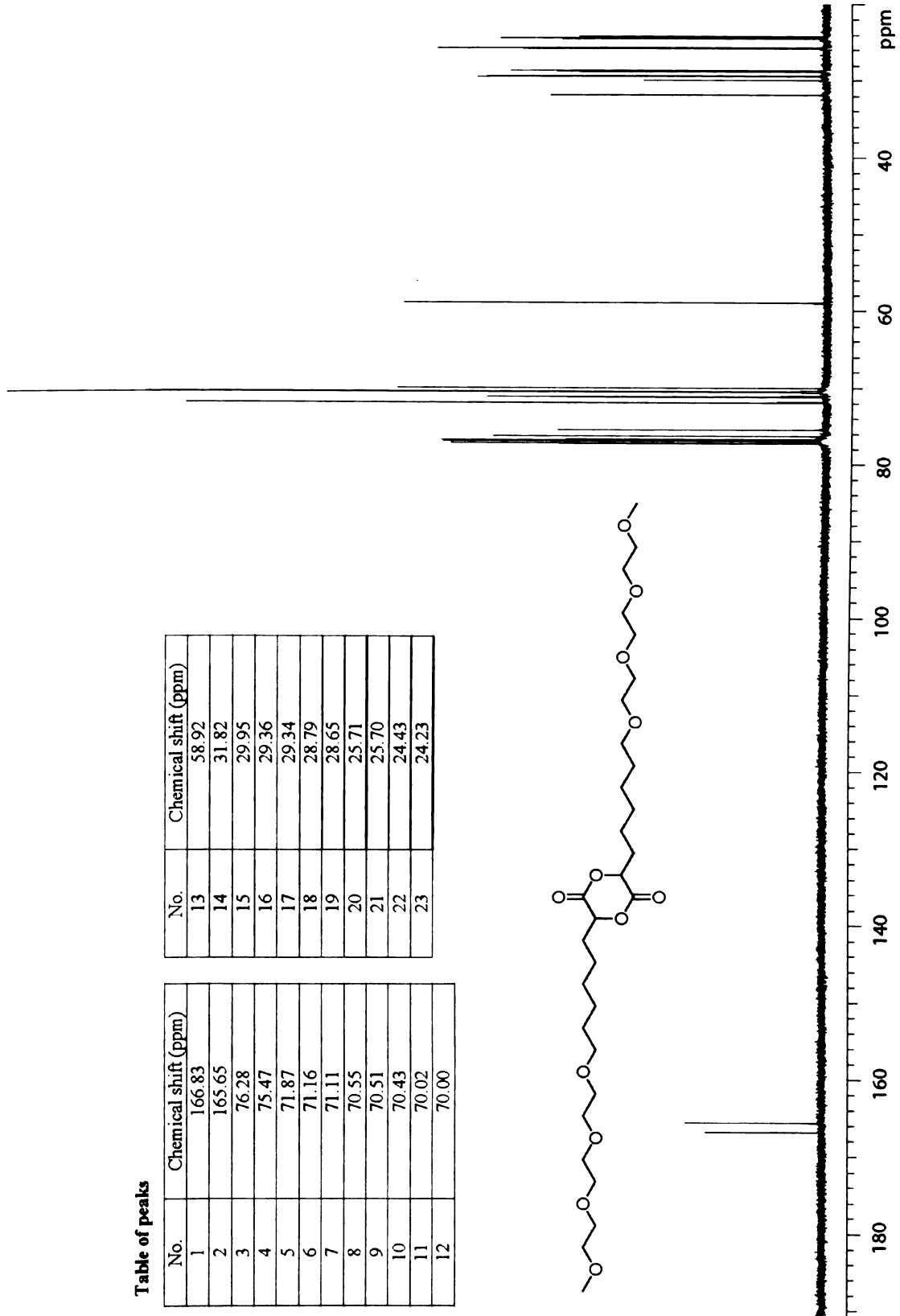
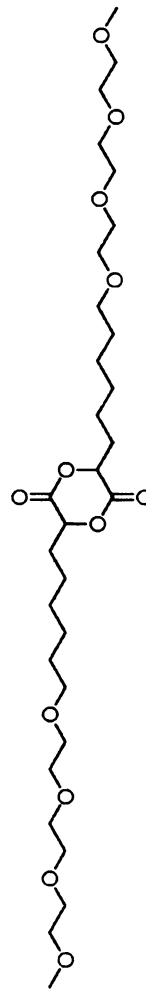


Appendix A 47. ¹H NMR spectrum of TriEG-C6 dimer

Table of peaks

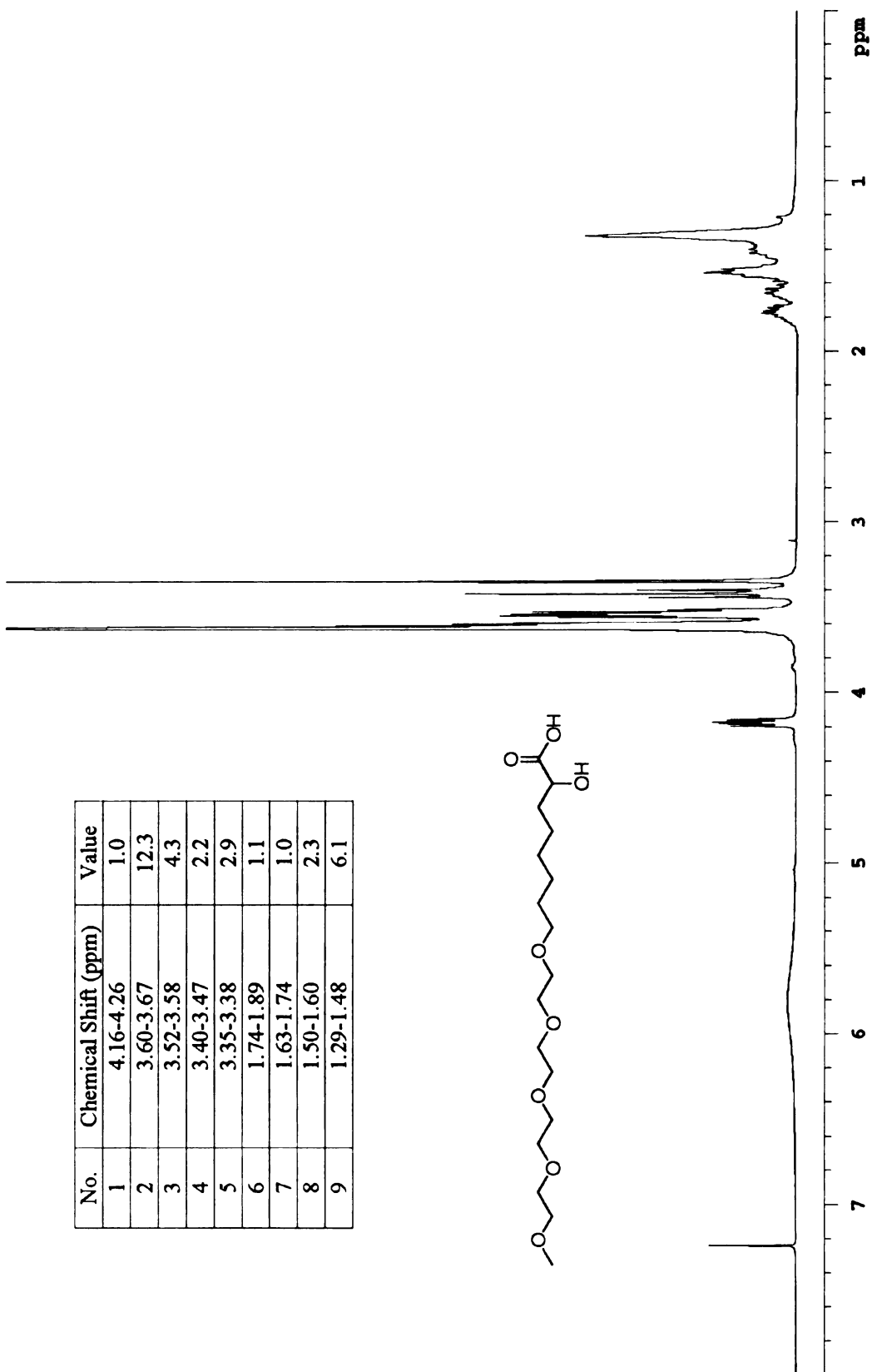
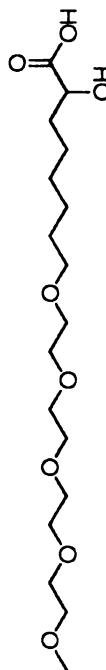
No.	Chemical shift (ppm)
1	166.83
2	165.65
3	76.28
4	75.47
5	71.87
6	71.16
7	71.11
8	70.55
9	70.51
10	70.43
11	70.02
12	70.00

No.	Chemical shift (ppm)
13	58.92
14	31.82
15	29.95
16	29.36
17	29.34
18	28.79
19	28.65
20	25.71
21	25.70
22	24.43
23	24.23

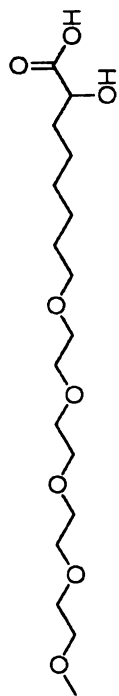


Appendix A 48. ^{13}C NMR spectrum of TriEG-C6 dimer

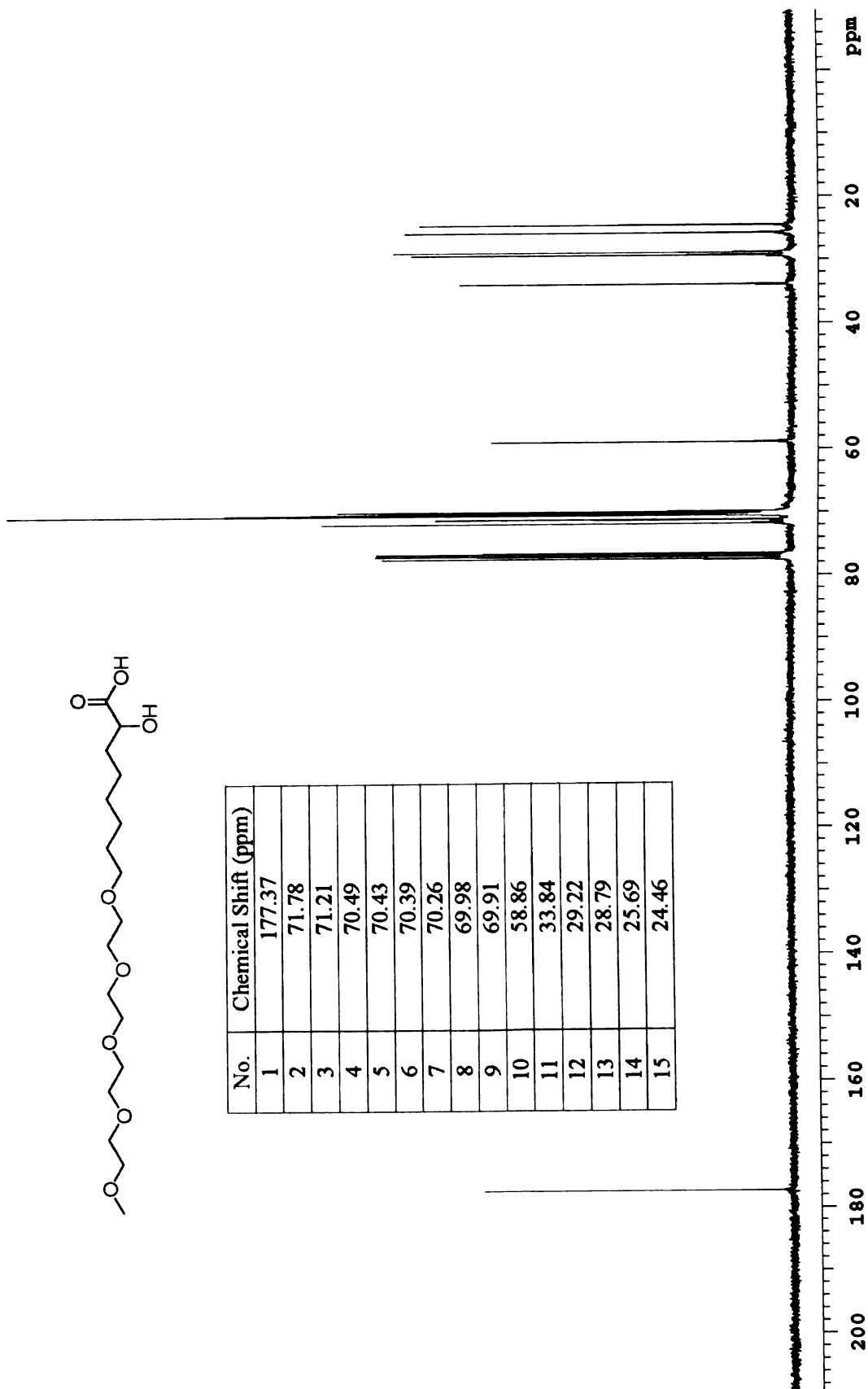
No.	Chemical Shift (ppm)	Value
1	4.16-4.26	1.0
2	3.60-3.67	12.3
3	3.52-3.58	4.3
4	3.40-3.47	2.2
5	3.35-3.38	2.9
6	1.74-1.89	1.1
7	1.63-1.74	1.0
8	1.50-1.60	2.3
9	1.29-1.48	6.1



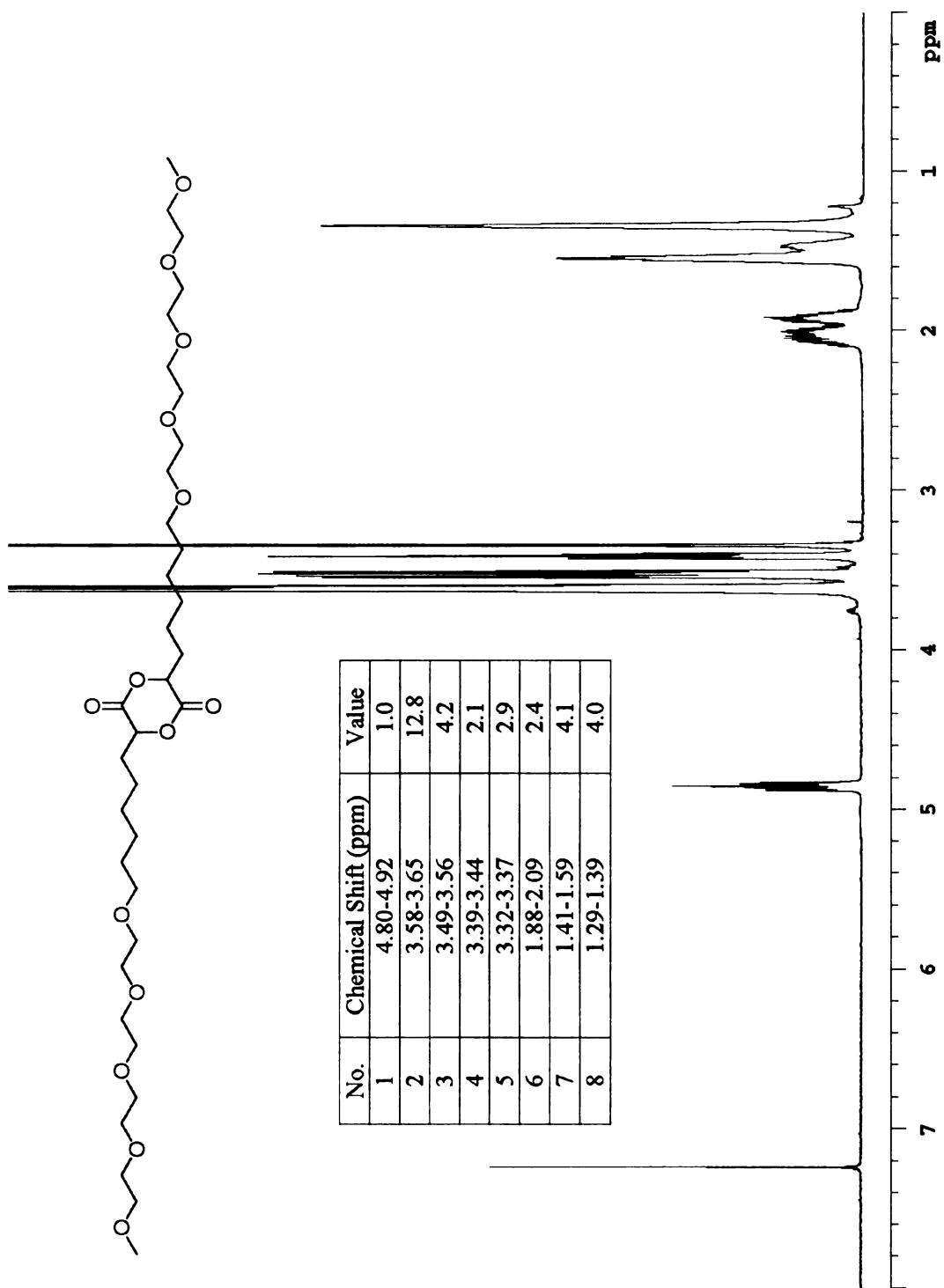
Appendix A 50. ^1H NMR spectrum of TetraEG-C6- α -hydroxy acid



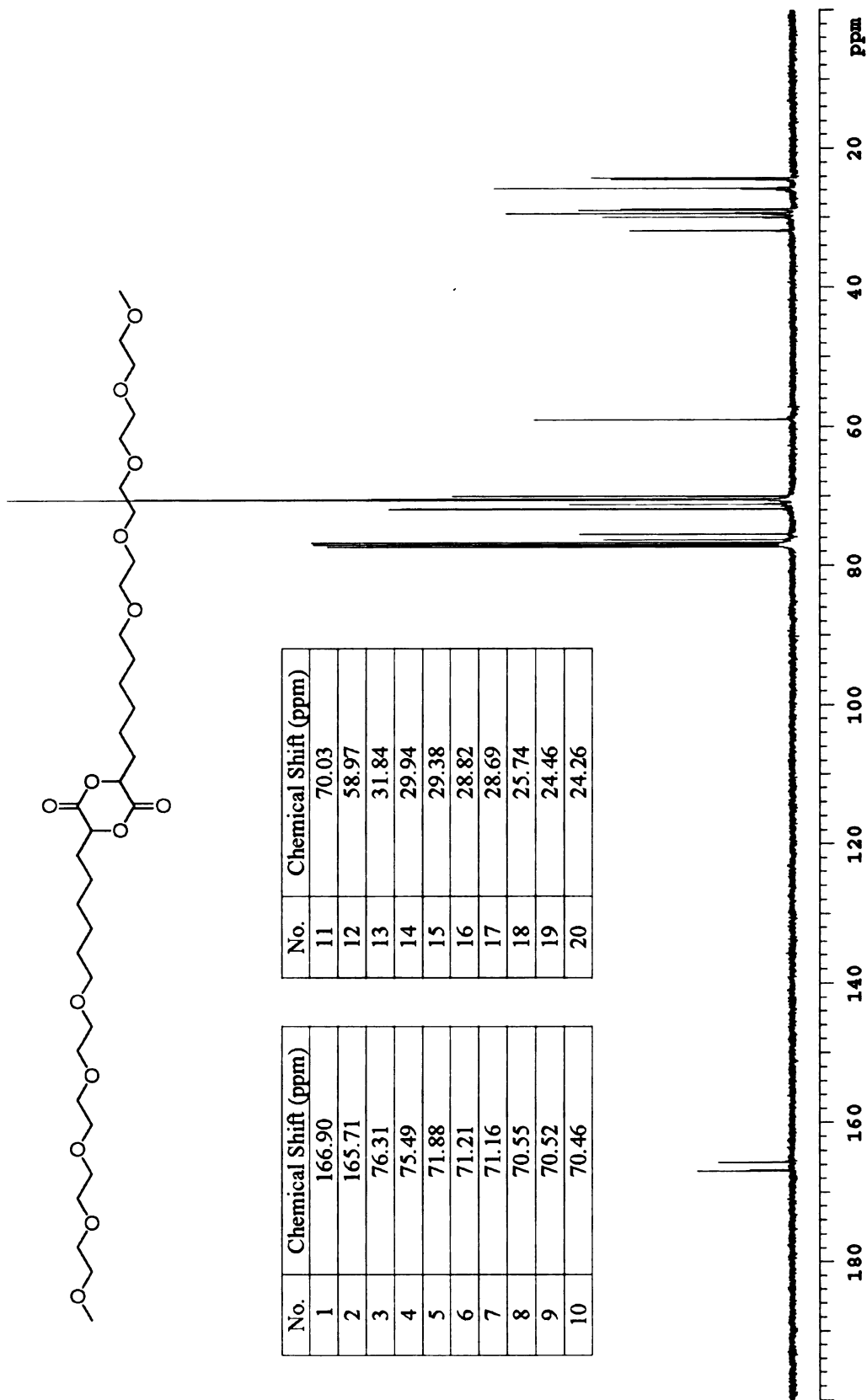
No.	Chemical Shift (ppm)
1	177.37
2	71.78
3	71.21
4	70.49
5	70.43
6	70.39
7	70.26
8	69.98
9	69.91
10	58.86
11	33.84
12	29.22
13	28.79
14	25.69
15	24.46



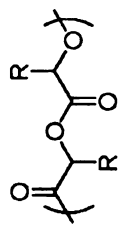
Appendix A 51. ^{13}C NMR spectrum of TetraEG-C6- α -hydroxy acid



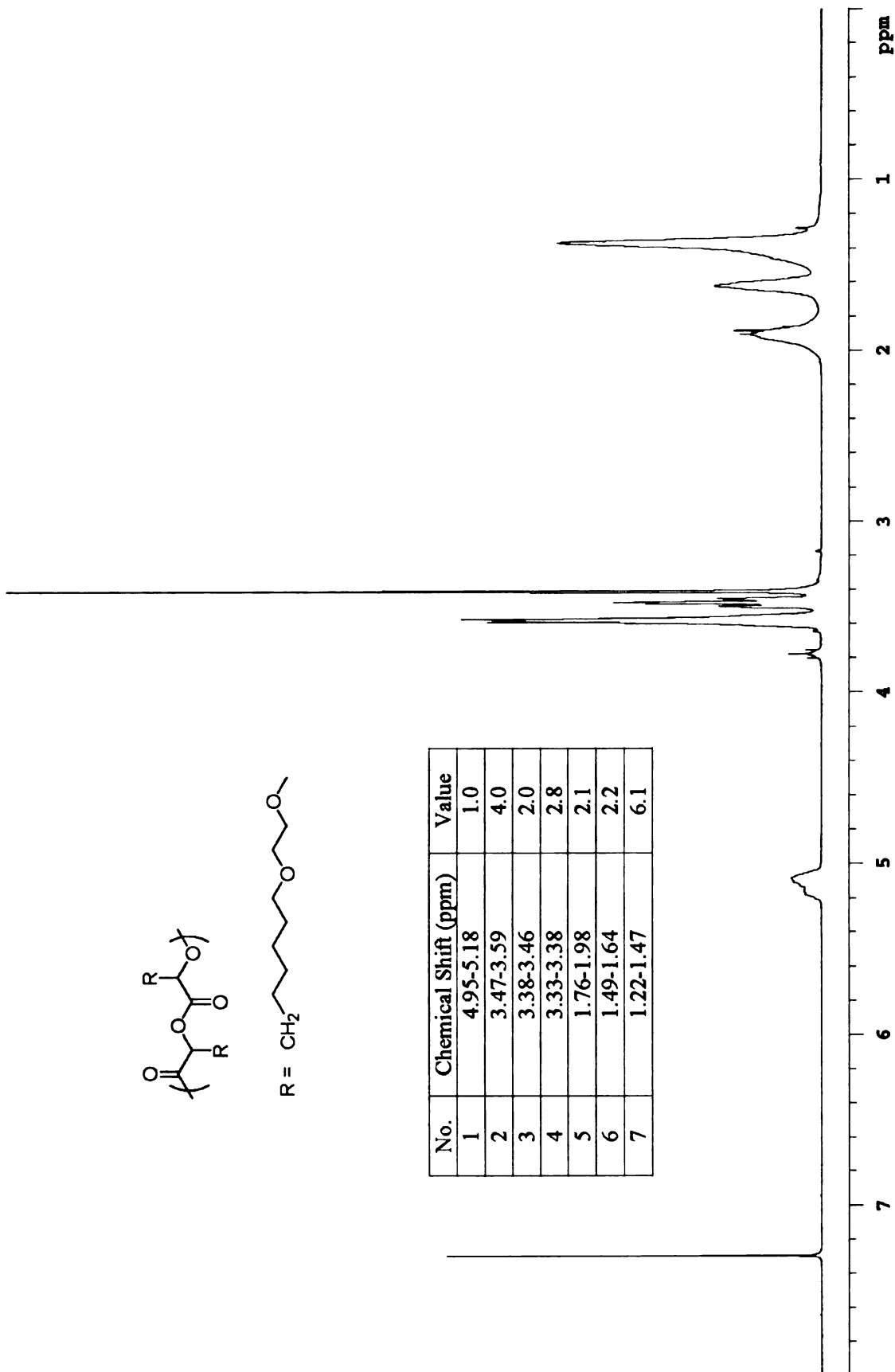
Appendix A 52. ^1H NMR spectrum of TetraEG-C6 dimer



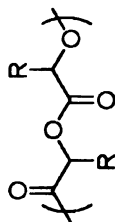
Appendix A 53. ¹³C NMR spectrum of TetraEG-C6 dimer



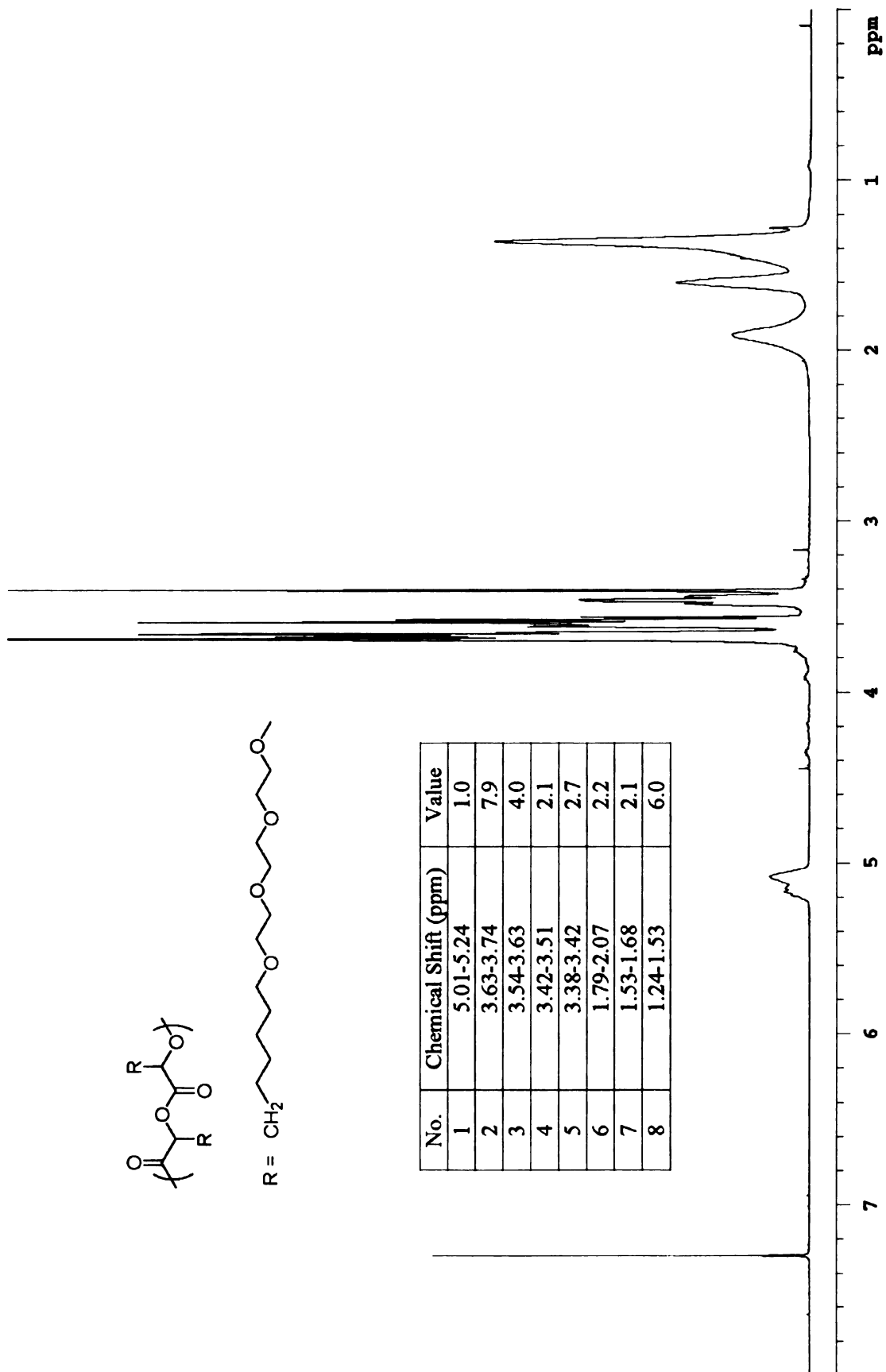
No.	Chemical Shift (ppm)	Value
1	4.95-5.18	1.0
2	3.47-3.59	4.0
3	3.38-3.46	2.0
4	3.33-3.38	2.8
5	1.76-1.98	2.1
6	1.49-1.64	2.2
7	1.22-1.47	6.1



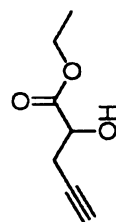
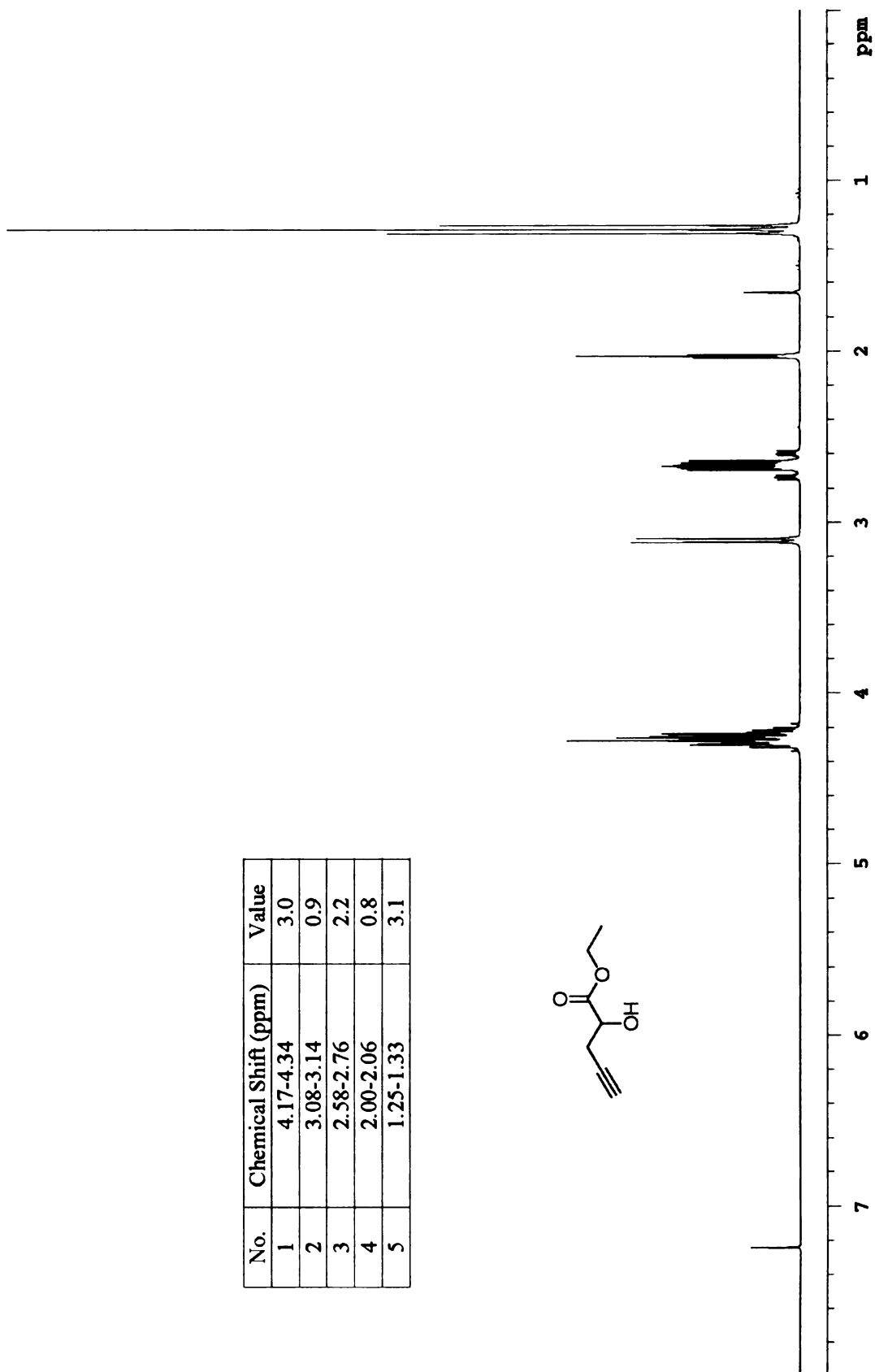
Appendix A 54. ¹H NMR spectrum of poly(MonoEG-C6)



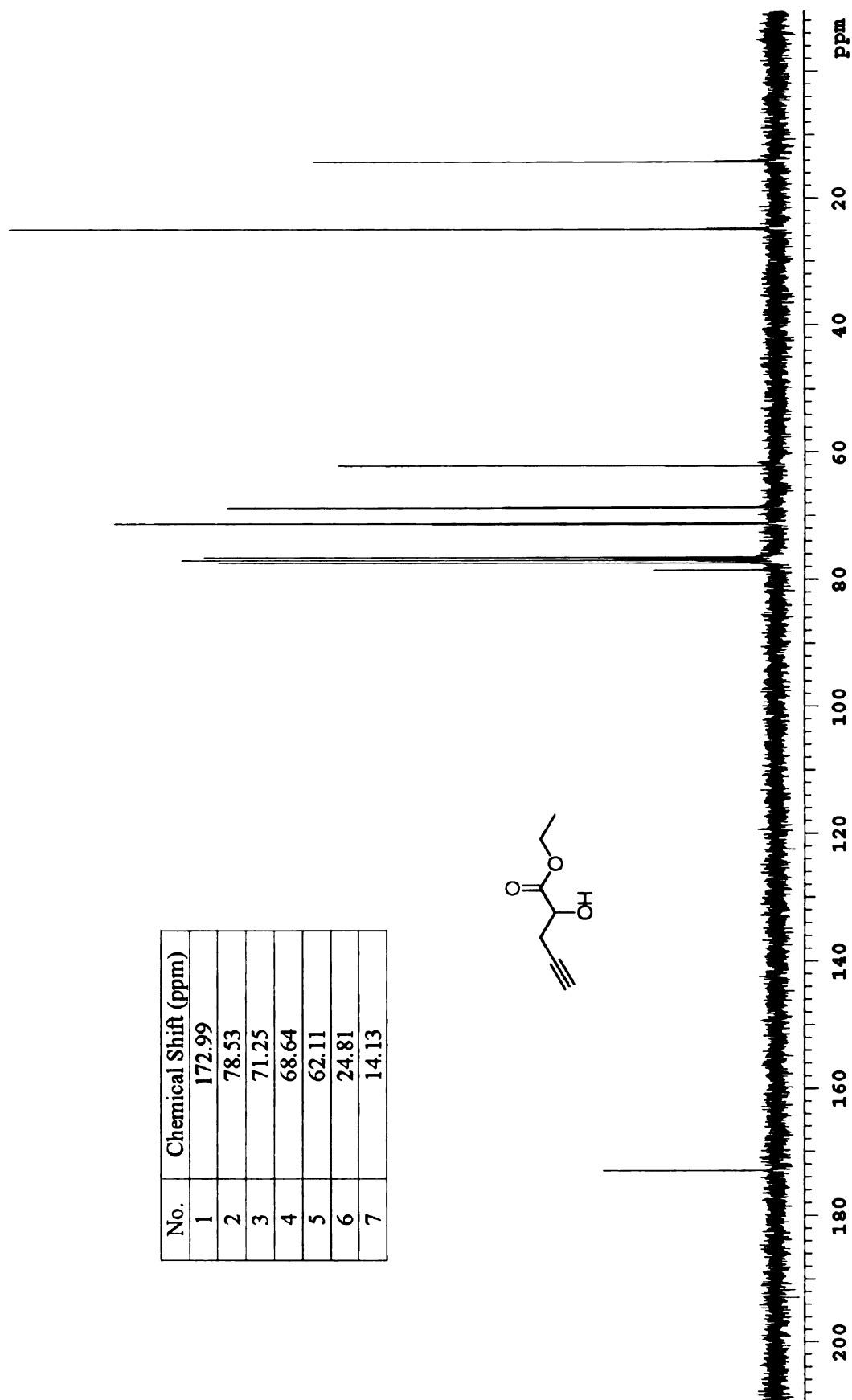
No.	Chemical Shift (ppm)	Value
1	5.01-5.24	1.0
2	3.63-3.74	7.9
3	3.54-3.63	4.0
4	3.42-3.51	2.1
5	3.38-3.42	2.7
6	1.79-2.07	2.2
7	1.53-1.68	2.1
8	1.24-1.53	6.0



Appendix A 56. ¹H NMR spectrum of poly(TriEG-C6)

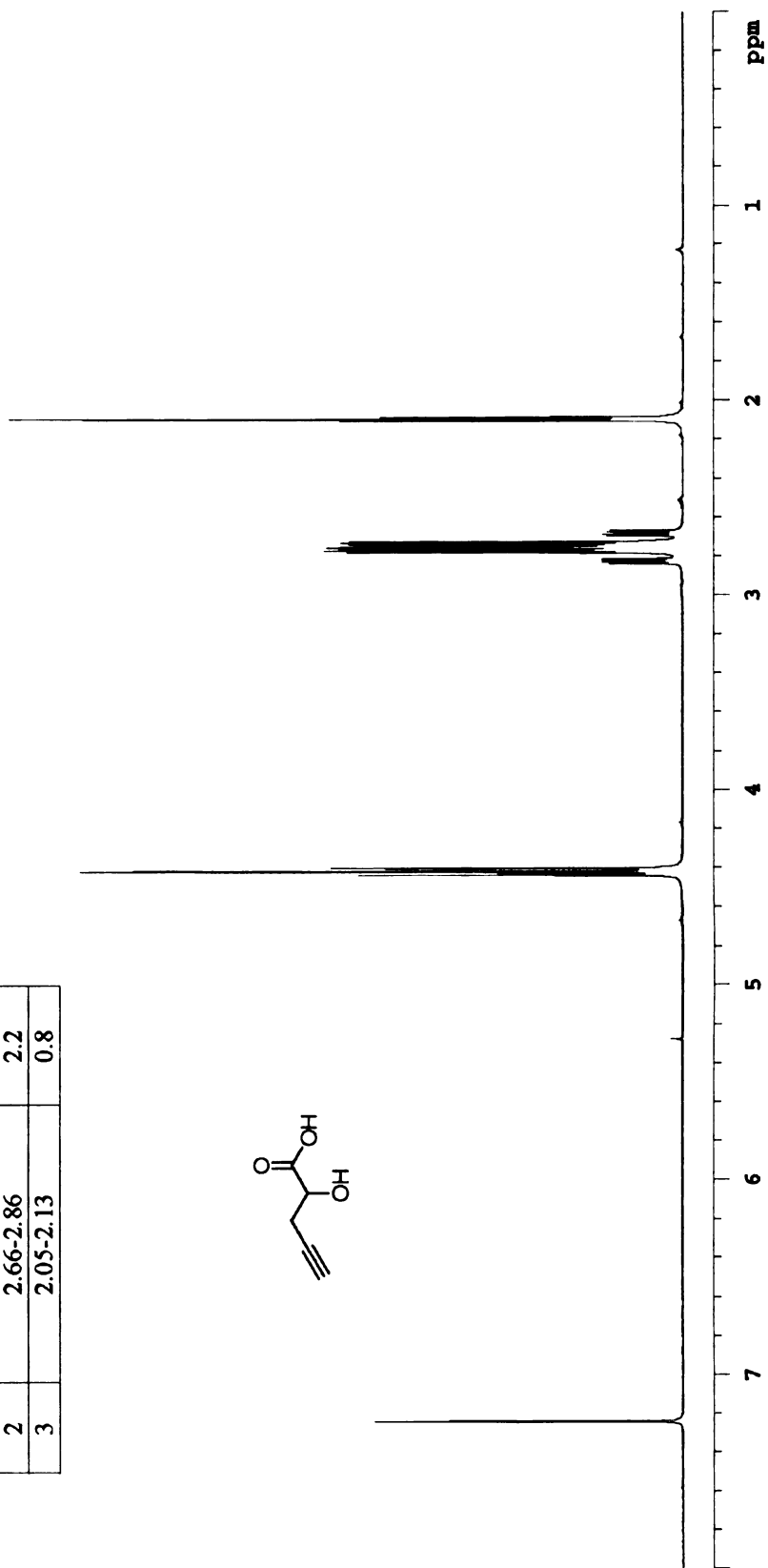
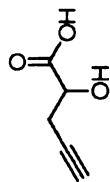


Appendix A 58. ¹H NMR spectrum of propargyl- α -hydroxy ethyl ester



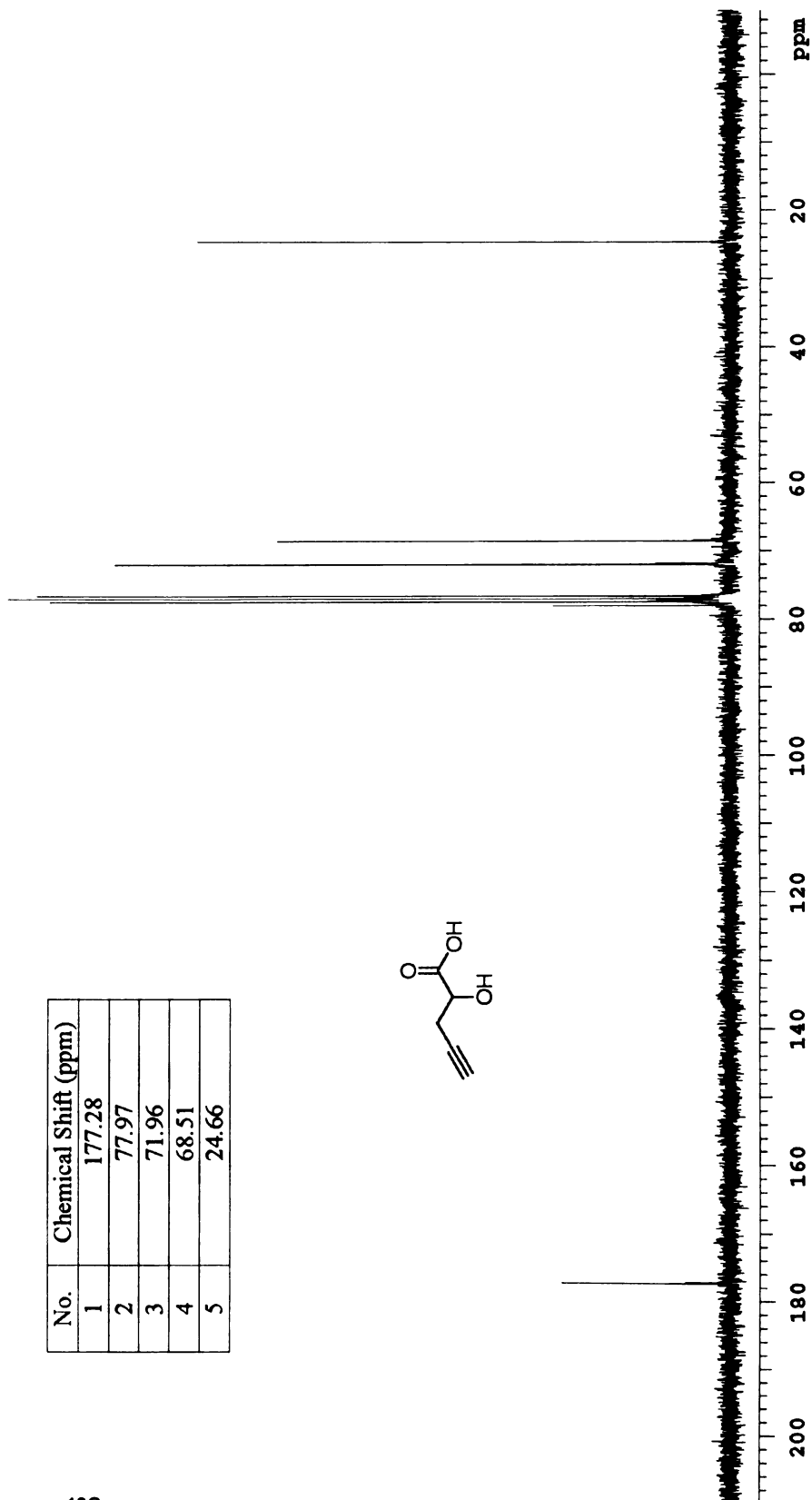
Appendix A 59. ^{13}C NMR spectrum of propargyl- α -hydroxy ethyl ester

No.	Chemical Shift (ppm)	Value
1	4.38-4.46	1.0
2	2.66-2.86	2.2
3	2.05-2.13	0.8

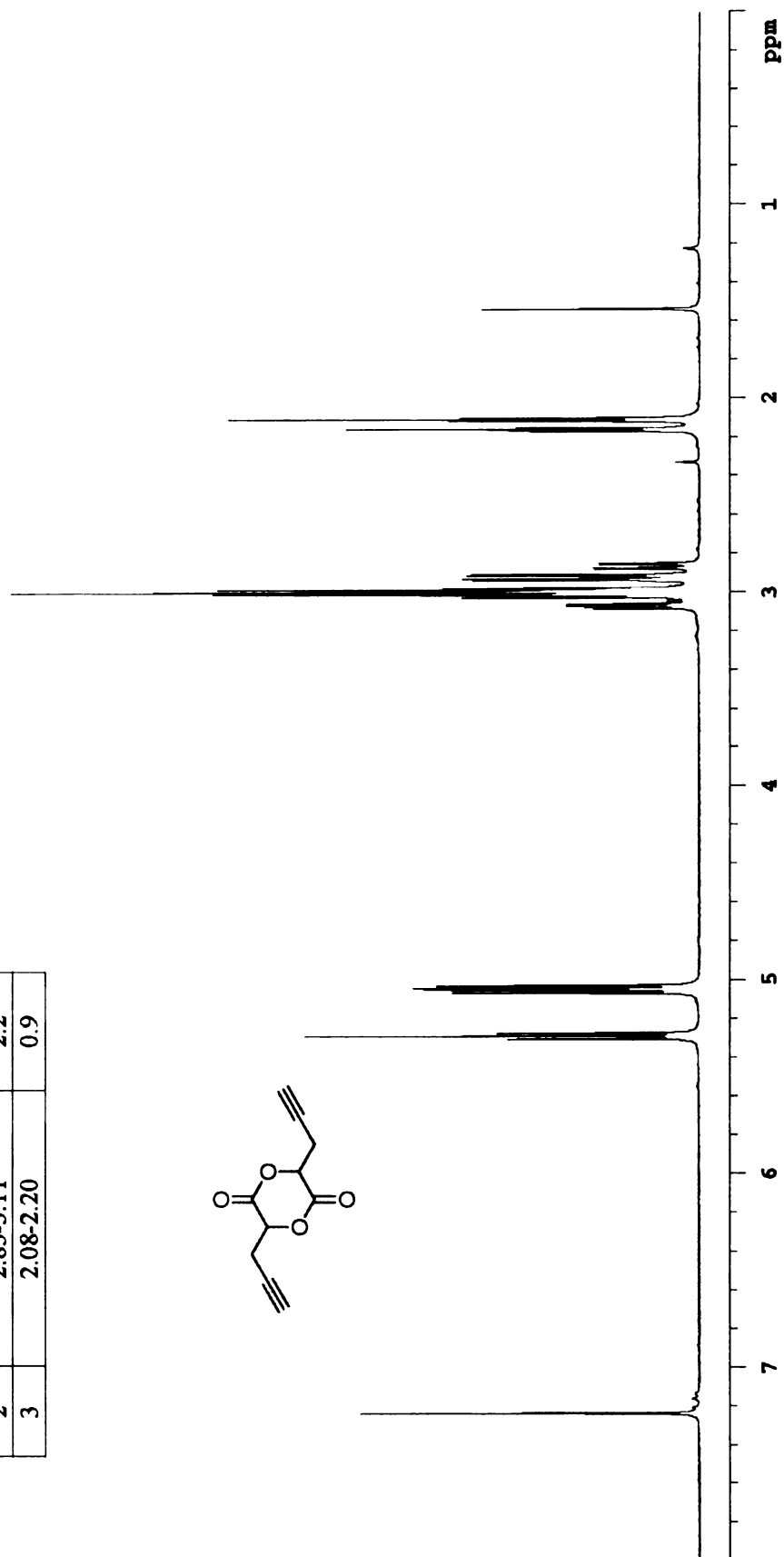
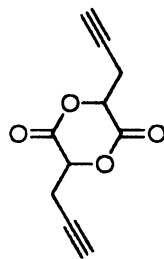


Appendix A 60. ^1H NMR spectrum of propargyl- α -hydroxy acid

Appendix A 61. ¹³C NMR spectrum of propargyl- α -hydroxy acid

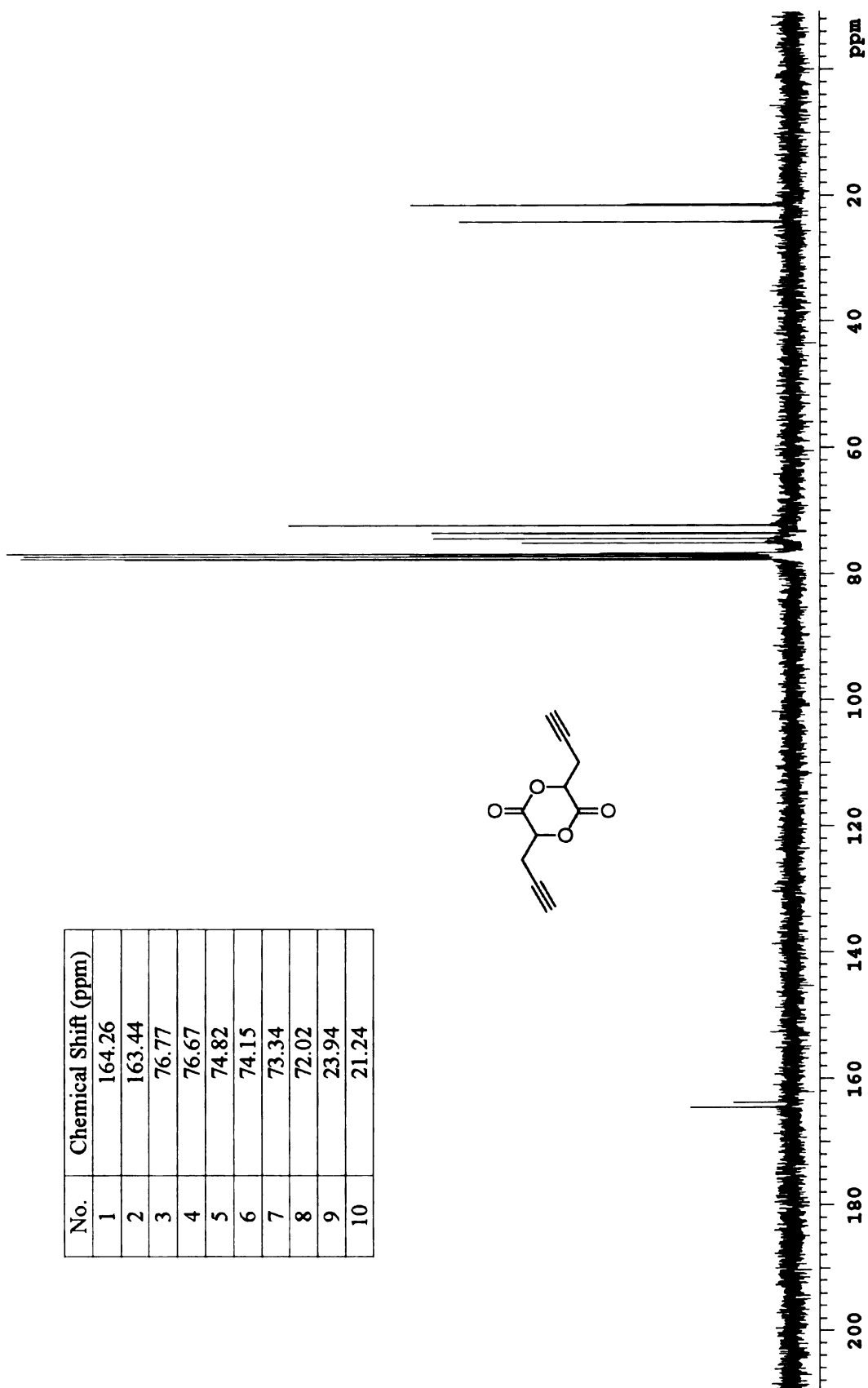
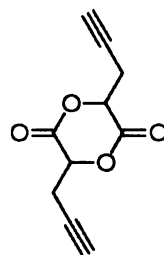


No.	Chemical Shift (ppm)	Value
1	5.01-5.33	1.0
2	2.83-3.11	2.2
3	2.08-2.20	0.9



Appendix A 62. ¹H NMR spectrum of propargyl glycolide

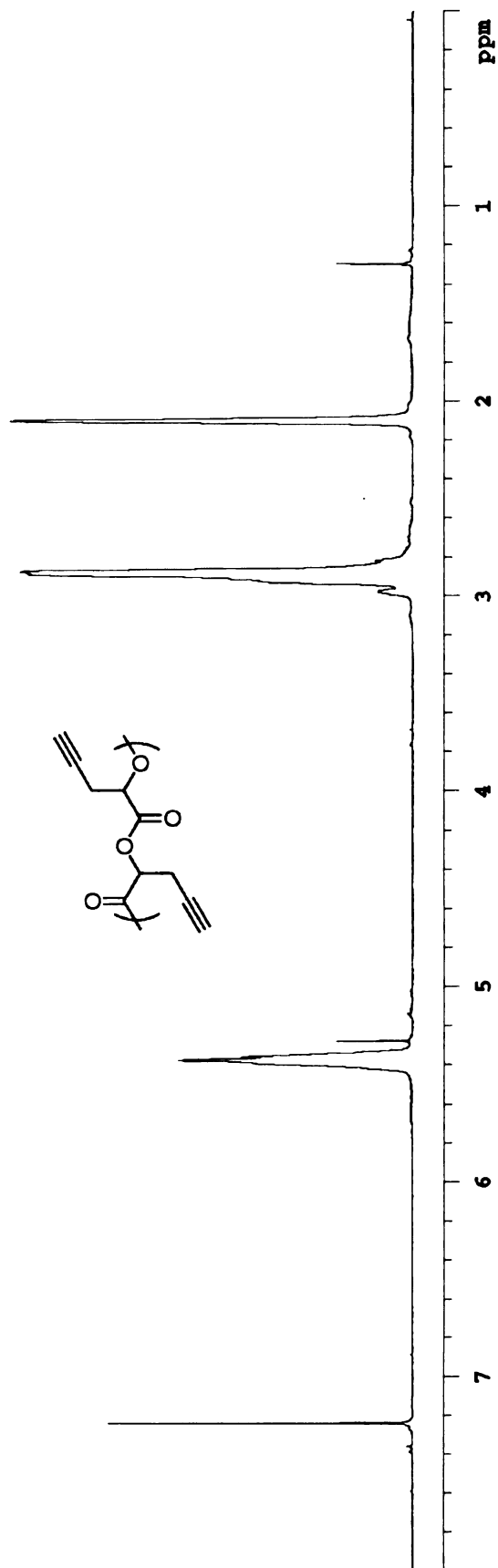
No.	Chemical Shift (ppm)
1	164.26
2	163.44
3	76.77
4	76.67
5	74.82
6	74.15
7	73.34
8	72.02
9	23.94
10	21.24

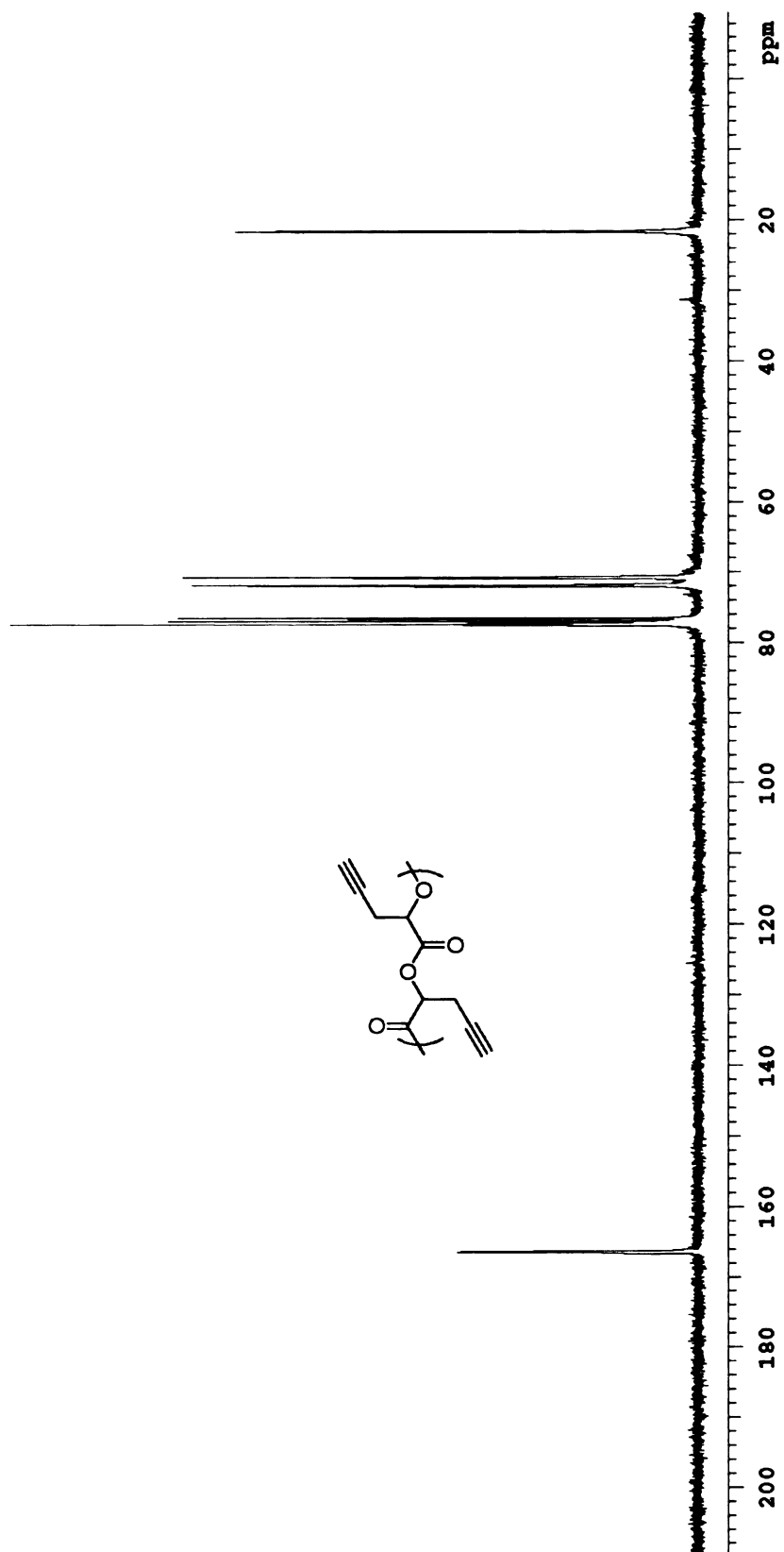


Appendix A 63. ¹³C NMR spectrum of propargyl glycolide

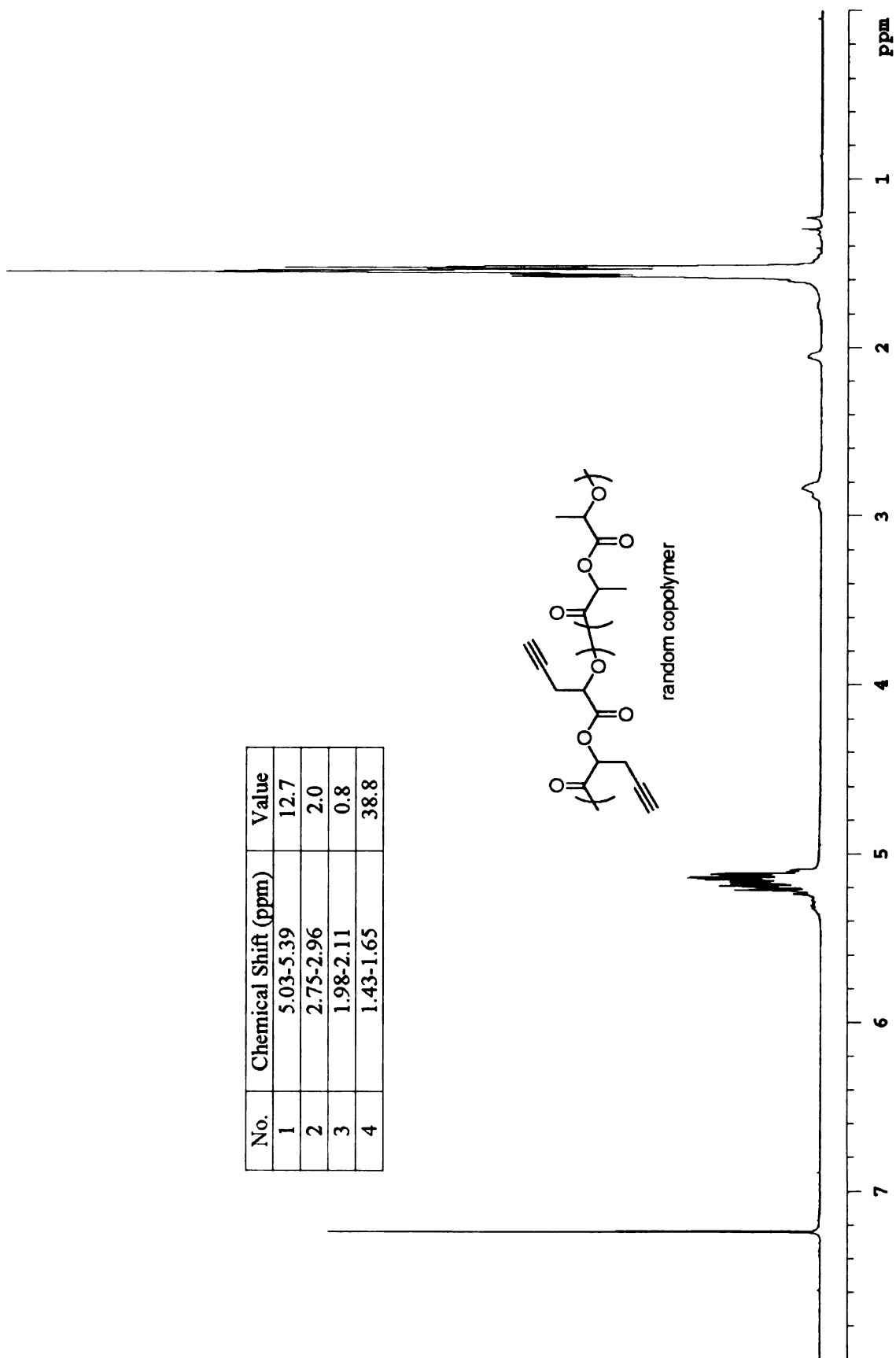
Appendix A 64. ¹H NMR spectrum of poly(propargyl glycolide)

No.	Chemical Shift (ppm)	Value
1	5.31-5.46	1.0
2	2.79-3.03	2.0
3	2.02-2.18	1.0

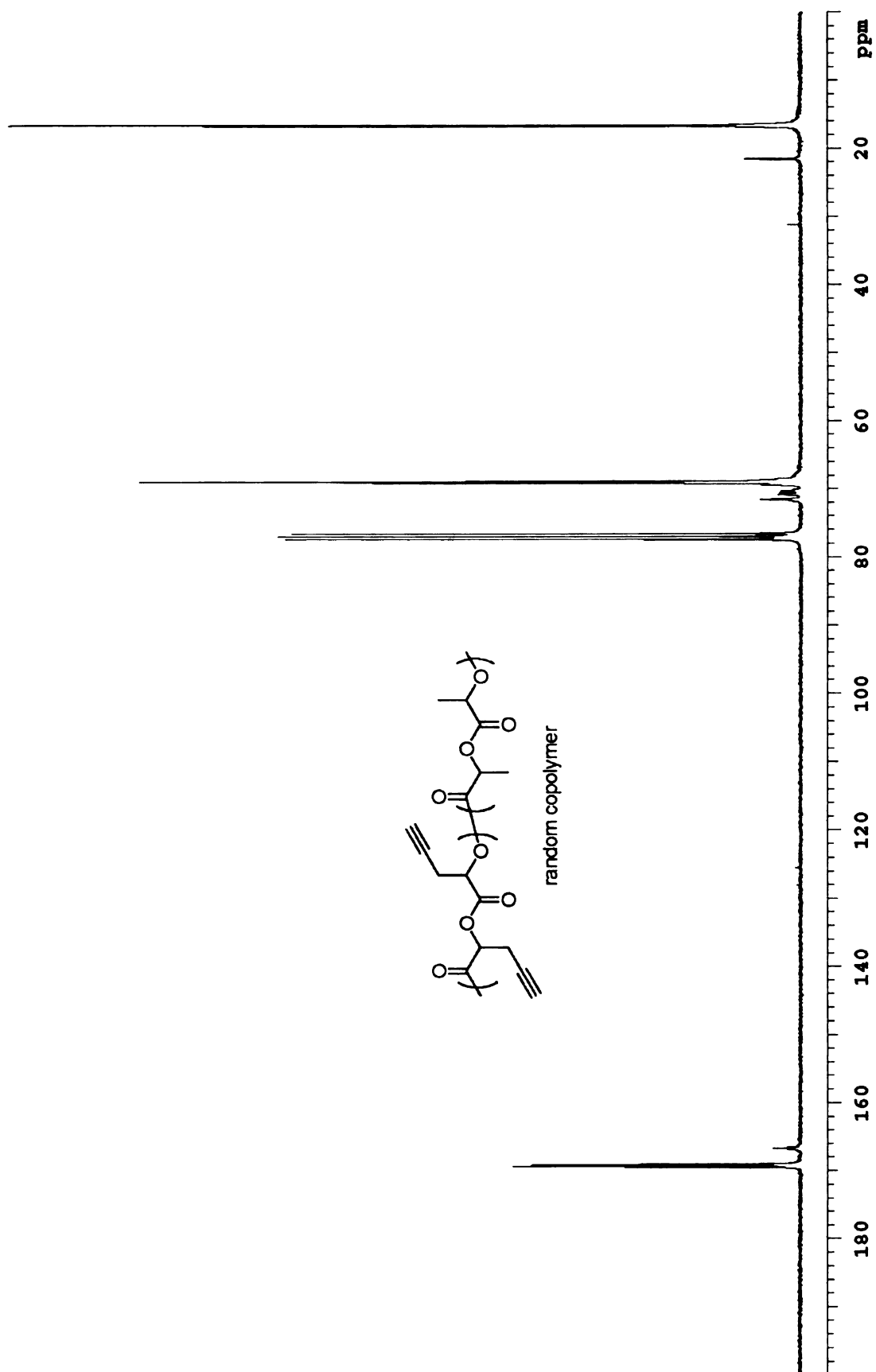




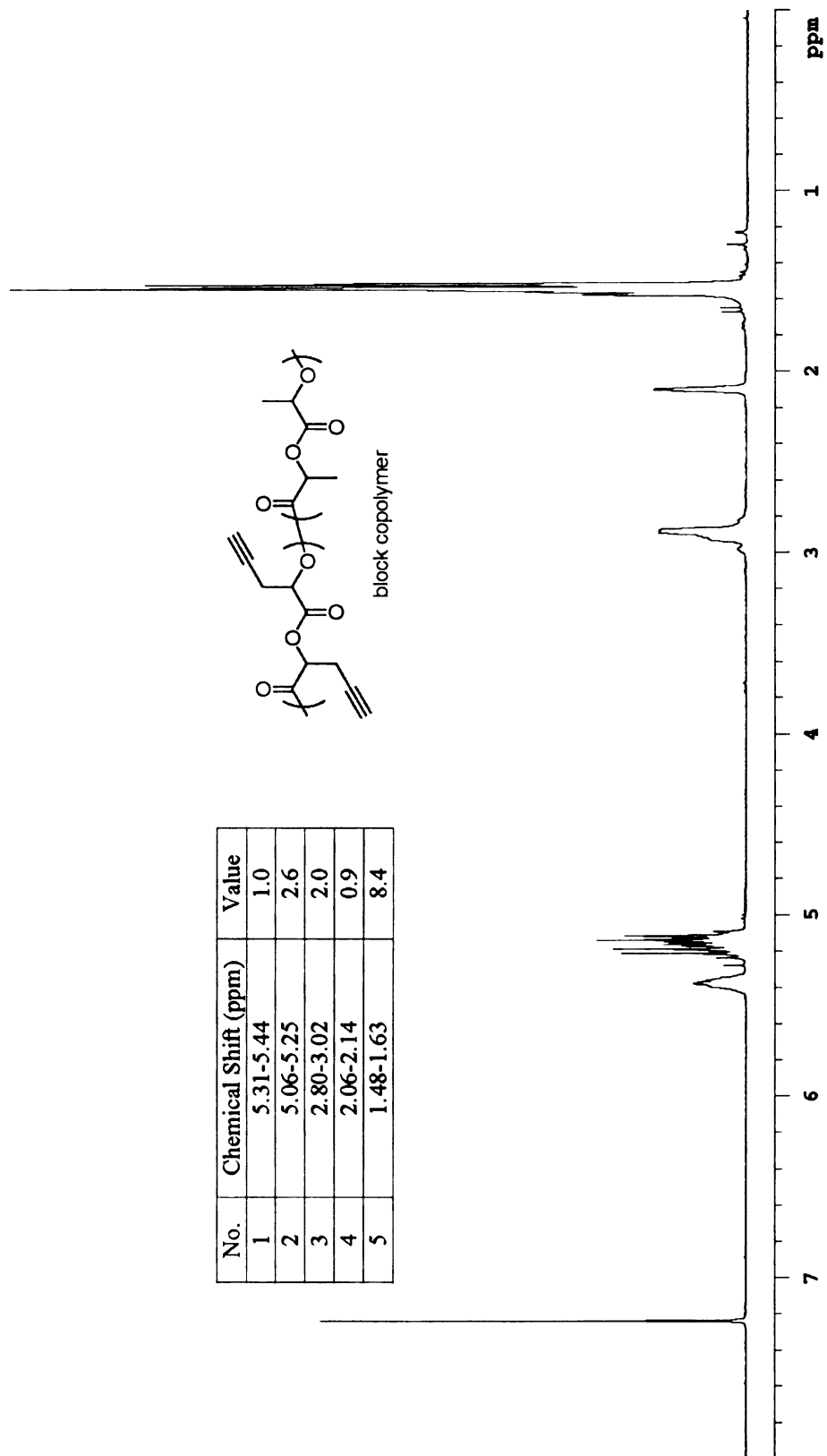
Appendix A 65. ^{13}C NMR spectrum of poly(propargyl glycolide)



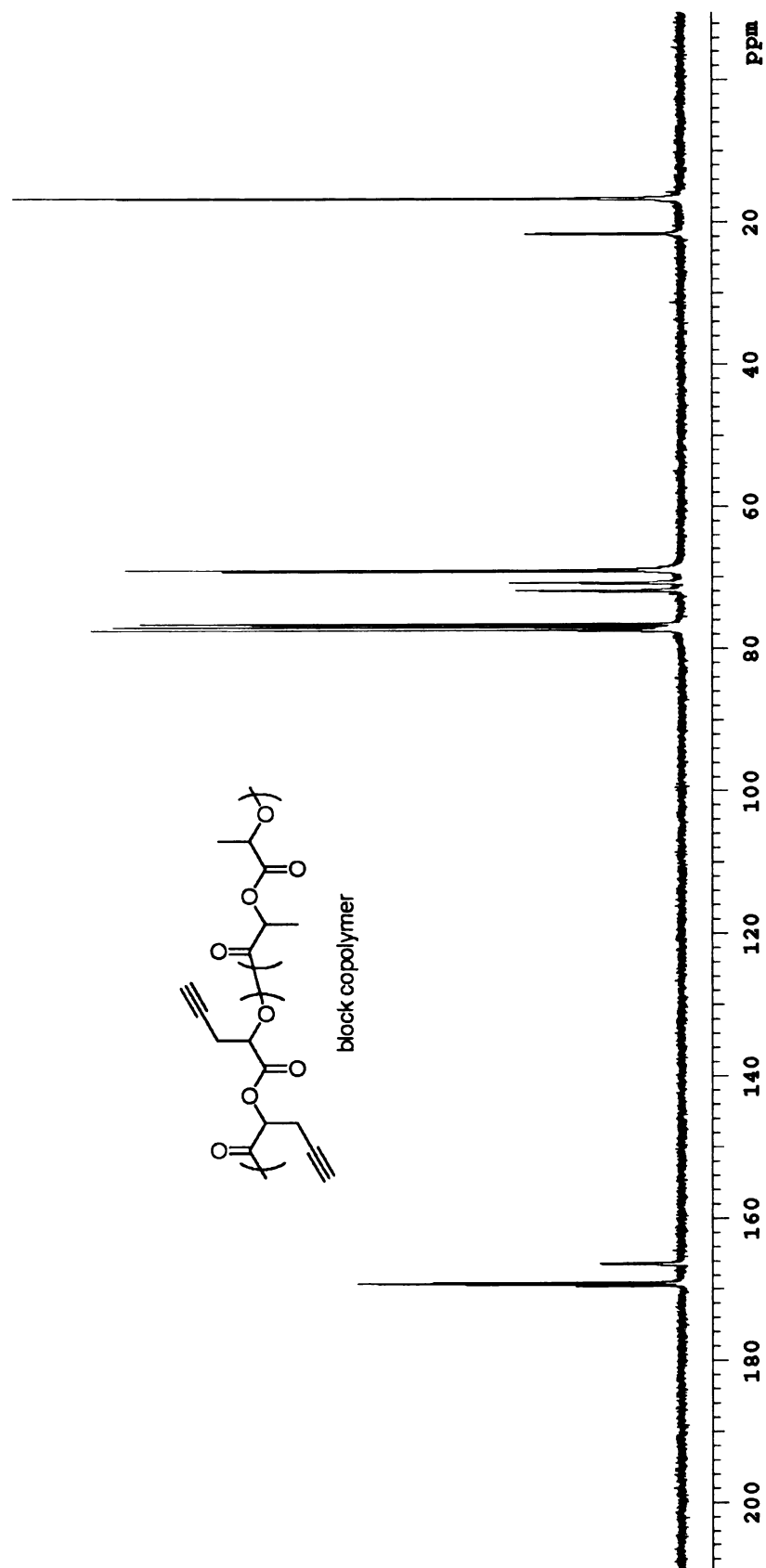
Appendix A 66. ^1H NMR spectrum of poly(propargyl glycolide) – *ran* - polylactide



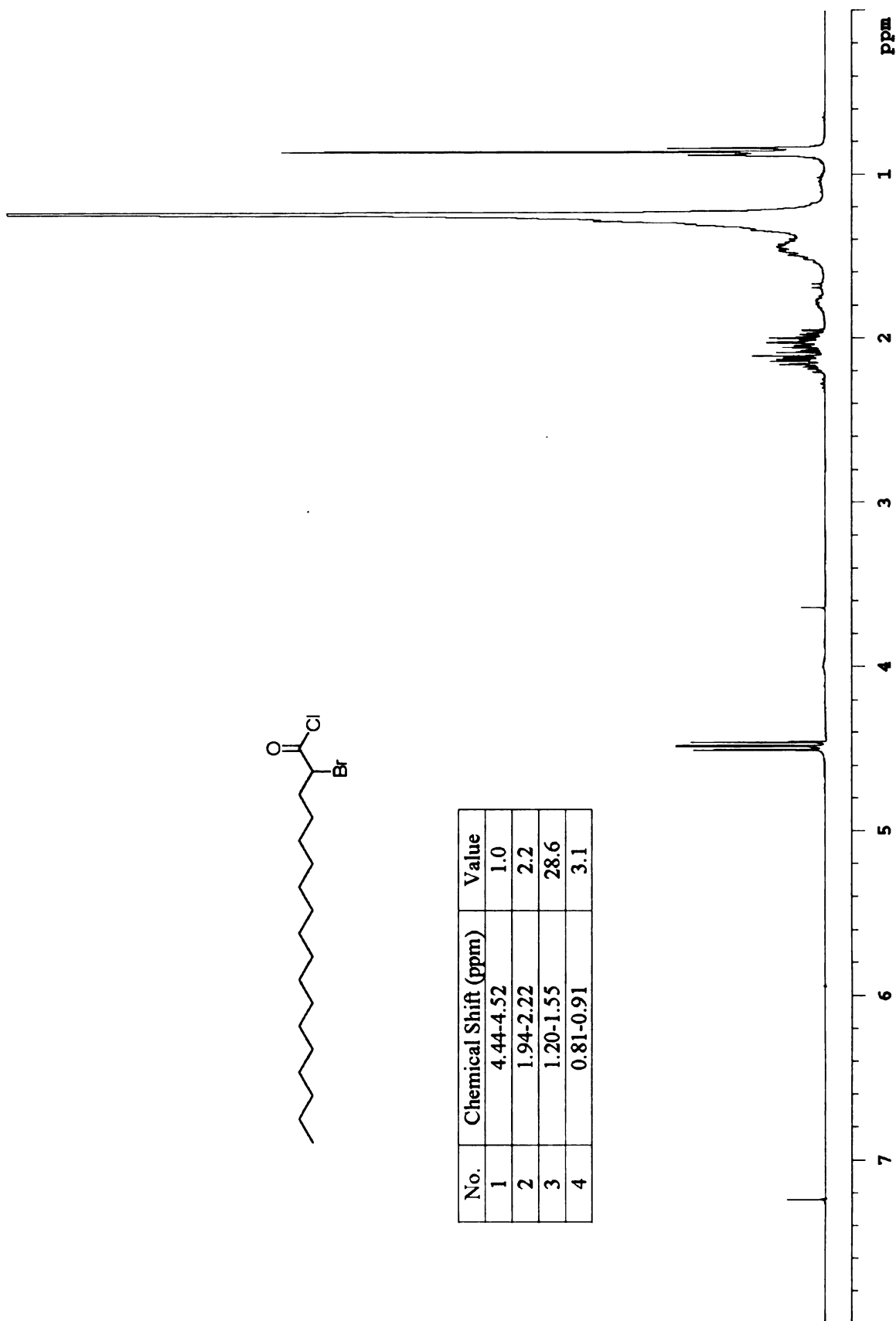
Appendix A 67. ^{13}C NMR spectrum of poly(propargyl glycolide) – *ran* - polylactide



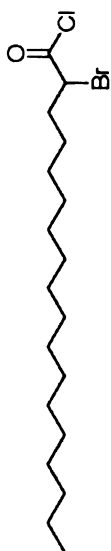
Appendix A 68. ^1H NMR spectrum of poly(propargyl glycolide) – *block* – polylactide



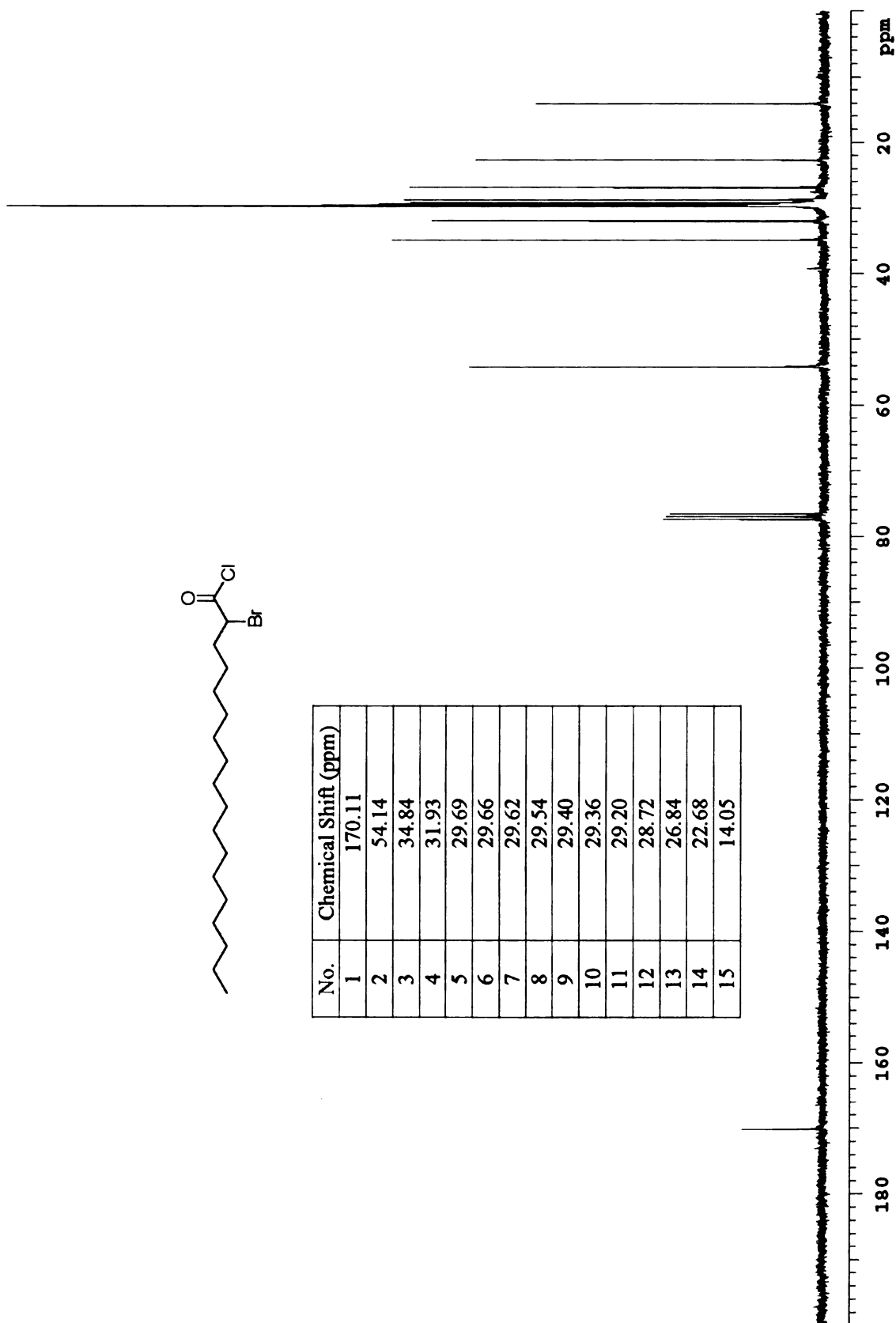
Appendix A 69. ^{13}C NMR spectrum of poly(propargyl glycolide) –block – polylactide



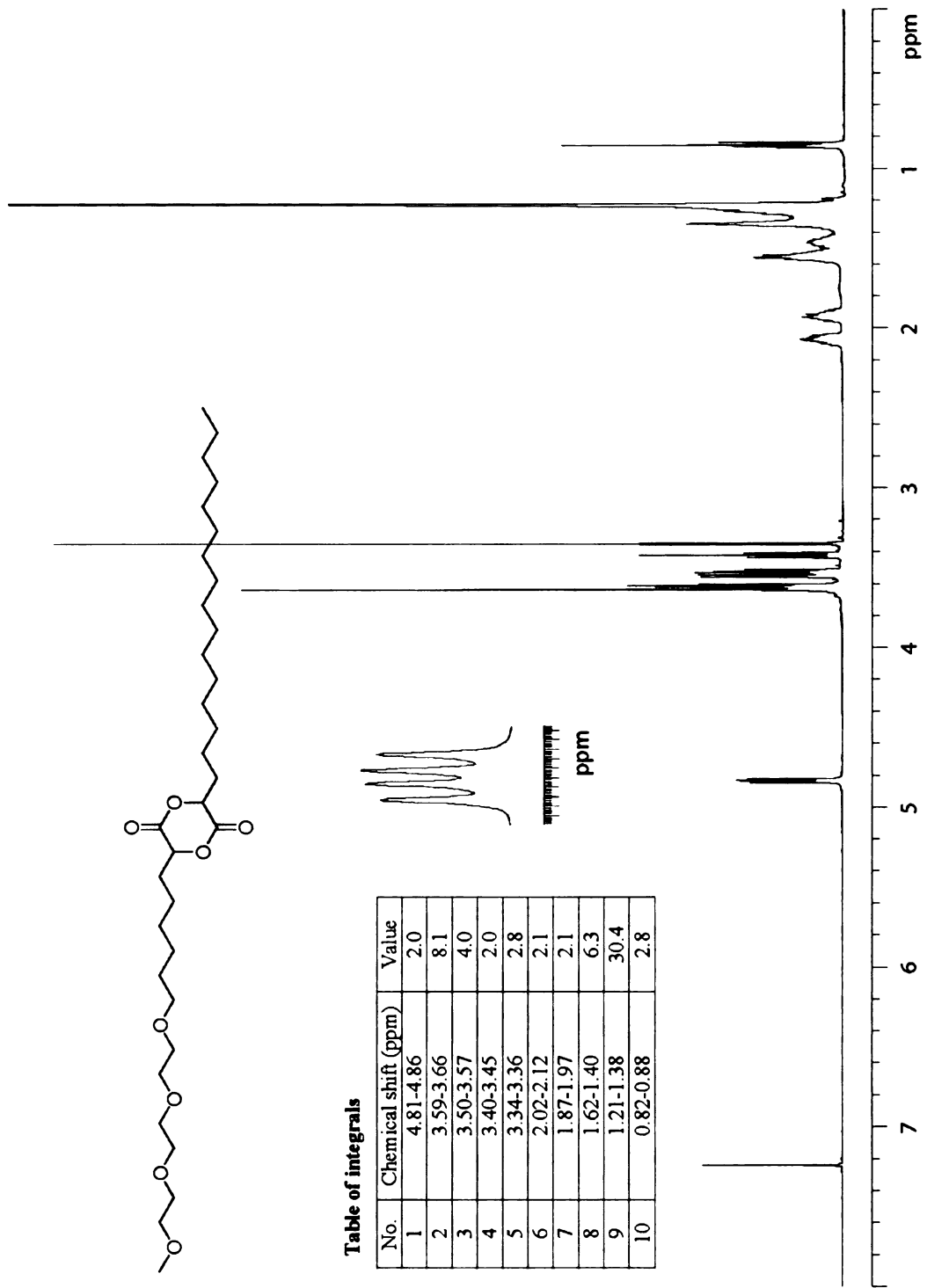
Appendix A 71. ¹H NMR spectrum of 2-bromooctadecanoyl chloride



No.	Chemical Shift (ppm)
1	170.11
2	54.14
3	34.84
4	31.93
5	29.69
6	29.66
7	29.62
8	29.54
9	29.40
10	29.36
11	29.20
12	28.72
13	26.84
14	22.68
15	14.05



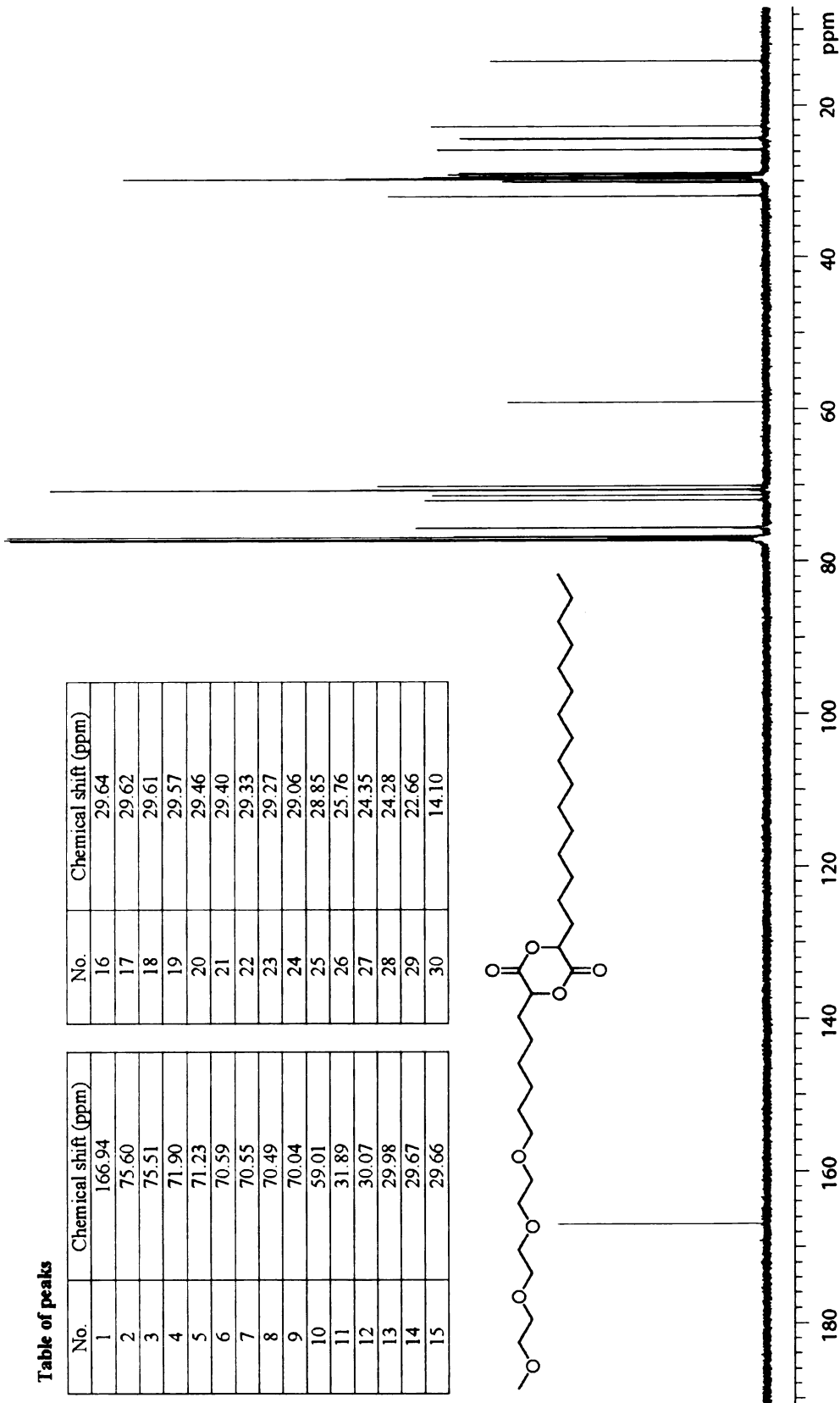
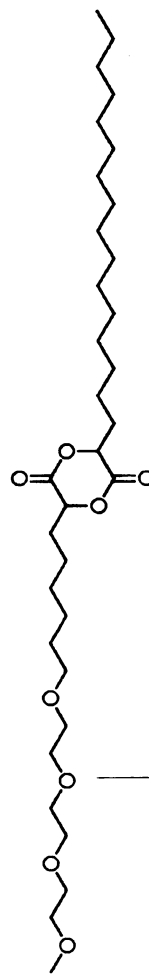
Appendix A 72. ¹³C NMR spectrum of 2-bromooctadecanoyl chloride



Appendix A 73. ¹H NMR spectrum of TriEG-C6-C16 dimer

Table of peaks

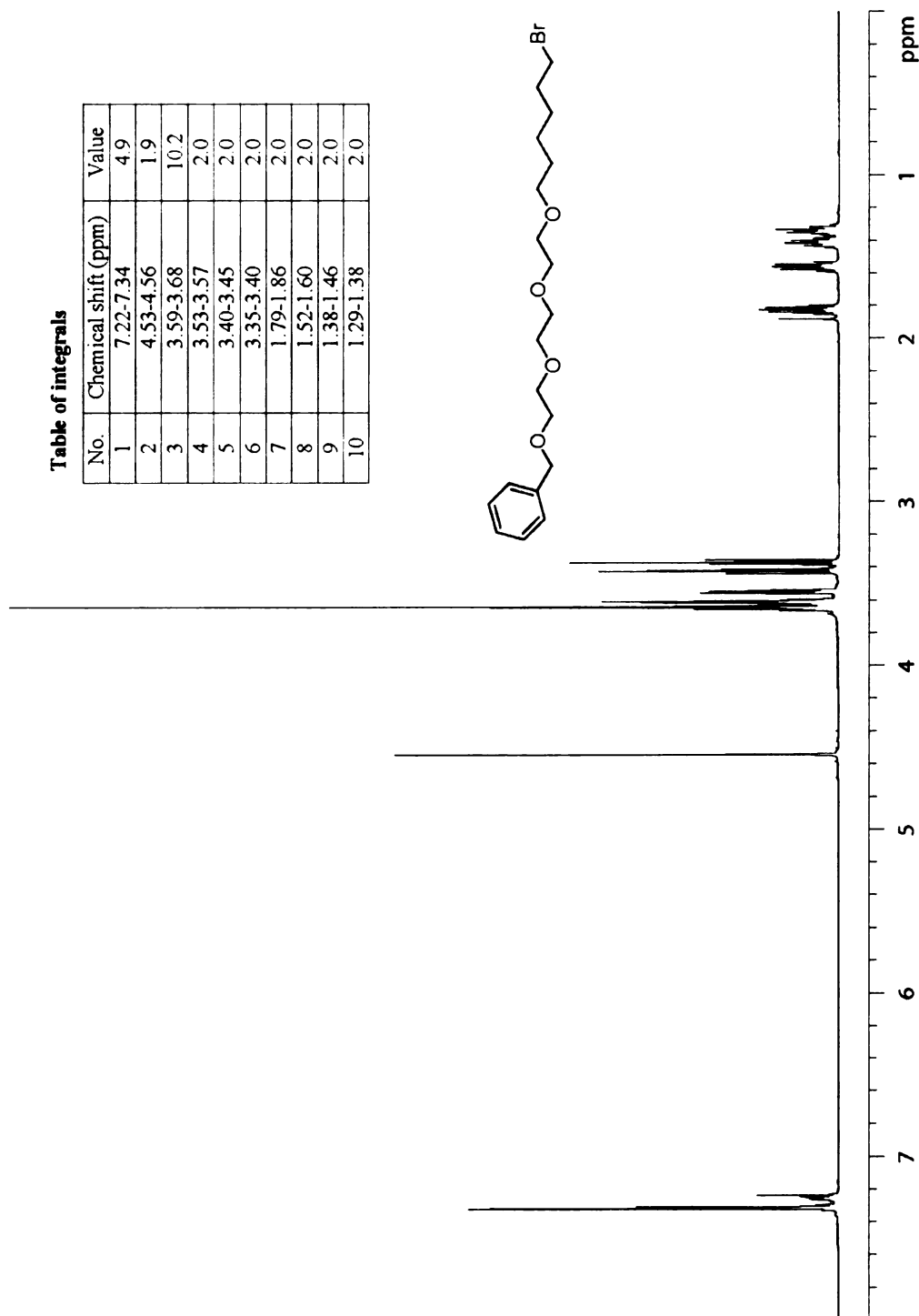
No.	Chemical shift (ppm)	No.	Chemical shift (ppm)
1	166.94	16	29.64
2	75.60	17	29.62
3	75.51	18	29.61
4	71.90	19	29.57
5	71.23	20	29.46
6	70.59	21	29.40
7	70.55	22	29.33
8	70.49	23	29.27
9	70.04	24	29.06
10	59.01	25	28.85
11	31.89	26	25.76
12	30.07	27	24.35
13	29.98	28	24.28
14	29.67	29	22.66
15	29.66	30	14.10



Appendix A 74. ^{13}C NMR spectrum of TriEG-C6-C16 dimer

Table of integrals

No.	Chemical shift (ppm)	Value
1	7.22-7.34	4.9
2	4.53-4.56	1.9
3	3.59-3.68	10.2
4	3.53-3.57	2.0
5	3.40-3.45	2.0
6	3.35-3.40	2.0
7	1.79-1.86	2.0
8	1.52-1.60	2.0
9	1.38-1.46	2.0
10	1.29-1.38	2.0



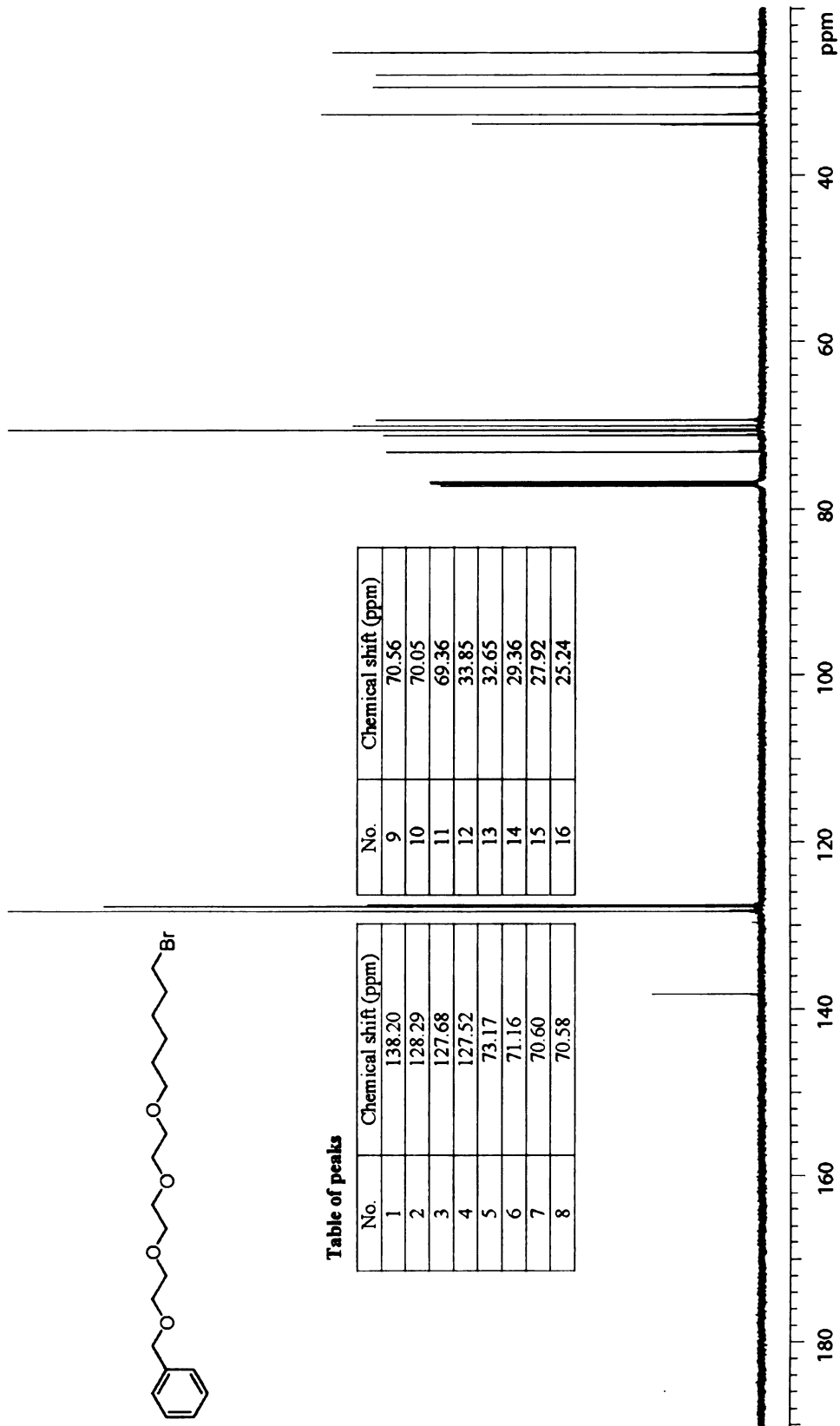
Appendix A 75. ¹H NMR spectrum of TriEG-monobenzyl-ether-C6 bromide



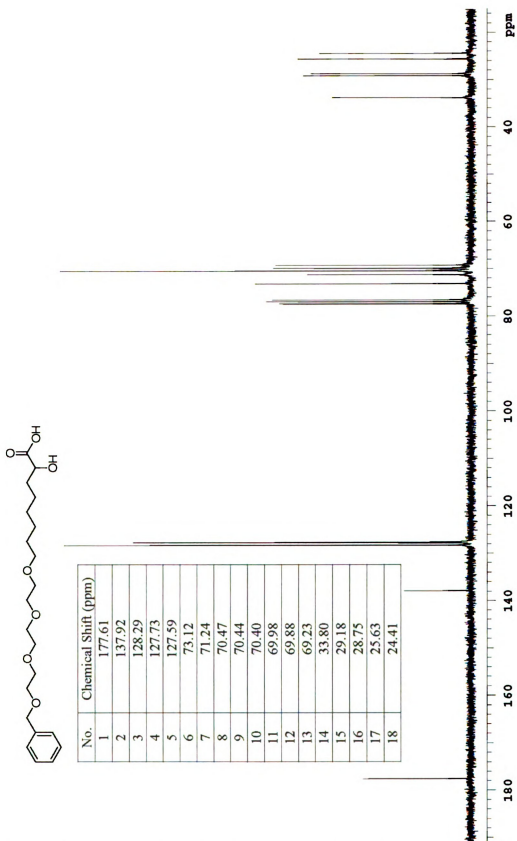
Table of peaks

No.	Chemical shift (ppm)
1	138.20
2	128.29
3	127.68
4	127.52
5	73.17
6	71.16
7	70.60
8	70.58

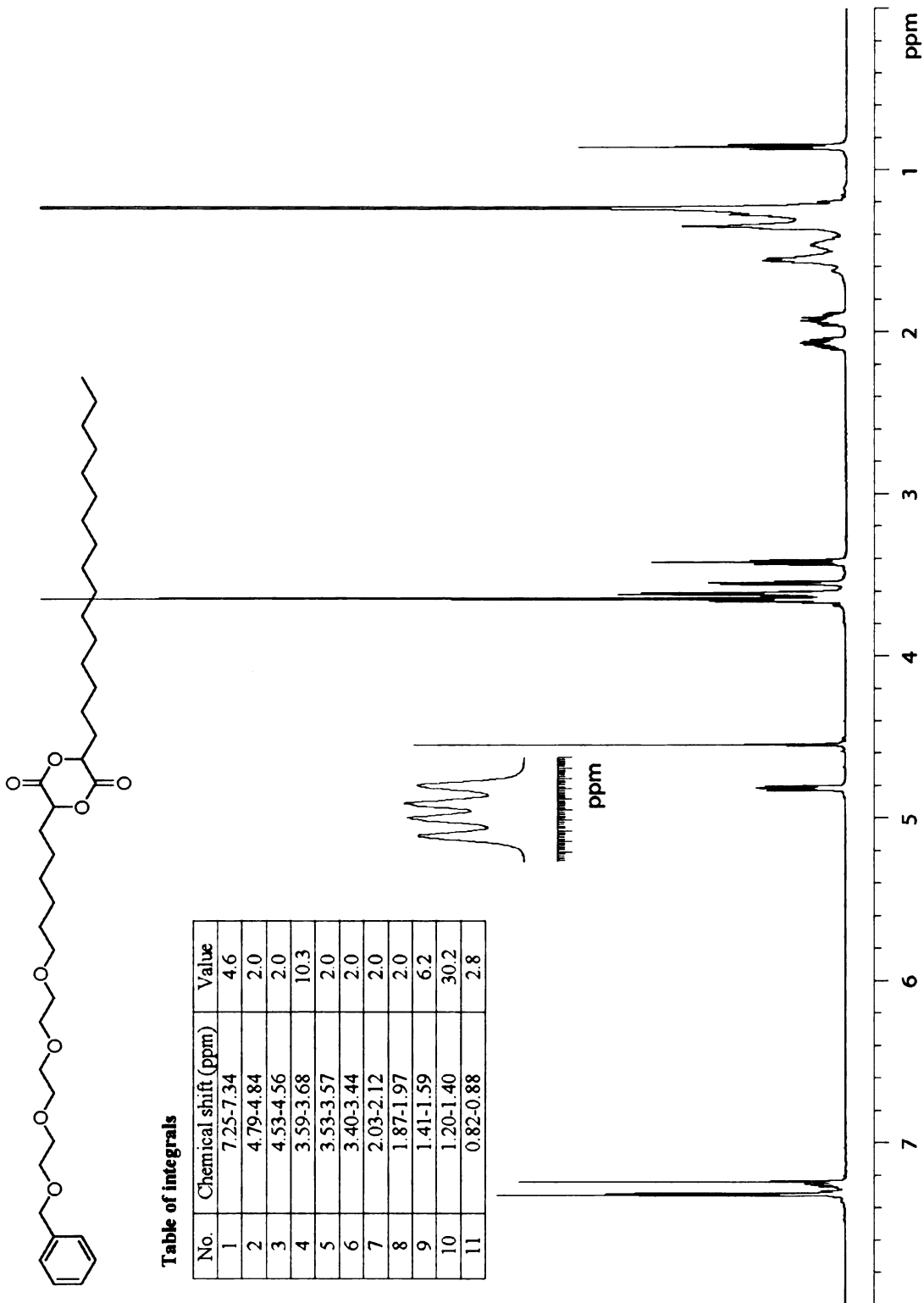
No.	Chemical shift (ppm)
9	70.56
10	70.05
11	69.36
12	33.85
13	32.65
14	29.36
15	27.92
16	25.24



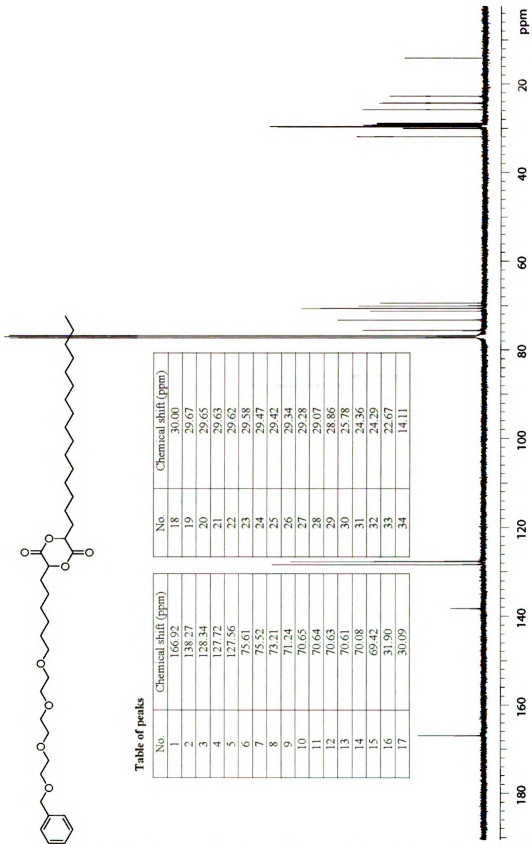
Appendix A 76. ¹³C NMR spectrum of TriEG-monobenzyl-ether-C6 bromide



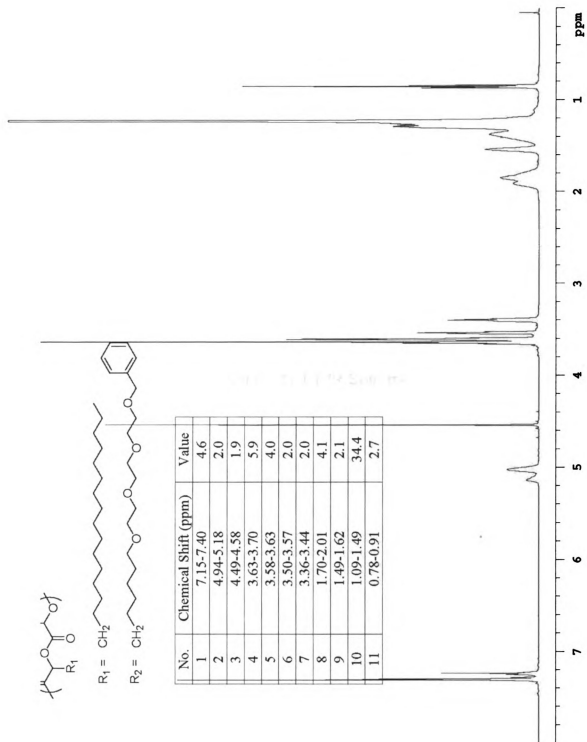
Appendix A 78. ^{13}C NMR spectrum of TriEG-monobenzyl-ether-C6- α -hydroxy acid



Appendix A 79. ¹H NMR spectrum of TriEG-monoethyl-ether-C6-C16 dimer

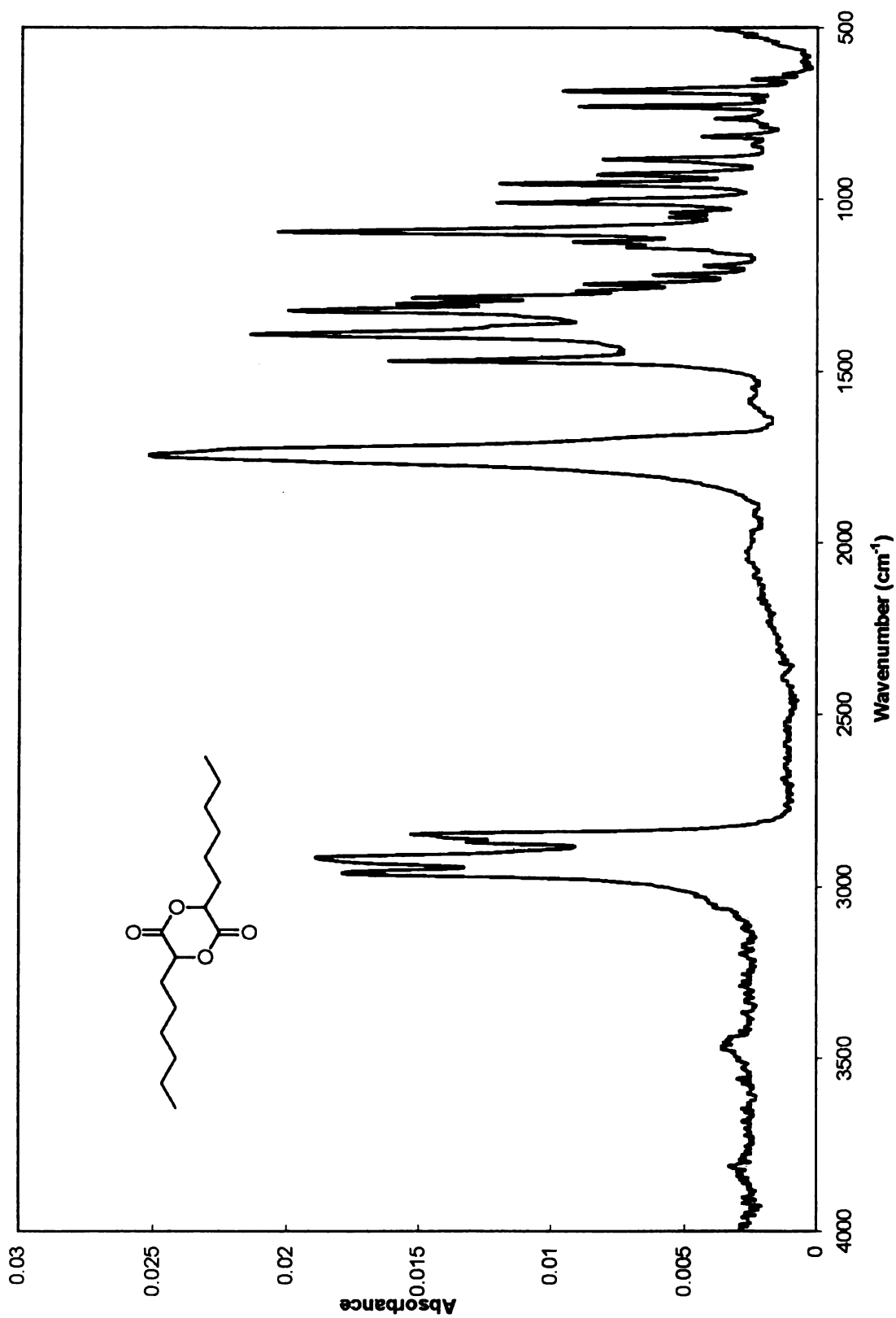


Appendix A 80. ^{13}C NMR spectrum of TriEG-monobenzyl-ether-C6-C16 dimer

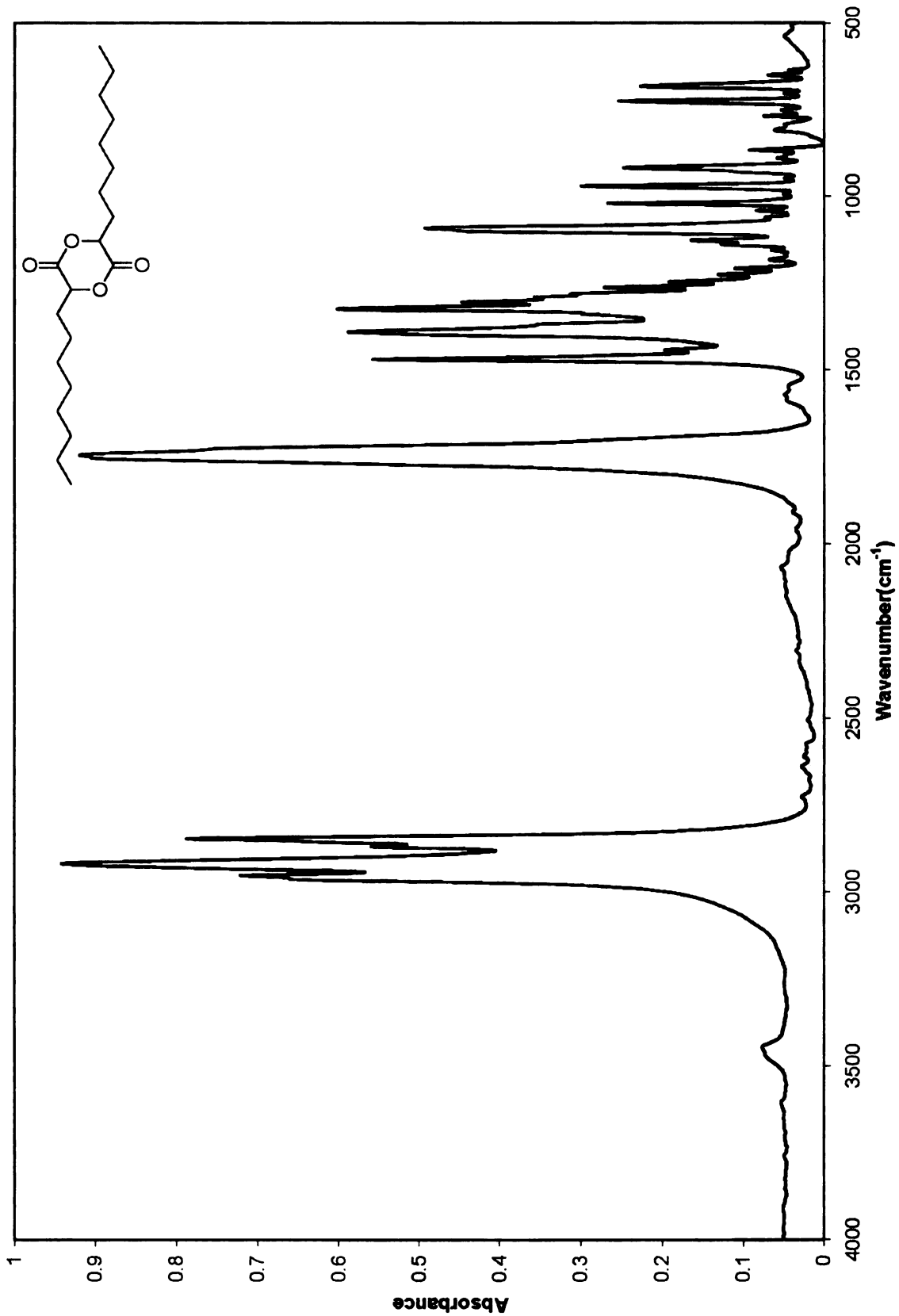


Appendix A 82. ^1H NMR spectrum of poly(TriEG-monobenzyl-ether-C6-C16)

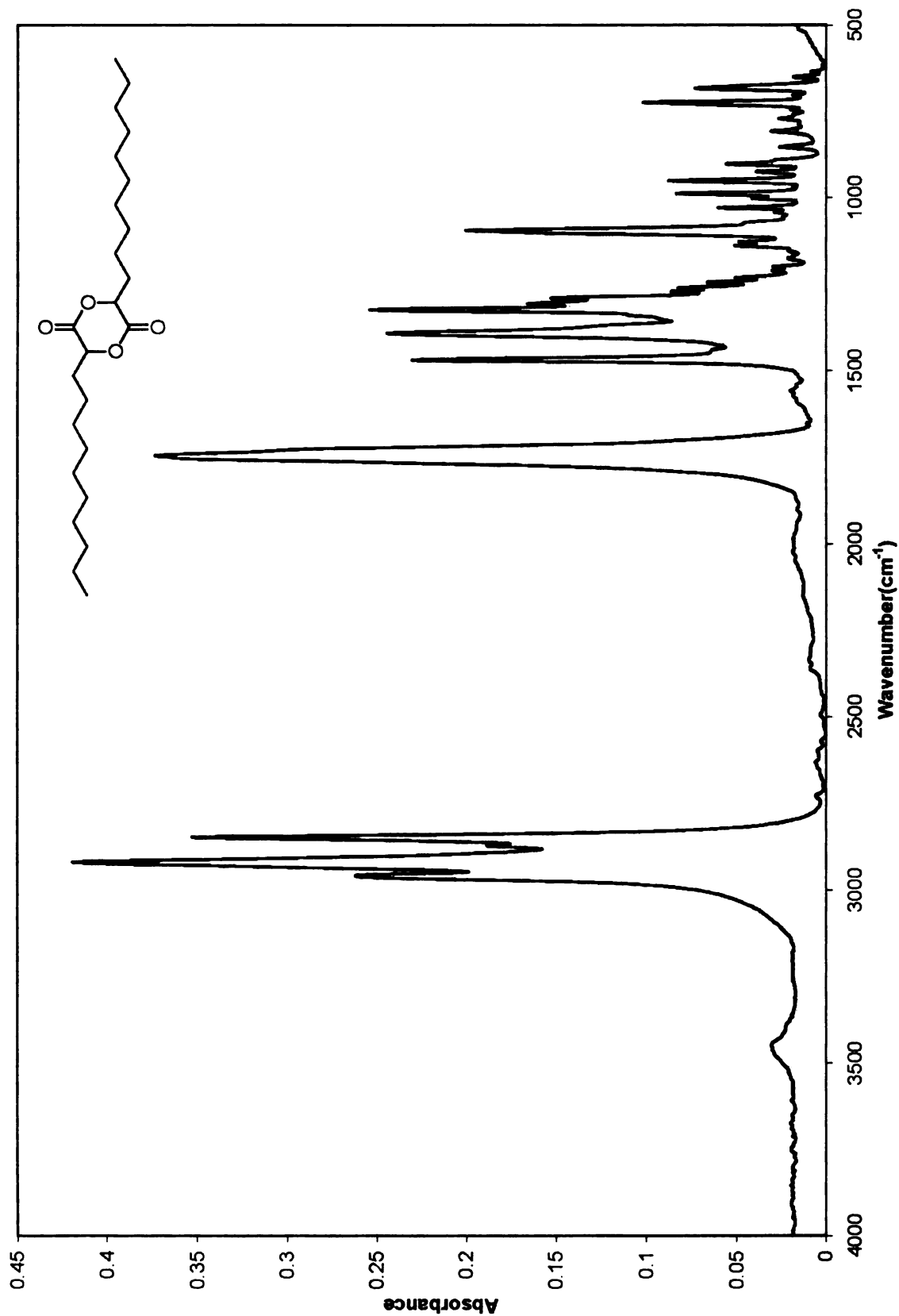
Appendix B. FT-IR Spectra



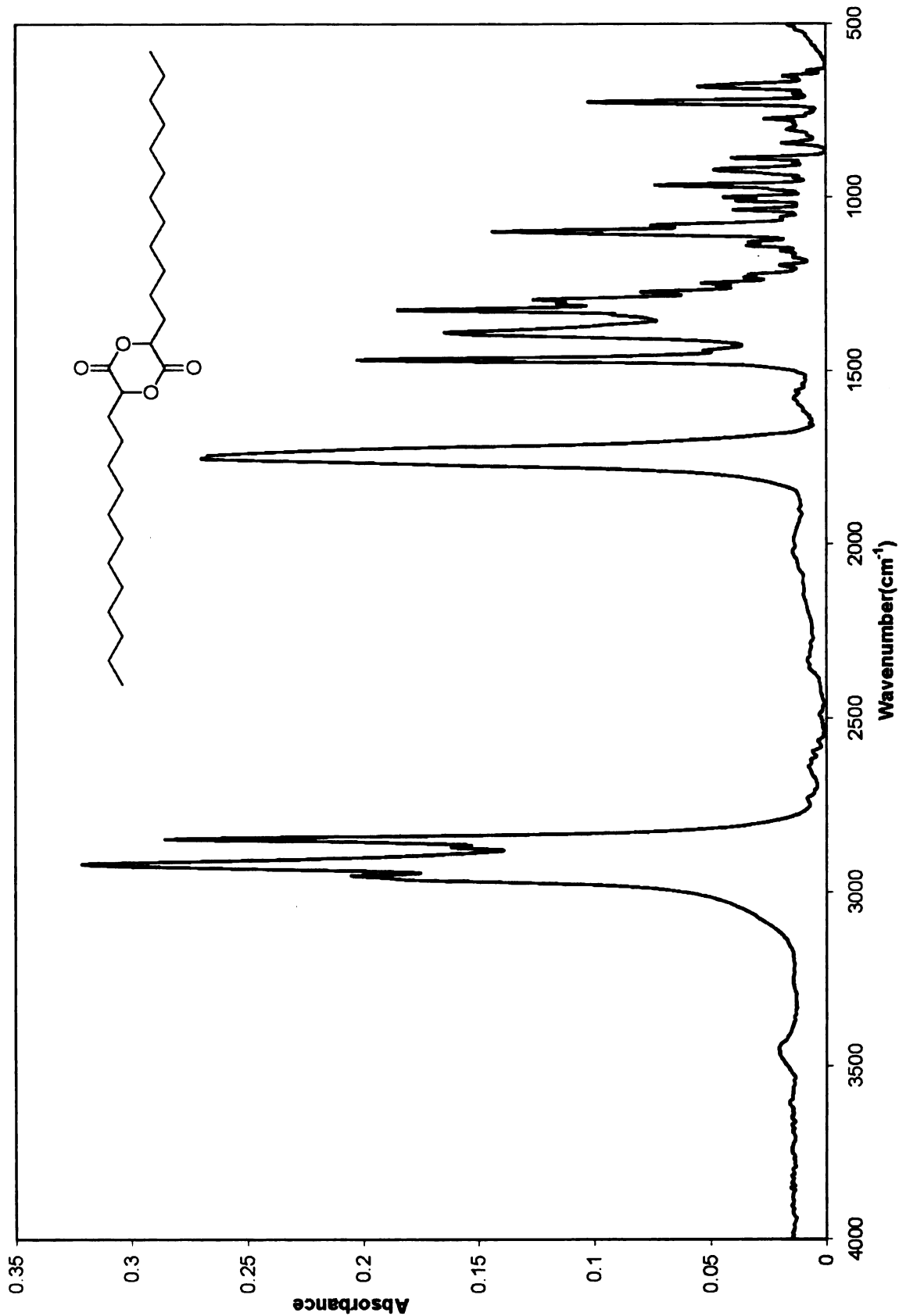
Appendix B 1. FT-IR spectrum of C6 dimer



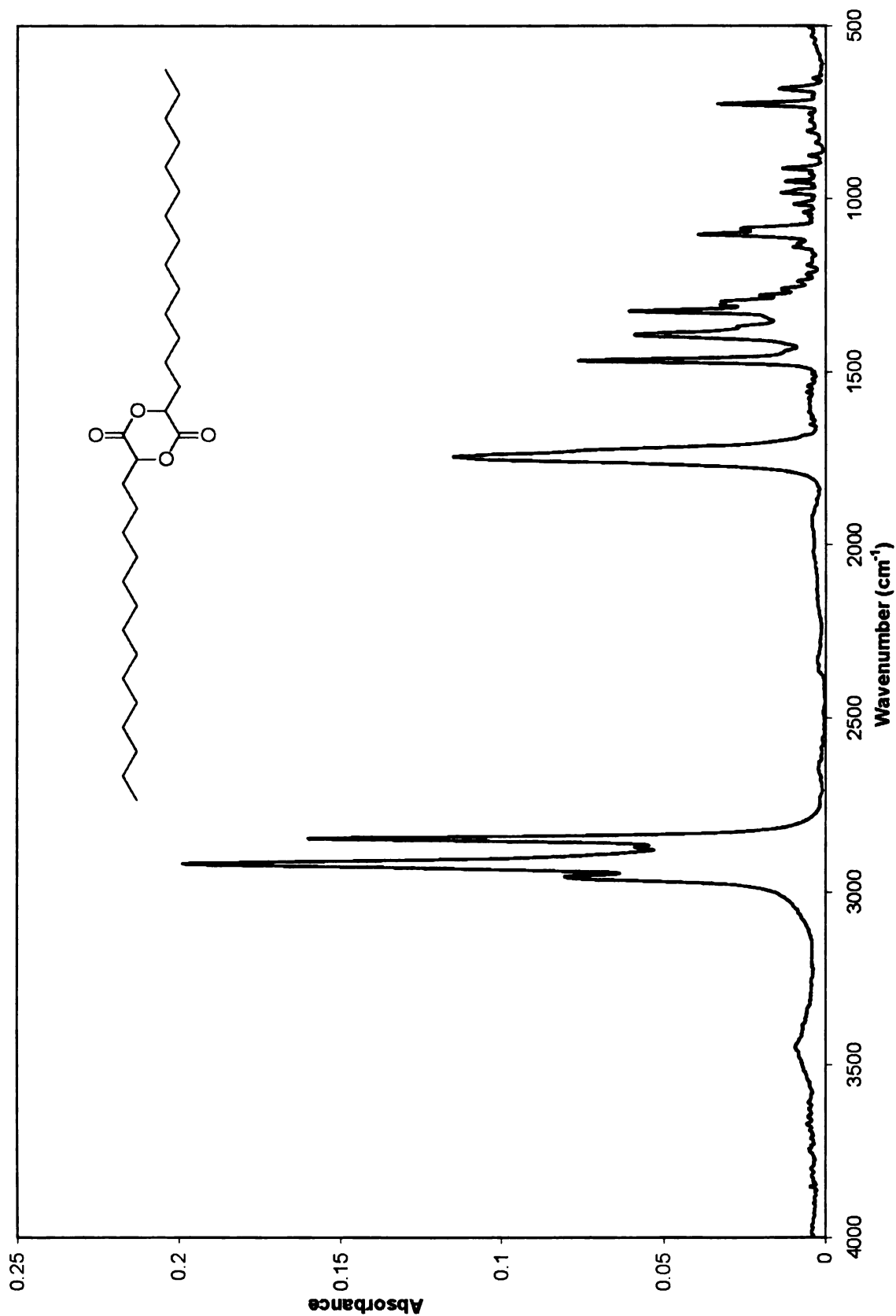
Appendix B 2. FT-IR spectrum of C8 dimer



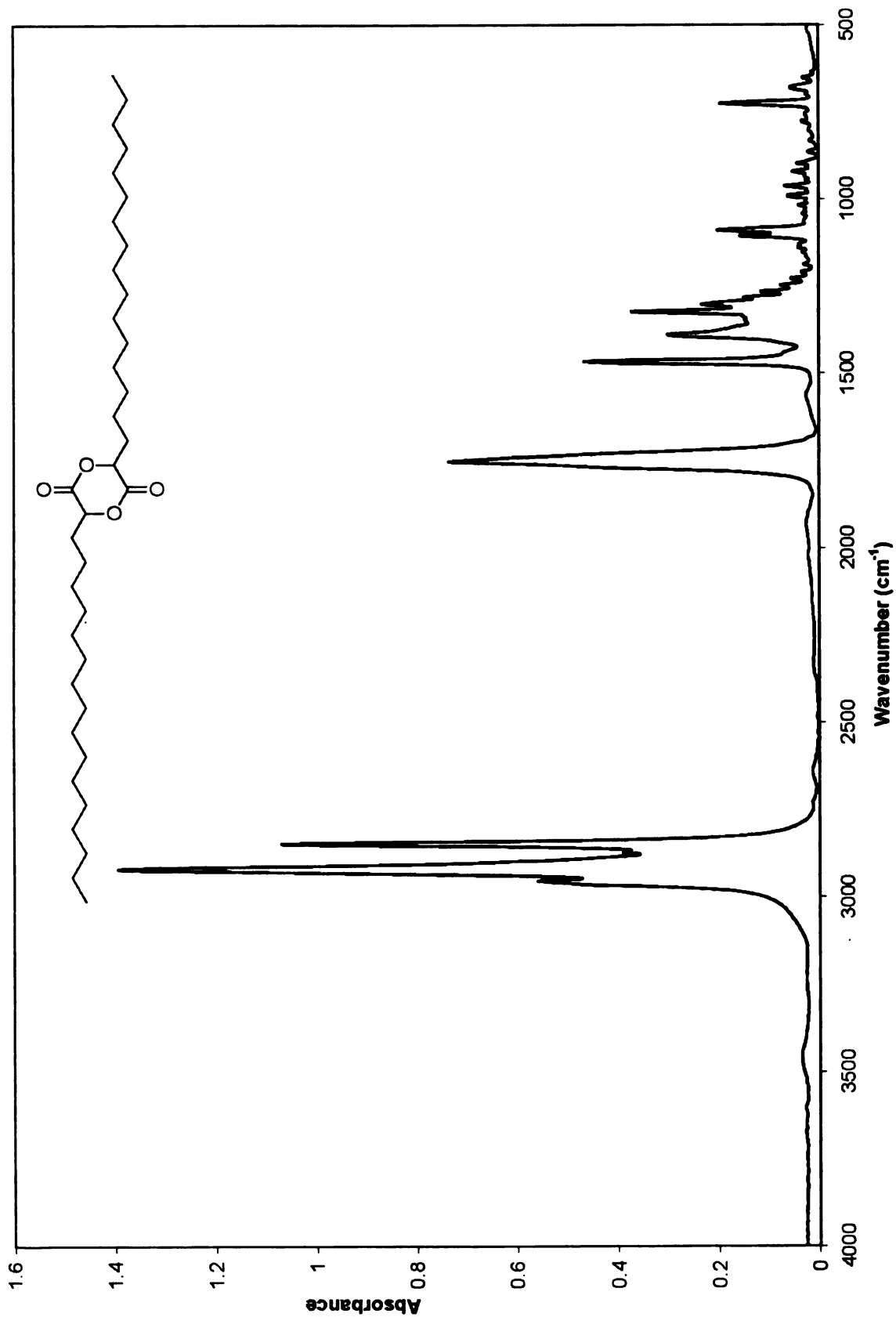
Appendix B 3. FT-IR spectrum of C10 dimer



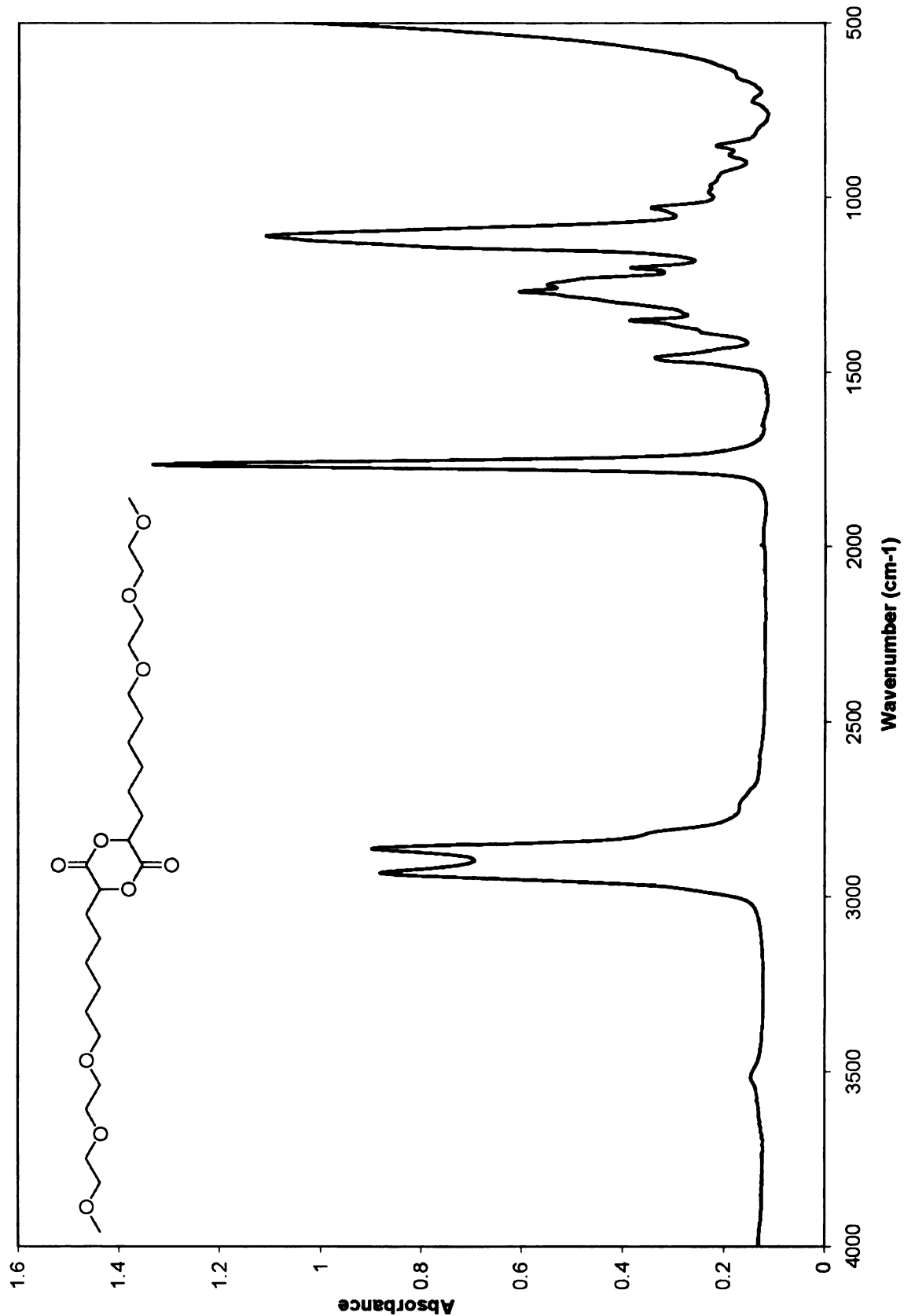
Appendix B 4. FT-IR spectrum of C12 dimer



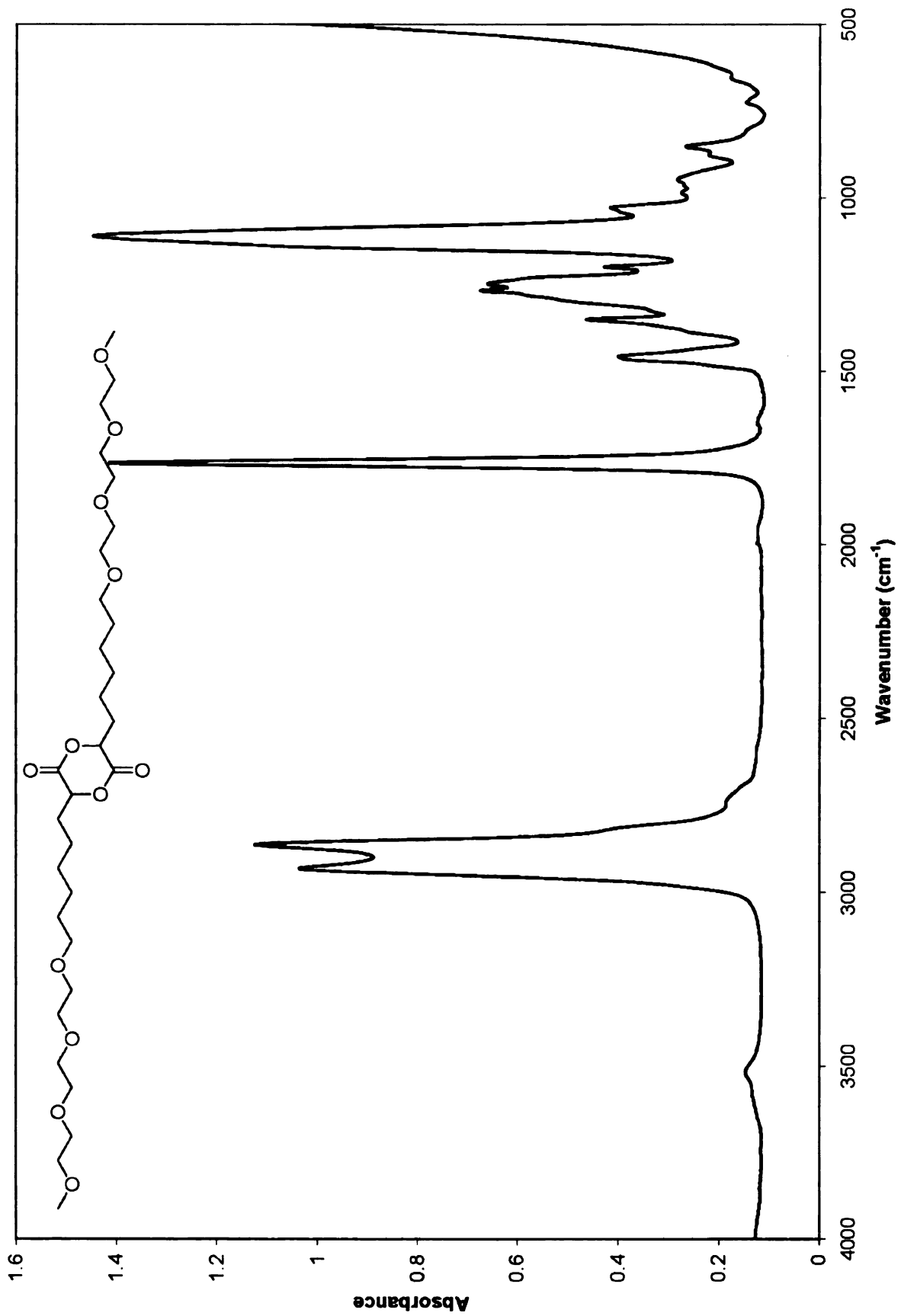
Appendix B 5. FT-IR spectrum of C14 dimer



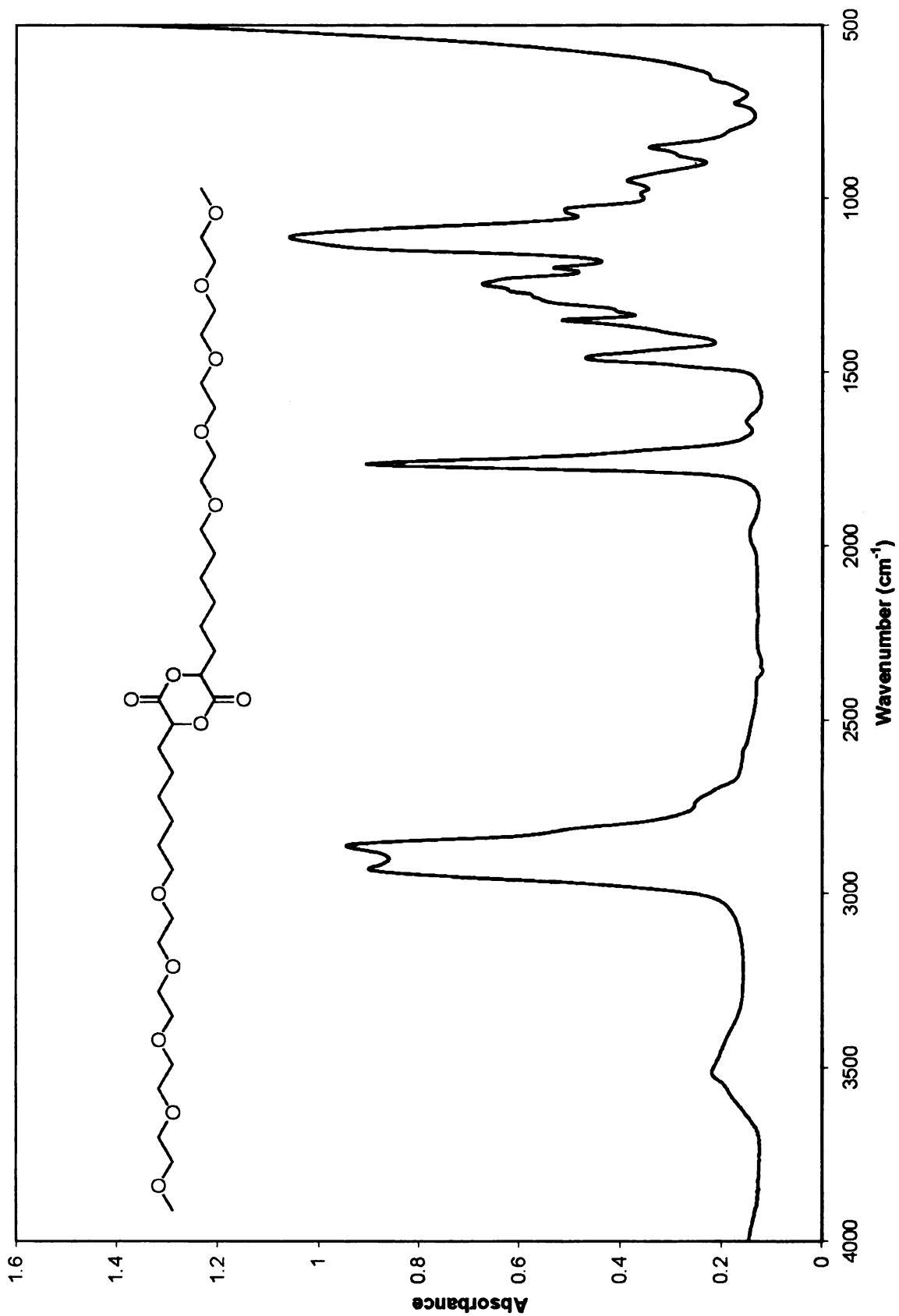
Appendix B 6. FT-IR spectrum of C16 dimer



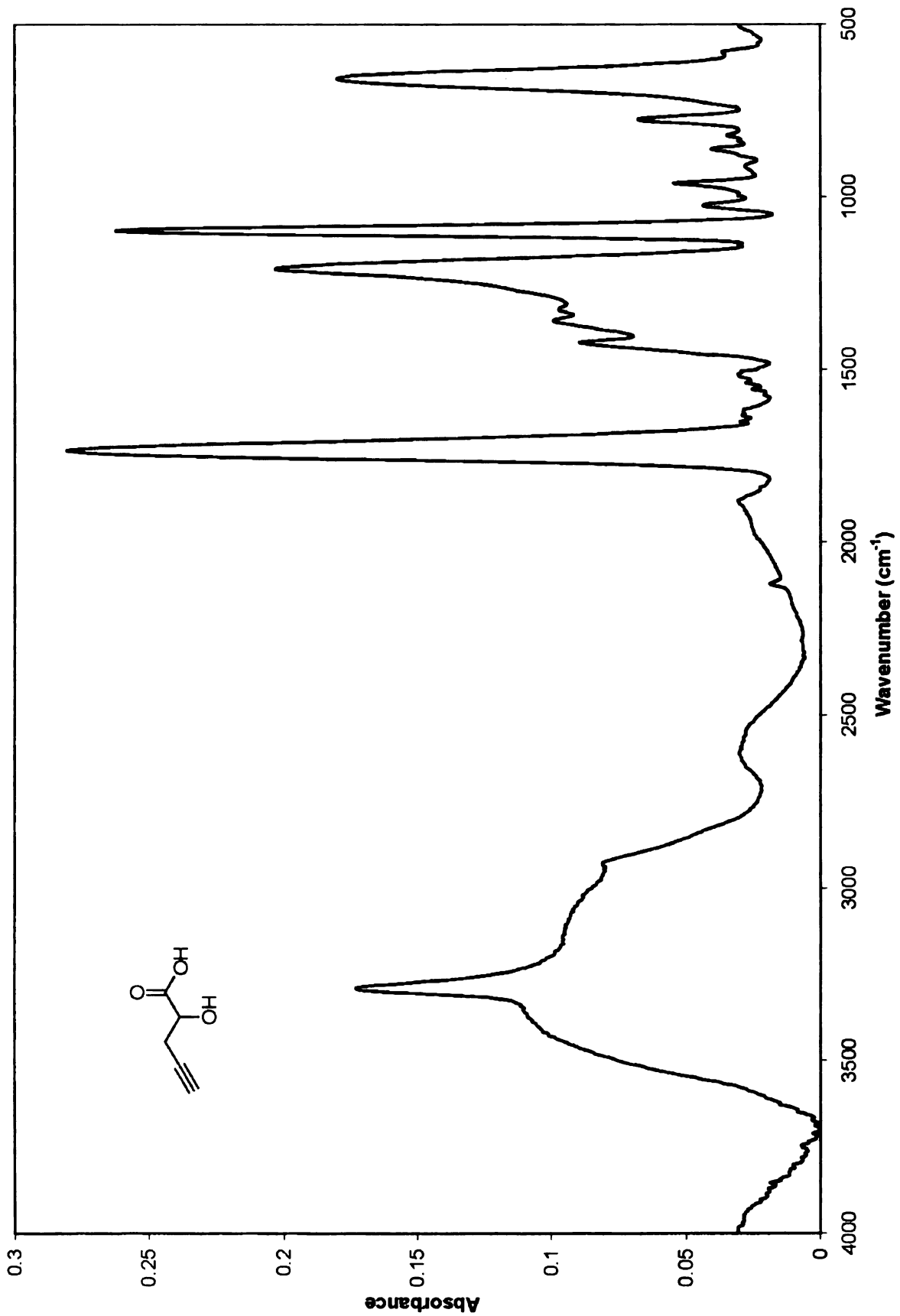
Appendix B 8. FT-IR spectrum of DiEG-C6 dimer



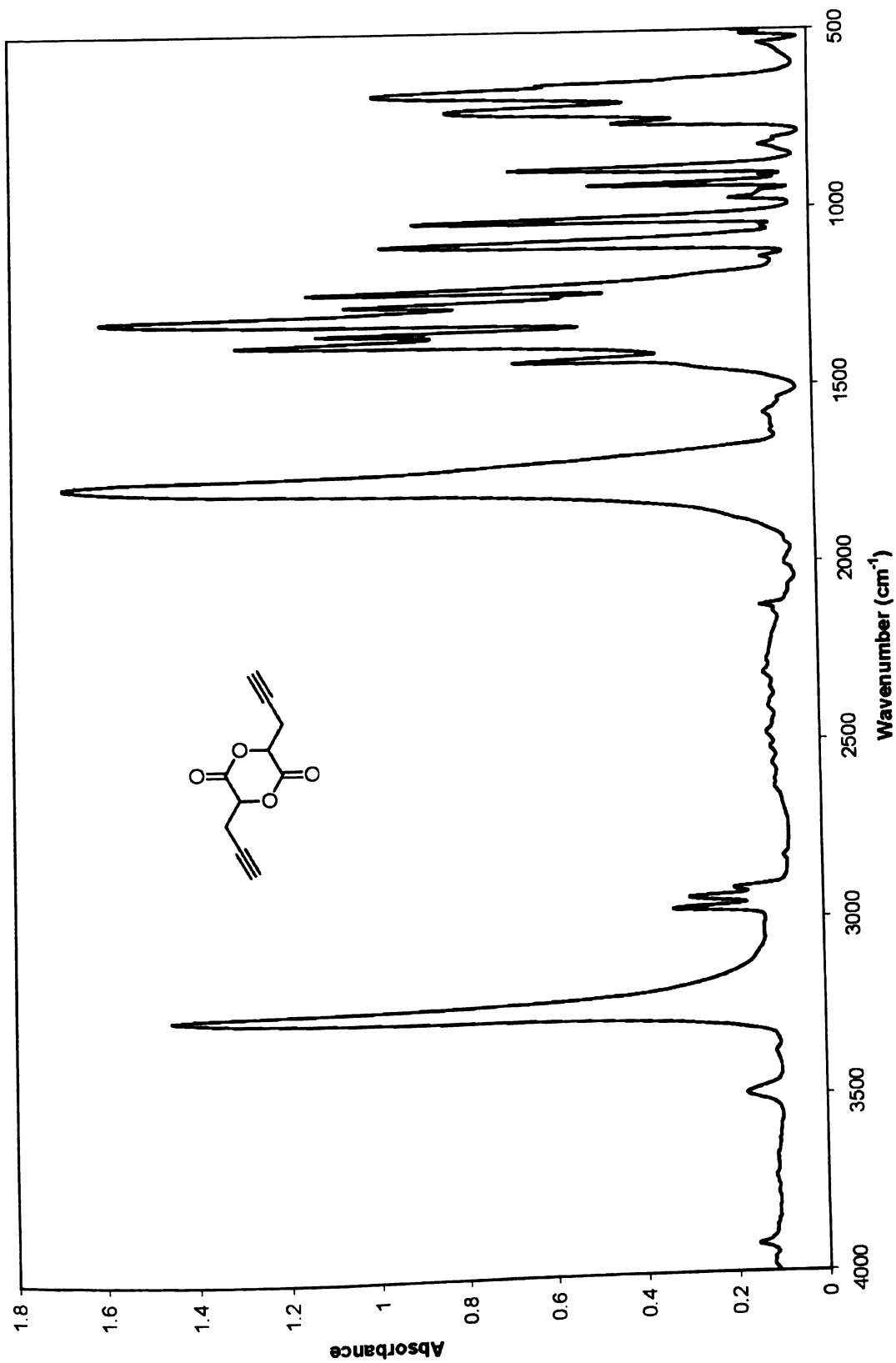
Appendix B 9. FT-IR spectrum of TriEG-C6 dimer



Appendix B 10. FT-IR spectrum of TetraEG-C6 dimer



Appendix B 11. FT-IR spectrum of propargyl- α -hydroxy acid



Appendix B 12. FT-IR spectrum of propargyl glycolide

References

1. Plate, N.A. and Shibaev, V.P., *J. Polym. Sci., Macromol. Rev.*, **1974** *8*, 117-253.
2. Daly, W.H., Poche, D., and Negulescu, I.I., *Prog. Polym. Sci.*, **1994** *19*, 79-135.
3. Greene, L. and Balachander, N., *Controlled-Release Delivery Systems for Pesticides*, **1999** 245-261.
4. Rehberg, C.E. and Fisher, C.H., *J. Am. Chem. Soc.*, **1944** *66*, 1203-7.
5. Rehberg, C.E. and Fisher, C.H., *Ind. Eng. Chem. Res.*, **1948** *40*, 1429-33.
6. Kaufman, H.S., Sacher, A., Alfrey, T., and Fankuchen, I., *J. Am. Chem. Soc.*, **1948** *70*, 3147-3147.
7. Greenberg, S.A. and Alfrey, T., *J. Am. Chem. Soc.*, **1954** *76*, 6280-5.
8. Shibaev, V.P., Petrukhin, B.S., Zubov, Y.A., Plate, N.A., and Kargin, V.A., *J. Polym. Sci., Polym. Chem.*, **1971** *9*, 2291-8.
9. Hsieh, H.W.S., Post, B., and Morawetz, H., *J. Polym. Sci., Polym. Phys.*, **1976** *14*, 1241-1255.
10. Jordan, E.F., Jr., Feldeisen, D.W., and Wrigley, A.N., *J. Polym. Sci., Polym. Chem.*, **1971** *9*, 1835-52.
11. Van Horne, W.L., *Ind. Eng. Chem. Res.*, **1949** *41*, 952-9.
12. Neher, H.T., Van Horne, W.L., and Bauer, L.V.N., **1952**, US 2623036
13. Van Horne, W.L., Bauer, L.V.N., and Neher, H.T., **1952**, US 2600451
14. Bauer, L.N., Neher, H.T., and Van Horne, W.L., **1953**, US 2642414
15. Tal'roze, R.V., Shibaev, V.P., and Plate, N.A., *J. Polym. Sci., Symp.*, **1974** *44*, 35.
16. Swern, D. and Jordan, E.F., *J. Am. Chem. Soc.*, **1948** *70*, 2334-2339.
17. Port, W.S., Hansen, J.E., Jordan, E.F., Jr., Dietz, T.J., and Swern, D., *J. Polym. Sci.*, **1951** *7*, 207-20.
18. Lutz, D.A. and Witnauer, L.P., *J. Polym. Sci., Polym. Lett.*, **1964** *2*, 31-&.

19. Morosoff, N., Morawetz, H., and Post, B., *J. Am. Chem. Soc.*, **1965** *87*, 3035-&.
20. Plate, N.A., Shibaev, V.P., Petrunkh.B, and Kargin, V.A., *J. Polym. Sci. Polym. Sym.*, **1968** *37*.
21. Goethals, E.J., Reyntjens, W., and Lievens, S., *Macromol. Symp.*, **1998** *132*, 57-64.
22. Reyntjens, W.G., Du Prez, F.E., and Goethals, E.J., *Macromol. Rapid Commun.*, **1999** *20*, 251-255.
23. Turner-Jones, A., *Makromol. Chem.*, **1964** *71*, 1-32.
24. Trafara, G., *Makromol. Chem.*, **1980** *181*, 969-977.
25. Trafara, G., Koch, R., Blum, K., and Hummel, D., *Makromol. Chem.*, **1976** *177*, 1089-1095.
26. Trafara, G., Koch, R., and Sausen, E., *Makromol. Chem.*, **1978** *179*, 1837-1846.
27. Magagnini, P.L., Andruzzi, F., and Benetti, G.F., *Macromolecules*, **1980** *13*, 12-15.
28. Magagnini, P.L., Lupinacci, D., Cotrozzi, F., and Andruzzi, F., *Makromol. Chem. Rapid Commun.*, **1980** *1*, 557-562.
29. Andruzzi, F., Lupinacci, D., and Magagnini, P.L., *Macromolecules*, **1980** *13*, 15-18.
30. Segre, A.L., Andruzzi, F., Lupinacci, D., and Magagnini, P.L., *Macromolecules*, **1983** *16*, 1207-1212.
31. Negulescu, I. and Vogl, O., *J. Polym. Sci., Polym. Lett.*, **1975** *13*, 17-22.
32. Kubisa, P., Negulescu, I., Hatada, K., Lipp, D., Starr, J., Yamada, B., and Vogl, O., *Pure Appl. Chem.*, **1976** *48*, 275-285.
33. Negulescu, I. and Vogl, O., *J. Polym. Sci., Polym. Chem.*, **1976** *14*, 2415-2431.
34. Negulescu, I. and Vogl, O., *J. Polym. Sci., Polym. Chem.*, **1976** *14*, 2995-3012.

35. Wood, J.S., Negulescu, I., and Vogl, O., *J. Macromol. Sci. Chem.*, **1977 A 11**, 171-194.
36. Overberger, C.G., Frazier, C., Mandelman, J., and Smith, H.F., *J. Am. Chem. Soc.*, **1953 75**, 3326-3330.
37. Quirk, R.P. and Ok, M.A., *Macromolecules*, **2004 37**, 3976-3982.
38. Wang, X., Ph.D. Thesis, *University of Akron, Akron, OH*, **1999**
39. Overberger, C.G., Arond, L.H., Wiley, R.H., and Garrett, R.R., *J. Polym. Sci.*, **1951 7**, 431-441.
40. Cowie, J.M.G. and Haq, Z., *Brit. Polym. J.*, **1977 9**, 241-245.
41. Cowie, J.M.G., *Pure Appl. Chem.*, **1979 51**, 2331-2343.
42. Arrighi, V., Triolo, A., McEwen, I.J., Holmes, P., Triolo, R., and Amenitsch, H., *Macromolecules*, **2000 33**, 4989-4991.
43. Arrighi, V., Holmes, P.F., Gagliardi, S., McEwen, Q., and Telling, M.T.F., *Appl. Phys. A-Mater.*, **2002 74**, S466-S468.
44. Lopez-Carrasquero, F., de Ilarduya, A.M., Cardenas, M., Carrillo, M., Arnal, M.L., Laredo, E., Torres, C., Mendez, B., and Muller, A.J., *Polymer*, **2003 44**, 4969-4979.
45. Holmes, P.F., Arrighi, V., McEwen, I.J., Qian, H., and Terrill, N.J., *Nucl. Instrum. Meth. B*, **2003 200**, 411-415.
46. Laupretre, F. and Genix, A.C., *Abstr. Pap. Am. Chem. Soc.*, **2003 225**, U643-U643.
47. Arrighi, V., McEwen, I.J., and Holmes, P.F., *Macromolecules*, **2004 37**, 6210-6218.
48. Genix, A.C. and Laupretre, F., *Macromolecules*, **2005 38**, 2786-2794.
49. Thierry, A., Skoulios, A., Lang, G., and Forestier, S., *Mol. Cryst. Liq. Cryst.*, **1978 41**, 125-128.
50. Watanabe, J., Ono, H., Uematsu, I., and Abe, A., *Macromolecules*, **1985 18**, 2141-2148.
51. Piskunov, M.V., Olonovskii, A.N., Stroganov, L.B., Talroze, R.V., Shibaev, V.P., and Plate, N.A., *Dokl. Akad. Nauk Sssr*, **1986 290**, 1396-1399.

52. Colomer, F.J.R., Ribelles, J.L.G., and Barralesrienda, J.M., *Macromolecules*, **1994** *27*, 5004-5015.
53. Lopezcarrasquero, F., Montserrat, S., Deilarduya, A.M., and Munozguerra, S., *Macromolecules*, **1995** *28*, 5535-5546.
54. Munoz-Guerra, S., Lopez-Carrasquero, F., Aleman, C., Morillo, M., Castelletto, V., and Hamley, I., *Adv. Mater.*, **2002** *14*, 203.
55. Morillo, M., de Ilarduya, A.M., and Munoz-Guerra, S., *Macromolecules*, **2001** *34*, 7868-7875.
56. Morillo, M., Martinez De Ilarduya, A., Alla, A., and Munoz-Guerra, S., *Macromolecules*, **2003** *36*, 7567-7576.
57. Chen, S.A. and Ni, J.M., *Macromolecules*, **1992** *25*, 6081-6089.
58. Prosa, T.J., Winokur, M.J., Moulton, J., Smith, P., and Heeger, A.J., *Macromolecules*, **1992** *25*, 4364-4372.
59. Yang, C., Orfino, F.P., and Holdcroft, S., *Macromolecules*, **1996** *29*, 6510-6517.
60. Hsu, W.P., Levon, K., Ho, K.S., Myerson, A.S., and Kwei, T.K., *Macromolecules*, **1993** *26*, 1318-1323.
61. Prosa, T.J., Winokur, M.J., and McCullough, R.D., *Macromolecules*, **1996** *29*, 3654-3656.
62. Chen, T.A., Wu, X.M., and Rieke, R.D., *J. Am. Chem. Soc.*, **1995** *117*, 233-244.
63. Tashiro, K., Kobayashi, M., Kawai, T., and Yoshino, K., *Polymer*, **1997** *38*, 2867-2879.
64. Park, K.C. and Levon, K., *Macromolecules*, **1997** *30*, 3175-3183.
65. Meille, S.V., Romita, V., Caronna, T., Lovinger, A.J., Catellani, M., and Belobrzechkaja, L., *Macromolecules*, **1997** *30*, 7898-7905.
66. Hu, X. and Xu, L.G., *Polymer*, **2000** *41*, 9147-9154.
67. Causin, V., Marega, C., Marigo, A., Valentini, L., and Kenny, J.M., *Macromolecules*, **2005** *38*, 409-415.
68. Ballauff, M., *Angew. Chem. Int. Ed.*, **1989** *28*, 253-267.

69. Clauss, J., Schmidtrohr, K., Adam, A., Boeffel, C., and Spiess, H.W., *Macromolecules*, **1992** 25, 5208-5214.
70. Galda, P., Kistner, D., Martin, A., and Ballauff, M., *Macromolecules*, **1993** 26, 1595-1602.
71. Sone, M., Wada, T., Harkness, B.R., and Watanabe, J., *Macromolecules*, **1998** 31, 8865-8870.
72. Sone, M., Harkness, B.R., Kurosu, H., Ando, I., and Watanabe, J., *Macromolecules*, **1994** 27, 2769-2777.
73. Watanabe, J., Harkness, B.R., Sone, M., and Ichimura, H., *Macromolecules*, **1994** 27, 507-512.
74. Sone, M., Harkness, B.R., Watanabe, J., Yamashita, T., Torii, T., and Horie, K., *Polym. J.*, **1993** 25, 997-1001.
75. Watanabe, J., Harkness, B.R., and Sone, M., *Polym. J.*, **1992** 24, 1119-1127.
76. Harkness, B.R. and Watanabe, J., *Macromolecules*, **1991** 24, 6759-6763.
77. Rodriguezparada, J.M., Duran, R., and Wegner, G., *Macromolecules*, **1989** 22, 2507-2516.
78. Kricheldorf, H.R. and Domschke, A., *Macromolecules*, **1996** 29, 1337-1344.
79. Schrauwen, C., Pakula, T., and Wegner, G., *Makromol. Chem.*, **1992** 193, 11-30.
80. Stern, R., Ballauff, M., Lieser, G., and Wegner, G., *Polymer*, **1991** 32, 2096-2105.
81. Helmermetzmann, F., Ballauff, M., Schulz, R.C., and Wegner, G., *Makromol. Chem.*, **1989** 190, 985-994.
82. Duran, R., Ballauff, M., Wenzel, M., and Wegner, G., *Macromolecules*, **1988** 21, 2897-2899.
83. Wenzel, M., Ballauff, M., and Wegner, G., *Makromol. Chem.*, **1987** 188, 2865-2873.
84. Fu, K., Sekine, N., Sone, M., Tokita, M., and Watanabe, J., *Polym. J.*, **2002** 34, 291-297.

85. Watanabe, J., Sekine, N., Nematsu, T., Sone, M., and Kricheldorf, H.R., *Macromolecules*, **1996** *29*, 4816-4818.
86. Fu, K., Nematsu, T., Sone, M., Itoh, T., Hayakawa, T., Ueda, M., Tokita, M., and Watanabe, J., *Macromolecules*, **2000** *33*, 8367-8370.
87. Majnusz, J., Catala, J.M., and Lenz, R.W., *Eur. Polym. J.*, **1983** *19*, 1043-1046.
88. Lee, J.L., Pearce, E.M., and Kwei, T.K., *Macromolecules*, **1997** *30*, 6877-6883.
89. Lee, J.L., Pearce, E.M., and Kwei, T.K., *Macromolecules*, **1997** *30*, 8233-8244.
90. Plachetta, C., Rau, N.O., and Schulz, R.C., *Mol. Cryst. Liq. Cryst.*, **1983** *96*, 141-151.
91. Nurulla, I., Morikita, T., Fukumoto, H., and Yamamoto, T., *Macromol. Chem. Phys.*, **2001** *202*, 2335-2340.
92. Basinska, T., *Macromol. Biosci.*, **2005** *5*, 1145-1168.
93. Veronese, F.M. and Pasut, G., *Drug Discovery Today*, **2005** *10*, 1451-1458.
94. Andruzzi, L., Senaratne, W., Hexemer, A., Sheets, E.D., Ilic, B., Kramer, E.J., Baird, B., and Ober, C.K., *Langmuir*, **2005** *21*, 2495-2504.
95. Kros, A., Gerritsen, M., Murk, J., Jansen, J.A., Sommerdijk, N.A.J.M., and Nolte, R.J.M., *J. Polym. Sci., Polym. Chem.*, **2001** *39*, 468-474.
96. Reppe, W., *Liebigs Ann. Chem.*, **1956** *601*, 81-138.
97. Watanabe, S., Fujishige, S., and Hirasa, O., *Kenkyu Hokoku - Sen'i Kobunshi Zairyo Kenkyusho*, **1991** *167*, 81-6.
98. Mathias, L.J., Canterbury, J.B., and South, M., *J. Polym. Sci., Polym. Lett.*, **1982** *20*, 473-479.
99. Aoshima, S., Oda, H., and Kobayashi, E., *J. Polym. Sci., Polym. Chem.*, **1992** *30*, 2407-2413.
100. Aoshima, S., Sugihara, S., Shibayama, M., and Kanaoka, S., *Macromol. Symp.*, **2004** *215*, 151-163.

101. Sugihara, S., Kanaoka, S., and Aoshima, S., *J. Polym. Sci., Polym. Chem.*, **2004** *42*, 2601-2611.
102. Sugihara, S., Hashimoto, K., Okabe, S., Shibayama, M., Kanaoka, S., and Aoshima, S., *Macromolecules*, **2004** *37*, 336-343.
103. Aoshima, S. and Hashimoto, K., *J. Polym. Sci., Polym. Chem.*, **2001** *39*, 746-750.
104. Aoshima, S. and Sugihara, S., *J. Polym. Sci., Polym. Chem.*, **2000** *38*, 3962-3965.
105. Okabe, S., Sugihara, S., Aoshima, S., and Shibayama, M., *Macromolecules*, **2003** *36*, 4099-4106.
106. Okabe, S., Sugihara, S., Aoshima, S., and Shibayama, M., *Macromolecules*, **2002** *35*, 8139-8146.
107. Sugihara, S., Kanaoka, S., and Aoshima, S., *Macromolecules*, **2005** *38*, 1919-1927.
108. Forder, C., Patrickios, C.S., Armes, S.P., and Billingham, N.C., *Macromolecules*, **1996** *29*, 8160-8169.
109. Bannister, D.J., Davies, G.R., Ward, I.M., and McIntyre, J.E., *Polymer*, **1984** *25*, 1600-1602.
110. Xia, D.W. and Smid, J., *J. Polym. Sci., Polym. Lett.*, **1984** *22*, 617-621.
111. Xia, D.W., Soltz, D., and Smid, J., *Solid State Ionics*, **1984** *14*, 221-224.
112. Fish, D., Xia, D.W., and Smid, J., *Makromol. Chem. Rapid Commun.*, **1985** *6*, 761-765.
113. Nwankwo, I., Xia, D.W., and Smid, J., *J. Polym. Sci., Polym. Phys.*, **1988** *26*, 581-594.
114. Ishizone, T., Han, S., Okuyama, S., and Nakahama, S., *Macromolecules*, **2003** *36*, 42-49.
115. Han, S., Hagiwara, M., and Ishizone, T., *Macromolecules*, **2003** *36*, 8312-8319.
116. Li, D., Jones, G.L., Dunlap, J.R., Hua, F., and Zhao, B., *Langmuir*, **2006** *22*, 3344-3351.

117. Regen, S.L. and Dulak, L., *J. Am. Chem. Soc.*, **1977** *99*, 623-625.
118. Mackenzie, W.M. and Sherrington, D.C., *Polymer*, **1980** *21*, 791-797.
119. Hallensleben, M.L. and Lucarelli, F., *Polym. Bull.*, **1996** *37*, 759-763.
120. Hallensleben, M.L. and Lucarelli, F., *Polym. Bull.*, **1996** *37*, 765-770.
121. Sinta, R. and Smid, J., *Macromolecules*, **1980** *13*, 339-345.
122. Zhao, B., Li, D.J., Hua, F.J., and Green, D.R., *Macromolecules*, **2005** *38*, 9509-9517.
123. Bjornholm, T., Greve, D.R., Reitzel, N., Hassenkam, T., Kjaer, K., Howes, P.B., Larsen, N.B., Bogelund, J., Jayaraman, M., Ewbank, P.C., and McCullough, R.D., *J. Am. Chem. Soc.*, **1998** *120*, 7643-7644.
124. de Boer, B., van Hutten, P.F., Ouali, L., Grayer, V., and Hadziioannou, G., *Macromolecules*, **2002** *35*, 6883-6892.
125. Futterer, T., Hellweg, T., Findenegg, G.H., Frahn, J., and Schluter, A.D., *Macromolecules*, **2005** *38*, 7443-7450.
126. Futterer, T., Hellweg, T., Findenegg, G.H., Frahn, J., and Schluter, A.D., *Macromolecules*, **2005** *38*, 7451-7455.
127. Zhang, C.M., Schlaad, H., and Schluter, A.D., *J. Polym. Sci., Polym. Chem.*, **2003** *41*, 2879-2889.
128. Kandre, R.M., Kutzner, F., Schlaad, H., and Schluter, A.D., *Macromol. Chem. Phys.*, **2005** *206*, 1610-1618.
129. Allcock, H.R., Napierala, M.E., Cameron, C.G., and OConnor, S.J.M., *Macromolecules*, **1996** *29*, 1951-1956.
130. Yoshida, T., Kanaoka, S., Watanabe, H., and Aoshima, S., *J. Polym. Sci., Polym. Chem.*, **2005** *43*, 2712-2722.
131. Yoshida, T., Seno, K.I., Kanaoka, S., and Aoshima, S., *J. Polym. Sci., Polym. Chem.*, **2005** *43*, 1155-1165.
132. Neugebauer, D., Theis, M., Pakula, T., Wegner, G., and Matyjaszewski, K., *Macromolecules*, **2006** *39*, 584-593.
133. Huisgen, R., *Proc. Chem. Soc.*, **1961** 357-369.

134. Rostovtsev, V.V., Green, L.G., Fokin, V.V., and Sharpless, K.B., *Angew. Chem. Int. Ed.*, **2002** *41*, 2596-+.
135. Bock, V.D., Hiemstra, H., and van Maarseveen, J.H., *Eur. J. Org. Chem.*, **2006** 51-68.
136. Wu, P., Feldman, A.K., Nugent, A.K., Hawker, C.J., Scheel, A., Voit, B., Pyun, J., Frechet, J.M.J., Sharpless, K.B., and Fokin, V.V., *Angew. Chem. Int. Ed.*, **2004** *43*, 3928-3932.
137. Joralemon, M.J., O'Reilly, R.K., Matson, J.B., Nugent, A.K., Hawker, C.J., and Wooley, K.L., *Macromolecules*, **2005** *38*, 5436-5443.
138. Wu, P., Malkoch, M., Hunt, J.N., Vestberg, R., Kaltgrad, E., Finn, M.G., Fokin, V.V., Sharpless, K.B., and Hawker, C.J., *Chem. Commun.*, **2005** 5775-5777.
139. Lee, J.W., Kim, B.-K., Kim, H.J., Han, S.C., Shin, W.S., and Jin, S.-H., *Macromolecules*, **2006** *39*, 2418-2422.
140. Tsarevsky, N.V., Sumerlin, B.S., and Matyjaszewski, K., *Macromolecules*, **2005** *38*, 3558-3561.
141. Opsteen, J.A. and van Hest, J.C.M., *Chem. Commun.*, **2005** 57-59.
142. Helms, B., Mynar, J.L., Hawker, C.J., and Frechet, J.M.J., *J. Am. Chem. Soc.*, **2004** *126*, 15020-15021.
143. Mynar, J.L., Choi, T.L., Yoshida, M., Kim, V., Hawker, C.J., and Frechet, J.M.J., *Chem. Commun.*, **2005** 5169-5171.
144. Sumerlin, B.S., Tsarevsky, N.V., Louche, G., Lee, R.Y., and Matyjaszewski, K., *Macromolecules*, **2005** *38*, 7540-7545.
145. Englert, B.C., Bakbak, S., and Bunz, U.H.F., *Macromolecules*, **2005** *38*, 5868-5877.
146. Malkoch, M., Thibault, R.J., Drockenmuller, E., Messerschmidt, M., Voit, B., Russell, T.P., and Hawker, C.J., *J. Am. Chem. Soc.*, **2005** *127*, 14942-14949.
147. Gao, H., Louche, G., Sumerlin, B.S., Jahed, N., Golas, P., and Matyjaszewski, K., *Macromolecules*, **2005** *38*, 8979-8982.
148. Lutz, J.F., Borner, H.G., and Weichenhan, K., *Macromol. Rapid Commun.*, **2005** *26*, 514-518.

149. Sen Gupta, S., Raja, K.S., Kaltgrad, E., Strable, E., and Finn, M.G., *Chem. Commun.*, **2005** 4315-4317.
150. Parrish, B., Breitenkamp, R.B., and Emrick, T., *J. Am. Chem. Soc.*, **2005** 127, 7404-7410.
151. Riva, R., Schmeits, P., Stoffelbach, F., Jerome, C., Jerome, R., and Lecomte, P., *Chem. Commun.*, **2005** 5334-5336.
152. Fernandez-Megia, E., Correa, J., Rodriguez-Meizoso, I., and Riguera, R., *Macromolecules*, **2006** 39, 2113-2120.
153. Rijkers, D.T.S., van Esse, G.W., Merkx, R., Brouwer, A.J., Jacobs, H.J.F., Pieters, R.J., and Liskamp, R.M.J., *Chem. Commun.*, **2005** 4581-4583.
154. Malkoch, M., Schleicher, K., Drockenmuller, E., Hawker, C.J., Russell, T.P., Wu, P., and Fokin, V.V., *Macromolecules*, **2005** 38, 3663-3678.
155. Diaz, D.D., Punna, S., Holzer, P., Mcpherson, A.K., Sharpless, K.B., Fokin, V.V., and Finn, M.G., *J. Polym. Sci., Polym. Chem.*, **2004** 42, 4392-4403.
156. Joralemon, M.J., O'Reilly, R.K., Hawker, C.J., and Wooley, K.L., *J. Am. Chem. Soc.*, **2005** 127, 16892-16899.
157. O'Reilly, R.K., Joralemon, M.J., Wooley, K.L., and Hawker, C.J., *Chem. Mater.*, **2005** 17, 5976-5988.
158. Beers, K.L., Gaynor, S.G., Matyjaszewski, K., Sheiko, S.S., and Moller, M., *Macromolecules*, **1998** 31, 9413-9415.
159. Matyjaszewski, K., Teodorescu, M., Miller, P.J., and Peterson, M.L., *J. Polym. Sci., Polym. Chem.*, **2000** 38, 2440-2448.
160. Shinoda, H. and Matyjaszewski, K., *Macromolecules*, **2001** 34, 6243-6248.
161. Shinoda, H., Miller, P.J., and Matyjaszewski, K., *Macromolecules*, **2001** 34, 3186-3194.
162. Hong, S.C., Pakula, T., and Matyjaszewski, K., *Macromol. Chem. Phys.*, **2001** 202, 3392-3402.
163. Lee, H.I., Matyjaszewski, K., Yu, S., and Sheiko, S.S., *Macromolecules*, **2005** 38, 8264-8271.

164. Jordan, E.F., Jr., Smith, S., Jr., Parker, W.E., Artymyshyn, B., and Wrigley, A.N., *J. App. Polym. Sci.*, **1978** *22*, 1509-28.
165. Jordan, E.F., Jr., Smith, S., Jr., Zabarsky, R.D., Austin, R., and Wrigley, A.N., *J. App. Polym. Sci.*, **1978** *22*, 1529-45.
166. Jordan, E.F., Jr., Smith, S., Jr., Zabarsky, R.D., and Wrigley, A.N., *J. App. Polym. Sci.*, **1978** *22*, 1547-67.
167. Port, W.S., O'Brien, J.W., Hansen, J.E., and Swern, D., *Ind. Eng. Chem. Res.*, **1951** *43*, 2105-7.
168. Sun, X.G. and Kerr, J.B., *Macromolecules*, **2006** *39*, 362-372.
169. Hou, W.H., Chen, C.Y., and Wang, C.C., *Polymer*, **2003** *44*, 2983-2991.
170. Meier-Haack, J., Lenk, W., Lehmann, D., and Lunkwitz, K., *J. Membrane Sci.*, **2001** *184*, 233-243.
171. Zheng, W.Y., Levon, K., Laakso, J., and Osterholm, J.E., *Macromolecules*, **1994** *27*, 7754-7768.
172. Chen, X.H., McCarthy, S.P., and Gross, R.A., *Macromolecules*, **1997** *30*, 3470-3476.
173. Chen, X.H., McCarthy, S.P., and Gross, R.A., *Macromolecules*, **1997** *30*, 4295-4301.
174. Schmidt, S.C. and Hillmyer, M.A., *Macromolecules*, **1999** *32*, 4794-4801.
175. Huang, J., Lisowski, M.S., Runt, J., Hall, E.S., Kean, R.T., Buehler, N., and Lin, J.S., *Macromolecules*, **1998** *31*, 2593-2599.
176. Yin, M. and Baker, G.L., **1999** *32*, 7711-7718.
177. Simmons, T.L. and Baker, G.L., *Biomacromolecules*, **2001** *2*, 658-663.
178. Liu, T., Simmons, T.L., and Baker, G.L., *PMSE Preprints*, **2003** *88*, 420-421.
179. Rozen, S. and Ben-David, I., *J. Org. Chem.*, **2001** *66*, 496-500.
180. Fairlamb, I.J.S., Dickinson, J.M., and Cristea, I.M., *Tetrahedron*, **2001** *57*, 2237-2246.

181. Dubois, P., Ropson, N., Jerome, R., and Teyssie, P., *Macromolecules*, **1996** *29*, 1965-1975.
182. Yamamoto, T., Komarudin, D., Maruyama, T., Arai, M., Lee, B.-L., Suganuma, H., Asakawa, N., Inoue, Y., Kubota, K., Sasaki, S., Fukuda, T., and Matsuda, H., *J. Am. Chem. Soc.*, **1998** *120*, 2047-2058.
183. Fukuzaki, H., Aiba, Y., Yoshida, M., Asano, M., and Kumakura, M., *Makromol. Chem.*, **1989** *190*, 2407-2415.
184. Doi, Y., Kaneshawa, Y., Kunioka, M., and Saito, T., *Macromolecules*, **1990** *23*, 26-31.
185. Guest, H.H., *J. Am. Chem. Soc.*, **1947** *69*, 300-302.
186. Kashinskii, V.N., Burba, A.A., Zulkarnaev, R.I., and Lapkin, I.I., *Zh. Obshch. Khim.*, **1984** *54*, 2767-2770.
187. Orito, K., Seki, Y., Suginome, H., and Iwadare, T., *Bull. Chem. Soc. Jpn.*, **1989** *62*, 2013-2017.
188. Sueur, L., *J. Chem. Soc.*, **1905** *87*, 1901.
189. Sueur, L., *J. Chem. Soc.*, **1904** *85*, 833.
190. Hoffman, A.S., *J. Control. Release*, **1987** *6*, 297-305.
191. Chen, G. and Hoffman, A.S., *Nature*, **1995** *373*, 49-52.
192. Alarcon, C.D.H., Pennadam, S., and Alexander, C., *Chem. Soc. Rev.*, **2005** *34*, 276-285.
193. Song, S.C., Lee, S.B., Jin, J.I., and Sohn, Y.S., *Macromolecules*, **1999** *32*, 2188-2193.
194. Lee, S.B., Song, S.C., Jin, J.I., and Sohn, Y.S., *Macromolecules*, **1999** *32*, 7820-7827.
195. Zhang, J.X., Qiu, L.Y., Jin, Y., and Zhu, K.J., *J. Bio. Mat. Res. Part A*, **2006** *76A*, 773-780.
196. Lee, B.H., Lee, Y.M., Sohn, Y.S., and Song, S.C., *Macromolecules*, **2002** *35*, 3876-3879.
197. Bhattarai, N., Ramay, H.R., Gunn, J., Matsen, F.A., and Zhang, M.Q., *J. Control. Release*, **2005** *103*, 609-624.

198. Chilkoti, A., Dreher, M.R., and Meyer, D.E., *Adv. Drug Deliv. Rev.*, **2002** *54*, 1093-1111.
199. Chilkoti, A., Dreher, M.R., Meyer, D.E., and Raucher, D., *Adv. Drug Deliv. Rev.*, **2002** *54*, 613-630.
200. Nath, N. and Chilkoti, A., *Adv. Mater.*, **2002** *14*, 1243.
201. Langer, R., *Acc. Chem. Res.*, **2000** *33*, 94-101.
202. Greenwald, D., Shumway, S., Albear, P., and Gottlieb, L., *J. Surg. Res.*, **1994** *56*, 372-377.
203. Gonzalez, R. and Ramshaw, B.J., *American Surgeon*, **2003** *69*, 471-476.
204. Carnahan, M.A., Middleton, C., Kim, J., Kim, T., and Grinstaff, M.W., *J. Am. Chem. Soc.*, **2002** *124*, 5291-5293.
205. MacDonald, R.T., McCarthy, S.P., and Gross, R.A., *Macromolecules*, **1996** *29*, 7356-7361.
206. Schmidt, P., Keul, H., and Hocker, H., *Macromolecules*, **1996** *29*, 3674-3680.
207. Li, S.M., Rashkov, I., Espartero, J.L., Manolova, N., and Vert, M., *Macromolecules*, **1996** *29*, 57-62.
208. Jeong, B., Bae, Y.H., Lee, D.S., and Kim, S.W., *Nature*, **1997** *388*, 860-862.
209. Allcock, H.R. and Dudley, G.K., *Macromolecules*, **1996** *29*, 1313-1319.
210. Parrish, B. and Emrick, T., *Macromolecules*, **2004** *37*, 5863-5865.
211. Rieger, J., Bernaerts, K.V., Du Prez, F.E., Jerome, R., and Jerome, C., *Macromolecules*, **2004** *37*, 9738-9745.
212. Benabdillah, K.M., Coudane, J., Boustta, M., Engel, R., and Vert, M., *Macromolecules*, **1999** *32*, 8774-8780.
213. Trollsas, M., Lee, V.Y., Mecerreyes, D., Lowenhielm, P., Moller, M., Miller, R.D., and Hedrick, J.L., *Macromolecules*, **2000** *33*, 4619-4627.
214. Kimura, Y., Shirotni, K., Yamane, H., and Kitao, T., *Macromolecules*, **1988** *21*, 3338-3340.

215. Mecerreyes, D., Miller, R.D., Hedrick, J.L., Detrembleur, C., and Jerome, R., *J. Polym. Sci., Polym. Chem.*, **2000** *38*, 870-875.
216. Vogeley, N.J., Baker, G.L., and Smith, M.R., *Abstr. Pap. Am. Chem. Soc.*, **2005** *229*, 946.
217. Dirks, A.J.T., van Berkel, S.S., Hatzakis, N.S., Opsteen, J.A., van Delft, F.L., Cornelissen, J.J.L.M., Rowan, A.E., van Hest, J.C.M., Rutjes, F.P.J.T., and Nolte, R.J.M., *Chem. Commun.*, **2005** *4172-4174*.
218. Jiang, X., Horton, J.M., Baker, G.L., and Smith, M.R., III, *Polym. Preprints*, **2005** *46*, 1040.
219. Bohlmann, F., Herbst, P., and Gleinig, H., *Chem. Ber.*, **1961** *94*, 948-57.
220. Uhrich, K. E., Cannizzaro, S. M., Langer, R. S., and Shakesheff, K. M. *Chem. Rev.* **1999**, *99*, 3181.
221. Prime, K. L., and Whitesides, G. M. *J. Am. Chem. Soc.* **1993**, *115*, 10714.
222. Gan, D., and Lyon, L. A. *Macromolecules* **2002**, *35*, 9634.
223. Kissel, T., Li Y., and Unger F. *Adv. Drug Deliv. Rev.* **2002**, *54*, 99-134.
224. Gaucher G., Dufresne M.H., Sant, V. P., Kang N., Maysinger D., and Leroux J.C. *J. Control. Release* **2005**, *109*, 169-188.
225. Li, S., Anjard, S., Rashkov, I., and Vert, M. *Polymer*, **1998**, *39*, 5421-5430.
226. Shah, S.S., Zhu, K.J., and Pitt, C.G. *J. Biomater. Sci., Polym. Ed.* **1994**, *5*, 421-431.
227. Taniguchi, I.; Mayes, A. M.; Chan, E. W. L.; Griffith, L. G. *Macromolecules* **2005**, *38*, 216-219.

MICHIGAN STATE UNIVERSITY LIBRARIES



3 1293 02845 5891